

**Elucidating the role of endothelial  $\alpha\beta 3$ -integrin  
in tumour growth and angiogenesis**

**Veronica Steri**

Ph.D.

School of Biological Sciences

University of East Anglia

*A Marco*

*“Non tutti quelli che vagano sono senza meta, soprattutto non coloro che cercano la verità, oltre la tradizione, oltre la definizione, oltre l'apparenza”.*

This copy of the thesis has been supplied on condition that anyone who consults it is understood to recognise that its copyright rests with the author and that use of any information derived there from must be in accordance with current UK Copyright Law. In addition, any quotation or extract must include full attribution (Number of words: 51490)

## ABSTRACT

Angiogenesis, the formation of new vessels from pre-existing ones, is essential for primary tumour growth as well as for metastasis, and endothelial cells play a central role in this process: they drive blood vessel formation in response to signals from the local environment by a mechanism that is integrin-dependent.

$\alpha\beta3$ -integrin seemingly poses an ideal anti-angiogenic target. Its expression is vastly up-regulated in neo-angiogenic vessels, while its expression in quiescent vasculature is minimal. However, anti-angiogenic therapy targeting  $\alpha\beta3$ -integrin has proven somewhat disappointing. In part, this may relate to the fact that  $\alpha\beta3$ -integrin is not expressed solely by endothelial cells, but across a wide range of cell types that each contribute to angiogenesis.

In this thesis, I describe my studies on understanding the role of  $\alpha\beta3$ -integrin as expressed specifically by endothelial cells in tumour growth and angiogenesis using endothelial specific  $\beta3$ -integrin deficient mice. I have shown that inducible deletion of endothelial  $\beta3$ -integrin inhibits tumour growth and angiogenesis preventatively, while its constitutive deletion is ineffective; furthermore, I have found that even the inducible deletion does not alter angiogenesis in already established tumours.

The findings described in this thesis re-establish  $\alpha\beta3$ -integrin as good anti-angiogenic target, but imply that timing and length of inhibition are critical factors to be considered when targeting endothelial  $\beta3$ -integrin-expression.

# CONTENTS

<b>ABSTRACT</b>	<b>3</b>
<b>CONTENTS</b>	<b>4</b>
<b>LIST OF FIGURES</b>	<b>13</b>
<b>LIST OF ABBREVIATIONS</b>	<b>17</b>
<b>1. INTRODUCTION</b>	<b>18</b>
<b>1.1 The vascular system</b>	<b>18</b>
<b>1.2 Blood vessel morphology</b>	<b>21</b>
1.2.1 Endothelial cells	21
1.2.2 Mural cells	21
1.2.3 Endothelial basement membrane	21
<b>1.3 Blood vessel development and physiology</b>	<b>22</b>
1.3.1 Vasculogenesis	22
1.3.2 Angiogenesis	22
1.3.3 Mechanism of sprouting angiogenesis	23
1.3.4 Vessel maturation	24
1.3.5 Vessel quiescence and permeability	25
<b>1.4 Molecular mechanisms of angiogenesis</b>	<b>25</b>
1.4.1 VEGF/VEGFR	25
1.4.2 Regulation of VEGFR2 activity	28
1.4.2.1 VEGFR2 promotes EC proliferation	29
1.4.2.2 VEGFR2 regulates EC migration	30
1.4.2.3 VEGFR2 controls EC survival and vessel permeability	31
<b>1.5 Pathological angiogenesis</b>	<b>32</b>
1.5.1 Tumour angiogenesis	32
1.5.2 Metastatic disease: vessels required	34
1.5.3 The role of immune cells in tumour angiogenesis	35
<b>1.6 Integrins</b>	<b>37</b>

1.6.1 Integrin structure	37
1.6.2 Integrin activation and signalling	39
1.6.3 Integrin in cancer	40
1.6.4 Vascular integrins	41
1.6.5 $\alpha\beta$ 3-integrin	41
1.6.5.1 $\alpha\beta$ 3-integrin signalling in angiogenesis	42
1.6.5.2 ECM ligands for $\alpha\beta$ 3-integrin	43
1.6.5.3 $\beta$ 3-integrin knock-out and knock-in models	43
1.6.5.4 $\alpha\beta$ 3-integrin inhibitors	45
<b>1.7 Anti-angiogenic therapy</b>	<b>45</b>
1.7.1 Clinically approved anti-angiogenic therapies	46
1.7.2 Concern and challenges of anti-angiogenic therapies	48
<b>1.8 Aims of the study</b>	<b>51</b>
<b>2. MATERIALS AND METHODS</b>	<b>52</b>
<b>2.1 MATERIALS</b>	<b>52</b>
<b>2.1.1 Chemicals</b>	<b>52</b>
<b>2.1.2 Consumables</b>	<b>52</b>
<b>2.1.3 Equipment and software</b>	<b>52</b>
<b>2.1.4 PCR</b>	<b>53</b>
2.1.4.1 Primers	53
2.1.4.2 Solutions and reagents	54
<b>2.1.5 Animals</b>	<b>54</b>
2.1.5.1 Surgical materials and reagents	54
<b>2.1.6 Histology</b>	<b>54</b>
2.1.6.1 Solutions and reagents	54
<b>2.1.7 Cells and tissues</b>	<b>55</b>
2.1.7.1 Cell Cultures	55
2.1.7.2 Solutions and reagents	56

2.1.7.3 Kits	57
<b>2.1.8 Western blotting</b>	<b>57</b>
2.1.8.1 Equipment	57
2.1.8.2 Solutions and reagents	57
2.1.8.3 Kits	57
<b>2.1.9 Antibodies</b>	<b>58</b>
<b>2.2 METHODS</b>	<b>59</b>
<b>2.2.1 Animals</b>	<b>59</b>
2.2.1.1 $\beta$ 3-integrin-floxed transgenic mice	60
2.2.1.2 Tie1Cre transgenic mice	60
2.2.1.3 Pdgfb-iCreER <sup>T2</sup> transgenic mice	60
2.2.1.4 tdTomato reporter mice	61
<b>2.2.2 PCR genotyping</b>	<b>61</b>
2.2.2.1 Genomic DNA isolation from tissues	62
2.2.2.2 Genomic DNA isolation from cells	62
2.2.2.3 $\beta$ 3-floxed PCR	62
2.2.2.4 Tie1Cre PCR	63
2.2.2.5 Pdgfb-iCre <sup>T2</sup> PCR	63
2.2.2.6 TdTomato PCR	63
2.2.2.7 Agarose gel electrophoresis	63
<b>2.2.3 <i>In vivo</i> tumour growth and metastasis assays</b>	<b>64</b>
2.2.3.1 Tumour cell lines	64
2.2.3.2 Growth and maintenance of tumour cell lines	65
2.2.3.3 Allografts	65
2.2.3.4 Tamoxifen treatments	66
2.2.3.5 Surgical resections	67
2.2.3.6 Quantification of tumour circulating cells	67
2.2.3.7 <i>In vivo</i> tumour permeability assay	68
2.2.3.8 Experimental metastasis assay	68
<b>2.2.4 Immunohistochemical analysis</b>	<b>68</b>

<b>2.2.4.1 Tumour sections</b>	<b>68</b>
2.2.4.1.1 Endomucin staining	69
2.2.4.1.2 $\alpha$ Smooth Muscle Actin/endomucin co-staining	69
2.2.4.1.3 Nidogen/endomucin co-staining	69
2.2.4.1.4 Focal Adhesion Kinase/endomucin co-staining	70
2.2.4.1.5 Live staining of luminal CD31	70
2.2.4.1.6 Analysis of tumour vascular phenotype	71
<b>2.2.4.2 Lung sections</b>	<b>72</b>
2.2.4.2.1 H&E staining	72
2.2.4.2.2 Endomucin staining	72
2.2.4.2.3 F4/80 staining	72
2.2.4.2.4 Analysis of lung metastatic phenotype	73
<b>2.2.4.3 Wholemounds of tumours</b>	<b>73</b>
2.2.4.3.1 Live staining of luminal $\beta$ 3-integrin	74
2.2.4.3.2 Analysis of Cre activity and specificity <i>in vivo</i>	74
<b>2.2.5 Ex vivo mouse aortic ring assay</b>	<b>74</b>
2.2.5.1 VEGF aortic angiogenesis in collagen gel	75
2.2.5.2 bFGF aortic angiogenesis in fibrin gel	75
2.2.5.3 Aortic ring staining	76
2.2.5.4 Protein isolation from aortae	76
<b>2.2.6 Cell isolations</b>	<b>77</b>
<b>2.2.6.1 Isolation of bone marrow cells</b>	<b>77</b>
<b>2.2.6.2 Isolation of platelets</b>	<b>78</b>
<b>2.2.6.3 Isolation of tumour endothelial cells</b>	<b>78</b>
2.2.6.3.1 Analysis of Tumour-Associated macrophages	79
<b>2.2.6.4 Isolation of lung endothelial cells</b>	<b>79</b>
2.2.6.4.1 Collagenase treatment of lungs	79
2.2.6.4.2 ICAM2 magnetic sorting	79
2.2.6.4.3 Generation of immortalized lung endothelial cells	80
2.2.6.4.4 Growth and maintenance of immortalized lung endothelial cells	81

2.2.6.4.5 Phenotypic analysis of immortalized lung endothelial cells	81
2.2.6.4.6 Analysis of macrophages in the pre-metastatic lung	82
<b>2.2.7 <i>In vitro</i> cell assays</b>	<b>83</b>
<b>2.2.7.1 Staining for endothelial cell markers and surface integrins</b>	<b>83</b>
<b>2.2.7.2 MTT Proliferation assay</b>	<b>84</b>
<b>2.2.7.3 Scratch wound assay</b>	<b>84</b>
<b>2.2.7.4 Endothelial cell adhesion assay</b>	<b>84</b>
<b>2.2.7.5 VEGF stimulation timecourse</b>	<b>84</b>
<b>2.2.7.6 Western blot analysis</b>	<b>85</b>
2.2.7.6.1 Sample preparation	85
2.2.7.6.2 SDS-PAGE protein separation	85
2.2.7.6.3 Wet Transfer	86
2.2.7.6.4 Immunoblotting	87
<b>2.2.8 Analysis of statistical significance</b>	<b>87</b>
<b>3. THE TIMING OF ENDOTHELIAL <math>\beta</math>3-INTEGRIN DELETION AFFECTS TUMOUR GROWTH AND ANGIOGENESIS <i>IN VIVO</i></b>	<b>87</b>
<b>RESULTS AND FIGURES</b>	<b>87</b>
<b>3.1 Inducible deletion of endothelial <math>\beta</math>3-integrin reduces tumour growth and inhibits angiogenesis, while the constitutive does not</b>	<b>87</b>
3.1.1 Constitutive deletion of endothelial $\beta$ 3-integrin	89
3.1.2 Inducible deletion of endothelial $\beta$ 3-integrin	89
3.1.3 Tumour models	90
3.1.3.1 B16F0	90
3.1.3.2 CMT19T	91
<b>3.2 <math>\beta</math>3-integrin does not impact on tumour vessel structure or function</b>	<b>92</b>
3.2.1 Structural analyses: pericyte and endothelial basement membrane coverage	92
3.2.2 Vascular functions: distribution and perfusion	93
<b>3.3 Validation of the two endothelial Cre models</b>	<b>94</b>

3.3.1 Bone marrow cell analysis	94
3.3.2 Platelet analyses	95
3.3.3 Analysis of Tomato Cre reporter activity	95
3.3.4 Analysis of Cre deletion efficiency	96
<b>3.4 The length of <math>\beta</math>3-integrin deletion dictates the angiogenic response</b>	<b>97</b>
3.4.1 Rationale of the long OHT treatment in the inducible model of $\beta$ 3-integrin deletion	97
3.4.2 Abrogation of the inhibitory tumour phenotype by long OHT treatment of $\beta$ 3-floxed/Pdgfb-iCreER <sup>T2</sup> mice	97
3.4.3 The inhibitory effects of inducible endothelial $\beta$ 3-integrin deletion are transient	98
3.4.4 Endothelial $\beta$ 3-integrin is not required when tumours have already established	99
<b>DISCUSSION</b>	<b>101</b>
<b>3.5 The <math>\alpha</math>v<math>\beta</math>3-integrin conundrum</b>	<b>113</b>
<b>3.6 Cre issues</b>	<b>115</b>
<b>3.7 Endothelial <math>\alpha</math>v<math>\beta</math>3-integrin-deficiency in the tumour vasculature</b>	<b>117</b>
<b>CONCLUSIONS</b>	<b>119</b>
<b>4. USING THE AORTIC RING ASSAY TO STUDY ENDOTHELIAL <math>\beta</math>3-INTEGRIN IN VESSEL SPROUTING</b>	<b>120</b>
<b>RESULTS AND FIGURES</b>	<b>120</b>
<b>4.1 Inducible deletion of <math>\beta</math>3-integrin inhibits VEGF-induced microvessel sprouting <i>ex vivo</i>, while the constitutive has the opposite effect</b>	<b>120</b>
<b>4.2 bFGF-induced microvessel sprouting <i>ex vivo</i> is not affected by deletion of endothelial <math>\beta</math>3-integrin expression</b>	<b>121</b>
<b>4.3 <i>Ex vivo</i> Cre activity in aortic rings</b>	<b>122</b>

<b>4.4 Microvessel sprouting is not suppressed by long OHT treatment of <math>\beta</math>3-floxed/Pdgfb-iCreER<sup>T2</sup> aortic rings</b>	<b>123</b>
<b>4.5 <math>\beta</math>3-integrin deletion is ineffective when microvessel sprouting has already begun</b>	<b>123</b>
<b>DISCUSSION</b>	<b>130</b>
<b>4.5 The aortic ring model</b>	<b>130</b>
<b>4.6 <math>\alpha</math>v<math>\beta</math>3-integrin in aortic angiogenesis</b>	<b>130</b>
<b>CONCLUSIONS</b>	<b>132</b>
<b>5. MECHANISTIC ANALYSIS OF THE ROLE OF ENDOTHELIAL <math>\beta</math>3-INTEGRIN: <i>IN VITRO</i> STUDIES</b>	<b>133</b>
<b>RESULTS AND FIGURES</b>	<b>133</b>
<b>5.1 <i>In vitro</i> cellular differences between the two Cre transgenic models</b>	<b>133</b>
5.1.1 Why use immortalized rather than primary endothelial cells?	133
5.1.2 Surface expression of endothelial integrin and adhesion properties	134
5.1.3 VEGF-induced migration and proliferation	135
<b>5.2 <i>In vitro</i> molecular differences between the two Cre transgenic models</b>	<b>136</b>
5.2.1 VEGFR2 analysis: total, surface, and phosphorylated levels	136
5.2.2 VEGF/VEGFR2 signalling analysis	138
<b>5.3 The differences observed in presence of <math>\beta</math>3-integrin inducible deletion are abolished by long OHT treatment <i>in vitro</i></b>	<b>139</b>
5.3.1 Molecular differences upon long OHT treatment	139
<b>DISCUSSION</b>	<b>150</b>
<b>5.4 <math>\alpha</math>v<math>\beta</math>3-integrin and VEGFR2 in angiogenesis: a complex marriage</b>	<b>150</b>
<b>5.5 Molecular compensation of other endothelial integrins</b>	<b>153</b>
<b>CONCLUSIONS</b>	<b>154</b>

<b>6. DEVELOPING MOUSE MODEL OF SPONTANEOUS METASTASIS TO ADDRESS THE ROLE OF ENDOTHELIAL <math>\beta</math>3-INTEGRIN</b>	<b>155</b>
<b>RESULTS AND FIGURES</b>	<b>155</b>
<b>6.1 Mouse models of metastasis</b>	<b>155</b>
6.1.1 CMT19T F1	156
6.1.2 B6 LV-1	158
<b>6.2 Endothelial <math>\beta</math>3-integrin deletion reduces CMT19T F1 spontaneous, but not experimental, metastasis</b>	<b>158</b>
6.2.1 The number of spontaneous CMT19T F1 lung metastases is reduced, but not their size or vascularisation, in the absence of endothelial $\beta$ 3-integrin	159
6.2.2 Tumour-Associated Macrophages are reduced in the CMT19T F1 metastatic lung when endothelial $\beta$ 3-integrin is absent	159
6.2.3 Loss of endothelial $\beta$ 3-integrin is sufficient to affect lung metastasis	160
<b>6.3 <i>In vivo</i> and <i>in vitro</i> mechanistic analysis of the role of endothelial <math>\beta</math>3-integrin in metastasis</b>	<b>161</b>
6.3.1 F4/80+ macrophages are also reduced in the CMT19T F1 pre-metastatic lung when endothelial $\beta$ 3-integrin is absent	161
6.3.2 Loss of endothelial $\beta$ 3-integrin within the tumour does not affect either vascular permeability, or circulating tumour cells <i>in vivo</i>	162
6.3.3 VEC Y731 phosphorylation is affected by endothelial $\beta$ 3-integrin <i>in vitro</i>	163
<b>DISCUSSION</b>	<b>169</b>
<b>6.4 Metastasis: the real killer</b>	<b>169</b>
<b>6.5 Metastasis models: not enough!</b>	<b>169</b>
<b>6.6 Is endothelial <math>\beta</math>3-integrin anti-metastatic?</b>	<b>171</b>
<b>6.7 Mechanisms of pre-metastatic niche formation</b>	<b>173</b>
<b>CONCLUSIONS</b>	<b>175</b>
<b>7. SUMMARY AND CONCLUSION</b>	<b>177</b>

<b>7.1 Novelty and significance</b>	<b>177</b>
<b>7.2 Final conclusions and future works</b>	<b>179</b>
<b>ACKNOWLEDGEMENTS</b>	<b>181</b>
<b>LIST OF PUBLICATIONS</b>	<b>182</b>
<b>REFERENCES</b>	<b>183</b>
<b>APPENDIX</b>	<b>201</b>

## LIST OF FIGURES

<b>Figure 1.1</b> The anatomy of man: the cardiovascular system	<b>18</b>
<b>Figure 1.2</b> Microscopic anatomy of vessel structure	<b>20</b>
<b>Figure 1.3</b> Schematic diagram of VEGFA isoforms	<b>26</b>
<b>Figure 1.4</b> Overview of VEGF/VEGFR binding	<b>27</b>
<b>Figure 1.5</b> Schematic overview of VEGF signalling pathways	<b>29</b>
<b>Figure 1.6</b> The role of Tumour-Associated Macrophages (TAM) in cancer	<b>36</b>
<b>Figure 1.7</b> Integrin receptor family	<b>38</b>
<b>Figure 1.8</b> Integrin intracellular signalling	<b>40</b>
<b>Figure 1.9</b> Overview of anti-angiogenic drugs in cancer	<b>46</b>
<b>Figure 3.1</b> Endothelial $\beta$ 3-integrin deletion in Tie1 and Pdgfb-iCreER <sup>T2</sup> models	<b>101</b>
<b>Figure 3.2</b> Tumour growth is not affected by differences in the genetic background	<b>102</b>
<b>Figure 3.3</b> Inducible deletion of endothelial $\beta$ 3-integrin reduces tumour growth and inhibits angiogenesis	<b>103</b>
<b>Figure 3.4</b> Tumour growth is not affected by the constitutive deletion of endothelial $\beta$ 3-integrin	<b>104</b>
<b>Figure 3.5</b> Endothelial $\beta$ 3-integrin does not affect pericyte or endothelial basement membrane coverage	<b>105</b>
<b>Figure 3.6</b> Vessel function is not impaired in the absence of endothelial $\beta$ 3-integrin	<b>106</b>
<b>Figure 3.7</b> Non-endothelial specificity of Tie1Cre and Pdgfb-iCreER <sup>T2</sup> promoters	<b>107</b>
<b>Figure 3.8</b> Analysis of Cre specificity and efficiency <i>in vivo</i>	<b>108</b>
<b>Figure 3.9</b> The length of endothelial $\beta$ 3-integrin deletion dictates the angiogenic response <i>in vivo</i>	<b>109</b>
<b>Figure 3.10</b> The effects of endothelial $\beta$ 3-integrin deletion are time-dependent	<b>111</b>
<b>Figure 4.1</b> Inducible deletion of $\beta$ 3-integrin inhibits VEGF (but not bFGF) microvessel sprouting <i>ex vivo</i> , while the constitutive has the opposite effect	<b>117</b>
<b>Figure 4.2</b> <i>Ex vivo</i> Cre activity in aortic rings	<b>119</b>
<b>Figure 4.3</b> The length of endothelial $\beta$ 3-integrin deletion dictates the angiogenic response <i>ex vivo</i>	<b>120</b>
<b>Figure 5.1</b> Immortalized lung endothelial cell phenotype	<b>142</b>

<b>Figure 5.2</b> Analysis of surface integrins and adhesive properties of $\beta$ 3-integrin deleted endothelial cells	<b>143</b>
<b>Figure 5.3</b> Analysis of VEGF-induced migration and proliferation in $\beta$ 3-integrin deleted endothelial cell	<b>144</b>
<b>Figure 5.4</b> Changes in VEGFR2 expression and activation	<b>145</b>
<b>Figure 5.5</b> VEGFR2 downstream signalling analyses	<b>146</b>
<b>Figure 5.6</b> Molecular differences are abolished by long OHT treatment	<b>147</b>
<b>Figure 5.7</b> Changes in FAK expression after deletion of endothelial $\beta$ 3-integrin	<b>149</b>
<b>Figure 6.1</b> Constitutive endothelial $\beta$ 3-integrin deletion reduces CMT19T F1 spontaneous, but not experimental, metastasis	<b>165</b>
<b>Figure 6.2</b> Constitutive deletion of endothelial $\beta$ 3-integrin does not affect average metastasis size or vascularisation, but fewer macrophages are present in the lung	<b>166</b>
<b>Figure 6.3</b> F4/80+ macrophages are reduced in CMT19T F1 pre-metastatic lungs when endothelial $\beta$ 3-integrin is absent	<b>167</b>
<b>Figure 6.4</b> Constitutive deletion of endothelial $\beta$ 3-integrin: <i>in vivo</i> and <i>in vitro</i> effects	<b>168</b>

## LIST OF ABBREVIATIONS

2D	Two-dimensional
3D	Three-dimensional
AJs	adherens junctions
Ang	Angiopoietin
APC	Allophycocyanin
bFGF	Basic fibroblast growth factor
BM	Basement membrane
BSA	Bovine serum albumin
CD	Cluster of differentiation
D-MEM	Dulbecco's Modified Eagle's Medium
DAPI	4',6-diamidino-2-phenylindole
DLL4	Delta-Like Ligand 4
DNA	Deoxyribonucleic acid
Enn.n	Embryonic day nn.n
EC	Endothelial cell
ECM	Extracellular matrix
EDTA	Ethylenediaminetetraacetic acid
EMT	Epithelial to Mesenchimal Transition
eNOS	Endothelial nitric oxide synthase
ERK	Extracellular signal-regulated protein kinase
FACS	Fluorescence activated cell sorter
FAK	Focal adhesion kinase
FCS	Foetal calf serum
FDA	Food and Drug Administration
FITC	Fluorescein isothiocyanate
FLK-1	Foetal liver kinase
FSC	Forward Scatter
GFP	Green fluorescent protein
H&E	Haematoxylin and eosin
HIF	Hypoxia-inducible factor
HUVEC	Human umbilical endothelial cell
HRP	Horse radish peroxidase
HSC	Haematopoietic stem cell
IB4	Isolectin B4

ICAM Intracellular cell adhesion molecule  
ICreER Tamoxifen inducible Cre recombinase  
IP3 Inositol 1, 4, 5-triphosphate  
JNK c-Jun kinase  
MAPK Mitogen-activated protein kinase  
MEK Mitogen-activated protein kinase/ERK kinase  
MLEC Mouse lung endothelial cell  
MMP Matrix metalloproteases  
mRNA Messenger ribonucleic acid  
MDSCs Myeloid derived suppressor cells  
N-CAD N-cadherin  
NCID Notch Intracellular Domain  
NRP Neuropilin  
OHT 4-hydroxytamoxifen  
OS Overall Survival  
PBS Phosphate buffered saline  
PC Pericyte  
PCR Polymerase chain reaction  
PDGF Platelet derived growth factor  
PDGFR Platelet derived growth factor receptor  
PVDF Polyvinyl difluoride  
PECAM Platelet endothelial cell adhesion molecule  
PFA Paraformaldehyde  
PI3K Phosphatidyl inositol-3-kinase  
PKC Protein kinase C  
PLC Phospholipase  
PIGF Placental growth factor  
PyMT Polyoma Middle T  
q-PCR Quantitative real-time polymerase chain reaction  
RNA Ribonucleic acid  
ROS Reactive oxygen species  
RTK Receptor Tyrosine Kinase  
S1P Sphingosine-1-phosphate  
SDS Sodium dodecyl sulphate  
SMA Smooth muscle actin  
SSC Side Scatter  
SAPK Stress Activated protein Kinase

Src tyrosin kinase Src (Sarcoma)  
TE Tris EDTA  
TEMED Tetramethylethylenediamine  
Tie Tyrosine kinase with immunoglobulin-like and EGF-like domains  
TJs tight junctions  
TKI Tyrosine Kinase Inhibitor  
TGF Transforming growth factor  
TAM Tumour Associated Macrophages  
TAN Tumour Associate Neutrophils  
TME Tumour Microenvironment  
TSAd T-cell specific adapter  
UV Ultraviolet  
VE-CAD VE-cadherin  
VEGF Vascular endothelial growth factor  
VEGFR Vascular endothelial growth factor receptor  
vSMC Vascular smooth muscle cell

# 1. INTRODUCTION

## 1.1 The vascular system

During the early stages of development the embryo receives its nutrition through diffusion (oxygen and nutrients diffuse across a short distance of 100-150  $\mu\text{m}$ ), but while growing bigger, it requires a specialized system to function as a major communication system between distant organs and tissues. Indeed, the vascular system, also known as the circulatory system, is the first organ that forms and becomes functional during embryonic development.

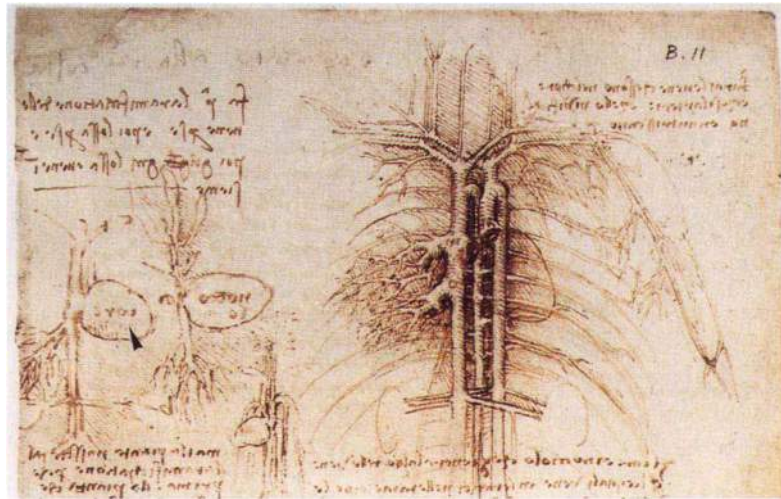


**Figure 1.1 The anatomy of man: the cardiovascular system**

Leonardo da Vinci's famous anatomy drawings explored the human body (1508). He firstly suggested the analogy between the vascular system and a tree speculating that blood vessels develop like a tree, starting from a seed (the heart) and expanding into trunk and branches (aorta and large vessels) as well as roots (small capillaries) (taken from Risau,1997).

In the adult, the vascular system is functionally divided in cardiovascular and lymphatic systems. Blood, heart and blood vessels form the cardiovascular system (Figure 1.1), whose function is to deliver oxygen and nutrients as well as clear carbon dioxide and metabolic products from tissues; whereas lymph, lymph nodes and lymphatic vessels form the lymphatic system, which serves to drain fluids from the extracellular spaces and move them back to the blood circulation (Purves *et al.*, 2004).

The cardiovascular system is a closed system composed of two functionally distinct but interconnected circulations: the systemic circulation in which the heart pumps

oxygenated blood through arteries and arterioles into capillaries whereby gases and metabolites are exchanged between the blood and surrounding tissues, then the deoxygenated blood is pumped back to the heart through venules and veins; and the lung circulation in which the deoxygenated blood is carried to the lungs to be reoxygenated and then back to the heart to be delivered systemically (Purves *et al.*, 2004).

## 1.2 Blood vessel morphology

The cardiovascular tree includes arteries, veins and capillaries. Cardiac contraction pumps high-pressure oxygenated blood flow through the arteries, which are characterized by the mechanical support of smooth muscle cells; while blood from the periphery returns under lower pressure to the heart through veins, which are characterized by specialized valve structures to maintain proper directional flow. Small caliber vessels (capillaries, arterioles and venules) enable the actual exchange of water and molecules between blood and the tissues.

Arterial-venous specification is genetically programmed, even before the first embryonic heart beat and results from the combination of hemodynamic and transcription factors, as well as, signaling molecules; all of which define the specification of blood vessel type during development (Swift and Weinstein, 2009). However, the maintenance of arterial-venous phenotype is susceptible to some degree of plasticity. In response to microenvironmental cues, vessels can undergo morphological and functional changes, which allows adaptation to the diverse needs of the various tissues/organs and also to account for inter-organ and intra-organ vessel heterogeneity.

Larger vessels consists of a three-layered structure: *tunica intima*, the inner layer, composed of an endothelial cell monolayer and basement membrane; *tunica media*, the middle layer, composed of vascular smooth muscle cells, collagen and elastic fibres, and *tunica adventitia*, the outer layer, composed of fibroblasts, collagen and elastic fibres (Figure 1.2). The *tunica adventitia* is also innervated and has its own blood supply, called *vasa vasorum*. These three layers are separated from each other by two thin sheets of elastic fibers: the *internal elastic lamina* between the *tunica intima* and *media* and the *external elastic lamina* between the *tunica media* and *adventitia*. These *elastic laminae*, together with the smooth muscle cells, regulate vessel tone and contraction acting on vessel diameter and blood flow. The wall of

smaller blood vessels is composed of vascular endothelial cells and mural cells (pericytes and vascular smooth muscle cells) surrounded by extracellular matrix.

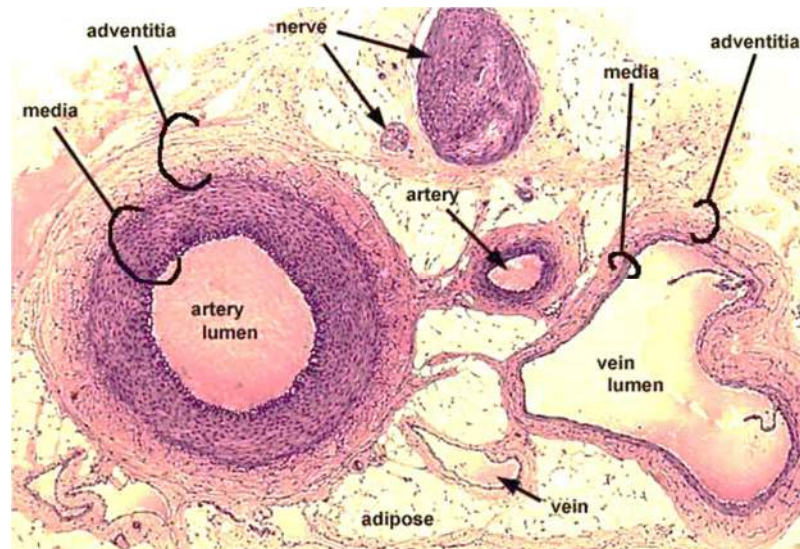


### Figure 1.2 Microscopic anatomy of vessel structure

Cross-sections of blood vessels displaying their characteristic 3-layered-structure of *tunica intima*, *tunica media* and *tunica adventitia*. While arteries have a thick elastic muscle layer which can handle the high pressure of the flowing blood, veins have a thin elastic muscle layer with semilunar valves which prevent the blood from flowing in the opposite direction. Nerves can be distinguished by the absence of lumen (taken from <http://wurstwisdom.com/>).

#### 1.2.1 Endothelial cells

Initially described as a “*layer of nucleated cellophane*” (Florey, 1966) endothelial cells (ECs) form a monolayer that lines the vessel lumen of the entire vascular system (Claever and Melton, 2003). In adults, approximately ten trillion cells form an almost 1 kg ‘organ’ which is far from being inert. As a barrier, the endothelium is semipermeable and regulates the transfer of small and large molecules through specific transport mechanisms and cellular junctional structures.

Endothelial cells also have metabolic and synthetic functions through the secretion of a large variety of mediators which control blood flow and vascular tone, hemostasis and coagulation, angiogenesis and tissue repair, inflammation and lipid catabolism. They act in autocrine, paracrine and endocrine manners affecting smooth muscle cells, platelets and immune cells. They display a remarkable phenotypic heterogeneity in different parts of the vascular system, such as to specifically meet the metabolic need of each organ and tissue.

### 1.2.2 Mural cells

Mural cells reside at the interface between the endothelium and the surrounding tissue (Gerhardt and Betsholtz, 2003). They are commonly subdivided in vascular smooth muscle cells (vSMCs) and pericytes. Vascular smooth muscle cells are associated with arteries and veins whereas pericytes are associated with the smallest diameter blood vessels (arterioles, capillaries, and venules), (Gaengel *et al.*, 2009). Pericytes were once known as “*Rouget cells*” after the first description by Rouget (Rouget, 1873) of perivascular cells adjacent to capillaries. Only in 1923, Zimmerman introduced the term “pericyte” to identify cells lying in close proximity of endothelial cells (Zimmerman, 1923).

Pericytes physically “sit” on top of endothelial cells in small caliber vessels (capillaries, arterioles and venules). They express a number of markers of differentiation such as  $\alpha$  Smooth Muscle Actin ( $\alpha$ SMA), desmin, chondroitin sulfate proteoglycan marker NG-2 and platelet-derived growth factor receptor  $\beta$  (PDGFR $\beta$ ). Nevertheless, there is no single molecular marker able to unequivocally identify pericytes. Moreover, the multiple markers which are commonly used are neither entirely specific, nor stable in their expression (Armulik *et al.*, 2011). Pericytes provide structural support and stability to the vascular endothelium: pericytes and endothelial cells act as a functional and physical unit through the establishment of cell-cell heterotypic contacts, synthesis and secretion of growth factors and common basement membrane that promote their mutual survival.

### 1.2.3 Endothelial basement membrane

Endothelial cells and pericytes are embedded in a specialized extracellular matrix (ECM), known as endothelial basement membrane (EBM). The endothelial basement membrane was first described in muscle by Bowman in 1840 and later observed in nearly all tissues (Davies and Sanger, 2005). It is a layered cell-adherent extracellular matrix that forms part of tissue architecture. In close proximity to the plasma membrane, it protects tissues from physical stresses and provides an interactive interface between the cellular and extracellular compartments. The endothelial basement membrane is rich in collagen type IV, laminin, entactin/nidogen, fibronectin and perlecan; but its composition and integrity are modified according to blood vessel type, tissue, developmental and/or physiological stage (Yurchenko, 2011).

The EBM primarily provides a scaffold for maintaining the organization of vascular endothelial cells into blood vessels; but it also exerts essential functions in supporting signalling events such as proliferation, migration, survival; all of which are critical for endothelial cells functions, in association with integrins and growth factors.

### **1.3 Blood vessel development and physiology**

During development, two processes of blood vessel formation can be distinguished, namely vasculogenesis and angiogenesis. By definition, vasculogenesis is the *de novo* formation of blood vessels and it primarily takes place during embryonic development; whereas angiogenesis is defined as the formation of new vessel from pre-existing ones.

#### **1.3.1 Vasculogenesis**

Early in development within the mesoderm, hemangioblasts which are mesoderm-derived precursor cells, connect with each other forming blood islands, whereby cells at the periphery flatten and differentiate into angioblasts (endothelial cell precursors), while the cells located in the central islands differentiate into haematopoietic stem cells (HSCs) (Risau and Flamme, 1995).

Angioblasts further differentiate into endothelial cells, which eventually fuse with each other, consequently forming lumenized vessels (Downs, 2003). The first vessels arise in the yolk sac and, then, the dorsal aorta and cardinal veins form in the embryo itself. After vasculogenesis has occurred, the primary vascular tree is subsequently remodelled through the process of angiogenesis. This leads to the formation of a mature vascular system in which vessels are morphologically and functionally distinguished into arteries and veins (Risau and Flamme, 1995).

#### **1.3.2 Angiogenesis**

The formation of new vessels can take place either by sprouting or non-sprouting angiogenesis, depending on whether endothelial cells proliferate (the former) or not (the latter). In sprouting angiogenesis, the extracellular matrix is proteolytically degraded by specific proteases, endothelial cells start to migrate and proliferate, forming a monolayer characterized by a tube like structure. Thereafter, the basal

lamina is remodelled and mural cells are recruited to stabilize the vascular wall and the blood flow is re-established (Carmeliet, 2000).

In contrast, non-sprouting angiogenesis (or intussusception) is a process by which single vessels split in two by extending the vessel wall into the lumen. This separation depends on the reorganisation of existing cells, without involving endothelial cell proliferation (Carmeliet, 2000). Irrespective of the way they are formed, new vessels undergo further remodelling processes, referred to as vessel maturation, which include stabilization of vessel structure by cell-cell, cell-ECM interactions and mural cell recruitment. Ultimately, excess endothelial cells or vascular segments are eliminated by vascular regression or pruning in order to construct and preserve a functionally efficient network (Risau, 1997).

### **1.3.3 Mechanism of sprouting angiogenesis**

For new blood vessel sprouts to form, pre-existing vessels dilate and become leaky in response to vascular endothelial growth factor (VEGF) which is up-regulated in hypoxic tissues (Giordano and Johnson, 2001). Endothelial cells lose inter-endothelial cell contacts and detach from surrounding vSMCs (Dvorak *et al.*, 1999).

This effect is further sustained by Angiopoietin2 (Ang2) binding to the endothelial cell tyrosine kinase receptor Tie2 (Tyrosine kinase with immunoglobulin-like and EGF-like domains-2), which has been implicated in the detachment of ECs from vSMCs, thereby destabilizing the endothelium (Scharpfenecker *et al.*, 2005). Secretion of proteinases of the matrix metalloproteinases (MMPs) or heparanase families by endothelial cells leads to ECM degradation (creating room for the endothelial cell to migrate) and the release of growth factors sequestered within it such as VEGF and basic fibroblast growth factor (bFGF) (Jakobsson *et al.*, 2006). These growth factors induce endothelial cell migration, proliferation and differentiation.

Sprouting angiogenesis involves the specification of endothelial cell populations: tip cells which migrate towards a VEGF gradient by extending filipodia at the leading edge of the new-forming vessel, followed by stalk cells which actively proliferate to elongate the sprout (Gerhardt *et al.*, 2003). The process of tip/stalk differentiation is under the control of VEGF and Notch signalling. VEGF promotes tip cell induction and induces the expression of the Notch ligand Delta-like 4 (DLL4), which activates Notch signalling in neighbouring cells via Notch Intracellular domain (NICD), thereby

suppressing VEGF receptor 2 (VEGFR2) expression and tip cell behaviour (Williams *et al.*, 2006).

Notch activity is required for stalk cell specification: they proliferate, form tubes and branches to elongate the vessel sprout. Tip and stalk cell are transient phenotypes, not fixed cell fates, and competition for tip cell position ensure the maximal efficiency of vascular sprouting (Geudens and Gerhardt, 2011). Importantly, adhesion molecules, such as integrins, are essential to promote endothelial cell proliferation and migration, followed by their assembly into cords and lumen formation (Eliceiri and Cheresh, 2001).

#### **1.3.4 Vessel maturation**

In order to become functional, newly formed blood vessels have to mature. This involves the recruitment of vascular smooth muscle cells and the deposition of new basement membrane. The recruitment of pericytes is mediated by Platelet-derived growth factor type-b (*Pdgfb*) and its receptor PDGFRB (von Tell *et al.*, 2006).

*Pdgfb* is expressed by endothelial cells and acts on pericytes which express its receptor. vSMCs express a number of molecules which have a paracrine effect on the endothelium such as Angiopoietins which includes Angiopoietin1 (Ang1) and Angiopoietin2 (Ang2). Ang1 is expressed by vSMCs, whereas Ang2 is primarily expressed by ECs. Binding of Ang1 to its Tie2 receptor on endothelial cells results in the activation of Akt (Protein kinase B, PKB), which in turn promotes endothelial cell quiescence and survival; whereas EC-Ang2 antagonizes Ang1 activity, thus destabilizing vessels and sensitizing them to pro-angiogenic signals. (Fiedler and Augustin, 2006).

vSMCs make focal contacts with endothelial cells and stabilize the vessel wall by inhibiting proliferation and migration of endothelial cells (Bergers and Song, 2005). Pericytes also express sphingosine-1-phosphate (S1P) which binds to S1P receptor on endothelial cells and regulates EC barrier properties by stabilizing VE-cadherin (VEC) junctions and increasing N-cadherin (N-CAD) expression (von Tell *et al.*, 2006). Additionally, the onset of blood flow remodels endothelial cell shape and patency and stabilizes vessel connections (vascular remodelling), while hypoperfused vessels regress and endothelial cells undergo apoptosis (vascular regression) (Potente *et al.*, 2011).

### **1.3.5 Vessel quiescence and permeability**

Quiescent endothelial cells named phalanx cells, as resembling the ancient Greek military formation (Mazzone *et al.*, 2009), adhere tightly by cell-cell junctions and form barriers which control the exchange of molecules and fluids between blood and tissues as well as extravasation of immune cells (Potente *et al.*, 2011). In the quiescent state, endothelial cell proliferation diminishes and it is contact-inhibited: only one in every 10,000 endothelial cells divides (Lampugnani *et al.*, 1997). Moreover, endothelial cells become less sensitive to growth factor stimulation, protected from apoptosis and in full control of permeability (Lampugnani *et al.*, 2003). Barrier function and endothelial cell permeability rely on junctional complexes including tight junctions (TJs) and adherens junctions (AJs), both of which contain proteins that mediate homophilic adhesion at the cell surface (Figure 1.3). TJs regulate paracellular permeability, whereas AJs are involved in cell-cell adhesion, cytoskeletal dynamics and intracellular signalling (Lampugnani and Dejana, 2007).

The main component of AJ is Vascular endothelial-cadherin (VEC) which is part of a protein complex comprising p120-catenin,  $\alpha$ - and  $\beta$ -catenin at site of cell-cell contacts (Dejana, 2004). Binding of VEGF to its receptor VEGFR2 leads to an activation of the kinase c-Src (cellular Src kinase), which in turn phosphorylates VEC. Phosphorylation of VEC results in the disruption of the complex thereby enhancing vascular permeability and leukocyte transmigration (Wallez *et al.*, 2007).

Conversely, VE-cadherin regulates VEGFR2 signalling through phosphatase Dep1 (CD148) which associates with VE-cadherin and attenuates tyrosine phosphorylation of VEGFR2 thereby suppressing receptor activity (Lampugnani *et al.*, 2003). VEC also controls endothelial cell survival: it is required for the VEGF-dependent survival signals through formation of a VEC/ $\beta$ -catenin/PI3K/VEGFR2 complex which leads to Akt survival signalling pathway and increased levels of the anti-apoptotic mediator Bcl2 (Carmeliet *et al.*, 1999).

## **1.4 Molecular mechanisms of angiogenesis**

### **1.4.1 VEGF/VEGFR**

Initially, Vascular Endothelial Growth Factors were identified as vascular permeability factor (VPF) (Senger *et al.*, 1983) because of their effect on permeability by promoting

intercellular adhesion molecule rearrangements, such as platelet endothelial cell adhesion molecule (PECAM-1) and VE-cadherin (Bates and Harper, 2002) and on vessel dilatation, by stimulating endothelial nitric oxide synthase (eNOS) (Kroll and Waltenberger, 1999). Currently, VEGFs are acknowledged primarily for their role as master regulators of angiogenesis (Ferrara *et al.*, 2003). They are dimeric cystein-linked secreted glycoproteins produced in response to hypoxia and upon stimulation with other growth factors. In mammals, the VEGF family includes VEGF-A, VEGF-B, VEGF-C, VEGF-D and PlGF (Placental Growth Factor). Furthermore, highly related proteins called VEGF-E and VEGF-F are found in *orf* virus and snake venom, respectively (Figure 1.3).

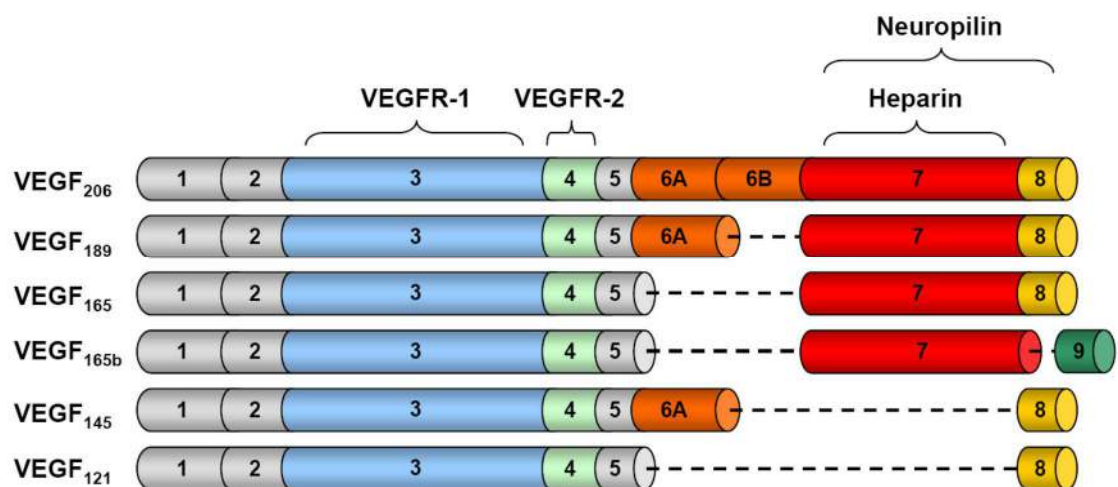


**Figure 1.3 Schematic diagram of VEGFA isoforms**

There are six isoforms of VEGF-A. Exons are indicated by numbers. Exon 3 (blue) is primarily involved in VEGF homodimerization and interactions with VEGFR-1. Interactions with VEGFR-2 are mainly mediated by exon 4 (green). Binding to heparin is mediated by exon 7 (red) and to neuropilins by exons 8 and 9 (red and yellow). Exon 9 (dark green) is expressed in the inhibitory VEGF165b variant.

The biological functions of VEGFs are mediated upon binding to type III receptor tyrosine kinase (RTK) Vascular Endothelial Growth Factor Receptors, namely VEGFR-1, VEGFR-2 and VEGFR-3 (Cebe-Suarez *et al.*, 2006). The receptors consist of seven extracellular immunoglobulin-like domains, a transmembrane domain, a regulatory juxtamembrane domain, an intracellular tyrosine kinase domain interrupted by a short peptide and the kinase insert domain, followed by a sequence carrying several tyrosine residues involved in recruiting downstream signalling molecules (Figure 1.4).

Each VEGF isoform binds specifically to a particular subset of VEGFRs with some degree of promiscuity though (Figure 1.5). Ligand-binding induces receptor

dimerisation, activation of the kinase domain and finally specific activation of distinct downstream pathways (Cebe-Suarez *et al.*, 2006). VEGFR signalling is further modulated upon recruitment of co-receptors (such as neuropilins and integrins) that additionally regulate signal strength, and timing and specificity of responses, thereby accounting for the complexity of VEGF-induced signals (Staton *et al.*, 2007). For instance, neuropilin1 (NRP1) has been shown to increase the binding affinity of VEGFA for VEGFR2 (Soker *et al.*, 1998). The best characterized variant of VEGFs is VEGFA (commonly referred to as VEGF) which signals through both VEGFR1 and VEGFR2, the latter being the most important receptor in angiogenic signalling.

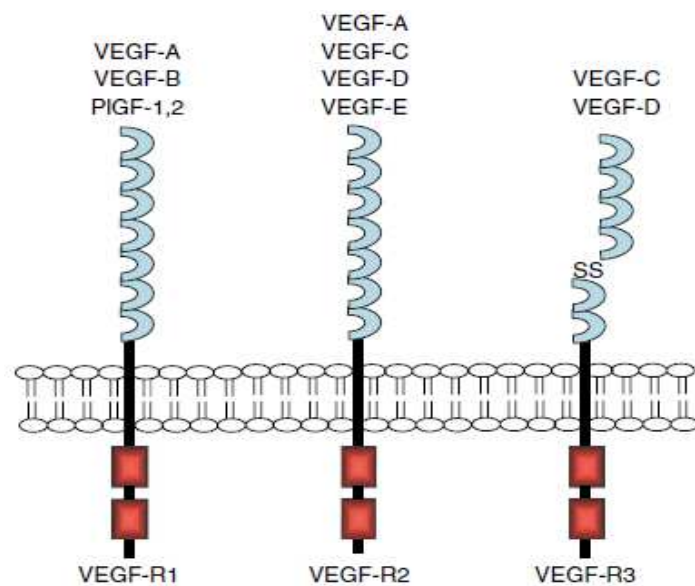


**Figure 1.4 Overview of VEGF/VEGFR binding**

Vascular Endothelial Growth Factor (VEGF) -A, -B and Placenta growth factor (PLGF) bind to VEGFR1, VEGFA to VEGFR2 and VEGFC and -D to VEGFR3. Proteolytic processing of VEGFC and -D enables them to bind VEGFR2 (taken from Staton *et al.*, 2007).

VEGFA is produced by several cell types including macrophages, keratinocytes, pancreatic cells, hepatocytes, vSMCs, embryonic fibroblasts and tumour cells (Ferrara *et al.*, 2003). Its expression is regulated by a plethora of stimuli such as other growth factors, inflammatory cytokines, hormones and hypoxia. Indeed, low concentration of oxygen activates the hypoxia inducible transcription factor-1 (HIF1) which in turn up-regulates VEGFA expression (Takahashi and Shibuya, 2005). VEGFA gene consists of nine exons separated by seven introns and alternative splicing gives rise to a number of functionally distinct isoforms (at least six isoforms in humans VEGFA 121, 145, 165, 183, 189 and 206) which differ in their ability to

bind heparin/heparan sulphate in the extracellular space and to neuropilin receptors and therefore have different signalling properties (Roy *et al.*, 2006).

VEGFR2 (Flk-1, in mouse) is produced as a 150-kDa protein, which is processed within the cell to a 200-kDa form and further glycosylated and expressed at the cell surface as a 230-kDa protein. During early embryogenesis, VEGFR2 is highly expressed in haematopoietic and endothelial cell precursors, haemangioblasts. At later developmental stages, the blood vascular expression of VEGFR2 decreases and, in adults, is upregulated under pathological conditions such as tumour angiogenesis (Shibuya and Claesson-Welsh, 2006). Non-endothelial cells, including neuronal cells, retinal cells, osteoclasts and megakaryocytes, can also express VEGFR2 (Otrock *et al.*, 2007).

The central role of VEGF/VEGFR axis in regulating angiogenesis is confirmed by a number of genetic studies. Both VEGFA and VEGFR2 knockout mice are embryonic lethal. Homozygous VEGFA knockouts die earlier, at E9, due to severe defects in the formation of blood islands, development of endothelial cells and reduced angiogenic sprouting (Carmeliet *et al.*, 1996). Whereas the deletion of a single allele of VEGFA in mice results in early vascular defects and embryonic lethality at E11-E12 (Carmeliet *et al.*, 1996; Ferrara *et al.*, 1996). Deletion of VEGFR2 in mice leads to embryonic lethality between E8.5 and E9.5 due to a lack of blood island formation in the yolk sac, an absence of vasculogenesis and severe defects in the development of endothelial and haematopoietic cells (Shalaby *et al.*, 1995).

#### **1.4.2 Regulation of VEGFR2 activity**

VEGFR2 is the main receptor in angiogenesis by transducing proliferation, migration and survival signals to endothelial cells (Figure 1.5). Like other RTKs, VEGFR2 activates upon VEGF-mediated receptor dimerization, whereas its activity is downregulated by receptor dephosphorylation via phosphatases such as SHP-1 and SHP-2 (Dougher *et al.*, 1999). Activated VEGFR2 is subsequently internalized into endocytic vesicles whereby it can be trafficked to the cell membrane through recycling (through early, late, and recycling endosomes) or degraded in lysosomes or proteasomes (Duval *et al.*, 2003). However, contrary to other RTKs, unstimulated VEGFR2 is only partially localised at the plasma membrane with a pool of receptor (40%) constantly internalized and recycled back to the surface (Berger and Ballmer-Hofer, 2011).

Ligand-induced dimerization leads to structural changes to the intracellular kinase domain following conformational rearrangement of the transmembrane and juxtamembrane domains. Both the juxtamembrane and intracellular domains have tyrosine phosphorylation sites which have an either regulatory or signalling function. Among the 19 tyrosine residues present in the intracellular domain of VEGFR-2, 5 of them (Y951, 1054, 1059, 1175 and 1214) have been identified as the most prominent phosphorylation sites (Shibuya and Claesson-Welsh, 2006).

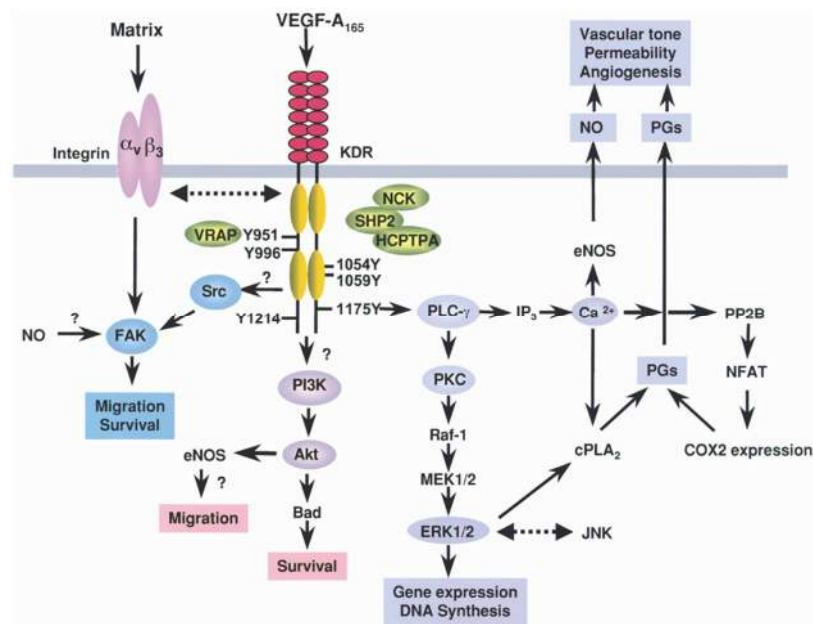


**Figure 1.5 Schematic overview of VEGF signalling pathways**

VEGF signalling is mediated via tyrosine kinase receptor whose activation occurs through ligand-induced dimerization and receptor autophosphorylation at multiple tyrosine residues in the intracellular domain (taken from Zachary, 2003).

#### 1.4.2.1 VEGFR2 promotes EC proliferation

Y1175 is clearly one of the most important VEGFR2 phosphorylation sites: it is implicated in the activation of many signalling pathways through phospholipase C $\gamma$  (PLC $\gamma$ ) (Takahashi *et al.*, 2001). In detail, PLC $\gamma$  promotes phosphatidylinositol 4,5-bisphosphate (PIP<sub>2</sub>) hydrolysis resulting in to 1,2-diacylglycerol (DAG) and inositol 1,4,5-trisphosphate (IP<sub>3</sub>). DAG activates Protein kinase C (PKC), whereas IP<sub>3</sub> acts on endoplasmic reticulum, resulting in the release of intracellular stored Ca<sup>2+</sup> in the cell cytoplasm. PKC leads to Ras-independent Raf activation which in turn, induces ERK 1/2 (Extracellular-signal Regulated protein Kinase 1/2) activity.

Activated ERK1/2 activates c-Jun by phosphorylation, which then translocates to the nucleus whereby it forms a transcriptional complex with c-Fos leading to DNA synthesis and cell proliferation (Zachary and Gliki, 2001). Y1175 importance has been further confirmed in knockin mice expressing a Y1175 mutant which dies *in utero* due to vascular defects, similar to those observed in VEGFR2 null mice (Sakurai *et al.*, 2005).

Y1054 and 1059 are homologous to regulatory residues conserved in all protein kinases and are autophosphorylation sites important for receptor activation (Cebe-Suarez *et al.*, 2006).

Y951 has been shown to mediate the binding to T-cell specific adapter (TSAD) which, then leads to c-Src activation thereby regulating actin stress fiber organization and migratory responses of endothelial cells (Matsumoto *et al.*, 2005). c-Src proto-oncogene is a non-receptor protein tyrosine kinase protein, it has an SH2 domain, an SH3 domain, and a tyrosine kinase domain and it is implicated in a wide variety of pathways, including cell proliferation.

VEGFR2 can promote proliferation upon the activation of the Ras-dependent signaling pathway impinging on MAP kinases such as ERK1/2 (Meadows *et al.*, 2001) or alternatively through PI3K/S6kinase/Akt signalling pathway, although conflicting data suggest that PI 3-kinase is not required. Moreover, c-Src and NO have also been identified as intracellular mediators of VEGFR2 mitogenic signaling (Cebe-Suarez *et al.*, 2006).

#### **1.4.2.2 VEGFR2 regulates EC migration**

With respect to migration, VEGFR2 signalling is mainly mediated by focal adhesion kinase (FAK), which regulates focal adhesion assembly and disassembly and the organization of the actin cytoskeleton (Abedi *et al.*, 1997). Focal adhesions are dynamic macromolecular structures required for cell adhesion and migration: they assemble, mature, and disassemble upon different cues transmitting both cellular signalling and mechanical signalling. (Petit and Thiery, 2000). The turnover of focal adhesions is essential for cell motility and the formation of the actin stress fibres occurs at the leading edge of the cell, whereby lamellipodia (flat extensions of plasma membrane) generate mechanical forces that alter local cytoskeletal dynamics.

Integrin transduce extracellular cues to the cytoskeleton via the activation of the tyrosine kinases Src and FAK.

FAK is a non-receptor tyrosine kinase which interacts with integrin via its FERM domain and gets activated upon integrin binding to autophosphorylate Y397, this induces subsequent binding of Src by the SH2 domain, leading to stable and increased activation of Src–FAK complex (Schaller et al., 1994). FAK also binds to with adaptor protein such paxillin and talin via its focal adhesion targeting (FAT) domain. VEGF/VEGFR2 via integrin cooperation induces FAK phosphorylation by recruiting this kinase to focal adhesions thereby promoting cell migration (Abedi et al., 1997).

VEGF-induced endothelial cell migration is also mediated by stress activated protein kinase 2, SAPK/p38 which induces phosphorylation of heat shock protein HSP27 (Rosseau et al, 2000). This then leads to actin reorganization and formation of stress fibers and lamellipodia thus promoting cell migration. Furthermore VEGFR2 can regulate the small GTPases Rho and Rac, which in turn modulate actin dynamics and cell contraction leading to endothelial cell migration (Zeng *et al.*, 2002).

#### **1.4.2.3 VEGFR2 controls EC survival and vessel permeability**

VEGFR2 is also essential for cell survival: it protects endothelial cells against apoptosis via the activation of the PI3-kinase/Akt pathway and by promoting the expression of anti-apoptotic molecules including the caspase inhibitor Bcl-2 (Gerber *et al.*, 1998). Moreover, VEGFR-2 provides survival signals through the formation of the tetrameric complex of VEGFR-2, PI3-kinase, VE-cadherin and  $\beta$ -catenin whose disruption inhibits the PI3-kinase/Akt pathway and induces endothelial cell apoptosis (Carmeliet *et al.*, 1999).

VEGF also regulates vascular permeability by loosening the junctions between endothelial cells, giving rise to the formation of transcellular gaps; indeed phosphorylation of major components of junctional complexes such as VE-cadherin,  $\beta$ -catenin, occludin has been described in response to VEGF (Dejana *et al.*, 1999; Esser *et al.*, 1998). Moreover, vessel dilation is controlled by NO which in turn is upregulated by Akt upon induction of endothelial NO synthase (eNOS) expression (Fulton *et al.*, 1999).

## 1.5 Pathological angiogenesis

Physiological angiogenesis is required to ensure adequate function and dynamic plasticity of the vascular system for tissue growth and homeostasis. As such, its dysregulation causes pathological conditions due either to insufficient angiogenesis (heart and brain ischemia, hypertension, osteoporosis and pre-eclampsia) or excessive and uncontrolled angiogenesis (cancer, eye diseases, arthritis, psoriasis, atherosclerosis) (Carmeliet and Jain, 2000).

### 1.5.1 Tumour angiogenesis

With respect to cancer, it is well established that the acquisition of an angiogenic phenotype (the so-called “angiogenic switch”) by cancer cells is required very early in the transformation process and it is considered a marker of malignant transformation as proposed in the fundamental review “The hallmarks of cancer: the next generation” by Hannah and Weinberg (2010). In 1939, Ide *et al.* first observed that tumour growth was accompanied by infiltration of newly formed blood vessels in a rabbit tumour model (Ide *et al.*, 1939). Less than 10 years later, in 1945, Algire and Chalkeley reported that transplanted tumour cells could induce vessel formation before tumour growth occurred and suggested that tumour explants require the development of a new vascular supply to grow (Algire *et al.*, 1945). Their work represented the first demonstration that tumours actively attract new blood vessels, the process that, 30 years later, would become known as “tumour angiogenesis”.

Tumours cannot grow bigger than a few millimeters in size until they acquire the ability to recruit their own blood supply. Avascular tumour masses, named dormant tumours were firstly identified in human autopsies, they can persist *in situ* or progress to an active vascular state which allows exponential cell growth and expansion, eventually leading to invasion and metastasis (Black and Welsh, 1993). Initially, tumour cells grow around existing vessels, hence, they do not need to induce angiogenesis; but when they do, they have been shown to exploit different strategies, aside from sprouting angiogenesis, to ensure their own blood supply. Tumour cells can release soluble factors, including VEGF, to recruit bone marrow derived cells (BMDCs, broadly defined as CD45+) at the site of primary tumours and metastatic lesions, which in turn produce angiogenic factors and sustain tumour angiogenesis (Wilson and Trumpp, 2006; Grunewald *et al.*, 2006).

Less defined and still debated, it is the role of endothelial precursor cells (EPCs, defined as CD34+/VEGFR2+) which have been firstly described as able to differentiate in Von Willebrand Factor (vWF)+ cells and form new vessels through vasculogenesis (Asahara *et al.*, 1997; Lyden *et al.*, 2001). Even though the number of EPCs in tumour vasculature is very low (<10%) and the lack of definitive and specific EPC markers has contributed to a wide variability of results (De Palma *et al.*, 2003), there is evidence supporting a correlation between the number of blood circulating EPCs and tumour recurrence and metastasis, thus suggesting their involvement in tumor progression (Naik *et al.*, 2008; Igreja *et al.*, 2007).

Tumours can induce the remodelling of pre-existing vessels in order to split and as a consequence increase them by intussusception. Intussusceptive angiogenesis has been observed both in mouse and human tumour models and reported to be happening on a time scale of minutes due to low energy requirements (Patan *et al.*, 2001). In highly vascularized stromal tissues, such as lung and brain, tumour cells can collectively migrate along the vessels and invade the surrounding tissue in a perivascular fashion through a mechanism known as vessel co-option (Holash *et al.*, 1999). Interestingly, tumour cells can re-program their gene expression to display an endothelial cell-like phenotype, therefore acquiring the capability of line vessel themselves (Maniotis *et al.*, 1999). This process defined as vascular mimicry seems to be independent of the canonical angiogenic factors such as VEGF and bFGF, while VE-cadherin and EphrinA2 have been shown to play a significant role: however the molecular mechanisms have not been thoroughly identified yet (Hendrix *et al.*, 2001).

Regardless of the mode, tumour vessels are abnormal in their structure and function (Jain, 2005). They are tortuous and dilated, they branch irregularly and they are leaky. Moreover, pericyte and basement membrane coverage are reduced and discontinuous. This structural disorganization creates a constitutive hypoxic environment which leads to a further enhanced production of pro-angiogenic factors by tumour cells thereby establishing a vicious cycle (Jain, 2005). From a clinical point of view, dysfunctional tumour vasculature causes reduced drug delivery and high fluid pressure due to vessel leakiness (Bergers and Hanahan, 2008). Taken together, these conditions significantly impair the efficacy of chemotherapy and radiotherapy which rely on the formation of oxygen radicals to exert their cytotoxic functions.

### 1.5.2 Metastatic disease: vessels required

Metastasis is the primary cause of tumour related death, lung and bone being the most common site for metastasis in breast and prostate cancers. Most metastatic lesions are not treated by surgery, as the presence of a single metastatic lesion frequently indicates wider systemic metastatic dissemination (Christofori, 2011; Yachida *et al.*, 2010). Metastatic dissemination is a multi-step process whereby vessels are used as a route by invasive cells to spread from the primary tumour by extravasating and entering the circulation (either blood or lymphatic), to then intravasate and colonize distant tissues and organs.

According to the Paget theory of “*seed and soil*” (Paget, 1989), tumour cells can only survive and grow if they encounter the right host environment, their appropriate “*soil*” and the vasculature plays a central role in contributing to the “*seeding*” of tumour cells during the process of metastasis. Indeed metastatic primary tumours can set pre-metastatic niche by providing the required growth factors, chemoattractants, adhesive molecules and proteinases to create a conducive microenvironment for tumour cells to engraft at distant sites and expand as metastatic outgrowths (Hiratsuka *et al.*, 2006; Kaplan *et al.*, 2005).

Tumours can directly pre-condition the vasculature releasing angiogenic factors which can facilitate extravasation of tumour cells as well as their intravasation at distant sites. As an example, high VEGF tumour levels promote the loosening of endothelial tight junctions, thus allowing extravasation of tumour cells into the circulation (Hanahan and Coussens, 2012). Enhanced FAK activity by tumour cells has been shown to reduce blood vessel barrier integrity through a VEGF/cSrc/VEC dependent mechanism, thereby increasing the passage of tumour cells through the endothelium (Jean *et al.*, 2014). In addition, the hypoxic *milieu* surrounding tumour vessels induces hypoxia inducible related genes including inducible nitric oxide synthase (iNOS) whose altered function impairs pericyte recruitment and, as a consequence, destabilizes the endothelium (Kashiwagi *et al.*, 2005). Significantly, endothelial HIF expression controls metastatic success: depending on which HIF isoform is expressed, it can act to both promote and inhibit metastasis through the regulation of NO homeostasis (Branco-Price *et al.*, 2012).

Tumours can also indirectly dictate changes which render the secondary microenvironment receptive to tumour cell colonization. As examples, tumours can

induce the mobilization of VEGFR1+ hematopoietic precursor cells from the bone marrow to home at pre-metastatic sites. Further, tumour secreted inflammatory chemoattractants (such as S100A8 and S100A9) can recruit myeloid cells at pre-metastatic sites (Hiratsuka *et al.*, 2006). BMDCs are the main source of MMP9 which in turn releases matrix-bound VEGF thereby prompting angiogenesis within metastatic tissues (Hiratsuka *et al.*, 2002).

### **1.5.3 The role of immune cells in tumour angiogenesis**

Over the last decades, a growing body of literature has highlighted the importance of the microenvironment for tumour growth and metastatic spread. The concept of tumour microenvironment has been broadened to include the influx of cells from the periphery in addition to the canonical cellular architecture of the tissue. Infiltration of immune cells in tumours was firstly observed by Virchow as early as the mid-nineteenth century (Balkwill and Mantovani, 2001). For a long time, it was believed that immune cells could recognize tumour cells as being foreign and efficiently eradicate them. This view was not only challenged by the evidence that tumour cells can escape host immune surveillance (Kim *et al.*, 2007), but also reversed by the findings that they can play a dual role in tumour progression: either induce anti-tumour immune responses or sustain tumour growth and metastasis (Mantovani *et al.*, 2008).

Tumour immune infiltrate consists of many cell subsets, including macrophages and neutrophils. Macrophages are key orchestrators of chronic inflammation and are functionally distinguished as M1 and M2 populations, M1 being potent effector cells that kill pathogens and tumours, while M2 tune inflammation and adaptive immunity (Galdiero *et al.*, 2013). Tumour-Associated Macrophages (TAMs) are recruited into the tumour-associated stroma and polarized toward a pro-tumoural M2 phenotype, thereby contributing to the establishment and maintenance of a chronic inflammation state which favours tumour growth and progression (Figure 1.6) (Sica and Mantovani, 2012). TAMs can sustain tumour growth through the production of growth factors, and they can promote tissue invasion and angiogenesis through the release of proteases and angiogenic molecules respectively. They can also inhibit antitumoural responses through the production of immunosuppressive cytokines (Sica and Mantovani, 2012). Macrophages are also associated with increased metastatic potential as demonstrated by studies in which their transfer or depletion significantly affects the frequency of metastatic nodules (enhanced or reduced respectively) (De

Nardo *et al.*, 2009; Joyce and Pollack, 2009). Studies have suggested that macrophages are recruited to the sites of tumour cell colonization while in their absence, tumour cell extravasation and survival is reduced thereby diminishing metastatic cell seeding efficiency. Furthermore, poor recruitment of macrophages within neoplastic lesions limits metastatic growth, even if metastatic lesions have already been established (Talmadge, 2013).

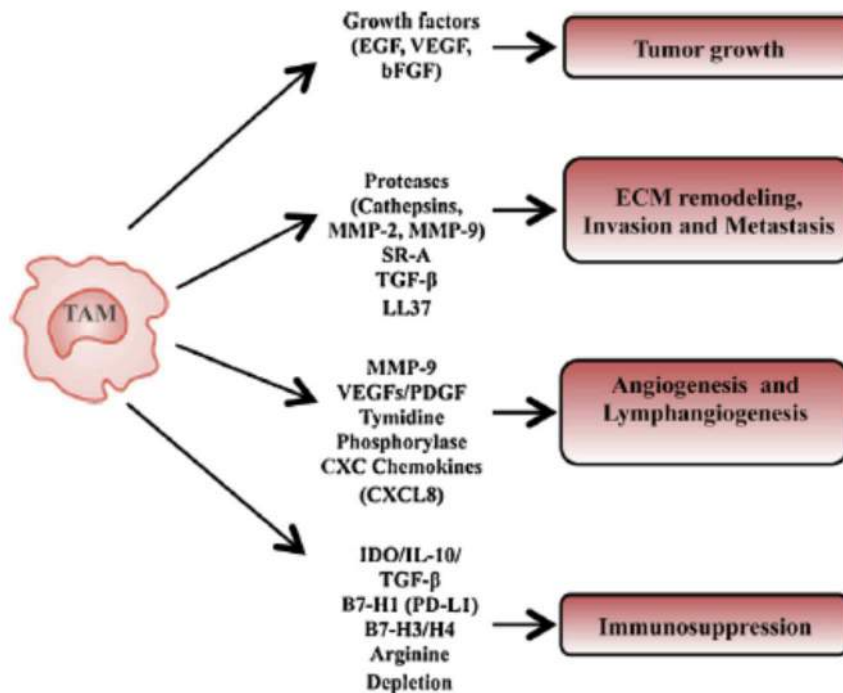


**Figure 1.6 The role of Tumour-Associated Macrophages (TAM) in cancer**

M2 polarized TAMs are recruited into the tumour microenvironment where they release a plethora of growth factors, proteolytic enzymes and cytokine which contribute to sustain tumour growth and invasion as well as block antitumoural immune responses (taken from Galdiero *et al.*, 2013).

Neutrophils are the most abundant leukocyte subset in the peripheral blood and they set the first line of defence against microbial organisms. Due to their very short life-span their role in tumour growth has been long disregarded; while only recently acknowledged as tumour infiltrating cells, playing an important role in tumour growth and progression (Mantovani *et al.*, 2011). Similarly to macrophages, they have both pro-tumoural and anti-tumoural functions, mirroring the same dualistic profile of N1 and N2. Tumour-Associated Neutrophils (TANs) can favour genetic instability of tumour cells through the release of Reactive Oxygen Species (ROS) and the activation of proteolytic enzymes through the release by nitric oxide derivatives (Sandhu *et al.*, 2000). The liberation of Neutrophil Elastase (NE) from their azurophil

granules has been shown to promote tumour cell proliferation and epithelial-to-mesenchymal-transition (EMT) in epithelial lung cancer cells (Houghton et al, 2010). Neutrophil infiltration can also enhance the metastatic potential via expression of pro-migratory and pro-invasive factors and can enhance angiogenesis by inducing the release of VEGF from the ECM, (Galdiero *et al.*, 2013). Furthermore, neutrophils can suppress anti-tumoural T CD8<sup>+</sup> responses by Transforming Growth Factor-  $\beta$  (TFG- $\beta$ ) production (Fridlender *et al.*, 2009).

In addition to TAMs and TANs, tumour growth has been found to be further sustained by the presence of a population of immunosuppressive cells referred to as myeloid derived suppressive cells (MDSCs) (Sica and Bronte, 2007). Morphologically, these populations consist of monocytes, granulocytes, and immature myeloid cells and are functionally identified by their capacity to suppress cytotoxic T-cell responses. MDSCs in mice are divided in monocytic MDSCs (CD11b<sup>+</sup>/Ly6C<sup>+</sup>) and granulocytic MDSCs (CD11b<sup>+</sup>/Ly6G<sup>+</sup>) (Galdiero *et al.*, 2013). Several mechanisms have been proposed for their immunosuppressive effects such as up-regulation of ROS and NO production, as well as the secretion of immunosuppressive cytokines, all of which contribute to suppress T cell proliferation and activation

## **1.6 Integrins**

### **1.6.1 Integrin structure**

Integrins are a family of cell adhesion receptors as well as signalling molecules which transduce signals bidirectionally across the plasma membrane and regulate essential functions such as cell proliferation, survival and migration (Avramides *et al.*, 2008). They are expressed by almost all cell types, including tumour cells. Together with immunoglobulin superfamily, cadherins and selectins, they constitute the four families of cell adhesion molecules that have been detected in angiogenic blood vessels (Eisenstein and Kramer, 1994).

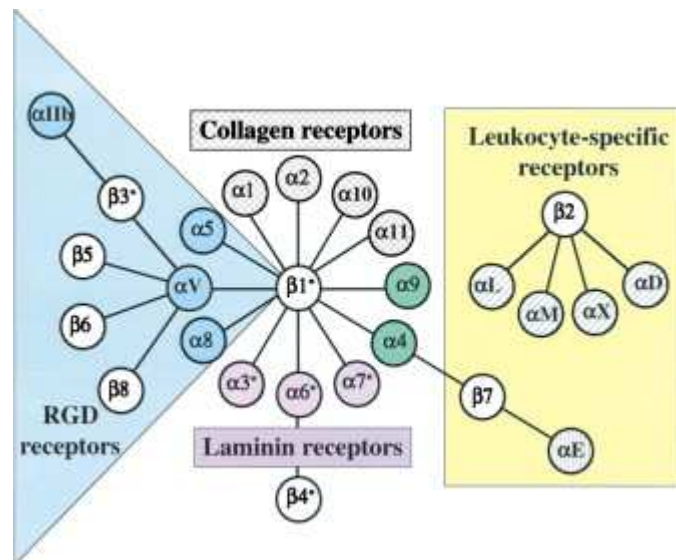


**Figure 1.7 Integrin receptor family**

The diagrams shows the mammalian subunits and their  $\alpha$ - $\beta$  associations: 8  $\beta$  subunits heterodimerize with 18  $\alpha$  subunits to form 24 distinct integrins. These are classified in subfamilies based on evolutionary relationships (displayed in different colours) and ligand specificity (taken from Hynes, 2002).

They are heterodimeric transmembrane glycoprotein composed of non-covalently bound  $\alpha$  and  $\beta$  subunits. There are 18 types of  $\alpha$  subunit and 8 different types of  $\beta$  subunit that have been identified in mammals and which can assemble into at least 24 distinct integrins (Hynes, 2002; Hodivala-Dilke *et al.*, 2003).

Each subunit consists of an extracellular domain, a single transmembrane region and a short cytoplasmic tail. The extracellular domains of both subunits form the ligand-binding site and the combination of  $\alpha$  and  $\beta$  subunits confers integrin ligand specificity (Humphries, 1990). The short cytoplasmic tail (fewer than 60 amino acids long) is present in all integrin subunits except for  $\beta4$  and  $\beta8$ ; it is not catalytic active and it associates with a set of proteins to mediate intracellular signalling. Integrins bind to components present in the ECM, such as laminin, collagen, fibronectin, vitronectin and different cell types have different integrin profiles (van der Flier and Sonnenberg, 2001).

Some integrins bind to a single ligand, others bind to multiple ligands, typically recognizing short peptide sequences in their ligands (such as the tripeptide Arg-Gly-Asp or RGD). In fact, they can be broadly divided into four main groups: collagen receptors, laminin receptors, RGD-ligand receptors and those with expression restricted to leukocytes (Figure 1.7).

## 1.6.2 Integrin activation and signalling

Integrins provide a physical connection between the extracellular compartment and the actin cytoskeleton (Hynes, 2002). They exert adhesive functions and have signal transduction capabilities, but they do not have any intrinsic enzymatic activity by themselves. They signal bidirectionally according to their activation states through “outside-in signalling” which mediates signals that are transduced intracellularly upon the binding to ECM ligands and the “inside-out signalling” which regulates the extracellular binding activity of integrins from inside of the cell through the induction of conformational changes in their structure (Giancotti and Ruoslahti, 1999; Ginsberg *et al.*, 2005). The adhesive properties of integrins rely on their activation, the process by which they switch from low to high binding affinity to ECM components, followed by their clustering at the plasma membrane, resulting in an increased avidity for their ligands. In fact, integrin subunits can bend to generate a conformational form in which the N-terminal domain is in close proximity to the cell membrane, forming a V-shape, and stabilised by inter-subunit clasps. This bent conformation represents a low affinity state for ligand binding (Takagi *et al.*, 2002)

Integrin activation is regulated both by intracellular activators (such as talin and kindlins) or suppressors (such as filamin) which bind to the short cytoplasmic tails of integrin subunits. The binding of an activator disrupts the inter-subunit clasps between the  $\alpha$  and  $\beta$  subunits by altering the angle of the transmembrane domain and causing their separation. This then transmits a conformational change to the extracellular domain which induces the transition to a conformation with a high affinity for ligand binding (Mould and Humphries, 2004). In their active state integrins form oligomeric complexes (process referred to as clustering) and this has been shown to occur following both inside-out and outside-in stimulation. Further integrin activity can be modulated by controlling integrin availability at the cell surface and within adhesive structures via their internalization and trafficking (Hynes, 2002).

The interaction of integrins with the actin cytoskeleton is important for their signalling functions (Figure 1.8). Integrins assemble at focal contact sites, where they associate with adaptor proteins and signalling molecules, thereby integrating adhesion to ECM with intracellular signalling pathways that control processes such as proliferation, migration, and survival. (Eliceri, 2001). Examples of adaptor proteins are talin, paxillin, vinculin. Signalling molecules include, FAK, members of the c-Src family of non-receptor tyrosine kinases, ERK1/2, c-Jun kinase/mitogen-activated protein

kinase (JNK/MAPK) and members of the Rho family of small GTPases (van der Flier and Sonnenberg, 2001). In endothelial cells, integrins play a central role in VEGF/VEGFR signalling. For instance,  $\beta 3$  integrins specifically bind to the extracellular domain of VEGFR2 resulting in increased receptor activation upon VEGF stimulation (Soldi *et al.*, 2000).

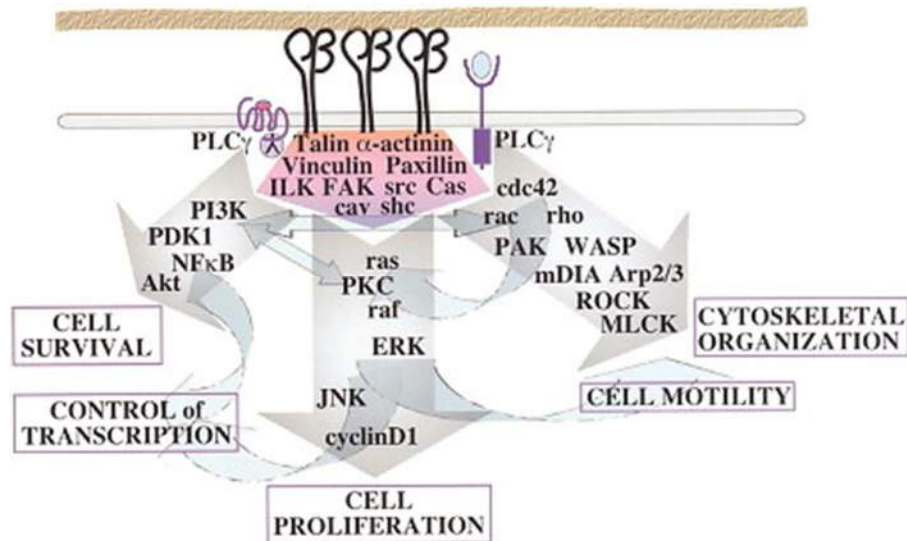


**Figure 1.8 Integrin intracellular signalling**

Signal transduction proteins associated with, or activated by integrins. Signalling molecules, such as FAK, c-Src, bind to and recruit additional signalling molecules, creating a complex signalling network that is intimately connected to the cytoskeleton network and regulate cell proliferation, survival and migration (adapted from Hynes, 2002).

### 1.6.3 Integrin in cancer

Integrin expression in cancer cells has been found to contribute to tumour progression and metastasis. Even if integrins are not oncogenic by themselves, they have been found to be involved in the tumour initiation process activated by some oncogenes (Bendas and Borsig, 2012; Koistinen and Heino, 2000). As such integrins have been investigated and developed as therapeutic targets (Desgrosseier and Cheresh, 2010) Increased expression of  $\alpha 5$ ,  $\beta 1$  and  $\beta 3$  integrin subunits has been shown to correlate with poor prognoses in patients with non-small lung cell carcinoma (Dingemans *et al.*, 2010). Constitutively active  $\beta 1$  integrin has been shown to drive metastasis *in vivo* (Kato *et al.*, 2012); whereas its ablation in pancreatic  $\beta$ -cells was found to decrease tumour growth, but to mediate metastatic dissemination in the mouse Rip-Tag model (Kren *et al.*, 2007). Integrins  $\alpha 5$ ,  $\beta 1$   $\alpha v$  and  $\beta 3$  have been

shown to be overexpressed in glioma, with  $\alpha\beta3$  integrin abundantly expressed at the tumour periphery of high grade gliomas and in the tumour vasculature (Gladson *et al.*, 1996).

$\alpha\beta3$ -integrin has been shown to cooperate with PDGFRB in glioma cells implicating  $\alpha\beta3$ -integrin in tumour invasion in gliomas which secrete high levels of PDGF (Ding *et al.*, 2003). Furthermore,  $\alpha\beta3$ -integrin has been shown to be overexpressed in breast and prostate cancers and to correlate with bone metastasis (Sheldrake and Patterson, 2009); whereas in pancreatic tumour, its increased expression is associated with increased MMP-2 activation of and lymph node metastasis (Hosotani *et al.*, 2002). Therefore, the critical role of integrins in cell adhesion and migration coupled with their dysregulated expression in different cancers have made integrins a focus of targeted drug design.

#### **1.6.4 Vascular integrins**

The first evidence that integrins were involved in angiogenesis was supported by their expression patterns in newly formed blood vessels. In particular, attention has been given to  $\alpha\beta3$ -integrin as although it is barely detectable in quiescent vessels, its expression is elevated greatly in angiogenic sprouts (Brooks *et al.*, 1994).

Vascular endothelial cells express several integrins including: the collagen receptors  $\alpha1\beta1$  and  $\alpha2\beta1$ ; the laminin receptors  $\alpha3\beta1$ ,  $\alpha6\beta1$  and  $\alpha6\beta4$ ; the fibronectin receptors  $\alpha4\beta1$  and  $\alpha5\beta1$ ; the osteopontin receptor,  $\alpha9\beta1$  and the vitronectin receptors  $\alpha\beta3$  and  $\alpha\beta5$ . Even though  $\alpha\beta3$  is referred to as the vitronectin receptor, on endothelium it can also bind to von Willebrand factor, fibronectin, osteopontin, thrombospondin, tumstatin as well as other ECM proteins, all of which contain a arginine-glycine-aspartic acid (RGD) peptide motif (Hodivala-Dilke *et al.*, 2003).

#### **1.6.5 $\alpha\beta3$ -integrin**

$\alpha\beta3$ -integrin has gathered much attention since it is expressed only by neo-angiogenic tumour vessels and not by normal ones thereby reducing the potential for side-effects from its blockade (Brooks *et al.*, 1994).  $\alpha\beta3$ -integrin is expressed in the endothelium of newly formed blood vessels: it is dramatically upregulated in tumour endothelium and in the vasculature at sites of inflammation and tissue repair (Brooks *et al.*, 1995).

Moreover its expression on tumour cells has been correlated with poor patient survival. However, in some human tumours (such as angiosarcomas) endothelial cell  $\alpha\beta 3$  levels decrease as malignant transformation progresses and vascular  $\alpha\beta 3$  levels have been found to be significantly lower in lung metastases from colorectal carcinomas compared to those in primary tumours (Robinson and Hodivala-Dilke, 2011) implying it might also exert an antiangiogenic role.

#### **1.6.5.1 $\alpha\beta 3$ -integrin signalling in angiogenesis**

At a molecular level, ligation of  $\alpha\beta 3$ -integrin induces the activation of MAPK (mitogen-activated protein kinase), FAK and c-Src, resulting in cell proliferation, survival and migration which are all steps endothelial cells undergo during the angiogenic process (Miranti and Brugge, 2002). Whereas unligated  $\alpha\beta 3$ -integrin negatively regulates cell survival and promotes apoptosis by recruiting caspase-8 to the plasma membrane in a process defined as Integrin-Mediated death (IMD) (Stupack *et al.*, 2001). The disruption of  $\alpha\beta 3$  ligation, either by neutralizing antibodies or by small RGD inhibitors, results in prevention of vessel formation *in vitro* and inhibition of tumour growth and angiogenesis *in vivo* in some models (Brooks *et al.*, 1995; Drake *et al.*, 1995; Hammes *et al.*, 1996; Kumar *et al.*, 2001).

Importantly,  $\alpha\beta 3$ -integrin and VEGFR2 have been shown to interact synergistically (Mahabeleshwar *et al.*, 2006). VEGFR2 activation induces  $\alpha\beta 3$ -integrin tyrosine phosphorylation that, in turn, is crucial for VEGF-induced VEGFR2 phosphorylation in a c-Src dependent mechanism. Indeed, knockin mice, expressing a mutant form of  $\alpha\beta 3$ -integrin unable to undergo cytoplasmic tyrosine phosphorylation (DiYF) display impaired pathological angiogenesis whereby tumour growth and associated neovascularisation were reduced significantly (Mahabeleshwar *et al.*, 2006).

Taken together these results suggest that  $\alpha\beta 3$ -integrin is required for pathological angiogenesis. In addition,  $\alpha\beta 3$ -integrin has been shown to associate with Neuropilin-1, a VEGF co-receptor that augments signalling through VEGFR2 (Robinson *et al.*, 2009) and with a number of pro-angiogenic growth factor receptors, substantiating the role of  $\alpha\beta 3$ -integrin as a positive regulator of angiogenesis (Miranti and Brugge, 2002).

### 1.6.5.2 ECM ligands for $\alpha\beta 3$ -integrin

The interactions of  $\alpha\beta 3$ -integrin with the extracellular environment determines endothelial cell behaviour and thus angiogenesis. Despite defined as “vitronectin receptor”,  $\alpha\beta 3$ -integrin can bind to other RGD-containing-ECM ligands such as fibronectin, fibrinogen, von Willebrand Factor (vWF), Osteopontin (OPN) and thrombospondin. Brooks *et al.* (1995) showed that  $\alpha\beta 3$ -integrin antagonists (RGD mimetics) induce endothelial cell death, implying that this integrin is pro-angiogenic and required for angiogenesis. In contrast Alghisi *et al.* (2009) reported that the RGD mimetic treatment of HUVECs (human umbilical endothelial cells) cultured on  $\beta 1$ -integrin ligands (such as laminins, collagens and fibronectin) led to  $\alpha\beta 3$ -integrin activation and associated with an increase in endothelial monolayer permeability; thereby suggesting  $\alpha\beta 3$ -integrin functions are dependent on ECM ligation. Further,  $\alpha\beta 3$ -integrin on HUVECs binds to acutely secreted von Willebrand factor (vWF) and sustains platelet adhesion (Huang *et al.*, 2009).

$\alpha\beta 3$ -integrin as expressed by other cell types is also affected by interaction with the extracellular matrix. For instance, in osteoclasts  $\alpha\beta 3$ -integrin binding to Osteopontin in osteoclasts results in a reduction in cytosolic  $\text{Ca}^{2+}$  which in turns regulates osteoclast function (Miyachi *et al.*, 1993); whereas it promotes migration in smooth muscle cells (Liaw *et al.*, 1995). Furthermore in melanoma cells,  $\alpha\beta 3$ -integrin function has been shown to be modulated by thrombospondin acts via CD47 (Integrin associated Protein-IAP) and to affect cell spreading and focal adhesion turnover (Gao *et al.*, 1996). In addition,  $\alpha\beta 3$ -integrin can also act together with  $\alpha 5\beta 1$ -integrin in promoting adhesion and spreading on fibronectin in M21 melanoma cells (Charo *et al.*, 1990).

### 1.6.5.3 $\beta 3$ -integrin knockout and knock-in mouse models

Unexpectedly, the genetic ablation of  $\beta 3$ -integrin not only supports tumour growth and tumour angiogenesis, it enhances these processes (Reynolds *et al.*, 2002; Taverna *et al.*, 2004), implying that, in contrast to what originally was thought,  $\beta 3$ -integrin is not required absolutely for tumour angiogenesis and indicating that it can also negatively regulate angiogenesis.  $\beta 3$ -integrin knock-out (KO) mice also display a bleeding phenotype due to the loss of  $\alpha \text{IIb}\beta 3$  integrin in platelets, which is required for platelet clotting (Hodivala-Dilke *et al.* 1999). Furthermore, the enhanced pathological angiogenesis displayed by  $\beta 3$  KO mice has been shown to be associated

with increased VEGFR2 expression and function (Reynolds *et al.*, 2004). This phenotype can be normalized by administering VEGFR-2 inhibitors, suggesting that a VEGFR2 compensatory mechanism may be involved in tumour angiogenesis when  $\alpha v\beta 3$  integrin is absent (Reynolds *et al.*, 2002).

DiYF knock-in mice (expressing a mutant  $\beta 3$ -integrin unable to undergo tyrosine phosphorylation) undergo normal embryonic development and organogenesis, but they show impaired normal and pathological angiogenesis (Mahabeleshwar *et al.*, 2006). Importantly, they do not show any compensatory changes in VEGFR2 signalling (Mahabeleshwar *et al.*, 2006) as reported for by  $\beta 3$  KO mice (Reynolds *et al.*, 2004).

Floxed mice with cell-specific conditional deletion of  $\beta 3$ -integrin in platelets and myeloid cells have also been generated (Morgan *et al.*, 2010). Consistently,  $\beta 3$  KO in platelets leads to a bleeding phenotype, but has no effect on tumor growth and angiogenesis. Interestingly, tumour growth is enhanced in myeloid  $\beta 3$  KO mice but without an increase in tumour angiogenesis. Moreover,  $\beta 3$ -integrin deletion in myeloid cells induced osteopetrosis (similar to that observed in the global  $\beta 3$  knockout mice) due to impaired osteoclast activity (Morgan *et al.*, 2010).

$\alpha v\beta 3$ -integrin is expressed by different cell types (pericytes, platelets, macrophages, bone marrow derived cells, fibroblasts, osteoclasts) each contributing in their own way to angiogenesis (Robinson and Hovidala-Dilke, 2011) and in fact both KO and DiYF angiogenic phenotype can be rescued by restoring wild-type expression of  $\beta 3$ -integrin in bone marrow derived cells, through bone marrow transplant (Reynolds *et al.*, 2002; Feng *et al.*, 2008). In line with this finding, the disruption of  $\beta 3$  expression in BMDCs has been shown to give rise to similar angiogenic phenotypes as the ones observed in  $\beta 3$  KO mice (Morgan *et al.*, 2010). This suggests that ablation of  $\beta 3$ -integrin in non-ECs may be responsible for the phenotypes seen in KO studies.

Collectively, the studies illustrate that  $\alpha v\beta 3$ -integrin can play both pro- and anti-angiogenic roles in tumour development depending on its level of expression, on the molecules with which it is interacting and on the cell type expressing it in complex ways we do not fully understand yet and as such we can not exploit them effectively in clinical settings (Robinson and Hovidala-Dilke, 2011). However, a major limitation of these genetic and pharmacological studies is the global nature of the imposed inhibition (e.g. multiple cell types are affected by both manipulations). Moreover a

systemically administered drug directed against  $\alpha v \beta 3$ -integrin is acting differently than a genetic alteration that abrogates the expression of the  $\beta 3$ -integrin subunit. In reality, both are blunt tools to dissect the complex cellular and molecular pathways regulated by this molecule (Atkinson *et al.*, 2014). More refined work is needed in order to clarify how  $\alpha v \beta 3$ -integrin regulates pathological angiogenesis.

#### **1.6.5.4 $\alpha v \beta 3$ -integrin inhibitors**

Preclinical *in vitro* studies have provided the rationale for the development of  $\alpha v \beta 3$ -integrin antagonists as anti-angiogenic agents (Brooks *et al.*, 1994). LM609 (mouse anti- $\alpha v \beta 3$  antibody) was fully humanized and known as Vitaxin, then MEDI-522. It has been developed by Astra-Zeneca as etaracizumab (Abegrin). Despite being well tolerated in Phase I trials (Delbaldo *et al.*, 2008), Abegrin did not show objective response in a Phase II trial for melanoma (Hersey *et al.*, 2010). It Abegrin is currently being tested in other clinical trials for solid tumors (metastatic melanoma (prostate and ovarian cancer) and auto-immune diseases (psoriasis, and rheumatoid arthritis. Furthermore, Abegrin has proven successful as a targeting ligand for molecular imaging agents (Liu *et al.*, 2010).

The most promising  $\alpha v \beta 3$  candidate was Cilengitide (RGD-peptide), which was first synthesized by Kessler and colleagues (Aumailley *et al.*, 1991) and subsequently identified using a cell-free receptor assay for the inhibition of integrins  $\alpha v \beta 3$  and  $\alpha v \beta 5$  but not  $\alpha 11 \beta 3$  (Smith *et al.*, 1990). Since  $\alpha v \beta 3$  is highly expressed in glioblastoma multiforme (on both tumour astrocytes and endothelial cells; Gladson and Cheresch, 1991), Cilengitide has been tested in patients with newly diagnosed glioblastoma.

Despite initial clinical trials have shown encouraging results: antitumor activity, including durable remissions, and increased survival for a subset of patients; the latest Phase III study (CENTRIC) aimed to test standard treatment in combination with Cilengitide have recently failed (see paragraph 1.7.2).

### **1.7 Anti-angiogenic therapy**

The concept that tumour angiogenesis may have therapeutic implications in the control of tumour growth was introduced by Folkman in 1971 (Folkman, 1971). Given the premise that tumours depend on angiogenesis for their growth, progression and

spread, targeting of tumour blood vessels has been considered a logical approach to target different tumours over the past decades (Carmeliet and Jain, 2000).

### 1.7.1 Clinically approved anti-angiogenic therapies

Ever since 1971, research in angiogenesis inhibition as a therapeutic strategy has led to the discovery of the molecular mechanisms of angiogenesis: pro- and anti-angiogenic molecules, their ligands and receptors, as well as their downstream signalling pathways have been identified and investigated as potential targets (listed in Figure 1.9).

SPECIFICITY	DRUG	TARGET	INDICATION	STATUS
Mono-target	Bevacizumab (AVASTIN)	VEGF-A	Mestastic CC, NSCLC, metastatic RCC	US/EU approved
	Cetuximab (ERBITUX)	EGFR	Head and neck SCC, CC	US/EU approved
	Panitumumab (VECTIBIX)	EGFR	Mestastic CC,	US/EU approved
	Trastuzumab (HERCEPTIN)	HER-2	HER2+ BC and GC	US/EU approved
Multi-target	Pazopanib (VOTRIENT)	VEGFR-1 -2 -3, PDGFR, KIT	Advanced RCC, tissue sarcoma	US/EU approved
	Sorafenib (NEXAVAR)	VEGFR-2 -3, PDGFR, KIT, Raf	HC, advanced RCC	US/EU approved
	Sunitinib (SUTENT)	VEGFR-1 -2 -3, PDGFR, KIT, FLT3, CSF-1R, RET	GIST, advanced RCC, PNETs	US/EU approved
	Vandetanib (CAPRELSA)	VEGFR-2, EGFR, KIT, RET	Medullary TC	US/EU approved
	Broad-spectrum	ATN-161	Av $\beta$ 3 - $\alpha$ v $\beta$ 1 integrins	CNS tumours, RCC
Cilengitide		$\alpha$ v $\beta$ 3 - $\alpha$ v $\beta$ 5 integrins	Glioma, GB	Not improved OS

#### Figure 1.9 Overview of anti-angiogenic drugs in cancer

List of main anti-angiogenic drugs with their specificity, target and approved indications. Since 2004, a huge panel of antiangiogenic inhibitors, either alone or in combination with cytotoxic and chemotherapy drugs, have been tested in clinical trials, and approved (adapted from Limaverde-Sousa *et al.*, 2014).

Due to its main role in angiogenesis, vascular endothelial growth factor (VEGF) and its receptors (VEGFR) have been the most widely studied targets (Hicklin and Ellis, 2005). This has resulted in the development of VEGF inhibitors, amongst which BEVACIZUMAB (a monoclonal anti-VEGF antibody-Avastin®) was the first

angiogenesis inhibitor that was shown to have a significant and clinically relevant survival benefit in phase III trial for advanced colorectal cancer (CC) and the first to be approved by the Food and Drug Administration (FDA) in 2004. In detail, BEVACIZUMAB was shown to extend both overall survival (OS) and progression free survival when combined with standard chemotherapy agents (irinotecan, 5-fluorouracil, leucovorin- IFL scheme) (Hurwitz *et al.*, 2004).

Shortly after that, the use of Bevacizumab was additionally approved for the treatment of metastatic breast cancer (MBB), hepatocellular carcinoma (HC), renal cell carcinoma (RCC), non small lung cell cancer (NSCLC), gastrointestinal stroma tumours (GIST) and glioblastoma (GBM). Besides Bevacizumab, other monoclonal antibodies designed to block epithelial growth factor (EGF/HER) receptors, such as cetuximab (Erbix), trastuzumab (Herceptin) and panitumumab (Vectibix) have been found to exhibit antiangiogenic functions due to crosstalk between the signalling pathways that involve VEGF (Walti *et al.*, 2013).

Moving from single target therapy to the second generation of anti-angiogenic drugs, broad-spectrum receptor tyrosine kinase inhibitors (TKIs) were subsequently approved for clinical use: SUNITINIB (Sutent®) for metastatic RCC and advanced pancreatic neuroendocrine tumours, PAZOPANIB (Votrient®) for metastatic RCC, SORAFENIB (Nexavar®) for unresectable HC and metastatic RCC and VANDETANIB (Zactima®) for medullary thyroid cancer (Walti *et al.*, 2013). These VEGFR inhibitors are also able to block other receptor targets such as Platelet derived growth factor receptor (PDGFR), Epidermal growth factor receptor (EGFR), c-Kit or RET, thereby preventing the establishment of resistance mechanisms associated with long-term monotherapy. Unlike antibodies, TKIs cross the cell membrane due to their small size and hydrophobicity, interacting directly with the intracellular domain of receptors and/or other signalling molecules. Several multi-target TKIs display activity as single agents, but they have also been investigated in combination as described for single-target anti-angiogenic treatments (Limaverde-Sousa *et al.*, 2014).

In addition to the above-mentioned drugs, several other molecules with anti-angiogenic activities have been developed and studied extensively both *in vivo* and *in vitro*. Integrins are a family of cell adhesion molecules that have been demonstrated to play a key role in tumour angiogenesis and metastasis and, as such, they have been exploited as therapeutic targets (Desgrosseliers and Cheresh, 2011).

Inhibitors of integrin activity include monoclonal antibodies such as VITAXIN (a humanized anti-integrin  $\alpha\beta 3$  monoclonal antibody) and peptides such as CILENGITIDE (a cyclic pentapeptide inhibitor mimicking the RGD motif recognized by  $\alpha\beta 3$ - and  $\alpha\beta 5$ -integrins) and ATN-161 (a fibronectin derived peptide recognized by  $\alpha 5\beta 1$  and  $\alpha\beta 3$ ) (Cai *et al.*, 2006; Reardon *et al.*, 2008; Khalili *et al.*, 2007). Peptides, compared to full size recombinant monoclonal antibodies, retain the activity of the parent molecule and have significant advantages such as low toxicity, high specificity and good tissue penetration due to their small size.

### 1.7.2 Concern and challenges of anti-angiogenic therapies

Although there is general consensus on the notion that targeting angiogenesis represents a clinically effective therapeutic strategy in oncology, in reality the multiple anti-angiogenic strategies which have been pursued, have proved largely disappointing. Despite initial encouraging results, BEVACIZUMAB, along with other anti-angiogenic drugs, failed to prove significant clinical efficacy, whereas showing a modest success represented by an increase in overall survival measured in the order of months (Bergers and Hanahan, 2008). Indeed, the FDA has revoked BEVACIZUMAB indication for the treatment of metastatic breast carcinoma in 2012 (Mackey *et al.*, 2012). In February 2013, Merck announced that CILENGITIDE had not passed a phase III clinical trial aimed at evaluating OS in glioblastoma patients when added to the current standard chemo-radiotherapy treatment (temozolomide and radiotherapy) (Soffietti *et al.*, 2014). In addition to that, VEGF blockade has been associated with an increase in tumour invasion and metastasis giving raise to safety concerns in clinical settings (Kerbel *et al.*, 2008), while the concept of normalization of the tumour vasculature (therefore improving the delivery of drugs and oxygen to tumours) has emerged as potentially beneficial in reducing tumour growth and metastatic dissemination (Jain, 2001).

Taken together this evidence calls into question the simple concept of the causal link between tumour growth and angiogenesis which needs to be further evaluated (Atkinson *et al.*, 2014). First of all, the molecular pathways regulating developmental and physiological angiogenesis might not necessarily recapitulate the mechanisms underlying tumour angiogenesis; second of all, *in vitro* and *in vivo* models used to test anti-angiogenic drugs do not completely reflect the heterogeneity of human cancers; finally, and partially related to this, the mode of action of these targets in patients is not fully understood yet, as well as the duration and dose of treatment

remain to be effectively determined since rebound tumour growth effect may happen after stopping anti-angiogenic drugs (Welti *et al.*, 2013).

Rather relevant, these drugs are employed for the treatment of patients with highly metastatic disease and, as such, displaying an already aggressive tumour phenotype, thereby possibly accounting for intrinsic refractoriness or subsequent acquired resistance to anti-angiogenic drugs (Leite de Oliveira *et al.*, 2011). Because angiogenesis is regulated by different factors, often displaying redundant functions, the inhibition of a single target is likely to increase the dependency on alternative pathways or to induce the selection of cells in which angiogenesis is driven by other factors.

Furthermore, the reasons for limited efficacy of anti-angiogenic approaches are likely the result of multiple factors relying both on tumour cells and the tumour microenvironment (Hanahan and Coussens, 2012). Tumour cells can produce pro-angiogenic molecules other than VEGF (VEGF-independence), they can switch between different modes of vascularization (angiogenesis independence), become tolerant to hypoxic conditions or metastatise via lymphatic vessels (vascular independence) thereby escaping VEGF (receptor) blockade. In addition, cancer stem cells can give rise to an alternative source of vascular cells with reduced sensitivity to VEGF inhibition (Welti *et al.*, 2013).

The unforeseen plasticity of tumour cells along with the dynamic characteristics of the tumour microenvironment still pose unresolved challenges which will require new anti-angiogenic strategies both in the form of alternative molecules and target cells such as the more genetically stable endothelial cells or pericytes and alternative therapeutic schemes, such as neoadjuvant or metronomic therapies (Welti *et al.*, 2013). Importantly, there is a need for more suitable preclinical models to investigate resistance mechanisms and how they can be effectively overcome; and, equally important, the need for clinically predictive biomarkers tailored for tumour type, stage and treatment (Leite de Oliveira *et al.*, 2011).

With respect to this last aspect, the identification and validation of predictable biomarkers is as relevant as the development of “drugable” targets. Faithful biomarkers will allow for the personalization of therapeutic regimes, for the evaluation of efficacy and toxicity of these treatments and, ideally, the prediction of resistance. Thus, it is compelling to further investigate the complex interplay of signalling

molecules and cells which are involved in tumour angiogenesis in order to overcome these limitations and to improve the efficacy of anti-angiogenic therapy in the clinics.

The importance of tumour microenvironment (TME) in promoting tumour growth and progression is now-increasingly accepted (Quail and Joyce, 2013). The stromal compartment also significantly affects tumour cells' abilities of developing resistance to treatments. Stromal cells, infiltrating immune cells and cancer associated fibroblasts can all produce pro-angiogenic molecules and recruit bone marrow derived cells, resulting in increased tumour angiogenesis independently of VEGF (receptor) inhibition. Furthermore, distinct signals can regulate angiogenesis in primary compared to metastatic tumours, implying that the efficacy of treatment is context- and time-dependent; nevertheless, treatments themselves can select for more aggressive tumour cell clones (Hanahan and Coussens, 2012).

Anti-angiogenic therapy, compared to traditional cancer therapies, has significant advantages; namely easy accessibility, broad applicability and, overall reduced toxicity when compared to the detrimental side effects of chemo/radiotherapies. However, given the current limitations, it seems unlikely that a single anti-angiogenic therapy will ever prove entirely effective. The challenge is to define an effective and rational combinational therapy that overcomes these limitations. Aside from targeting tumour vessel structure thereby improving the delivery of drugs and oxygen to tumours, as a complementary approach to improve traditional anti-angiogenic therapy, another new concept that is emerging is to target vascular sprouts by manipulating endothelial cell metabolism (Rivera and Bergers, 2014). Additionally combining therapeutic approaches over single therapies is potentially a way of synergizing therapeutic effect as well as overcome resistance.

### **1.8 Aims of the study**

This study was undertaken to elucidate the role of endothelial  $\beta$ 3-integrin in pathological angiogenesis *in vivo*.

My aims were:

To generate two different endothelial-specific  $\beta$ 3-integrin-deficient mouse models:

- a constitutively-deleted  $\beta$ 3-integrin-floxed Tie1Cre model,

- a drug inducible  $\beta$ 3-integrin-floxed  $Pdgfb$ -iCreER<sup>T2</sup> model,

and to then use these two models to dissect the role of endothelial  $\beta$ 3-integrin during tumour angiogenesis;

2) For any phenotype observed in (1) to begin to unravel the molecular basis of  $\beta$ 3-integrin function in endothelial cells (*in vitro* and *ex vivo*);

3) To develop spontaneous metastasis models in order to further investigate the involvement of endothelial  $\beta$ 3-integrin in tumour invasion and metastatic dissemination *in vivo*.

## 2 MATERIALS AND METHODS

### 2.1 MATERIALS

#### 2.1.1 Chemicals

Bulk chemicals were obtained from the following companies:

- Sigma-Aldrich (Poole, UK)
- Thermo Scientific (Rockford, USA,)

#### 2.1.2 Consumables

- Plates (6-12-96-wells) flasks (T25-75-175), dish for tissue culture (10 cm): Thermo Scientific
- Test tubes (0.5-1.5 ml): Eppendorf (Stevenage, UK)
- Test tubes (10-50 ml falcon): BD Bioscience (Oxford, UK)
- FACS tubes: BD Bioscience
- Syringe (20 ml) and needles (19 G): Plastipack (St Leonards-on-Sea, UK)/BD Bioscience
- Filters (0.4-0.7  $\mu\text{m}$ ): Millipore (Watford, UK)
- Poly-L-Lysine coated microscope slides and glass coverslips (10 mm): Thermo Scientific

#### 2.1.3 Equipment and software

- UV BioDoc-It Imaging System: UVP (Cambridge, UK)
- FUJIFILM Luminescent Image Analyzer LAS-1000plus: Fujifilm UK (Bedford, UK).
- NanoDrop: Thermo Scientific
- 96-well Fast Thermal Cycler: Applied Biosystems (Invitrogen)
- UV/Vis Spectrometer Microplate Reader: BMG Labtech (Aylesbury, UK)
- Axioplan epifluorescent microscope: Zeiss (Cambridge, UK)
- Microtome and vibratome: Leica (Milton Keynes, UK)
- Tissue Lyser: Qiagen (Manchester, UK)
- Accuric C6 flow cytometer: BD Bioscience
- ImageJ software for densitometric analysis: software available at the National Institutes of Health web site
- GraphPad Prism software for statistical analyses

- Axiovision software for fluorescent image analysis
- CELLQUEST software for flow cytometry analysis

## **2.1.4 PCR**

### **2.1.4.1 Primers**

PCR analysis of genetically engineered mice was carried out using the following oligonucleotide primers:

#### **$\beta$ 3-floxed PCR**

Forward primer: 5'-TTGTTGGAGGTGAGCGAGTC-3'

Reverse primer: 5'-GCCCAGCGGATCTCCATCT-3'

#### **Tie1Cre PCR**

Forward primer: 5'-GCC TGC ATT ACC GGT CGA TGC AAC GA-3'

Reverse primer: 5'-GTG GCA GAT GGC GCG GCA ACA CCA TT-3'

#### **Pdgfb-iCreER<sup>T2</sup> PCR**

Forward primer: 5'-GCC GCC GGG ATC ACT CTC-3'

Reverse primer: 5'-CCA GCC GCC GTC GCA ACT-3'

#### **TdTomato PCR**

oIMR9020: 5'-AAG GGA GCT GCA GTG GAG TA-3'

oIMR9021: 5'-CCG AAA ATC TGT GGG AAG TC-3'

oIMR9103: 5'-GGC ATT AAA GCA GCG TAT CC-3'

oIMR9105: 5'-GGC ATT AAA GCA GCG TAT CC-3'

#### **Semi-qPCR**

RT-PCR analysis of peripheral blood mononuclear cells was carried out using the following oligonucleotide primers:

#### **Luciferase**

Forward primer: 5'-GTTCGTACATCTCATCTACCTCC-3'

Reverse primer: 5'-CTTTAGGCAGACCAGTAGATCCAG-3'

#### **GADPH**

Forward primer: 5'-TCACTGCCACCCAGAAGAC-3'

Reverse primer: 5'-TGTAGGCCATGAGGTCCAC-3'

#### **2.1.4.2 Solutions and reagents**

- Tail lysis buffer was made of 0.2% SDS, 100 mM Tris-base, 200 mM NaCl, 5 mM EDTA and 0.5 mg/ml proteinase K.
- PCR Master Mix (MegaMix Blue, Cambio; Cambridge, UK) consists of a licensed Taq DNA polymerase, dNTPs, MgCl<sub>2</sub>, reaction buffer and enzyme stabiliser.
- TE buffer consists of 10 mM Tris-base and 1 mM EDTA.
- TAE buffer 50X solution consists of 104 g Tris-base, 55 g orthoboric acid and 10 ml 0.2 M EDTA made up to 1 litre in distilled H<sub>2</sub>O.
- RNA isolation kit: Qiagen
- M-MLV RT kit: Promega (Southampton, UK)

#### **2.1.5 Animals**

##### **2.1.5.1 Surgical materials and reagents**

- Suture wound clips, surgical sutures: VetTech (Congleton, UK)
- Syringe (2 ml) and needles (21 G): Plastipack/BD Bioscience
- Sterile dissection instruments
- Isoflurane: Baxter (Newbury, UK)
- Tamoxifen (21-day-slow release 5 mg pellet): Innovative Research of America (Sarasota, Florida, USA)
- Matrigel (0.7% solution): BD Bioscience
- FITC-dextran (low MW 4300): Sigma-Aldrich

#### **2.1.6 Histology**

##### **2.1.6.1 Solutions and reagents**

- Paraformaldehyde fixing solution consists of 4% paraformaldehyde in PBS.
- PBLEC consists of PBS containing 1% Tween-20, 1mM CaCl<sub>2</sub>, 1mM MgCl<sub>2</sub> and 0.1 mM MnCl<sub>2</sub>.
- Washing solution consists of 0.1% TRITON X-100 in PBS.
- Permeabilising solution for aortic rings consists of 0.25% TritonX-100 in PBS.

- Sodium citrate antigen retrieval buffer consists of 10mM tri-sodium citrate and 0.05% Tween-20 at pH 6.
- Trypsin-based antigen retrieval buffer consists of 0.0025% trypsin in 0.1% CaCl<sub>2</sub> at pH 7.8.
- Mayer's Hemotoxylin: Sigma-Aldrich
- Eosin-phloxine B: Sigma-Aldrich
- Sudan Black (0.1% solution): Sigma-Aldrich
- Formamide: Life Technologies
- Prolong Gold Antifade reagent with DAPI: Invitrogen (Paisley, UK)
- Vectashield mounting medium with DAPI: Vector Laboratories (Peterborough, UK)
- DePeX mounting solution: Fisher Scientific (Loughborough, UK).
- Protein block (serum free): Dako (Ely, UK)

## **2.1.7 Cells and tissues**

### **2.1.7.1 Cell Cultures**

- Mouse Lung Endothelial Cell (MLEC) medium consists of:
  - 1:1 mixture of DMEM low glucose+Glutamax (Invitrogen):Ham's F12+Glutamax (Invitrogen)
  - 20% Fetal bovine serum (FCS), heat inactivated (HyClone, Invitrogen)
  - 50 µg/ml Heparin from sodium salt, from porcine intestinal mucosa (Sigma-Aldrich)
  - 25 mg of endothelial mitogen (AbD Serotec, Oxford,UK)
  - 2 mM L-Glutamine (Invitrogen)
  - 100 U/ml Penicillin/ 100 µg/ml Streptomycin (Invitrogen)
- Immortalized Mouse Lung Endothelial Cell (Im-MLEC) medium consists of:
  - 1:1 mixture of DMEM low glucose+Glutamax (Invitrogen):Ham's F12+Glutamax (Invitrogen)
  - 10% Fetal bovine serum (FCS), heat inactivated (HyClone, Invitrogen)
  - 50 µg/ml Heparin from sodium salt, from porcine intestinal mucosa (Sigma-Aldrich)
  - 2 mM L-Glutamine (Invitrogen)
  - 100 U/ml Penicillin/ 100 µg/ml Streptomycin (Invitrogen)
- Tumour cell medium consists of:
  - DMEM high glucose+Glutamax (Invitrogen)

10% Fetal bovine serum (FCS), heat inactivated (HyClone, Invitrogen)

2 mM L-Glutamine (Invitrogen)

100 U/ml Penicillin/ 100 µg/ml Streptomycin (Invitrogen)

- GgP+E packaging cell culture medium consists of:  
DMEM high glucose+Glutamax (Invitrogen)  
15% Fetal bovine serum (FCS), heat inactivated (HyClone, Invitrogen)  
2 mM L-Glutamine (Invitrogen)  
100 U/ml Penicillin/ 100 µg/ml Streptomycin (Invitrogen)

### **2.1.7.2 Solutions and reagents**

- Solution for tumour digestion consists of Hank's Balanced Salt Solution (HBSS, Invitrogen) supplemented with 0.2% collagenase IV (Invitrogen), 0.01% hyaluronidase (Invitrogen) and 0.01% DNase I (Invitrogen).
- Solution for lung digestion consists of PBS supplemented with 0.1% collagenase I (Invitrogen), 1 mM CaCl<sub>2</sub> and 1mM MgCl<sub>2</sub>.
- Anti-coagulant buffer solution consists of 38 mmol/L citric acid, 75 mmol/L sodium citrate and 100 mmol/L dextrose.
- Matrix coating solution consists of PBS supplemented with 0.1% gelatin (Sigma-Aldrich), Purecol (30 µg/ml, Nutacon BV, Netherlands), human plasma fibronectin (10 µg/ml, Millipore) and mouse multimeric vitronectin (2 µg/ml; Patriecell, Nottingham, UK).
- FACS buffer consists of PBS supplemented with 1% Fetal bovine serum and 10mM HEPES (1M solution, Invitrogen).
- Permeabilising solutions for cells consists of PBS supplemented with 0.5% NP40 (Sigma-Aldrich).
- Blocking solution for cells consists of PBS supplemented with 0.1% Bovine Serum Albumin (BSA, Thermo Scientific) and 0.2% Triton X-100 (Sigma-Aldrich).
- VEGF-A164 was made in house according to the method published by Krilleke *et al.*, (2007)
- bFGF: Peprotech (London, UK)
- Collagen I (rat tail): Millipore
- Laminin (L2020): Sigma-Aldrich
- Fibrinogen from bovine plasma: Sigma-Aldrich
- Thrombin from bovine plasma: Sigma-Aldrich

- Aprotinin from bovine lung: Sigma-Aldrich
- OptiMEM: Invitrogen
- Dulbecco's phosphate buffered saline (PBS): Invitrogen
- Dynabeads sheep anti-rat IgG: Life Technologies
- 0.25% trypsin/EDTA: Gibco, Invitrogen
- Red blood lysis buffer (10X): eBioscience (Hatfield, UK)
- Polybrene: Sigma-Aldrich
- Dimethylsulfoxide (DMSO): Sigma-Aldrich

### **2.1.7.3 Kits**

- Dynabeads Antibody Coupling Kit: Life Technologies
- Vybrant MTT Cell Proliferation Assay Kit: Life Technologies

## **2.1.8 Western Blotting**

### **2.1.8.1 Equipment**

- Vertical gel and transfer apparatus/1mm-thick gel cassettes/10- or 15-well combs: Bio-Rad Laboratories (Hertfordshire, UK)
- PROTRAN nitrocellulose membrane: Fisher Scientific
- Filter paper/sponges: Whatman (GE Healthcare)

### **2.1.8.2 Solutions and reagents**

- ESB lysis buffer consists of 65mM Tris-HCl, 60mM sucrose and 3% SDS at pH 7.4.
- NuPAGE LDS Sample Buffer (4X): Invitrogen
- NuPAGE Sample Reducing Agent (10X): Invitrogen
- Ponceau solution consists of 0.1% Ponceau red (Sigma-Aldrich) and 1% acetic acid in distilled H<sub>2</sub>O.
- Primary antibody solution consists of 5% BSA and 0.1% Tween-20 (Thermo Scientific) in PBS.
- Blocking solution consists of 5% non-fat milk protein (Thermo Scientific) and 0.1% Tween-20 in PBS.
- Acrylamide resolving gel consists of:  
8% acrylamide solution (Protogel, National Diagnostics; Hesse, UK)  
0.1% SDS

0.1% ammonium persulfate

TEMED

distilled H<sub>2</sub>O

- Acrylamide stacking gel consists of:  
5% acrylamide solution (30%, Protogel, National Diagnostics)  
0.1% SDS  
0.1% ammonium persulphate  
TEMED  
distilled H<sub>2</sub>O
- Running buffer (in 1L of distilled H<sub>2</sub>O) consists of:  
25 mM Tris-base  
192 mM glycine  
0.1% SDS
- Transfer buffer (in 1L of distilled H<sub>2</sub>O) consists of:  
25 mM Tris base  
192 mM glycine  
20% ml methanol

### **2.1.8.3 Kits**

- Bio-Rad DC Protein Assay kit: Bio-Rad Laboratories (Hertfordshire, UK)
- ECL kit: Bio-Rad Laboratories

### **2.1.9 Antibodies**

- Antibodies for immunohistological analysis were as follows: anti-endomucin (clone V.7C7, Santa Cruz Biotechnology, Santa Cruz, CA, USA); anti- $\alpha$ SMA (clone EPR5368, Abcam, Cambridge, UK); anti-nidogen (made in house, kind gift from Ulrike Mayer; UEA, Norwich, UK); FAK (clone 77/FAK, BD Bioscience); NG-2 (clone 132.39, Millipore); FITC-IB4 (Sigma-Aldrich) and FITC-conjugated anti-F4/80 (clone BM8, eBioscience). Appropriate Alexa Fluor (488-546-555) conjugated secondary antibodies (Invitrogen) were used at 1:500.

- Antibodies for systemic injection were as follows: PE-conjugated anti- $\beta$ 3-integrin (clone 2C9.G3, eBioscience) and PE-conjugated anti-CD31 (Clone 390, eBioscience).
- Antibodies for magnetic sorting were as follows: anti-CD31 antibody (Cat.no. MCA1334GA, AbD Serotec) and anti-ICAM-2 (Cat.no. MCA2295EL, AbD Serotec).
- Primary antibodies for flow cytometry were all used at 1:200 in FACS buffer and purchased from eBioscience: FITC-conjugated anti-CD45 (clone A20); FITC-conjugated anti-Ly6G (clone RB6-8C5); FITC-conjugated anti-CD3 (clone 17A2); Alexa Fluor 488-conjugated anti-CXCR4 (CD184, clone 2B11); FITC-conjugated anti-F4/80 (clone BM8); PE-conjugated anti-CD11b (clone M1/70); PE-conjugated anti- $\alpha$ 1 (clone Ha31/8, Cambridge Bioscience, Cambridge, UK); PE-conjugated anti- $\alpha$ 2 (clone DX5); PE-conjugated anti- $\alpha$ 5 (clone HMA5-1); PE-conjugated anti- $\alpha$ v (clone RMV-7) and PE-conjugated anti- $\beta$ 1 (clone HMB1-1). Appropriate PE/FITC labelled isotype-matched controls were from eBioscience.
- Primary antibodies for Western Blot analysis were all used at 1:1000 and purchased from Cell Signaling Technology (Hitchin, UK), unless noted otherwise: anti-phospho (Y1175) VEGFR2 (clone 19A10); anti-VEGFR2 (clone 55B11); anti- $\beta$ 3-integrin (Cat.no. 4702); anti- $\beta$ 5 integrin (Cat.no.4708); anti-phospho (Thr202/Tyr204) p44/42 MAPK ERK1/2 (clone D13.14.4E); anti-p44/42 MAPK ERK1/2 (clone 137F5 ); anti-phospho (Ser 1248) PLC $\gamma$ 1 (clone D25A9); anti-PLC $\gamma$ 1 (clone D9H10); anti-phospho (Y416) c-Src (clone D49G4); anti-c-Src (clone 36D10); anti-phospho (Y397) FAK (clone D20B1); anti-phospho (Y861) FAK (Millipore, Cat.no.PS1008); anti-FAK (Cat.no.3285); anti-phospho (Thr180/Y182) p38 (clone 12F8); anti-p38 (clone D13E1); anti-phospho (Y731) VE-cadherin (Abcam, Cat.no.27776) anti-VE-cadherin (Abcam, Cat.no.33168); and anti-HSC70 (clone B-6, Santa Cruz Biotechnology). Appropriate horseradish peroxidase (HRP)-conjugated secondary antibodies (Invitrogen) were all used at 1:2000.

## 2.2 METHODS

### 2.2.1 Animals

All mice were bred in the Disease Modelling Unit of the Biomedical Research Centre at the University of East Anglia, and used in accordance with UK Home Office

Regulations and the European Legal Framework for the Protection of animals used for scientific purposes (European Directive 86/609/EEC).

### **2.2.1.1 $\beta$ 3-integrin-floxed transgenic mice**

In order to examine the role of endothelial  $\beta$ 3-integrin specifically in pathological angiogenesis, I took advantage of endothelial-specific  $\beta$ 3-integrin-deficient mice (Morgan *et al.*, 2010). The  $\beta$ 3-integrin-floxed allele was generated by gene target insertion of embryonic stem cells that resulted in the insertion of loxP sites flanking exon 1 of the *Itgb3* ( $\beta$ 3-integrin) gene. Mice carrying a loxP-flanked allele of the *Itgb3* gene (*Itgb3<sup>flox</sup>*) were kindly provided by Katherine Weilbaecher (School of Medicine, Washington University of St. Louis). Homozygous mice (*Itgb3<sup>flox/flox</sup>*) were crossed with Tie1Cre or Pdgfb-iCreER<sup>T2</sup> transgenic mice in order to generate Tie1Cre;*Itgb3<sup>flox/flox</sup>* and Pdgfb-iCreER;*Itgb3<sup>flox/flox</sup>* on a mixed C57BL6/129 background. They will be hereafter be referred to as  $\beta$ 3-floxed/Tie1Cre and  $\beta$ 3-floxed/Pdgfb-iCreER<sup>T2</sup> mice for consistency with our published work (Steri *et al.*, 2014).

### **2.2.1.2 Tie1Cre transgenic mice**

In Tie1Cre transgenic mice (Gustafsson *et al.*, 2001), Cre Recombinase (Gu *et al.*, 1993) expression is directed to endothelial cells by the mouse *Tie1* promoter (Ilijin *et al.*, 1999). Tie1Cre mice were originally provided by Reinhard Fässler (Max Planck, Martinsried, Germany). This promoter has been reported to drive Cre-induced expression of the LacZ reporter gene in endothelial cells as early as E8, and expression in endothelial cells persists throughout embryogenesis and in adult mice (Gustafsson *et al.*, 2001). Therefore, the use of this transgenic mouse strain allows excision of floxed gene in endothelial cells during embryogenesis after E8 and into adulthood.  $\beta$ 3-floxed mice on a mixed C57BL6/129 genetic background were crossed with Tie1Cre transgenic mice on C57BL6 genetic background to generate mice with the conditional deletion of  $\beta$ 3-integrin in endothelial cells. Mice will be hereafter be referred to as  $\beta$ 3-floxed/Tie1 Cre positive and, their negative counterparts,  $\beta$ 3-floxed /Tie1Cre negative will be used as control.

### **2.2.1.3 Pdgfb-iCreER<sup>T2</sup> transgenic mice**

To further examine the role of  $\beta$ 3-integrin in pathological angiogenesis in a more clinically relevant model, I took advantage of an inducible endothelial cell-specific  $\beta$ 3-

integrin-deficient mouse model. *Pdgfb-iCreER<sup>T2</sup>* transgenic mice were kindly provided by Marcus Fruttiger (UCL Institute of Ophthalmology, UCL, London). In *Pdgfb-iCreER<sup>T2</sup>* transgenic mice, the tamoxifen inducible form of Cre Recombinase (*iCreER<sup>T2</sup>*) is under the transcriptional control of *Pdgfb* gene, which is predominantly expressed by endothelial cells; therefore allowing the genetic targeting of the endothelium in postnatal mice. In the absence of tamoxifen, the *iCreER<sup>T2</sup>* protein is expressed in endothelial cells but retained in the cytoplasm because it is sequestered by HSP-90 (Claxton *et al.*, 2008). Whereas in presence of tamoxifen (referred to as tamoxifen or OHT), *iCreER<sup>T2</sup>* is translocated to the nucleus where it induces the deletion of the  $\beta$ 3-floxed gene.  $\beta$ 3-floxed mice on a mixed C57BL6/129 genetic background were crossed with *Pdgfb-iCreER<sup>T2</sup>* transgenic mice on a mixed C57BL6/129 genetic background to generate mice with the inducible deletion of  $\beta$ 3-integrin in endothelial cells. They will be hereafter be referred to as  $\beta$ 3-floxed/*Pdgfb-iCreER<sup>T2</sup>* positive mice and, their negative counterpart,  $\beta$ 3-floxed/*Pdgfb-iCreER<sup>T2</sup>* negative mice as control. Tamoxifen has been administered equally in  $\beta$ 3-floxed/*Pdgfb-iCreER<sup>T2</sup>* positive and negative mice.

#### **2.2.1.4 tdTomato reporter mice**

To verify that both endothelial specific Cres induced equally efficient and specific recombination of the target gene in endothelial cells, *Tie1Cre* and *Pdgfb-iCreERT2* positive mice were crossed with tdTomato reporter line (Madisen *et al.*, 2010) on a C57BL6/129 mixed background. TdTomato Cre reporter mice (kindly provided by Professor Ulrike Mayer; UEA, Norwich, UK) were generated by the insertion in the *Rosa26* locus of a loxP-flanked DNA STOP cassette under the transcriptional control of a strong and ubiquitous promoter, preventing the expression of the downstream tomato reporter gene. When crossed with *Tie1Cre* and *Pdgfb-iCreER<sup>T2</sup>* positive mice, the STOP sequence is removed by Cre, therefore the fluorescent reporter is strongly expressed. TdTomato heterozygous mice were used for the crossing with endothelial specific Cre transgenics. Endothelial cells isolated from *Tie1Cre* positive/TdTomato heterozygous or *Pdgfb-iCreER<sup>T2</sup>* positive/TdTomato heterozygous cells displayed a bright red fluorescence which was used to compare the pattern of Cre expression in the two endothelial specific models.

#### **2.2.2 PCR genotyping**

##### **2.2.2.1 Genomic DNA isolation from tissues**

Ear (at weaning) or tail (at the end of each *in vivo* experiment as internal control) snips from mice were used for genotyping. Tissues were digested overnight at 56°C in a 96-well PCR plate in 100 µl of tail buffer supplemented with 0.5 mg/ml proteinase K. DNA was precipitated by adding 100 µl of isopropanol to each well and then centrifuging the plate at 2500 rpm for 20 minutes. Isopropanol was removed by gently inverting the plate and the pellet was dried at 56°C for about 30 minutes. DNA was then resuspended in 200 µl of TE buffer and solubilised overnight at room temperature.

#### **2.2.2.2 Genomic DNA isolation from cells**

For this purpose, endothelial cells were plated at  $2 \times 10^5$  cells/well in a 6-well-plate, grown to 80-90% confluency and lysed in 500 µl/well of Tail Lysis Buffer supplemented with 0.5 mg/ml proteinase K. Cell lysates were collected in eppendorf tubes and incubated overnight at 56°C. NaCl 5M (250 µl/tube) was added and tubes were vortexed for 30 seconds. Samples were then centrifuged at 14000 rpm for 10 minutes and the supernatant was carefully transferred to fresh tubes. DNA was precipitated by adding 100 µl of isopropanol to each tube, then samples were centrifuged at 2500 rpm for 20 minutes. Isopropanol was removed by pipetting, DNA was resuspended in 200 µl of TE buffer and solubilised overnight at room temperature.

#### **2.2.2.3 $\beta$ 3-floxed PCR**

For each PCR reaction (total 10 µl), 1 µl of DNA template was mixed with 0.04 µl of 10 µM forward primer, 0.04 µl of 10 µM reverse primer and 8.2 µl of MegaMix Blue reagent. PCR reaction conditions were as follows: denaturation at 95°C, 30 seconds; extension at 56°C, 30 seconds and annealing at 72°C, 30 seconds. Thirty-five amplification cycles were performed, preceded by an initialisation step at 95°C for 2 minutes and terminated with a final elongation step at 72°C for 8 minutes. PCR products are 182-bp (wild-type) and 272-bp ( $\beta$ 3 integrin-floxed allele).

#### **2.2.2.4 Tie1Cre PCR**

For each PCR reaction (total 10 µl), 0.8 µl of DNA template was mixed with 0.08 µl of 10 µM forward primer, 0.08 µl of 10 µM reverse primer and 9.1 µl of MegaMix Blue reagent. PCR reaction conditions were as follows: denaturation at 95°C, 1 minute;

annealing at 67°C, 90 seconds and extension at 72°C, 1 minute. Thirty-five amplification cycles were performed, preceded by an initialisation step at 95°C for 4 minutes and terminated with a final elongation step at 72°C for 10 minutes. The Tie1-Cre transgene PCR product is 600-bp.

#### **2.2.2.5 Pdgfb-iCre<sup>T2</sup> PCR**

For each PCR reaction (total 10 µl), 0.8 µl of DNA template was mixed with 0.08 µl of 10 µM forward primer, 0.08 µl of 10 µM reverse primer and 9.1 µl MegaMix Blue reagent. PCR reaction conditions were as follows: denaturation at 94°C, 30 seconds; annealing at 57.5°C, 45 seconds and extension at 72°C, 1 minute. Thirty-four amplification cycles were performed, preceded by an initialisation step at 94°C for 4 minutes and terminated with a final elongation step at 72°C for 10 minutes. The Pdgfb-iCre<sup>T2</sup> PCR product is 443-bp.

#### **2.2.2.6 TdTomato PCR**

For each PCR reaction (total 10 µl), 0.8 µl of DNA template was mixed with 0.08 µl 7.5 µM of each of the four primers, and 8.8 µl MegaMix Blu reagent. PCR reaction conditions were as follows: denaturation at 94°C, 20 seconds; annealing at 61°C, 30 seconds and extension at 72°C, 30 seconds. Thirty-five amplification cycles were performed, preceded by an initialisation step at 94°C for 3 minutes and terminated with a final elongation step at 72°C for 2 minutes. PCR products are 297-bp (wild-type) and 196-bp (TdTomato allele).

#### **2.2.2.7 Agarose gel electrophoresis**

PCR products from all above described PCRs were separated on a 1.8% agarose gel. Agarose gels were made by mixing 1.8 g of agarose with 70 ml distilled H<sub>2</sub>O, microwaving at full power for 3-5 minutes until the agarose dissolved, and adding 28 ml distilled H<sub>2</sub>O, 2 ml 50X TAE buffer and 5 µl of 10 mg/ml Ethidium Bromide. The agarose solution was poured into a large gel and 20-well-forming combs were inserted into the gel. The amplified PCR products (10 µl) were loaded into the gel and separated at 100 V for about 1 hour. Bands of PCR products were visualised under UV light and photographed using the UV Gel Image Capture System box.

## **2.2.3 In vivo tumour growth and metastasis assays**

### **2.2.3.1 Tumour cell lines**

#### **B16F0**

B16F0 mouse melanoma cell line was employed for *in vivo* tumour growth assays (Fidler, 1973). B16F0 were passaged when they reached ~80-90% confluency. Tumour cells were detached with 0.25% trypsin:EDTA, collected in Falcon tubes, counted and then centrifuged for 5 minutes at 1200 rpm. The supernatant was removed and tumour cells were washed in PBS. They were finally resuspended in PBS ( $1 \times 10^6$  cells/100  $\mu$ l per injection) according to the total number of injections and kept on ice until their use.

#### **CMT19T**

CMT19T is a mouse lung carcinoma cell line derived from the CMT167 cell line and was employed for *in vivo* tumour growth assays (Layton and Franks, 1986). CMT19T were passaged when they reached ~80-90% confluency. Tumour cells were detached with 0.25% trypsin:EDTA, collected in Falcon tubes, counted and then centrifuged for 5 minutes at 1200 rpm. The supernatant was removed and tumour cells were washed in PBS. They were finally resuspended in PBS ( $1 \times 10^6$  cells/100  $\mu$ l per injection) according to the total number of injections and kept on ice until their use.

#### **CMT19T F1**

CMT19TF1 carcinoma cell line was derived from a single round of *in vivo* selection of CMT19T cells, which had spontaneously metastasised to lung. CMT19TF1 metastatic cells were isolated by digesting the lung tissue as described in paragraph 2.2.6.4, expanded and Mycoplasma tested. CMT19TF1 were passaged when they reached ~80-90% confluency. Tumour cells were detached with 0.25% trypsin:EDTA, collected in Falcon tubes, counted and then centrifuged for 5 minutes at 1200 rpm. The supernatant was removed and tumour cells were washed in PBS. They were finally resuspended in PBS ( $1 \times 10^6$  cells/100  $\mu$ l per injection) according to the total number of injections and kept on ice until their use.

## **B6 LV-1**

B6 LV-1 breast carcinoma cell line was derived from multiple rounds of *in vivo* selections of C57BL/6 compatible MMTV-PyMT cells, which had spontaneously metastasised to bone after left ventricle injection. B6-LV1 tumours cells are also green fluorescent protein (GFP) and luciferase (LUC) tagged. B6 LV-1 cell line was generated and kindly provided by Katherine Weilbaecher (School of Medicine, Washington University of St.Louis). B6 LV-1 were passaged when they reached ~80-90% confluency. Tumour cells were detached with 0.25% trypsin:EDTA, collected in Falcon tubes, counted and then centrifuged for 5 minutes at 1200 rpm. The supernatant was removed and tumour cells were washed in PBS. They were finally resuspended in PBS ( $2 \times 10^5$  cells/50  $\mu$ l per injection in 1:1 Matrigel mix) according to the total number of injections and kept on ice until their use.

### **2.2.3.2 Growth and maintenance of tumour cell lines**

Cell lines were grown in tissue culture flasks and maintained in the appropriate culture media at 37°C with a humidified atmosphere of 5% CO<sub>2</sub> in air. Tumour cells were expanded through subsequent passages to obtain the desired number of cells as required for injections. Additional tumour cells were further grown to be frozen down in freezing medium (10% DMSO in Foetal Bovine Serum) at  $10^6$  cells/cryogenic vial. Vials were initially stored at -80°C for and subsequently transferred to a liquid nitrogen tank for long-term storage.

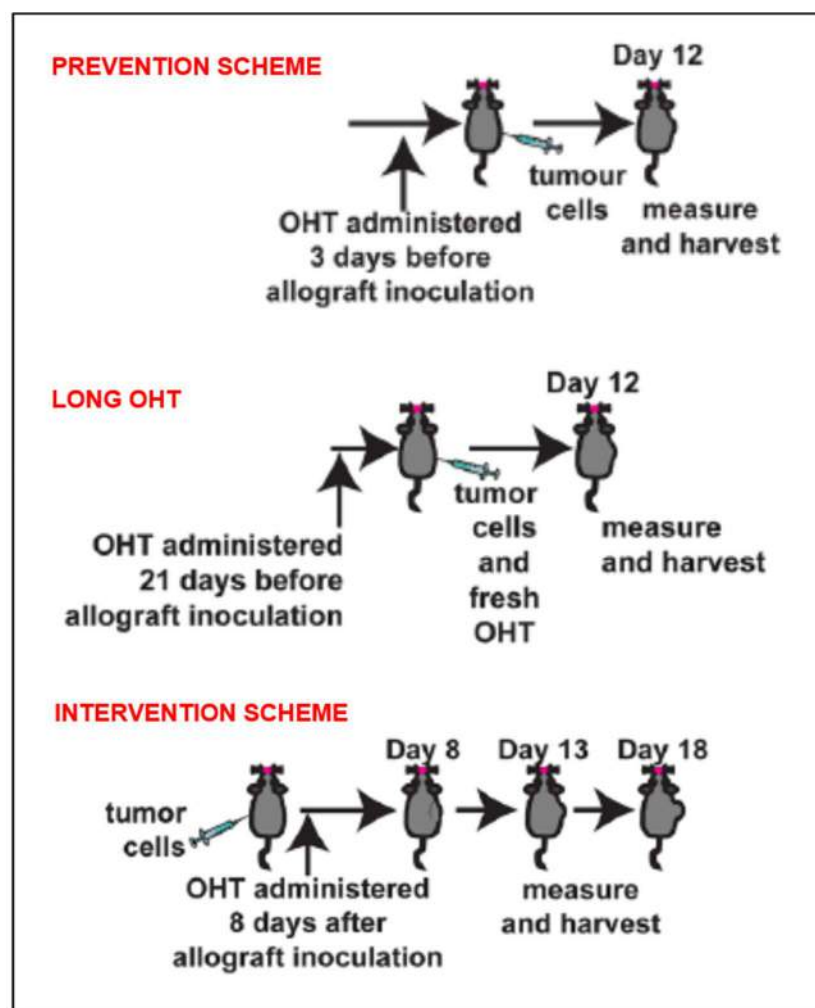
### **2.2.3.3 Allografts**

6 to 8-week-old age-matched mice ( $\beta$ 3-floxed/Tie1Cre positive and negative mice,  $\beta$ 3-floxed/Pdgfb-iCreER<sup>T2</sup> positive and negative mice, Tie1Cre positive/tdTomato heterozygous and Pdgfb-iCreER<sup>T2</sup> positive/tdTomato heterozygous) were anaesthetized with isoflurane inhalant and B16F0, CMT19T and CMT19TF1 tumour cells were administered by subcutaneous injection ( $1 \times 10^6$  cells resuspended in PBS, 100  $\mu$ l per injection), while B6 LV-1 were administered by mammary fat pad injection with Hamilton syringe ( $2 \times 10^5$  cells resuspended in PBS, 50  $\mu$ l per injection in 1:1 Matrigel mix, final volume 100  $\mu$ l per injection). Tumour growth curves were established measuring tumours in two dimension with digital callipers from the outside of the mice every other day starting from the onset of a palpable mass. Tumour volumes were calculated according to the formula for the volume of a sphere:

tumour volume ( $\text{mm}^3$ ) =  $\text{width}^2 \times \text{length} \times 0.52$ . The day of sacrifice (between day 12 and 20 depending on tumour cell line/experimental scheme) mice were euthanized by cervical dislocation and their tumours were excised with surgical scissors, photographed for macroscopic appearance and weighed in addition to a final caliper measurement.

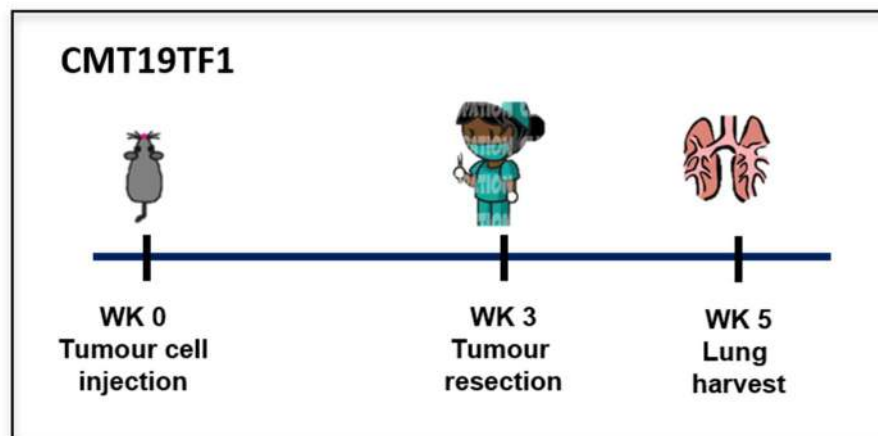
#### 2.2.3.4 Tamoxifen treatments

$\beta 3$ -floxed/Pdgfb-iCreER<sup>T2</sup> positive and negative and Pdgfb-iCreER<sup>T2</sup> positive/tdTomato heterozygous mice were anaesthetized with isoflurane inhalant and slow release (5 mg, 21-day release) tamoxifen pellets were implanted subcutaneously into the scruff of the neck 3 days before tumour cell injection (PREVENTION SCHEME) or 8 days after tumor cell injection (INTERVENTION SCHEME). For long OHT treatment a second pellet was implanted 21 days after the first pellet, at the same time as tumour cell injections.



### 2.2.3.5 Surgical resections

In order to be able to investigate distant site metastases, surgical resection of the primary tumour was performed to allow metastasis to occur.  $\beta$ 3-floxed/Tie1Cre positive and negative mice were anaesthetized with isoflurane inhalant. The day of resection (between day 14 and 20 depending on tumour cell line), CMT19TF1 or B6 LV-1 tumours were surgically resected after taking measurements with a digital caliper. Mice were housed for a further 2 to 4 weeks (depending on tumour cell line) before they were sacrificed in order to harvest lungs/bones (sites of metastases). They were euthanized by cervical dislocation and lungs were inflated with 3.7% formaldehyde in PBS by tracheal injection.



### 2.2.3.6 Quantification of tumour circulating cells

B6 LV-1 tumour cells are luciferase tagged and this allowed for their quantification in peripheral blood samples by LUC-RT PCR. To quantify the amount of tumour circulating cells, peripheral blood from 14-day-B6 LV-1 tumour bearing mice was collected in order to isolate nucleated cells. Mice were lethally anaesthetized and blood from the *vena cava* was collected in eppendorf tubes containing anticoagulant buffer. Blood samples were centrifuged for 7 minutes at 300 rpm. The resulting cell enriched plasma fraction was transferred to a fresh tube and resuspended in 1 mL of Red blood lysis buffer. After 5 minutes, samples were centrifuged for 7 minutes at 2000 rpm. The supernatant was carefully discarded and PBS was added for washing. Samples were centrifuged again (7 minutes at 2000 rpm) and the final pellet was resuspended in 1 mL RNA-Bee for RNA extraction and isopropanol precipitation.

RNA quality and concentration were assessed via NanoDrop. cDNA synthesis was performed using Moloney Murine Leukemia Virus Reverse Transcriptase (M-MLV RT) according to the manufacturer's protocol. Luciferase PCR conditions were as follows: denaturation at 95°C, 10 seconds; extension at 55°C, 30 seconds and annealing at 72°C, 10 seconds. Thirty-nine amplification cycles were performed, preceded by an initialisation step at 95°C for 3 minutes and terminated with a final elongation step at 72°C for 1 minute. Luciferase PCR product is 182-bp. As control for the reaction, total RNA and subsequent cDNA synthesis from cultured B6 LV-1 tumour cells was included. GADPH RT-PCR was performed as a loading control.

### **2.2.3.7 *In vivo* tumour permeability assay**

In pathological conditions that promote increased vascular permeability (such as tumour angiogenesis) the endothelium becomes permeable to small proteins. This condition allows for extravasation of low molecular weight FITC Dextran in the tumour tissues which can be assessed by quantitative measurement of the fluorescent dye incorporated per weight or volume of tissue. 14-day-B6 LV-1 tumour bearing mice  $\beta$ 3-floxed/Tie1Cre positive and negative mice were lethally anaesthetized and injected systemically with low molecular weight FITC-dextran (final 1% in 200  $\mu$ l PBS per injection). After 30 minutes, tumours were harvested, measured and FITC-dextran was extracted by immersion in formamide buffer for 48 hours at 37°C. 200  $\mu$ l of formamide solution was taken from each sample and transferred to a 96-well-plate for fluorescence quantification (excitation wavelength 490 nm; emission wavelength 520 nm). Fluorescence reading values were then normalized to tumour volumes.

### **2.2.3.8 Experimental metastasis assay**

CMT19T F1 tumour cells were injected systemically ( $0.5 \times 10^6$  cells/100  $\mu$ l per tail vein injection) in  $\beta$ 3-floxed/Tie1Cre positive and negative mice. Prior to injection, mice were warmed (10-15 minutes) by placing the animal in warming box to dilate the veins. After 2 weeks, mice were euthanized and lungs were harvested for histological analysis and metastasis evaluation.

## **2.2.4 Immunohistochemical analyses**

### **2.2.4.1 Tumour sections**

For subsequent immunohistochemical analysis, tumours were bisected at the midline and fixed in PFA for 24 hours. Fixed tumours were dehydrated through a graded series of ethanols (50% - 70% - 90% - 95% - 100%, 2 changes 1 hour each) to xylene (overnight), and finally embedded with the cut face toward the blade in liquid paraffin (62°C, two changes of two hour each under vacuum). Tumours were transferred to histology cassettes and left to solidify at room temperature. Paraffin blocks were sectioned on a microtome, 5µm-thick sections were mounted onto glass slides and dried overnight at 37°C. Before staining, paraffin sections were deparaffinized in xylene and rehydrated in a graded series ethanol (100% - 95% - 90% - 70% - 50%, two changes of ten minutes each).

#### **2.2.4.1.1 Endomucin staining**

To quantify tumour blood vessels, paraffin sections of size-matched tumours were stained for endomucin (a blood vascular endothelial cell marker; Morgan *et al.*, 1999). Paraffin sections were rinsed in PBS and blocked by incubating with serum-free blocking solution for 30 minutes at 37°C. Subsequently, sections were incubated with rat anti-mouse endomucin antibody diluted 1:500 in PBLEC overnight at 4°C. Paraffin sections were washed in PBLEC 3 times for 5 minutes at room temperature, then incubated for 2 hours with Alexa-546 donkey anti-rat antibody diluted 1:200 in PBLEC. Paraffin sections were washed in PBS 0.1% TRITON X-100, 3 times for 5 minutes. Sections were finally counterstained with 0.1% Sudan Black for 10 minutes, cleared and mounted with Prolong Gold Antifade reagent containing DAPI.

#### **2.2.4.1.2 αSmooth Muscle Actin/endomucin co-staining**

To evaluate vessel-pericyte association in tumour vessels, paraffin sections of size-matched tumours were double-stained for α Smooth Muscle Actin (αSMA, a pericyte marker; Gerhardt and Betsholtz, 2003) and endomucin. Paraffin sections were rinsed in PBS and antigen retrieval was carried out by boiling sections in sodium citrate buffer for 20 minutes. Paraffin sections were then incubated with serum-free blocking solution for 30 minutes at 37°C. Subsequently, sections were incubated with rabbit anti-mouse αSMA antibody diluted 1:1000 and rat anti-mouse endomucin diluted 1:500 antibody in PBLEC overnight at 4°C. Paraffin sections were washed in PBLEC 3 times for 5 minutes at room temperature, then incubated for 2 hours with Alexa-546 donkey anti-rabbit and Alexa-488 donkey anti-rat antibodies, diluted 1:200 in PBLEC. Paraffin sections were then washed in PBS 0.1% TRITON X-100, 3 times for 5

minutes. Sections were finally counterstained with 0.1% Sudan Black for 10 minutes, cleared and mounted with Prolong Gold Antifade reagent containing DAPI.

#### **2.2.4.1.3 Nidogen/endomucin co-staining**

To assess endothelial basement membrane deposition in tumour vessels, paraffin sections of size-matched tumours were double-stained for nidogen (an endothelial basement membrane marker; Kohfeldt *et al.*, 1998) and endomucin. Paraffin sections were rinsed in PBS and antigen retrieval was carried out by boiling sections in sodium citrate buffer for 20 minutes. Paraffin sections were incubated with serum-free blocking solution for 30 minutes at 37°C. Subsequently, sections were incubated with rabbit anti-mouse nidogen antibody diluted 1:1000 and rat anti-mouse endomucin, antibody diluted 1:500 in PBLEC overnight at 4°C. Paraffin sections were washed in PBLEC 3 times for 5 minutes at room temperature, then incubated for 2 hours with Alexa-546 donkey anti-rabbit and Alexa-488 donkey anti-rat antibodies, diluted 1:200 in PBLEC. Paraffin sections were then washed in PBS 0.1% TRITON X-100, 3 times for 5 minutes. Sections were finally counterstained with 0.1% Sudan Black for 10 minutes, cleared and mounted with Prolong Gold Antifade reagent containing DAPI.

#### **2.2.4.1.4 Focal Adhesion Kinase/endomucin co-staining**

To examine focal adhesion complexes along tumour vessels, paraffin sections of size-matched tumours were double-stained for Focal Adhesion Kinase (FAK, Petit and Thiery, 2000) and endomucin. Paraffin sections were rinsed in PBS and antigen retrieval was carried out by boiling sections in sodium citrate buffer for 20 minutes. Paraffin sections were incubated with serum-free blocking solution for 30 minutes at 37°C. Subsequently, sections were incubated with rabbit anti-mouse FAK antibody diluted 1:100 and rat anti-mouse endomucin antibody diluted 1:500 in PBLEC overnight at 4°C. Paraffin sections were washed in PBLEC 3 times for 5 minutes at room temperature, then incubated for 2 hours with Alexa-546 donkey anti-rabbit and Alexa-488 donkey anti-rat antibodies, diluted 1:200 in PBLEC. Paraffin sections were then washed in PBS 0.1% TRITON X-100, 3 times for 5 minutes. Sections were finally counterstained with 0.1% Sudan Black for 10 minutes, cleared and mounted with Prolong Gold Antifade reagent containing DAPI.

#### **2.2.4.1.5 Live staining of luminal CD31**

To examine tumour vessel function in terms of patency and perfusion, 10 minutes prior to sacrifice, tumour bearing-mice were lethally anaesthetized and injected systemically with PE-conjugated anti-mouse CD31 antibody (5µg/100µl in PBS). Before tumour harvest, mice were perfuse-fixed by systemic injection of PFA. Tumours were fixed for an 2 additional hours and then embedded in 5% melted agarose. Agarose blocks were left to solidify at room temperature and then sectioned on a vibratome. 20-40 µm vibratome sections were collected in 24-well-plates, permeabilised in 0.25% Triton X-100 for 30 minutes, washed in PBLEC 3 times for 15 minutes and then incubated with serum-free blocking solution for 30 minutes at 37°C. Sections were incubated with rat anti-mouse-endomucin antibody diluted 1:500 in PBS overnight at 4°C. Sections were then washed in PBS 0.1% TRITON X-100 three times for 15 minutes and then incubated with Alexa-488 donkey anti-rat antibody, diluted 1:200 in PBLEC for 2 hours at room temperature. Vibratome sections were finally washed in PBS 0.1% TRITON X-100 3 times for 15 minutes, transferred to glass slides and then mounted with Prolong Gold Antifade reagent containing DAPI.

#### **2.2.4.1.6 Analysis of tumour vascular phenotype**

Images were acquired on an Axioplan epifluorescent microscope and tissue area was quantified using ImageJ software. The characterisation of tumour vascular phenotype was performed as follows:

- tumour blood vessel density was assessed as number of endomucin positive vessels across the entire tumour area;
- pericyte coverage was assessed as number of double positive αSMA/endomucin vessels per field. Ten fields for each tumour section were counted;
- endothelial basement membrane deposition was assessed as number of double positive nidogen/endomucin vessels per field. Ten fields for each tumour section were counted;
- endothelial FAK levels were assessed as number of double positive FAK/endomucin vessels per field. Ten field for each tumour section were counted;
- pattern of vessel distribution was visualized as the distribution of endomucin staining in the whole tumour area;

- depth of perfusion was quantified as maximum depth of double positive CD31/endomucin vessels from the tumour border (in  $\mu\text{m}$ ). Ten fields for each tumour section were measured.

#### **2.2.4.2 Lung sections**

Lungs from  $\beta 3$ -floxed/Tie1Cre positive and negative mice were fixed in PFA for 24 hours. Fixed lungs were dehydrated through a graded series of ethanols (50% - 70% - 90% - 95% - 100%, 2 changes 1 hour each) to xylene (overnight), and finally embedded in liquid paraffin (62°C, two changes of two hour each under vacuum). Lungs were transferred to histology cassettes and left to solidify in paraffin at room temperature. Paraffin blocks were sectioned on a microtome, 5 $\mu\text{m}$ -thick sections were mounted onto glass slides and dried overnight at 37°C. Before staining, paraffin sections were deparaffinised in xylene and rehydrated in a graded series ethanol (100% - 95% - 90% - 70% - 50%, two changes of ten minutes each).

##### **2.2.4.2.1 H&E staining**

Following deparaffinisation, lung sections were stained with Mayer's Hemotoxylin for 8 minutes and then rinsed under warm tap water for 10 minutes. Following a rinse in distilled water and 95% ethanol (10 dips), sections were counterstained in eosin-phloxine B solution for 1 minute. Slides were then dehydrated as follows: 70% - 95% - 100% - xylene two changes of ten minutes each. Slides were finally mounted with DEPEX mounting solution.

##### **2.2.4.2.2 Endomucin staining**

To examine lung blood vessels, sections of were stained for endomucin as described in 2.2.4.1.1.

##### **2.2.4.2.3 F4/80 staining**

Following deparaffinisation, antigen retrieval of lung sections was performed in trypsin buffer where slides were immersed at 37°C for 5 minutes. Paraffin sections were rinsed in PBS and blocked by incubating with serum-free blocking solution for 30 minutes at 37°C. Subsequently, sections were incubated with rat anti-mouse F4/80-FITC conjugated antibody diluted 1:100 in PBS overnight at 4°C. Paraffin

sections were then washed in PBS 0.1% TRITON X-100, 3 times for 5 minutes. Sections were finally counterstained with 0.1% Sudan Black for 10 minutes, cleared and mounted with Prolong Gold Antifade reagent containing DAPI.

#### **2.2.4.2.4 Analysis of lung metastatic phenotype**

Images were acquired on an Axioplan epifluorescent microscope and tissue area was quantified using ImageJ software. The characterization of lung metastatic phenotype was performed as follows:

- total number of lung metastases;
- area of lung covered by metastases expressed as ratio of metastatic area against total lung area (%);
- blood vessel density in metastases was assessed by counting the total number of endomucin positive vessels within metastatic lung areas;
- infiltrating macrophages were assessed as total number of F4/80 positive cells within metastatic lung areas.

#### **2.2.4.3 Wholemounds of tumours**

To assess Cre Recombinase activity, tomato fluorescence in tumours grown in Tie1Cre positive/tdTomato heterozygous and Pdgfb-iCreER<sup>T2</sup> positive/tdTomato heterozygous mice was used as a readout for its distribution in tumour tissue. Before tumour harvest, mice were perfuse-fixed by systemic injection of PFA. Tumours were dissected, fixed for 2 additional hours and then embedded in 5% melted agarose. Agarose blocks were left to solidify at room temperature and then sectioned on a vibratome. 20-40 µm vibratome sections were collected in 24-well-plates, permeabilised in 0.25% Triton X-100 for 30 minutes, washed in PBS 3 times for 15 minutes and then incubated with serum-free blocking solution for 30 minutes at 37°C. Sections were incubated with rat anti-mouse endomucin antibody diluted 1:500 in PBS overnight at 4°C. Sections were then washed in PBS 0.1% TRITON X-100 3 times for 15 minutes and then incubated with Alexa-488 donkey anti-rat antibody diluted 1:200 in PBLEC for 2 hours at room temperature. Vibratome sections were finally washed in PBS 0.1% TRITON X-100 3 times for 15 minutes, transferred to glass slides and then mounted with Prolong Gold Antifade reagent containing DAPI.

#### **2.2.4.3.1 Live staining of luminal $\beta$ 3-integrin**

To assess Cre endothelial specificity *in vivo*, endothelial  $\beta$ 3-integrin was stained *in vivo* within the tumour vasculature. 10 minutes prior to sacrifice,  $\beta$ 3-floxed/Tie1Cre and  $\beta$ 3-floxed/Pdgfb-iCreER<sup>T2</sup> positive and negative tumour bearing mice were lethally anaesthetized and injected systemically with PE-conjugated anti- $\beta$ 3-integrin (5 $\mu$ g/100 $\mu$ l in PBS). Before tumour harvest, mice were perfusion-fixed by systemic injection of PFA. Tumours were dissected, fixed for 2 additional hours and then embedded in 5% melted agarose. Agarose blocks were left to solidify at room temperature and then sectioned on a vibratome. 20-40  $\mu$ m vibratome sections were collected in 24-well-plates, permeabilized in 0.25% Triton X-100 for 30 minutes, washed in PBS 3 times for 15 minutes and then incubated with serum-free blocking solution for 30 minutes at 37°C. Sections were incubated with FITC-conjugated Isolectin-B4 (IB4, 2  $\mu$ g/ml in PBS) overnight at 4°C. Vibratome sections were finally washed 3 times PBS 0.1% TRITON X-100 3 times for 15 minutes, transferred to glass slides and then mounted with Prolong Gold Antifade reagent containing DAPI.

#### **2.2.4.3.2 Analysis of Cre activity and specificity *in vivo***

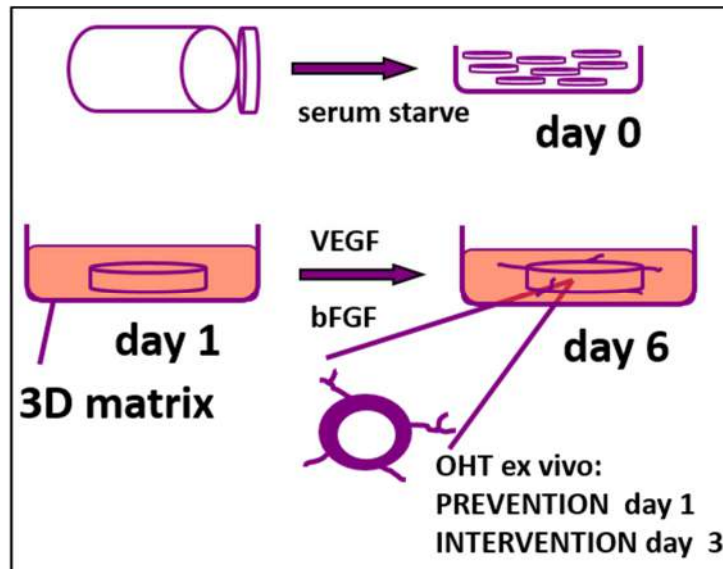
Images were acquired on an Axioplan epifluorescent microscope and tissue area was quantified using ImageJ software. The analysis of Tomato Cre Recombinase reporter activity *in vivo* was performed as follow:

- endothelial specific Cre activity was assessed as double positive endomucin/tomato vessels across the whole tumour area;
- endothelial specific Cre efficiency was assessed as double positive  $\beta$ 3-integrin/IB4 vessels across the whole tumour area.

#### **2.2.5 *Ex vivo* aortic ring assay**

The aortic ring assay was performed as described by Baker *et al.*, (2011). Animals were euthanized by cervical dislocation and sterilized by spraying with 70% ethanol. The chest cavity was opened using surgical scissors. Thoracic aortae from  $\beta$ 3-floxed/Tie1Cre positive and negative mice,  $\beta$ 3-floxed/Pdgfb-iCreER<sup>T2</sup> positive and negative mice, Tie1Cre positive/*tdTomato* heterozygous and Pdgfb-iCreER<sup>T2</sup> positive/*tdTomato* heterozygous mice (2 months or older) were dissected, cut into

rings of approximately 0.5 mm in width and serum-starved in OptiMEM overnight at 37°C.



#### 2.2.5.1 VEGF aortic angiogenesis in collagen gel

Aortic rings were embedded in a 96-well-plate (one ring per well) containing Collagen I gel (1 mg/ml in DMEM-H<sub>2</sub>O mix) on ice to prevent polymerisation, while embedding the ring under the dissection microscope. After collagen polymerisation (for 30 minutes at 37°C), rings were fed with OptiMEM supplemented with 2.5% FBS and VEGF (30 ng/ml), then incubated at 37°C. Aortic rings from  $\beta 3$ -floxed/Pdgfb-iCreER<sup>T2</sup> positive and negative mice and from Pdgfb-iCreER<sup>T2</sup> positive/TdTomato heterozygous mice were also supplemented with OHT (1  $\mu$ M). Unstimulated rings were used as controls. Rings were fed every 2 days with fresh medium with or without VEGF (30 ng/mL). Sprouting microvessels were counted after 6 days after fixation and staining. For intervention scheme, OHT (1  $\mu$ M) was added 3 days after ring embedding and the sprouting microvessels were counted at day 8.

#### 2.2.5.2 bFGF aortic angiogenesis in fibrin gel

Aortic rings were embedded in a 96-well-plate (one ring per well) containing fibrin gel. The catalysis of polymerization of fibrinogen (3 mg/ml) into fibrin required thrombin addition (1U/ml) to the fibrinogen solution on ice. After fibrin polymerisation (for 10 minutes at room temperature), rings were fed with OptiMEM supplemented with bFGF (30 ng/ml) and aprotonin (10 ng/ml), then incubated at 37°C. Aortic rings from

$\beta$ 3-floxed/Pdgfb-iCreER<sup>T2</sup> positive and negative mice and from Pdgfb-iCreER<sup>T2</sup> positive/tdTomato heterozygous mice were also supplemented with OHT (1  $\mu$ M). Unstimulated rings were used as control. Rings were fed every 2 days with fresh medium with or without bFGF (30 ng/mL). Sprouting microvessels were counted after 6 days after fixation and staining.

### **2.2.5.3 Aortic ring staining**

6 or 8 day-rings were fixed with 4% PFA, permeabilized with 0.25% Triton X-100 and incubated with serum-free blocking solution for 30 minutes at 37°C. Aortic rings were stained with FITC-conjugated IB-4 diluted 1:2000 in PBLEC overnight at 4°C. Rings were then washed PBS 0.1% TRITON X-100 3 times for 15 minutes, excised from the gel, transferred to glass slides and then mounted with Vectashield mounting medium.

Aortic rings from Tie1Cre positive/tdTomato heterozygous and Pdgfb-iCreER<sup>T2</sup> positive/tdTomato heterozygous mice were costained with FITC-conjugated IB4 diluted 1:2000, plus rabbit anti-mouse NG-2 (a pericyte marker; Gerhardt and Betsholtz, 2003) antibody diluted 1:1000 in PBLEC overnight at 4°C. For NG-2 detection, rings were then washed PBS 0.1% TRITON X-100 3 times for 15 minutes and then incubated with Alexa-546 donkey anti-rabbit antibody, diluted 1:200 in PBLEC for 2 hours at room temperature. Rings were finally washed in PBS 0.1% TRITON X-100 3 times for 15 minutes, excised from the gel, transferred to glass slides and then mounted with Vectashield mounting medium.

Phase contrast and fluorescent images were taken using an inverted microscope equipped with a camera. Microvessel sprouting was quantified by counting the number of sprouts per ring, whereas endothelial specific Cre Recombinase activity was evaluated as double positive endomucin/tdTomato microvessels and single tdTomato positive/NG-2 negative microvessels.

### **2.2.5.4 Protein isolation from aortae**

Aortae from  $\beta$ 3-floxed/Tie1Cre and  $\beta$ 3-floxed/Pdgfb-iCreERT2 positive and negative mice were separately collected for protein isolation. Whole aortae (3 per genotype) were transferred to eppendorf tubes and mashed with a 1.5-ml tube pestle. Aortic tissue was then lysed in ESB sample buffer for subsequent Western blot analyses

(see paragraph 2.2.7.6). The efficiency of Cre recombinase was measured by densitometry as a reduction of  $\beta$ 3-integrin protein level in aortic tissue.

## **2.2.6 Cell isolations**

### **2.2.6.1 Isolation of bone marrow cells**

Bone marrow cells were isolated from long bones (femurs and tibiae) of  $\beta$ 3-floxed/Tie1Cre positive and negative mice to investigate Tie1Cre-non-specific activity as the *Tie1* gene is expressed in bone marrow cells.  $\beta$ 3-floxed/Pdgfb-iCreER<sup>T2</sup> positive and negative mice were included in the analysis for the sake of consistency. Mice were euthanized by cervical dislocation, sterilized by spraying with 70% ethanol and back legs were dissected using surgical scissors. Skin and muscle tissues were removed from bones and their extremities cut off. Bones were transferred into a 0.5 ml eppendorf with a hole in its end and placed within a bigger 1.5 ml eppendorf. Samples were centrifuged for 2 minutes at 7000 rpm.

Bone marrow cells were pelleted in the 1.5 ml eppendorf, while the 0.5 eppendorf containing the bones was discarded. Cells were then resuspended in FACS buffer and counted to be plated at the cell concentration of  $5 \times 10^5$  cells/well in a 96-well-plate for subsequent flow cytometry. Bone marrow cells were co-stained with and PE-conjugated anti- $\beta$ 3-integrin and the following antibodies for hematopoietic cell lineage markers: FITC-conjugated anti-CD45, FITC-conjugated anti-Ly6G, FITC-conjugated anti-CD3, Alexa Fluor488-conjugated anti-CXCR4 (CD184) and FITC-conjugated anti-F4/80. All antibodies were diluted 1:200 in FACS Buffer. After incubating 20 minutes on ice, bone marrow cells were washed 2 times in PBS to remove unbound antibody and pelleted by centrifugation.

Acquisition of samples was performed on Accuri C6 flow-cytometer ( $1 \times 10^5$  cells per sample were collected). FACS analyses included unstained and isotope control samples which were used to determine appropriate gates and voltages. Data were analysed with CELLQUEST software. The gating strategy was as follows: a polygon gate was created on a FSC-A (Forward Scatter Area) vs. SCA-A (Side Scatter Area) plot to select for viable cells and exclude debris (Live gate), followed by a quadrant plot displaying the resulting daughter population to compare the percentage of bone marrow cell subpopulations (CD45+, Ly6G+, CD3+, CXCR4+), which were co-expressing  $\beta$ 3-integrin or not.

### 2.2.6.2 Isolation of platelets

Platelet isolation from peripheral blood was performed in  $\beta 3$  flox/flox/Pdgfb-iCreER<sup>T2</sup> positive and negative mice to investigate Pdgfb-iCre-non-specific activity, as the *Pdgfb* gene is expressed in megakaryocytes.  $\beta 3$ -floxed/Tie1Cre positive and negative mice were included in the analysis for the sake of consistency. Mice were lethally anaesthetized and peripheral blood from the *vena cava* was collected in 1.5 ml eppendorf tubes containing anti-coagulant buffer. Blood samples were centrifuged for 7 minutes at 300 rpm. The resulting platelet rich plasma was transferred to a fresh tube and centrifuged for 7 min at 2000 rpm. The supernatant was carefully discarded and the final pellet was lysed in ESB lysis buffer in order to be processed by Western blot to quantify total levels of  $\beta 3$  integrin protein in platelets (see paragraph 2.2.7.6).

### 2.2.6.3 Isolation of tumour endothelial cells

Tumour bearing  $\beta 3$ -floxed/Tie1Cre and  $\beta 3$ -floxed/Pdgfb-iCreER<sup>T2</sup> positive and negative mice were euthanized by cervical dislocation and sterilized by spraying with 70% ethanol. B16F0 or CMT19T tumours were dissected using surgical scissors and placed in Hank's Balanced Salt Solution (HBSS). They were finely minced with a scalpel and enzymatically digested in HBSS containing 0.2% collagenase IV, 0.01% hyaluronidase and 0.01% DNase I for 1 hour at 37°C under gentle agitation. Tumour cell digests were passed 3 times through a 19G needle by using a 20 ml syringe and then filtered through a 70 $\mu$ m mesh to produce a single cell suspension. Tumour cells were pelleted by low speed-centrifugation for 5 minutes at 1000 rpm. After centrifugation, cells were resuspended in HBSS containing 2% BSA and 0.6% sodium citrate. Cell yield was determined in a hemocytometer and viability assessed by trypan blue exclusion.

Tumour endothelial cell separation was performed by magnetic separation using rat anti-mouse CD31 coupled to magnetic beads. Dynabeads Antibody Coupling Kit was used to covalently couple the anti-CD31 antibody to the surface of magnetic beads according to the manufactures' instructions. Tumour cells suspensions were incubated with anti-CD31 coupled-Dynabeads at a ratio of 30 beads per target cell (estimated at 1% of total cell count) at 4°C for 25 minutes and with occasional agitation. Bound cells were separated from unbound cells on a magnetic sorter, which allowed the bead-bound cells to be separated from the non-bead-bound cells and the remaining cell suspension was discarded carefully. To assess the degree of Cre

Recombinase efficiency *in vivo*, CD31 positive tumour endothelial cells were lysed in ESB lysis buffer and prepared for Western blot (see paragraph 2.2.7.6).

#### **2.2.6.3.1 Analysis of Tumour-Associated Macrophages**

In order to assess  $\beta$ 3-integrin expression levels in Tumour-Associated Macrophages (TAMs), tumour cells were isolated from tumours grown in  $\beta$ 3-floxed/Tie1Cre positive and negative mice. Tumour cell suspensions (isolated as described in 2.2.6.3, but without performing CD31 magnetic separation) were collected in FACS tubes and 1 ml of red blood lysis buffer was added for 1 minutes. Cell were centrifuged for 5 minutes at 1000 rpm and resuspended in FACS buffer. Tumour cells were then plated in a 96-well-plate ( $5 \times 10^5$  cells/well) and co-stained with PE-conjugated anti-mouse  $\beta$ 3-integrin and FITC-conjugated anti-mouse F4/80 (macrophage marker, Schmierer *et al.*, 2012) diluted 1:200 in FACS buffer. After a 20 minute incubation with primary antibodies on ice, tumour cells were washed 2 times in PBS to remove unbound antibody and pelleted by centrifugation.

Acquisition of samples was performed on Accuri C6 flow-cytometer ( $1 \times 10^5$  cells per sample were collected). FACS analysis included unstained and isotope control samples which were used to determine appropriate gates and voltages. Data were analysed with CELLQUEST software. The gating strategy was as follows: a polygon gate was created on a FSC-A (Forward Scatter Area) vs. SCA-A (Side Scatter Area) plot to select for viable cells and exclude debris (Live gate), followed by a quadrant plot displaying the resulting daughter population to compare the percentage of tumour associated macrophages (F4/80+), which were co-expressing or not  $\beta$ 3-integrin.

#### **2.2.6.4 Isolation of lung endothelial cells**

Primary lung endothelial cell isolation from  $\beta$ 3-floxed/Tie1Cre and  $\beta$ 3-floxed/Pdgfr- $\beta$ CreER<sup>T2</sup> positive and negative 6 to 8 week-old mice was carried out in multiple steps as described below.

##### **2.2.6.4.1 Collagenase treatment of lung**

All dissection procedures were performed under sterile conditions in a tissue culture hood. Animals were euthanized by cervical dislocation and sterilized by spraying with 70% ethanol. The chest cavity was opened using surgical scissors and lungs

dissected using forceps. Lungs were rinsed briefly by immersing first in 70% ethanol and subsequently in Ham's F12 medium supplemented with penicillin and streptomycin.

Tissues were minced with a scalpel into small pieces until a fine homogenate was produced and digested in 0.1 % Collagenase I supplemented with 1 mM CaCl<sub>2</sub> and 1mM MgCl<sub>2</sub> for 1 hour at 37°C. Lung digests were passed 3 times through a 19G needle by using 20 ml syringe and then filtered through a 70µm mesh to produce a single cell suspension. Lung cells were then centrifuged for 5 minutes at 1200 rpm and resuspended in Mouse Lung Endothelial Cell (MLEC) medium. Cell suspensions were plated into pre-coated-tissue culture 6-well-plates which were coated with coating solution which was removed just prior to cell plating. Lung endothelial cells from each mouse were cultured as single isolates. After overnight incubation at 37°C and 5% CO<sub>2</sub>, lung endothelial cells were washed 3 times with PBS to remove cell debris and red blood cells, and refed with fresh MLEC medium.

#### **2.2.6.4.2 ICAM-2 magnetic sorting**

Positive magnetic sorting was performed using an antibody against an endothelial cell marker, ICAM-2 (Intracellular Cell Adhesion Molecule 2). When cells reached approximately 70% confluency, the medium was removed, replaced with fresh MLEC and cells were incubated at 4°C for 30 minutes. Cells were then washed in PBS and incubated at 4°C for 30 minutes in PBS containing rat anti-mouse ICAM-2 antibody diluted 1:1000. Following antibody incubation, cells were washed in PBS and incubated with MLEC containing 1 µl/ml of sheep anti-rat IgG Dynabeads at 4°C for 30 minutes. Cells were washed three times to remove unbound beads and then trypsinized with 0.25% trypsin:EDTA. Detached cells were resuspended in MLEC, collected in an eppendorf tube and put on a magnetic sorter, which allowed the bead-bound cells to be separated from the non-bead-bound cells. Since the beads were attached to ICAM-2 positive cells, the remaining cell suspension was carefully discarded. Bound cells were resuspended in MLEC and plated into a pre-coated-tissue culture 6-well-plate. Cells were fed every 2 days until colonies of approximately 20-30 cells were apparent. When they neared confluency, an additional ICAM-2 positive sorting was performed in order to enhance the endothelial cell purity.

#### **2.2.6.4.3 Generation of immortalized lung endothelial cells**

Due to their slow growth and limited capacity to divide in culture, it is difficult to obtain sufficient quantities of primary lung endothelial cells to perform extensive *in vitro* analyses. I therefore opted to immortalize lung endothelial cells via Polyoma-Middle-T-antigen lentiviral infection (May *et al.*, 2005). The mouse GgP+E cell line was employed for the production of polyoma-middle-T-antigen lentiviral vectors (May *et al.*, 2005). After thawing, GgP+E packaging cells were seeded at  $1.5 \times 10^6$  cells in T25 flasks and, when cultures were confluent, cells were detached with 0.25% trypsin:EDTA. At the following passage, GgP+E cells were seeded  $2 \times 10^6$  cells/T25 flask, fed the next day with 2 ml of culture medium and, on the third day, the conditioned medium was collected.

The Polyoma-Middle-T virus conditioned medium centrifuged at 2800 rpm for 15 minutes and filtered through a  $0.45 \mu\text{m}$  strainer. After filtration, the supernatant was aliquoted and stored at  $-80^\circ\text{C}$ . ICAM-2 positive lung endothelial cells were immortalized by incubating with polyoma-middle-T-antigen virus conditioned medium in presence of polybrene ( $8 \mu\text{g/ml}$ ) to increase infection efficiency. The virus-containing medium was replaced 6 hours later with fresh MLEC medium and the same procedure was repeated the following day.

#### **2.2.6.4.4 Growth and maintenance of immortalized lung endothelial cells**

Immortalized lung endothelial cells were cultured at  $37^\circ\text{C}$  with 5%  $\text{CO}_2$  in air in Mouse Immortalized Lung Endothelial Cell medium (ImMLEC). Cells were usually passaged when they reached ~80-90% confluency and used up to passage 15. Early passage (3-6) immortalized lung endothelial cells were frozen down in freezing medium (10% DMSO in Foetal Bovine Serum) at  $10^6$  cells/cryogenic vial. Vials were initially stored at  $-80^\circ\text{C}$  and subsequently transferred to a liquid nitrogen tank for long-term storage.

#### **2.2.6.4.5 Phenotypic analysis of immortalized lung endothelial cells**

In order to characterize the phenotype of immortalized lung endothelial cell cultures, flow cytometry, immunocytochemistry and Western blot analyses were performed. The endothelial cell markers ICAM-2 and CD31 were evaluated by flow cytometric analyses. Subconfluent immortalized lung endothelial cells were trypsinized, resuspended in FACS buffer and plated in a 96-well-plate ( $5 \times 10^5$  cells/well). Staining was performed using PE-conjugated anti-mouse ICAM-2 antibody and PE-conjugated anti-mouse CD31 antibody, diluted 1:200 in FACS buffer. After a 20

minute incubation with primary antibody on ice, cells were washed 2 times in PBS to remove unbound antibody and pelleted by centrifugation.

Acquisition of samples was performed on an Accuri C6 flow-cytometer (1x10<sup>5</sup> cells per sample were collected). FACS analysis included unstained and isotope control samples which were used to determine appropriate gates and voltages. Data were analysed with CELLQUEST software. The gating strategy was as follows: a polygon gate was created on a FSC-A (Forward Scatter Area) vs. SCA-A (Side Scatter Area) plot to select for viable cells and exclude debris (Live gate), followed by a histogram plot displaying the resulting daughter population to visualize the subpopulations expressing ICAM-2 and CD31 respectively. The endothelial cell marker VE-cadherin (VEC) was evaluated by immunocytochemistry. Subconfluent immortalized lung endothelial cells were trypsinized and seeded in a 6-well-plate (2x10<sup>5</sup> cells/well) containing 10 mm glass coverslips (previously acid washed and coated with a coating solution overnight at 4°C). Cells were left to adhere overnight and then fixed with PFA on coverslips for 10 minutes at room temperature. Cells were washed with PBS 3 times for 5 minutes and permeabilised with NP40 solution for 10 minutes at room temperature.

Cells were washed again in PBS for 3 times for 5 minutes and blocked for 10 minutes at room temperature. Cells were then incubated with rabbit anti-mouse VEC antibody diluted 1:100 for 1 hour at room temperature. Following antibody incubation, cells were washed with PBS to remove unbound antibody and incubated with Alex Fluor-555 anti-rabbit antibody diluted 1:200 in PBS for 1 hour at room temperature. Finally coverslips were washed in PBS and mounted on glass slides with Prolong Gold Anti-fade reagent containing DAPI. Images were acquired on an Axioplan epifluorescent microscope. To assess the degree of Cre recombinase efficiency *in vitro*, immortalized lung endothelial cells were plated at 2x10<sup>5</sup> cells/well in a 6-well-plate, grown until ~ 80-90% confluency and lysed in 500 µl/well in ESB lysis buffer for Western blot analyses to quantify total level of β3-integrin protein (see paragraph 2.2.7.6).

#### **2.2.6.4.6 Analysis of macrophages in the pre-metastatic lung**

To examine myeloid cells infiltration in the lung during the pre-metastatic phase, flow cytometry analysis was performed. Lungs from β3-floxed/Tie1Cre positive and negative mice in which CMT19TF1 cells had been grown, were isolated at the time

of surgical resection of the primary tumour. Lung cell suspensions (isolated as described in 2.2.6.4.1) were collected in FACS tubes and 1 ml of red blood lysis buffer was added for 1 minutes. Cells were centrifuged for 5 minutes at 1000 rpm and resuspended in FACS buffer. Lung cells were then plated in a 96-well-plate ( $5 \times 10^5$  cells/well). Staining was performed with FITC anti-CD45 and PE anti-CD11b antibodies to detect myeloid cells and FITC anti-F4/80 and APC-eFluor 780 anti- $\beta$ 3-integrin antibodies. All antibodies were diluted 1:200 in FACS buffer. After a 20 minute incubation with primary antibodies on ice, lung cells were washed 2 times in PBS to remove unbound antibody and pelleted by centrifugation.

Acquisition of samples was performed on an Accuri C6 flow-cytometer ( $1 \times 10^7$  cells per sample were collected). FACS analysis included unstained and isotope control samples which were used to determine appropriate gates and voltages. The gating strategy was as follows: a polygon gate was created on the FSC-A (Forward Scatter Area) vs. FSC-H (Forward Scatter Height) plot to select for Single cells that passed by the lasers individually. These cells were then viewed on a FSC-A vs. SCA-A (Side Scatter Area) plot to select for viable cells and exclude debris (Live gate), following by a quadrant plot displaying the resulting daughter population to quantify myeloid cell (CD45+/CD11b+) and  $\beta$ 3-integrin expressing macrophage ( $\beta$ 3+/F4/80+) subpopulations.

### **2.2.7 *In vitro* cell assays**

$\beta$ 3-floxed/Tie1Cre and  $\beta$ 3-floxed/Pdgfb-iCreER<sup>T2</sup> positive and negative immortalized lung endothelial cells were employed to study the cellular and molecular differences between the two transgenic models *in vitro*.

#### **2.2.7.1 Staining for endothelial cell markers and surface integrins**

In order to examine changes in surface integrin expression upon  $\beta$ 3-integrin deletion, I performed flow cytometry analyses. Subconfluent immortalized lung endothelial cells were trypsinized, resuspended in FACS buffer and plated in a 96-well-plate ( $5 \times 10^5$  cells/well). The presence of  $\alpha$ 1,  $\alpha$ 2,  $\alpha$ 5,  $\alpha$ v,  $\beta$ 1 and  $\beta$ 3-integrin subunits on the cell surface were examined using PE-fluorescently labelled anti-mouse antibodies diluted 1:200 in FACS buffer. After a 20 minute incubation with primary antibodies on ice, cells were washed 2 times in PBS to remove unbound antibody and then pelleted by centrifugation.

Acquisition of samples was performed on an Accuri C6 flow-cytometer ( $1 \times 10^5$  cells per sample were collected). FACS analysis included unstained and isotope control samples which were used to determine appropriate gates and voltages. Data were analysed with CELLQUEST software. The gating strategy was as follows: a polygon gate was created on a FSC-A (Forward Scatter Area) vs. SCA-A (Side Scatter Area) plot to select for viable cells and exclude debris (Live gate), followed by a histogram plot displaying the resulting daughter population to visualize the subpopulation expressing the single integrin subunits.

### **2.2.7.2 MTT Proliferation assay**

Immortalized lung endothelial cells were seeded at  $1 \times 10^4$  cells/well in OptiMEM supplemented with 2% FBS in a 96-well-plate and stimulated with VEGF (30 ng/ml). Unstimulated cells were used as a control. After 24 and 48 hours the medium was removed and replenished with fresh before adding 12 mM MTT 3-(4,5-dimethylthiazol-2-yl)-2,5-diphenyltetrazolium bromide. Cells were then incubated for 4 hours at 37°C. The insoluble product of MTT conversion was solubilized by the addition of DMSO (50  $\mu$ l/well) and absorbance was measured at 540 nm. Absorbance values were normalized to the DMSO negative control and the rate of proliferation was determined as relative to absorbance values in unstimulated cells.

### **2.2.7.3 Scratch wound assay**

Immortalized lung endothelial cells were seeded in 6-well-plates ( $4 \times 10^5$  cells/well) and cultured until they reached confluence. Cells were serum-starved for 3 hours in OptiMEM, then a scratch wound was introduced with a 200  $\mu$ l-pipette tip and photographed as a zero time point. OptiMEM was replaced to remove scratched cells and cells were incubated with fresh OptiMEM supplemented with VEGF (30 ng/ml). Unstimulated cells were used as a control. To assess the rate of migration cells were photographed in the following 24 hours, using an inverted phase-contrast microscope. Axiovision software was used for measuring the scratch width and the average distance between leading cells in 3 positions (three points of the scratch wound; top, centre, bottom). Scratches were re-photographed, and the percentage of migration was determined relative to the scratch width at the zero time point.

#### **2.2.7.4 Endothelial cell adhesion assay**

96-well-plates were coated with single matrix compounds (collagen I, 10µg/ml; fibronectin, 10µg/ml; laminin I, 10µg/ml; vitronectin, 10µg/ml) at 4°C overnight. The following day, the coating solution was removed and 96-well-plates were blocked with 2% BSA for 1 hour at 37°C. BSA and plastic only separate wells were used as negative and positive controls for cell adhesion, respectively. Immortalized lung endothelial cells were seeded at  $1 \times 10^4$  cells/well into the coated well and incubated for 60 minutes at 37°C. Cells were gently washed with PBS 3 times to remove non-adhered cells. Attached cells were fixed with PFA for 10 minutes and subsequently stained with Methylene Blue (0.01% in 0.01M borate buffer) for 30 minutes. Stained cells were then washed with water and incubated with destain solution (1:1 mix EtOH:HCl 0.1M) for 10 minutes. Absorbance was measured at 630 nm and assessed in 8 replicates per condition. The OD value of cells adhered to fibronectin was assigned the value of 100% and relative adhesion was calculated.

#### **2.2.7.5 VEGF stimulation time course**

Changes in expression of total and phosphorylated levels of VEGFR2 and its downstream effectors (ERK1/2, FAK, p38, PLCγ) were assessed by Western blot analyses after a time course of VEGF stimulation.  $4 \times 10^5$  cell/well were plated in a 6-well-plate and grown until they reached 80-90% confluency. Cells were starved for 3 hours in OptiMEM and then stimulated with VEGF (30 ng/ml) for 5-10-15-30-60 minutes at 37°C. Unstimulated cells were used as a control. Cells were washed three times with PBS, scraped off using a cell scraper and lysed in ESB lysis buffer for subsequent Western blot analyses.

#### **2.2.7.6 Western blot analysis**

##### **2.2.7.6.1 Sample preparation**

ESB lysed cells and tissues were transferred to cap-locked tubes containing acid washed glass beads and homogenized with a tissue lyser at 50 Hertz for 2 minutes. Homogenates were centrifuged at 10000 rpm for 10 minutes at room temperature, to pellet insoluble material. Supernatants were transferred to new tubes and analysed for protein concentration. Samples were either immediately used or stored at -20°C

for future use. Frozen samples were thawed on ice and then vortexed briefly to obtain homogeneous lysates.

Protein concentrations were quantified using the Bio-Rad DC Protein Assay Kit. BSA standards of known concentrations were prepared alongside unknown samples. The protein concentration in each sample was determined as follows: 5  $\mu$ l of standard or unknown sample was mixed with 200  $\mu$ l of Bio-Rad Reagent B and with 25  $\mu$ l of a solution obtained by mixing 1 ml of Reagent A with 20  $\mu$ l of Reagent S, and incubated for 15 minutes at room temperature. After incubation, the absorbance was measured at 750 nm using a spectrophotometer. The protein concentrations of the unknowns were obtained from the standard curve plotted using GraphPad Prism software.

#### **2.2.7.6.2 SDS-PAGE protein separation**

A vertical gel apparatus was used for all polyacrylamide gels electrophoresis. For the proteins of interest (ranging from 40-kDa to 250-kDa) 8% acrylamide running gels were used. The running gel was poured into a gel cassette. After polymerisation, the stacking gel was loaded onto the resolving gel. Immediately, a 10- or 15-well comb was inserted and the gel was left to polymerise.

The gel apparatus was assembled and running buffer was poured into the gel tank. Equal amounts of protein from the lysates (10–20  $\mu$ g) were prepared for electrophoresis by diluting with 1X NuPAGE-LDS sample buffer supplemented with DTT. Samples were boiled at 95°C for 5 minutes, centrifuged at 10000 rpm for 1 minute and loaded into separate wells along with a well containing molecular weight protein ladder. The proteins underwent electrophoresis at 100 V, until the samples reached the bottom of the gel.

#### **2.2.7.6.3 Wet Transfer**

Once the proteins had been separated, the gel was removed from the electrophoresis cassette and transferred from the gel to nitrocellulose membrane using a transfer apparatus. The gel was positioned in a cassette next to the nitrocellulose membrane and between filter paper and fibre sponges all pre-wetted in cooled transfer buffer. Air bubbles during the assembly of the cassette were removed by rolling out with a plastic pipette. The cassette was assembled in the transfer apparatus, immersed in

transfer buffer, and proteins transferred to the membrane at 30 V for 2 hours at room temperature.

#### **2.2.7.6.4 Immunoblotting**

Once transferred, the membrane was stained with 0.1% Ponceau red to ensure complete and even transfer of all proteins. The membrane was rinsed with distilled H<sub>2</sub>O to remove excess stain. Nitrocellulose membranes were blocked in 5% milk protein, 0.1% Tween-20 in PBS for 30 minutes at room temperature, rinsed 3 times for 5 minutes with PBS 0.1% Tween-20 and incubated overnight at 4°C with primary antibody. Primary antibodies were all used at 1:1000 in PBS, 5% BSA, 0.1% Tween-20. The blots were then washed 3 times for 5 minutes with PBS 0.1% Tween-20, and incubated with the appropriate horseradish peroxidase (HRP)-conjugated secondary antibody diluted 1:2000 in 5% milk 0.1% Tween-20 for 2 hours at room temperature.

The membranes were finally washed 3 times with PBS for 5 minutes with 0.1% Tween-20 and developed. Immunoreactive bands were visualised by incubating the membranes with ECL chemiluminescence reagents for 1 minute. Chemiluminescence was detected on a Fujifilm LAS-3000 darkroom. Densitometry of band intensities was obtained using ImageJ software. Band densities were normalised to HSC-70 to make quantitative measurements of proteins of interest.

#### **2.2.8 Analysis of statistical significance**

Data sets were analysed for significance using Student's t test.  $P < 0.05$  was considered statistically significant. Unless otherwise indicated, results are the mean  $\pm$  SEM from at least 3 independent experiments.

### **3. THE TIMING OF ENDOTHELIAL $\beta$ 3-INTEGRIN DELETION AFFECTS TUMOUR GROWTH AND ANGIOGENESIS *IN VIVO***

Since  $\alpha$ v $\beta$ 3-integrin is expressed by a variety of cells, all of which can contribute to angiogenesis (Robinson and Hodivala-Dilke, 2011), I took a genetic *in vivo* approach to dissect the role of the endothelial-specific expression of  $\beta$ 3-integrin and test how its genetic targeting influences tumour growth and angiogenesis. In this chapter, I will describe my findings on the effect of the ablation of  $\beta$ 3-integrin on tumour growth and angiogenesis in two different endothelial specific Cre models where, unexpectedly, I observed divergent effects depending on when deletion occurred. I will also present validation data which confirm that  $\beta$ 3-integrin was effectively and specifically deleted in a similar fashion in the two Cre models.

## **RESULTS AND FIGURES**

### **3.1 Inducible loss of endothelial $\beta$ 3-integrin reduces tumour growth and inhibits angiogenesis, while the constitutive one does not**

In order to investigate whether ablation of  $\beta$ 3-integrin in endothelial cells had any effect on tumour growth and tumour associated angiogenesis, a genetic strategy based on Cre-loxP recombination was employed.  $\beta$ 3-integrin floxed mice (Morgan *et al.*, 2010), whereby the first exon of the  $\beta$ 3-integrin subunit gene (*Itgb3*) is flanked by loxP sites, were crossed with Tie1Cre transgenic mice (Gustaffson *et al.*, 2001) and with Pdgfb-iCreER<sup>T2</sup> transgenic mice (Claxton *et al.*, 2008).

Both *Tie1* and *Pdgfb* promoters drive Cre expression in endothelial cells, thereby restricting  $\beta$ 3 integrin deletion to vascular cells. The timing of deletion is different in the two transgenic lines. The *Tie1* promoter is expressed from E 8 allowing excision of floxed genes in endothelial cells by Cre recombinase activity during embryogenesis and in adulthood, acting as a cell-specific knock-out (as described in paragraph 3.1.1). Pdgfb-iCreER<sup>T2</sup> generates tamoxifen inducible endothelial cell-specific deficient mice, whereby Cre recombinase is activated in upon 4-hydroxytamoxifen administration, thereby mimicking a pharmacological treatment (as described in paragraph 3.1.2).

### 3.1.1 Constitutive deletion of endothelial $\beta$ 3-integrin

*Itgb3* floxed mice are viable and demonstrate functional activity of the *Itgb3* floxed allele (Morgan *et al.*, 2010). They will be hereafter be referred to as  $\beta$ 3-floxed mice. Mice expressing Cre recombinase under the control of the *Tie1* promoter (Gustafsson *et al.*, 2001) were intercrossed with homozygous  $\beta$ 3-floxed mice through multiple generations in order to generate  $\beta$ 3-floxedTie1Cre positive progeny, where  $\beta$ 3-integrin was genetically ablated in endothelial cells.

By cross-breeding to ROSA26R-lacZ reporter mice (Soriano, 1999), Gustafsson *et al.* (2001) have shown that Cre expression in Tie1Cre transgenic mice is expressed in endothelial cells as early as E8-E8.5. However, Cre recombinase activity in Tie1Cre positive animals was also reported to be present in certain neuronal populations and in a proportion (20%) of hematopoietic cells.

The presence of *Tie1Cre* transgene (600 bp) was determined by PCR analysis of DNA from tissues (earsnip or tail) or from cultured lung endothelial cells isolated from  $\beta$ 3-floxed/Tie1Cre mice (Figure 3.1A). Furthermore, the efficiency of Cre mediated recombination of the  $\beta$ 3-floxed gene was demonstrated by Western blot analysis, whereby lysates from  $\beta$ 3-floxed/Tie1Cre positive lung endothelial cells showed  $\beta$ 3-integrin protein expression reduction by approximately 70% when compared to protein lysates from  $\beta$ 3-floxedTie1Cre negative lung endothelial cells (Figure 3.1C).

### 3.1.2 Inducible deletion of endothelial $\beta$ 3-integrin

Alongside the endothelial specific Tie1Cre transgenic line, mice expressing Cre recombinase under the control of the *Pdgfb* promoter (Claxton *et al.*, 2008) were intercrossed with homozygous *Itgb3* floxed mice through multiple crosses in order to generate  $\beta$ 3-integrin/Pdgfb-iCreER<sup>T2</sup> positive progeny, where the genetic deletion of  $\beta$ 3-integrin could be induced in endothelial cells upon 4-hydroxytamoxifen administration. Claxton *et al.* (2008) have generated a modified Cre recombinase by fusion to a mutant form of the human estrogen receptor (ER<sup>T2</sup>), which is insensitive to naturally occurring estrogen; but selectively responsive to the artificial ligand 4-hydroxytamoxifen (hereafter referred to as OHT).

In  $\beta$ 3-floxed/Pdgfb-iCreER<sup>T2</sup> positive mice, Cre recombinase activity is present in endothelial cells within 48 hours after administration of 3-mg-OHT dose via oral

gavage, as assessed by X-Gal staining in a ROSA26R-lacZ background (Soriano, 1999). Nonetheless, recombination activity was also described in megakaryocytes.

The presence of the *Pdgfb-iCreER<sup>T2</sup>* transgene (473 bp) was evaluated by PCR analysis of DNA from tissues (earsnip or tail) or from cultured lung endothelial cells isolated from  $\beta$ 3-floxed/*Pdgfb-iCreER<sup>T2</sup>* mice (Figure 3.1A). The effective induction of  $\beta$ 3-integrin deletion was further confirmed at the protein level by Western blot analysis, whereby lysates from  $\beta$ 3-floxed/*Pdgfb-iCreER<sup>T2</sup>* positive lung endothelial cells showed  $\beta$ 3-integrin protein expression reduction by approximately 75%, when compared to protein lysates from  $\beta$ 3-floxed/*Pdgfb-iCreER<sup>T2</sup>* negative lung endothelial cells (Figure 3.1C).

### 3.1.3 Tumour models

B16F0 is a non-metastatic variant of the B16 cell line (Fidler, 1973). CMT19T is a mouse lung carcinoma cell line which has been derived from the more aggressive CMT167 (Layton and Franks, 1986). Both tumour cell lines are commonly used in tumour studies (Giavazzi and Decio, 2014; Kostourou *et al.*, 2013; Tavora *et al.*, 2014).

To determine whether the genetic background of the two endothelial Cre transgenic mice affected the ability of tumour cells to grow, tumour growth was assessed over time. Tie1Cre and *Pdgfb-iCreER<sup>T2</sup>* transgenic mice were injected subcutaneously with CMT19T tumour cells. Tumour growth was monitored by external caliper measurement every other day, starting from day 6 until day 12, when mice were sacrificed and tumours were harvested. No significant difference was detected in tumour growth when comparing  $\beta$ 3-floxed/Tie1Cre and  $\beta$ 3-floxed/*Pdgfb-iCreER<sup>T2</sup>* negative tumours, implying that tumour cells could equally grow in both transgenic models (Figure 3.2).

#### 3.1.3.1 B16F0

To study the effect of endothelial  $\beta$ 3-integrin deletion on tumour growth, Tie1Cre and *Pdgfb-iCreER<sup>T2</sup>* transgenic mice were injected subcutaneously with B16F0 melanoma cells. In  $\beta$ 3-floxed//*Pdgfb-iCreER<sup>T2</sup>* mice, Cre activity (therefore  $\beta$ 3-integrin deletion) was induced in endothelial cells by subcutaneous implantation of slow release 5-mg-tamoxifen pellets.

Unless otherwise specified, OHT treatment was administered 3 days before tumour cells injection (PREVENTION SCHEME) and both Pdgfb-iCreER<sup>T2</sup> positive and negative mice were treated. This allowed equal treatment of both mice groups and  $\beta$ 3-floxed/Pdgfb-iCreER<sup>T2</sup> negative mice served as control for possible OHT-induced side effects.

Over the time frame of 12 days, B16F0 allograft tumours grew significantly less in  $\beta$ 3-floxed//Pdgfb-iCreER<sup>T2</sup> positive mice as compared to their Cre negative littermate controls (Figure 3.3A). In contrast, tumour size was not significantly affected in  $\beta$ 3 flox/flox/Tie1-Cre mice (Figure 3.3A). If anything, there was a trend for subcutaneously-injected B16F0 tumours to grow larger in Tie1Cre positive mice compared to their Cre negative littermate controls.

To examine the effect of endothelial  $\beta$ 3-integrin deletion on tumour angiogenesis, blood vessel density was quantified by counting the numbers of endomucin+ blood vessels (a blood vascular endothelial cell marker; Morgan *et al.*, 1999) per unit area, across entire midline tumour sections from size-matched tumours which had been processed for immunohistological analysis (Figure 3.3C-3.4C). Consistent with growth, tumour angiogenesis was also significantly decreased in  $\beta$ 3-floxed//Pdgfb-iCreER<sup>T2</sup> positive tumours as compared to  $\beta$ 3-floxed//Pdgfb-iCreER<sup>T2</sup> negative tumours (Figure 3.3A); whilst not in tumours grown in  $\beta$ 3-floxed/Tie1Cre mice, where no significant difference was observed between Cre positive and negative tumours (Figure 3.4A).

Taken together, these results suggest that  $\beta$ 3-integrin expression on endothelium only affects tumour growth and angiogenesis when its inducible deletion, but not when its deletion has occurred through development (constitutive deletion).

### **3.1.3.2 CMT19T**

Further confirmation of the role of endothelial  $\beta$ 3-integrin in tumour growth and angiogenesis was accomplished by using the CMT19T cell line. CMT19T tumours were grown subcutaneously for 12 days in  $\beta$ 3-floxed//Tie1Cre and  $\beta$ 3-floxed/Pdgfb-iCreER<sup>T2</sup> mice following a prevention scheme. Both tumour size and tumour angiogenesis were significantly decreased in  $\beta$ 3-floxed//Pdgfb-iCreER<sup>T2</sup> positive mice as compared to  $\beta$ 3-floxed//Pdgfb-iCreER<sup>T2</sup> negative mice (Figure 3.3B) consistent with the results I obtained in the B16F0 model.

In contrast, Tie1Cre induced deletion had no effect on either CMT19T tumour growth or angiogenesis (Figure 3.4B), suggesting that the constitutive deletion of endothelial  $\beta$ 3-integrin behaved differently than the inducible deletion. CMT19T tumour growth and vessel density in  $\beta$ 3-floxed//Tie1Cre positive and negative mice actually reflected the same pattern observed in B16F0 studies, whereby they were both slightly increased in  $\beta$ 3-floxed/Tie1Cre positive mice compared to  $\beta$ 3-floxed/Tie1Cre negative mice, although neither of them reached statistical significance.

Overall using two mouse tumour cell lines, B16F0 melanoma and CMT19T carcinoma, I obtained similar results; this contributes to strengthening our findings. Therefore, I conclude that endothelial  $\beta$ 3-integrin is affecting tumour growth and tumour angiogenesis in a time dependent manner.

### **3.2 $\beta$ 3-integrin does not impact on tumour vessel structure or function**

Tumour vasculature is structurally and functionally abnormal (Jain, 2005). Given the importance of pericyte coverage and endothelial basement membrane support for vessel structure and function, I asked whether reduced tumour growth and angiogenesis in the presence of the inducible endothelial  $\beta$ 3-integrin deletion was linked to vascular defects in tumour vessels. Therefore, I assessed pericyte coverage and endothelial basement membrane deposition in B16F0 and CMT19T allografts by colocalization with pericyte and basement membrane markers through immunohistological analyses. Further, I characterized the pattern of vascular distribution and the degree of blood perfusion through the tumour vasculature by intravenous injection of phycoerythrin (PE) conjugated CD31 (also known as Platelet endothelial cell adhesion molecule - PECAM) to highlight vessel lumens *in vivo*.

#### **3.2.1 Structural analyses: pericyte and endothelial basement membrane coverage**

Histological analyses of 12-day CMT19T tumour vessels by double immunostaining for endomucin and  $\alpha$ Smooth Muscle Actin ( $\alpha$ SMA which identifies vSMCs and pericytes; Gerhardt and Betsholtz, 2003) revealed that the absence of  $\beta$ 3-integrin in endothelial cells had no effect on pericyte recruitment or organization along vessels, regardless of the time of the deletion. Indeed, there was no significant difference in the number of endomucin+/ $\alpha$ SMA+ vessels in either  $\beta$ 3-floxed/Tie1Cre positive or

$\beta$ 3-floxed//Pdgfb-iCreER<sup>T2</sup> positive tumours compared to their Cre negative counterparts (Figure 3.5A-3.5B).

A similar immunohistological analysis based on the colocalization of endomucin and nidogen (an endothelial basement membrane marker; Kohfeldt *et al.*, 1998) in 12-day CMT19T tumour vessels showed no difference in endothelial basement membrane deposition either in the presence or absence of endothelial  $\beta$ 3-integrin. Likewise, the time when deletion occurred seemed to be irrelevant: no significant difference in the number of endomucin+/nidogen+ vessels was detected when drawing comparisons between  $\beta$ 3-floxed/Tie1Cre and  $\beta$ 3-floxed/Pdgfb-iCreER<sup>T2</sup> positive tumours (Figure 3.5A-3.5B).

### **3.2.2 Vascular functions: distribution and perfusion**

To evaluate defects in vessel function, vessel distribution and perfusion were assessed by immunohistological analysis in vibratome sections. This analysis was conducted only in CMT19T tumours because of the softness of B16F0 tumours which makes them unsuitable for vibratome/thick sectioning. Vessel distribution was analysed by endomucin staining in vibratome sections of tumours grown in  $\beta$ 3-floxed/Tie1Cre and  $\beta$ 3-floxed/Pdgfb-iCreER<sup>T2</sup> mice. No difference in the pattern of distribution of tumour vessels was observed when comparing  $\beta$ 3-floxed/Tie1Cre negative and positive and  $\beta$ 3-floxed/Pdgfb-iCreER<sup>T2</sup> negative tumours to one another (Figure 3.6A). However, vessels were significantly reduced in number in  $\beta$ 3-floxed/Pdgfb-iCreER<sup>T2</sup> positive tumours, likely due to the fact that they were significantly less vascularized after 12 days of growth (Figure 3.3B).

The degree of vessel perfusion was assessed by *in vivo* intravenous injection of PE-CD31 in  $\beta$ 3-floxed/Tie1Cre and  $\beta$ 3-floxed/Pdgfb-iCreER<sup>T2</sup> CMT19T tumour bearing mice, just before sacrifice (day12). The quantification of the depth of perfusion was performed on histological sections, whereby CD31+ patent vessels were colocalized with endomucin+ staining (Figure 3.6B). The depth of patent vessels was similar when comparing  $\beta$ 3-floxed/Tie1Cre negative and positive and  $\beta$ 3-floxed/Pdgfb-iCreER<sup>T2</sup> negative tumours to one another. However, patent vessels penetrated deeper in  $\beta$ 3-floxed/Pdgfb-iCreER<sup>T2</sup> positive tumours, likely due to the fact that they were significantly smaller after 12 days of growth (Figure 3.6C).

Taken together these data indicate that during B16F0 and CMT19T tumour associated angiogenesis, neither pericyte coverage, endothelial membrane deposition, vessel distribution, nor vessel patency are altered by endothelial  $\beta$ 3-integrin deletion, irrespectively of when the deletion occurs.

### 3.3 Validation of the two endothelial Cre models

My findings uncover a time-dependent role for endothelial  $\beta$ 3-integrin in regulating tumour growth and angiogenesis, which likely is not due to structural and/or functional alterations of the tumour vasculature. In order to investigate this effect mechanistically, I first decided to test whether the non-endothelial expression of the two promoters, accounting for  $\beta$ 3-integrin deletion in cell types other than endothelial cells, was responsible for the difference between the two models. In fact, both *Tie-1* and *Pdgfb* promoters reportedly have some degree of non endothelial activity: *Tie-1* is also expressed by a proportion ( $\approx$ 20%) of bone marrow derived hematopoietic cells (Gustaffson *et al.*, 2001), while *Pdgfb* is also expressed by megakaryocytes which are platelet precursors (Claxton *et al.*, 2008). To address this point, I examined  $\beta$ 3-integrin expression levels in bone marrow derived cells and platelets isolated from  $\beta$ 3-floxed/*Tie1*Cre and  $\beta$ 3-floxed/*Pdgfb*-iCreER<sup>T2</sup> mice.

#### 3.3.1 Bone marrow cell analysis

To characterise  $\beta$ 3-integrin expression in the hematopoietic compartment, bone marrow derived cells isolated from femours of  $\beta$ 3-floxed/*Tie1*Cre positive and negative mice were analyzed by flow cytometric analyses. Cell suspensions were co-stained with PE-conjugated anti- $\beta$ 3 integrin and Fluorescein isothiocyanate (FITC)-conjugated antibodies against the hematopoietic markers CD45, Ly6G, CD3, CXCR4 (CD184) as described by Feng *et al.*, (2008) to selectively quantify the level of  $\beta$ 3-integrin within each bone marrow derived cell sub-population.

I found that the percentage of  $\beta$ 3-floxed/*Tie1*Cre positive bone marrow derived cells expressing  $\beta$ 3-integrin was significantly decreased in all the hematopoietic sub-populations, except for CXCR4+ bone marrow derived cells, when compared to  $\beta$ 3-floxed/*Tie1*Cre negative bone marrow derived cells (Figure 3.6A). In line with Feng findings, that  $\beta$ 3 integrin expression on CXCR4+ BMDC is required for their recruitment and retention at sites of angiogenic site, this suggest that the angiogenic phenotype observed in  $\beta$ 3-floxed/*Tie1*Cre mice is not likely the result of the leakiness

of the Tie1 promoter in the bone marrow compartment. In contrast, the same analysis performed on bone marrow derived cells isolated from  $\beta 3$ -floxed/Pdgfb-iCreER<sup>T2</sup> positive and negative mice showed no difference in  $\beta 3$ -integrin expression in any of the subpopulations assessed, thus confirming that *Pdgfb* is not active in bone marrow derived cells (Figure 3.6A).

The same authors have also shown that tumour infiltrating bone marrow derived cells localizing in perivascular areas of tumours were predominantly F4/80+ macrophages. In line with these observations, I analysed  $\beta 3$ -integrin expression in F4/80+ tumour-associated macrophages isolated from  $\beta 3$ -floxed/Tie1-Cre positive and negative tumours. Cell suspensions from tumour digests were double-stained with PE-conjugated anti- $\beta 3$  integrin and FITC-conjugated anti-F4/80, and the level of expression of  $\beta 3$ -integrin in F4/80+ cells was quantified by flow cytometric analysis. No significant difference was found in the percentage of  $\beta 3$ -integrin+/F4/80+ cells when comparing tumour associated macrophages isolated from  $\beta 3$ -floxed/Tie1Cre positive and negative tumours (Figure 3.7B), despite total bone marrow F4/80+ cells were reduced in  $\beta 3$ -floxed/Tie1Cre positive mice. This finding supports the conclusion that the angiogenic phenotype in  $\beta 3$ -floxed/Tie1Cre mice is not due to difference in tumour associated macrophage infiltration.

### 3.3.2 Platelet analyses

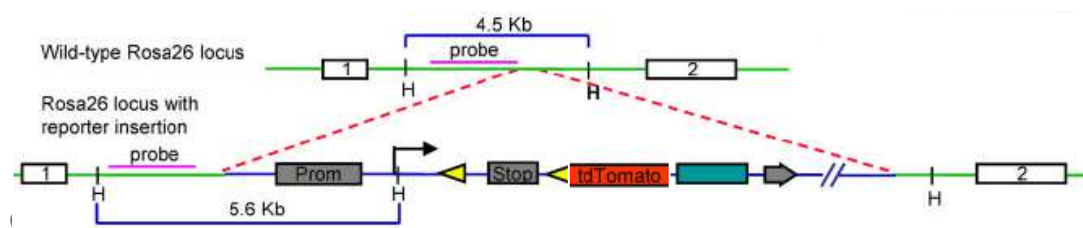
Peripheral blood was collected from the vena cava of anesthetized Tie1Cre and Pdgfb-iCreER<sup>T2</sup> mice before sacrifice and processed for platelet separation. Isolated platelets were lysed and Western blot analysis was performed to quantify  $\beta 3$ -integrin expression levels. They were unaltered between  $\beta 3$ -floxed/Pdgfb-iCreERCreER<sup>T2</sup> positive and negative platelets (Figure 3.7C). Further, I confirmed that there was no change in  $\beta 3$ -integrin expression in platelets isolated from in  $\beta 3$ -floxed/Tie1Cre positive and negative mice as expected (Figure 3.7C).

These data support the hypothesis that the difference observed in tumour growth and angiogenesis between the two transgenic models is likely due to endothelial cell specific deletion of  $\beta 3$  integrin.

### 3.3.3 Analysis of Tomato Cre reporter activity

Following on from the analysis of the non-endothelial activity of the *Tie1* and *Pdgfb* promoters, it was compelling to validate the two endothelial models in terms of activity and specificity of the Cre recombinase in the context of the tumours themselves.

In order to assess Cre recombinase activity *in vivo*, a reporter transgenic mouse line was employed. Tie1Cre and *Pdgfb*-iCreER<sup>T2</sup> positive mice were crossed with the tdTomato reporter line (Madisen *et al.*, 2010), whereby the Rosa26 locus has been modified by targeted insertion of a strong and ubiquitous promoter, followed by a floxed-STOP cassette controlling the tdTomato gene (as shown below).



*Pdgfb*-iCreERCreER<sup>T2</sup> positive/tdTomato heterozygous mice, harvested after 12 days and thick whole-mount sections were examined after co-staining for endomucin to highlight vessels. At high magnification, tomato positive cells (representing active Cre recombinase) colocalized with endomucin+ vessels in both Tie1Cre positive/tdTomato heterozygous and *Pdgfb*-iCreER<sup>T2</sup> positive/tdTomato heterozygous tumours, suggesting that Cre recombinase is specifically active in endothelial cells within the tumour tissue in both transgenic models (Figure 3.8A). In addition to that, analysis of CMT19T whole-mount tumour sections at lower magnification, showed that Tomato Cre reporter activity was widespread in both Cre models, confirming that substantial deletion was achieved (Figure 3.8A).

### 3.3.4 Analysis of Cre deletion efficiency

Cre recombinase activity as measured by fluorescence of the tdTomato reporter gene is an indirect evaluation and is not necessarily equivalent to effective protein ablation. Therefore, the efficiency of Cre driven deletion has been assessed by measuring  $\beta$ 3-integrin protein levels by Western blot analysis from 12-day tumour endothelial cells comparing Cre positive against Cre negative tumour endothelial cells isolated from both transgenic models (Figure 3.1B).

Importantly, the decrease of  $\beta$ 3-integrin protein level was similar when comparing in  $\beta$ 3-floxed/Tie1Cre and  $\beta$ 3-floxed/Pdgfb-iCreER<sup>T2</sup> positive tumour associated endothelial cells, proving the efficiency of the deletion was comparable in the two models. In addition, Cre driven deletion within the tumour vasculature was evaluated *in vivo* by colocalization of FITC IsolectinB4 (IB4) with intravenously injected PE-conjugated anti- $\beta$ 3 integrin antibody (which allowed endothelium targeting) on whole-mount tumour sections. The histological analysis revealed that  $\beta$ 3-integrin in tumour vessels was effectively deleted in both Cre models (Figure 3.7B).

From these additional analyses, I conclude that Cre recombinase is similarly specific and efficient in deleting  $\beta$ 3-integrin in tumour endothelial cells in both transgenic models, thereby allowing for a more direct comparison between them.

### **3.4 The length of $\beta$ 3-integrin deletion dictates the angiogenic response**

The validation data, heretofore, are likely to exclude the possibility that intrinsic differences between the two endothelial transgenic models explains the dichotomous effects I observed when comparing the two models. Rather, they suggest they differ in the amount of time  $\beta$ 3-integrin has been depleted.

#### **3.4.1 Rationale of the long OHT treatment in the inducible model of $\beta$ 3-integrin deletion**

In order to pinpoint the time dependency of endothelial  $\beta$ 3-integrin inhibitory effect on tumour growth and angiogenesis, I performed an *in vivo* “rescue” tumour experiment, whose rationale is based on the following question: could the effect of the inducible  $\beta$ 3-integrin deletion be abrogated by extending the time of its deletion?

In other words, would extending OHT treatment prior to allograft implantation in  $\beta$ 3-floxed/Pdgfb-iCreER<sup>T2</sup> mice mimic the angiogenic phenotype observed in  $\beta$ 3-floxed/Tie1-Cre mice?

#### **3.4.2 Abrogation of the inhibitory tumour phenotype by long OHT treatment of $\beta$ 3-floxed/Pdgfb-iCreER<sup>T2</sup> mice**

The rescue experiment consisted of administering OHT treatment to  $\beta$ 3-floxed/Pdgfb-iCreER<sup>T2</sup> mice for 21 days (referred to as “long OHT”) before subcutaneous tumour cell injections. Since OHT was administered by subcutaneous implantation of slow

release pellets, which lasted for only 3 weeks, a second OHT pellet was implanted at the same time as CMT19T tumour cell injection. CMT19T tumours were then harvested 12 days later, corresponding to a total of 33 days of OHT treatment; their size and vessel density were assessed.

Consistent with the hypothesis that it is the length of endothelial  $\beta$ 3-integrin deletion which affects tumour growth and angiogenesis, no differences were observed in either tumour size or degree of vascularization when comparing long OHT  $\beta$ 3-floxed/Pdgfb-iCreER<sup>T2</sup> positive and negative mice (Figure 3.9A-3.9C). In line with these findings, no structural defects in tumour vasculature were noted after immunofluorescent analysis of pericyte coverage and endothelial basement membrane deposition, as described in paragraph 3.2 (Figure 3.9D). Therefore, the inhibitory effects observed upon inducible deletion of endothelial  $\beta$ 3-integrin (15 days of OHT treatment in total - referred to as “short OHT”) were completely abolished if the OHT treatment was extended prior to allograft administration.

In order to ascertain that Cre recombinase was active *in vivo* over an extended time course, endothelial cells from long OHT  $\beta$ 3-floxed/Pdgfb-iCreER<sup>T2</sup> tumours were isolated at the end of the experiment (day 33) and  $\beta$ 3-integrin protein levels were quantified by Western blot analyses. Indeed, long OHT  $\beta$ 3-floxed/Pdgfb-iCreER<sup>T2</sup> positive tumour endothelial cells displayed a significant reduction of  $\beta$ 3-integrin expression compared to their Cre negative counterparts (Figure 3.9B). These results strongly support the conclusion that it is the length of endothelial  $\beta$ 3-integrin deletion which dictates the angiogenic response during tumour growth.

### **3.4.3 The inhibitory effects of inducible endothelial $\beta$ 3-integrin deletion are transient**

To further investigate whether the effect of inducible endothelial  $\beta$ 3-integrin deletion on tumour growth and angiogenesis was durable, I extended the time of growth of CMT19T allografts in  $\beta$ 3-floxed/Pdgfb-iCreER<sup>T2</sup> mice after short OHT treatment. CMT19T tumours were grown until day 18 (corresponding to an additional 6 days) after their injection. These analyses could not be performed with B16F0 allografts because they grow extremely rapidly beyond day 12 and were likely to exceed the legal size limit allowed for tumour growth in mice in accordance with UK Home Office Regulations.

Tumour growth was monitored with external caliper measurements in live mice while tumours were growing. Tumours were significantly smaller in  $\beta 3$ -floxed/Pdgfb-iCreER<sup>T2</sup> positive mice compared  $\beta 3$ -floxed/Pdgfb-iCreER<sup>T2</sup> negative mice at day 8 and 13 (Figure 3.10A).

However, at day 18 when tumours were harvested and analyzed to assess their growth and angiogenesis, there was no significant difference in size when comparing  $\beta 3$ -floxed/Pdgfb-iCreER<sup>T2</sup> positive and negative tumours, even though vessel density still was significantly decreased (Figure 3.10A). Endothelial cells from  $\beta 3$ -floxed/Pdgfb-iCreER<sup>T2</sup> positive and negative tumours were isolated at the end of the experiment (day 18) and  $\beta 3$ -integrin protein levels were quantified by Western blot analyses.  $\beta 3$  flox/flox/Pdgfb-iCreER<sup>T2</sup> positive tumour endothelial cells displayed a significant reduction of  $\beta 3$ -integrin expression compared to their respective Cre negative controls, proving that endothelial  $\beta 3$ -integrin was effectively deleted for the extended time of the experiment (Figure 3.10A).

Unfortunately, but perhaps not surprisingly, these findings show that the inhibitory effects observed with the inducible endothelial  $\beta 3$ -integrin deletion are transient and dissipate over time. This also suggests that  $\beta 3$ -integrin independent compensation mechanisms take over as tumour growth progresses in the continued presence of  $\beta 3$ -integrin suppression.

#### **3.4.4 Endothelial $\beta 3$ -integrin is not required when tumours have already established**

To test whether inducible endothelial  $\beta 3$ -integrin deletion had an effect also on tumour progression, I used a more clinically relevant model of tumour growth whereby CMT19T tumour cells were implanted subcutaneously and OHT was administered 8 days later (hereafter referred to as "INTERVENTION SCHEME"), after angiogenic tumours had already been established.

CMT19T tumour sizes were then assessed 5 and 10 days after OHT treatment (corresponding to days 13 and 18 from point of allograft implantation). Despite  $\beta 3$ -integrin being effectively deleted in tumour associated endothelial cells at day 18, no significant differences in size were observed at either time point when comparing  $\beta 3$ -floxed/Pdgfb-iCreER<sup>T2</sup> positive and negative mice (Figure 3.10B).

In addition, CMT19T tumours were harvested and processed for histological analyses and vessel density quantification. In line with the tumour growth data, angiogenesis did not appear to be altered in  $\beta 3$ -floxed/Pdgfb-iCreER<sup>T2</sup> positive tumours (Figure 3.10B).

Overall, these data suggest that the effects of an inducible endothelial  $\beta 3$ -integrin deletion during tumour angiogenesis are context dependent: the deletion exerts an inhibitory effect by preventing establishing tumours to grow by reducing their degree of angiogenesis, but the deletion has no effect on already established tumours.

**Figure 3.1 Endothelial  $\beta$ 3-integrin deletion in Tie1Cre and Pdgfb-iCreER<sup>T2</sup> models**

(A) Representative genotyping PCR analysis for detecting the presence of Tie1Cre and Pdgfb-iCreER<sup>T2</sup> transgenes (600 and 443 bp respectively). DNA was extracted from ears or tails of  $\beta$ 3-floxed/Tie1Cre and  $\beta$ 3-floxed/Pdgfb-iCreER<sup>T2</sup> transgenic mice. All mice were genotyped twice: at weaning and at the end of each experiment (L=ladder).

(B) Representative Western blot analysis of endothelial  $\beta$ 3-integrin and VEGFR2 expression in tumour associated endothelial cells isolated from 12-day-tumours grown in  $\beta$ 3-floxed/Tie1Cre and  $\beta$ 3-floxed/Pdgfb-iCreER<sup>T2</sup> positive and negative mice. HSC 70 provided a loading control. Bar graphs show  $\beta$ 3 integrin densitometric quantification relative to HSC 70 expression (mean  $\pm$  SEM; n=3 experiments; \*\*p<0.01).

(C) Representative Western blot analysis of endothelial  $\beta$ 3-integrin and VEGFR2 expression in endothelial cells isolated from  $\beta$ 3-floxed/Tie1Cre and  $\beta$ 3-floxed/Pdgfb-iCreER<sup>T2</sup> positive and negative mice. HSC 70 provided a loading control. Bar graphs show  $\beta$ 3 integrin densitometric quantification relative to HSC 70 expression (mean  $\pm$  SEM; n=3 experiments; \*\*p<0.01).

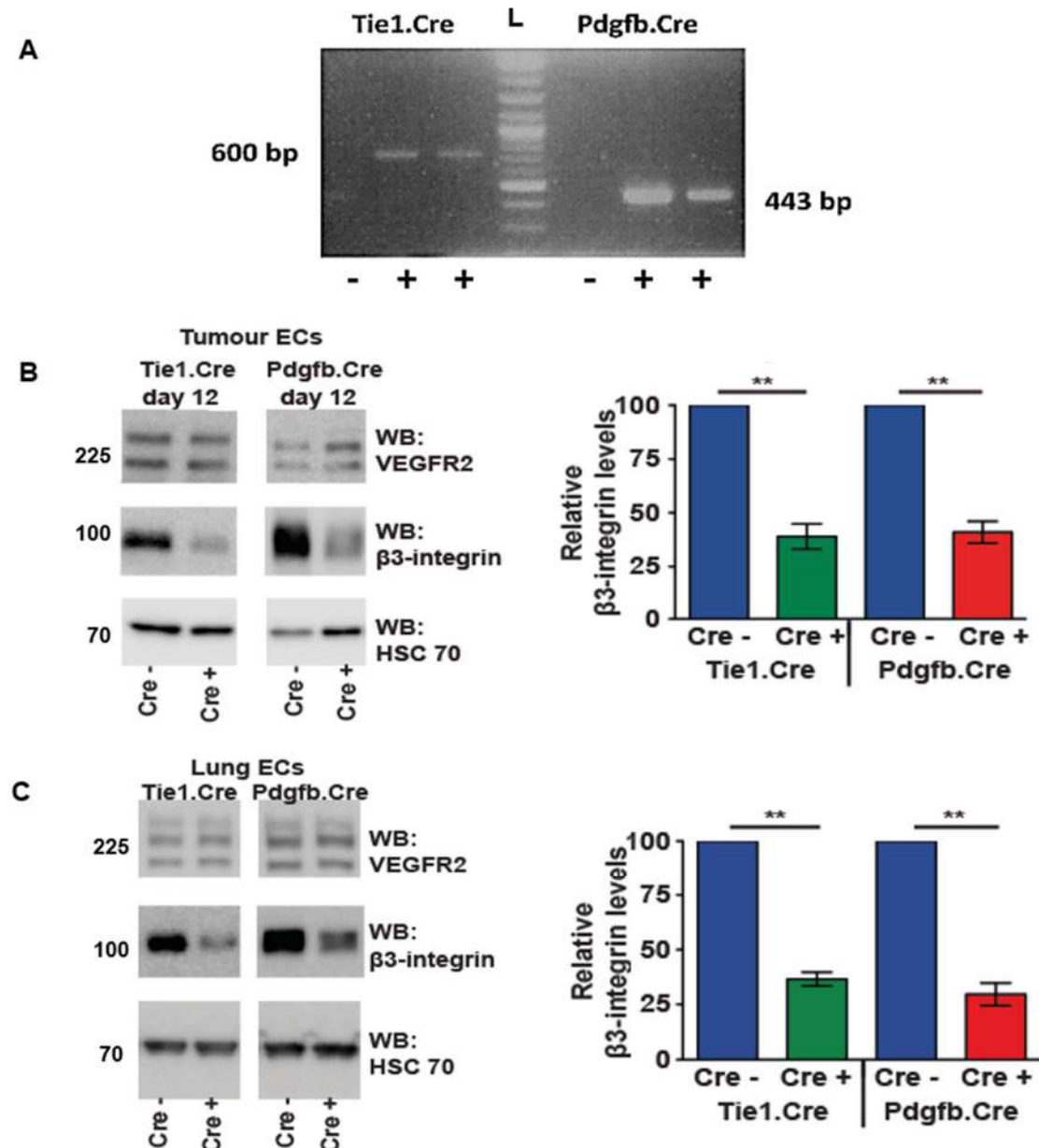


### Figure 3.2 Tumour growth is not affected by differences in the genetic background

CMT19T tumour growth was established measuring tumours in two dimension with digital caliper from the outside of the mice, every other day starting from the onset of a palpable mass (day 6) in  $\beta$ 3-floxed/Tie1Cre and  $\beta$ 3-floxed/Pdgfb-iCreER<sup>T2</sup> positive and negative mice. Tumour volumes were calculated according to the formula for the volume of a sphere: tumour volume (mm<sup>3</sup>) = width<sup>2</sup> × length × 0.52. Mice were sacrificed at day 12, tumours were removed, photographed for macroscopic appearance (bottom insets) and weighted in addition to a final caliper measurement. Bar graph shows mean tumour volume (+/- SEM, n=5 mice per genotype, \*\*<0.01). From a direct comparison, the only significant reduction in tumours size was detected in  $\beta$ 3-floxed/Pdgfb-iCreER<sup>T2</sup> positive 12-day-tumours, whereas tumours grew similarly in  $\beta$ 3-floxed/Tie1-Cre and  $\beta$ 3-floxed/Pdgfb-iCreER<sup>T2</sup> negative mice.

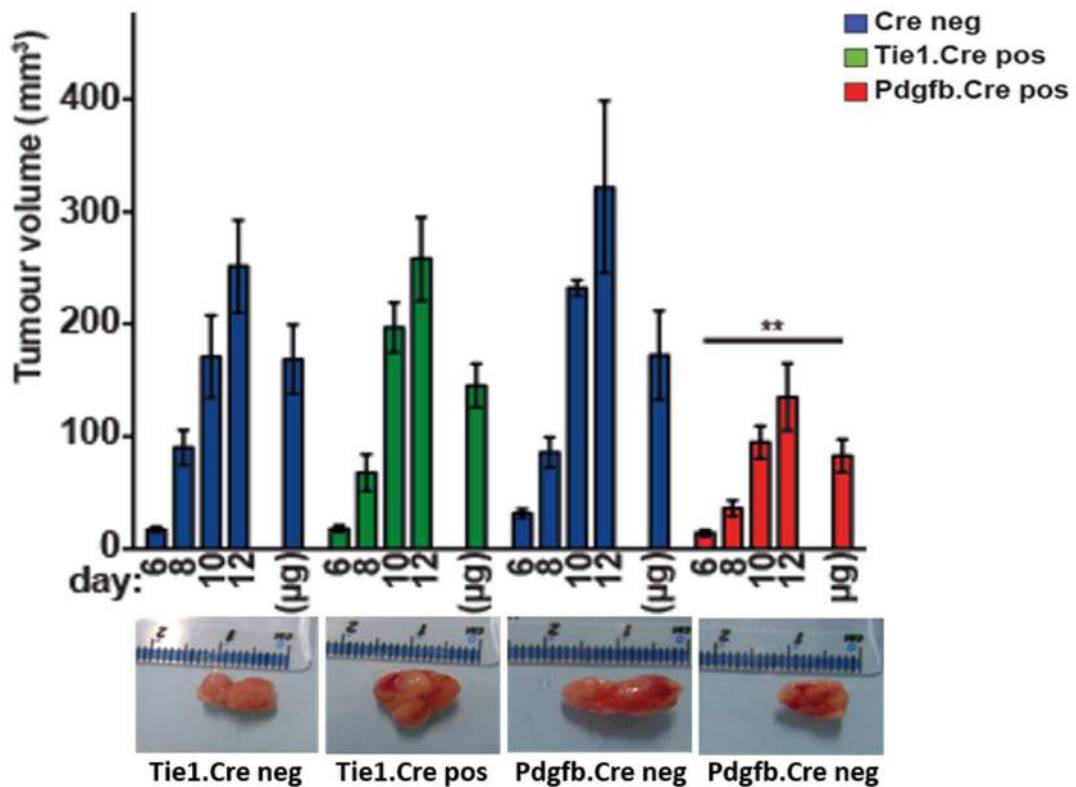


### Figure 3.3 Inducible deletion of endothelial $\beta 3$ -integrin reduces tumour growth and inhibits angiogenesis

Tumour growth is inhibited in  $\beta 3$ -floxed/Pdgfb-iCreER<sup>T2</sup> positive mice, when OHT is administered 3 day prior to tumour allograft implantation.  $\beta 3$ -floxed/Pdgfb-iCreER<sup>T2</sup> positive and negative mice were given subcutaneous injections of B16F0 (A) and CMT19T (B) tumour cells. 12-day-old tumour volume was significantly decreased in Cre positive mice when compared to Cre negative controls. Bar graphs show mean tumour volume (+/- SEM). Data are representative of 3 independent experiments (n=5 mice per genotype, \*\**p*<0.01). Tumour blood vessel density was also reduced in  $\beta 3$ -floxed/Pdgfb-iCreER<sup>T2</sup> positive B16F0 (A) and CMT19T (B) tumours. Blood vessel density was assessed by counting the total number of endomucin positive vessels across entire tumour sections. Bar graphs show mean vessel number per mm<sup>2</sup> (+/- SEM) for both tumour types (n=5 mice per genotype, \*\**p*<0.01). (C) Representative immunofluorescent images of tumour blood vessels stained with endomucin (in red) of 12-day-old tumours grown in  $\beta 3$ -floxed/Pdgfb-iCreER<sup>T2</sup> positive and negative mice. Arrows point to examples of vessels. DAPI (blue) was used as a nuclear counterstain (scale bar=50 $\mu$ m).

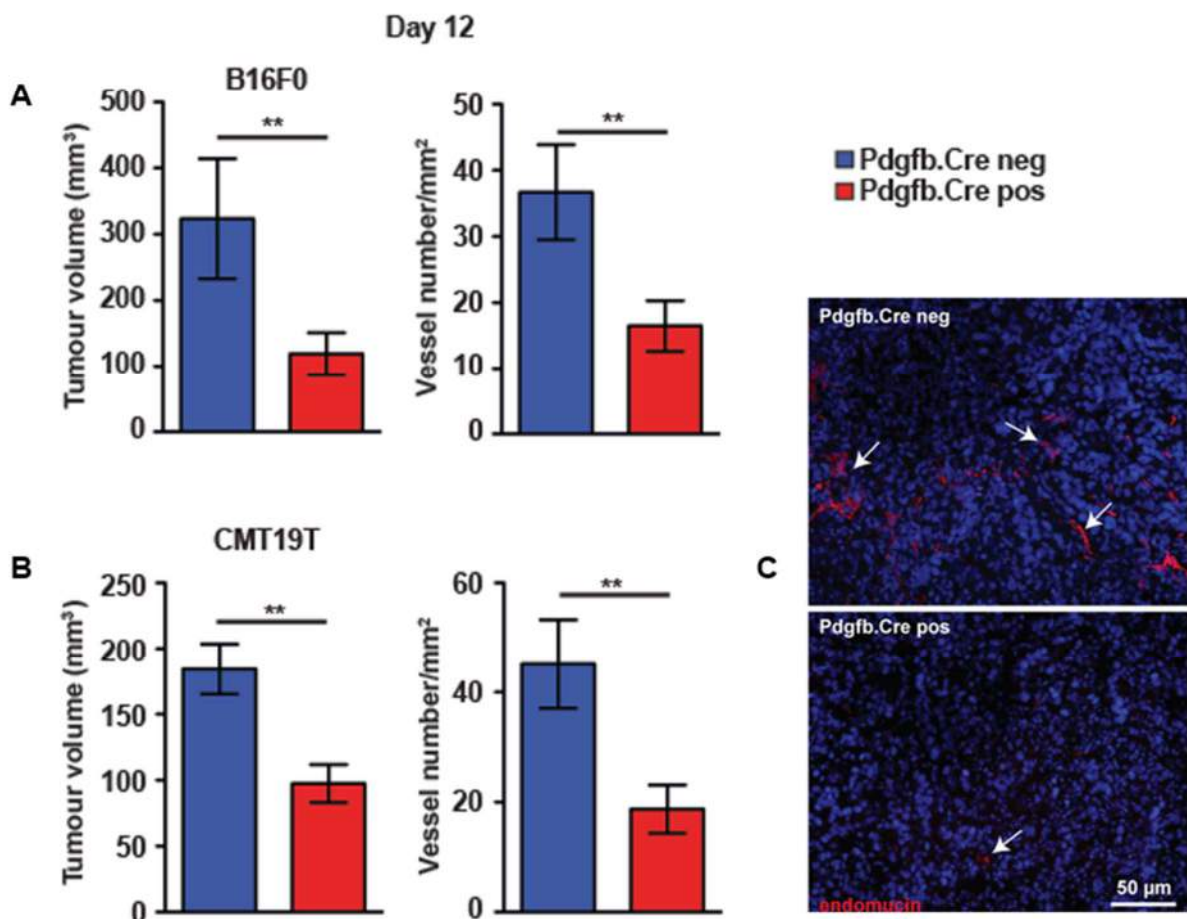


### Figure 3.4 Tumour growth is not affected by the constitutive deletion of endothelial $\beta$ 3-integrin

No difference in B16F0 (A) and CMT19T (B) tumour growth is observed in  $\beta$ 3-floxed/Tie1Cre mice. 12-day-old tumour volume showed no statistical difference between Cre positive and negative mice. Bar graphs show mean tumour volume (+/- SEM). Data are representative of 3 independent experiments (n= 5 mice per genotype, NS=not significant). No difference in tumour blood vessel density was observed in  $\beta$ 3-floxed/Tie1Cre B16F0 (A) and CMT19T (B) tumours between Cre positive and negative mice. Blood vessel density was assessed by counting the total number of endomucin positive vessels across entire tumour sections. Bar graphs show mean vessel number per mm<sup>2</sup> (+/- SEM) for both tumour types, (n=5 mice per genotype, NS=not significant). (C) Representative immunofluorescent images of tumour blood vessels stained with endomucin (in red) of 12-day-old tumours grown in  $\beta$ 3-floxed/Tie1Cre positive and negative mice. Arrows point to examples of vessels. DAPI (blue) was used as a nuclear counterstain (scale bar=50 $\mu$ m).

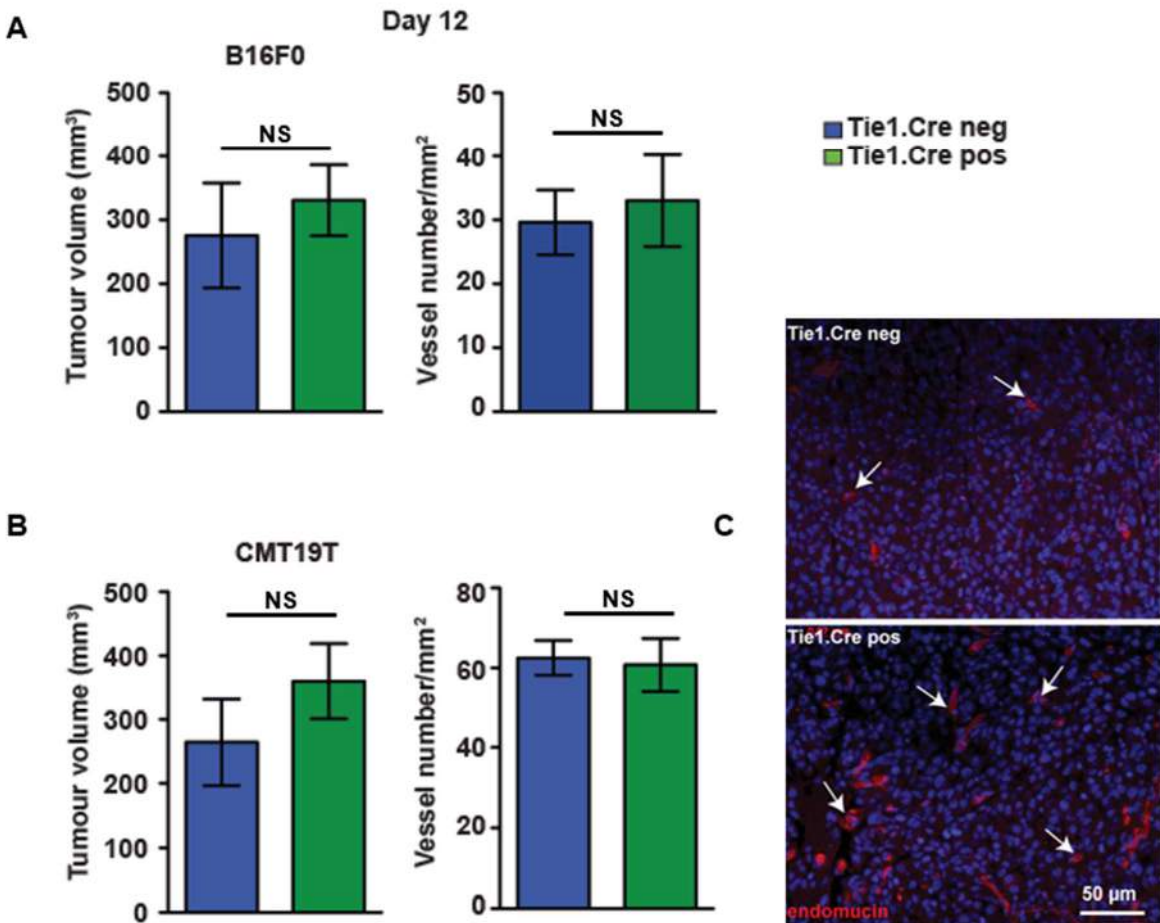


**Figure 3.5 Endothelial  $\beta$ 3-integrin does not affect pericyte or endothelial basement membrane coverage**

Pericyte association and endothelial basement membrane support were analyzed by immunofluorescence analysis. Representative immunofluorescence images of endothelial cells co-stained with endomucin (endothelial cell marker, in green) and  $\alpha$ SMA (pericyte marker, in red) or nidogen (basement membrane marker, in red) in sections of 12-day-old tumours grown in  $\beta$ 3-floxed/Pdgfb-iCreER<sup>T2</sup> mice (**A**) and  $\beta$ 3-floxed/Tie1Cre mice (**B**). Arrows point to examples of colocalization. DAPI (blue) was used as a nuclear counterstain (scale bar=100  $\mu$ m). Right, relative quantification of the level of pericyte and basement membrane coverage show no difference in tumours grown in  $\beta$ 3-floxed/Pdgfb-iCreER<sup>T2</sup> positive mice (**A**) and  $\beta$ 3-floxed/Tie1Cre positive mice (**B**) compared to Cre negative controls. Bar graphs represent the percentage of double-positive cells across each field (+/- SEM, n=10 fields per section, NS=not significant).

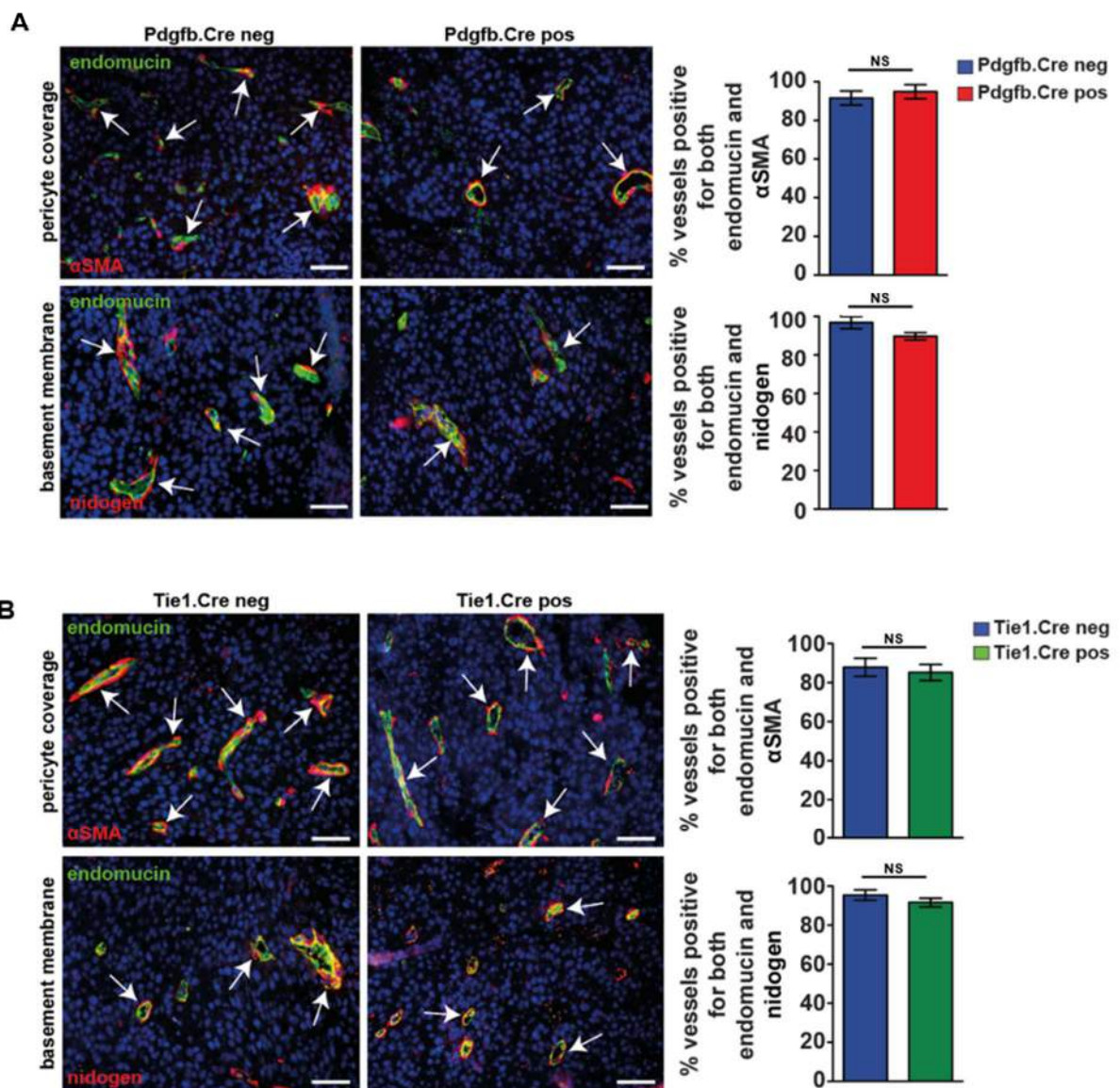


### Figure 3.6 Vessel function is not impaired in the absence of endothelial $\beta 3$ -integrin

(A) Vessel distribution was evaluated in vibratome sections stained with endomucin (endothelial cell marker, in green) in tumours grown in  $\beta 3$ -floxed/Tie1Cre and  $\beta 3$ -floxed/Pdgfb-iCreER<sup>T2</sup> mice. DAPI (blue) was used as a nuclear counterstain. No difference in tumour vasculature distribution was observed (scale bar=400  $\mu$ m).

(B) Vessel perfusion was evaluated by systemic injection of PE-CD31 (in red) in  $\beta 3$ -floxed/Tie1Cre and  $\beta 3$ -floxed/Pdgfb-iCreER<sup>T2</sup> mice, 10 minutes before sacrifice. Vibratome sections were costained with endomucin (in green). Double-arrows indicate the depth of perfused vessel penetrance from the tumour edge.

(C) Bar graph shows the mean depth of penetration in  $\mu$ m (+/- SEM) in tumours grown in mice of the indicated genotypes (n=3 mice per genotype, 5 fields per section, \*\*p<0.01, NS=not significant).

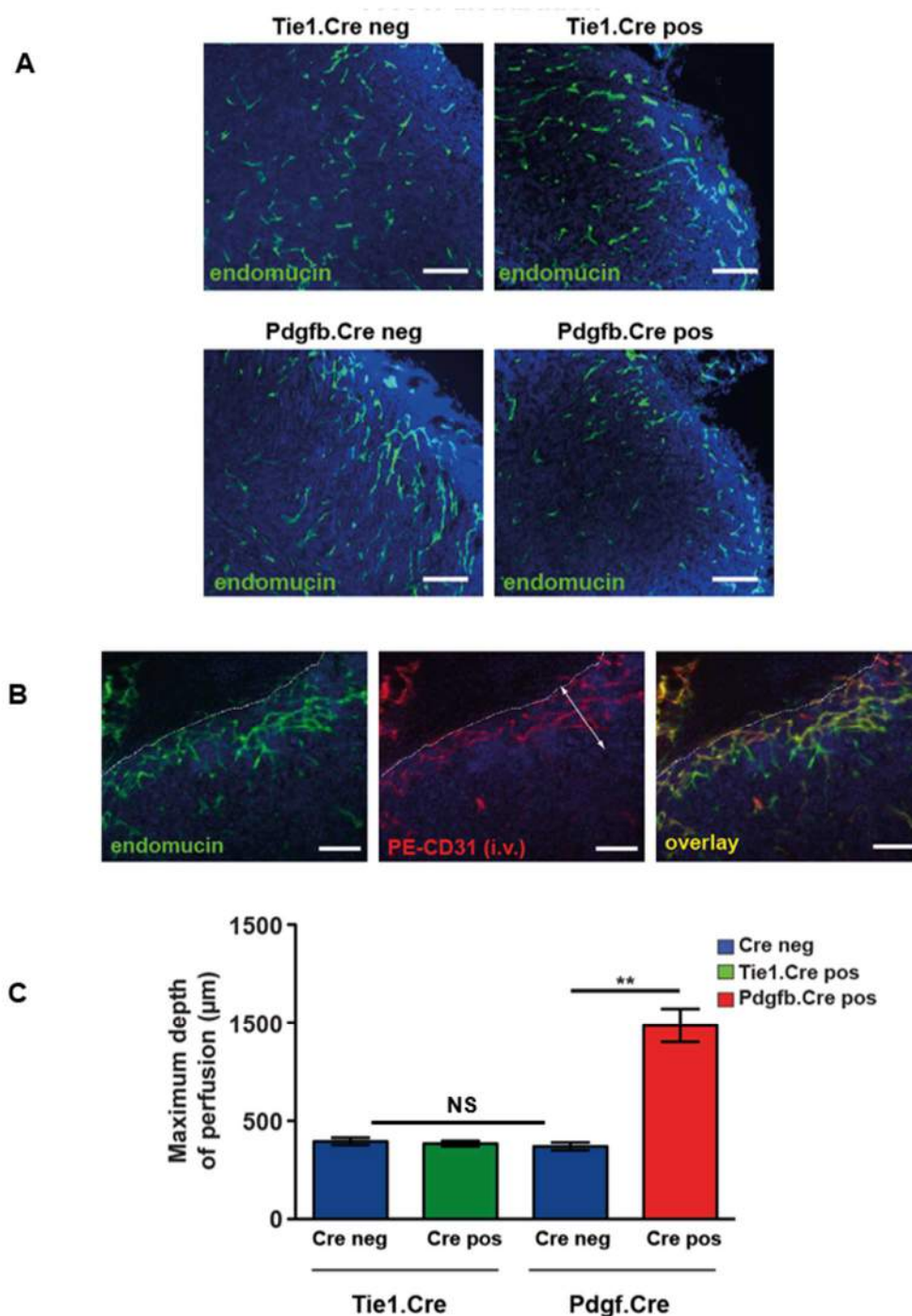


### Figure 3.7 Non-endothelial specificity of Tie1Cre and Pdgfb-iCreER<sup>T2</sup> promoters

(A)  $\beta$ 3-integrin was deleted in bone marrow derived cells derived from  $\beta$ 3-floxed/Tie1Cre positive mice, but not from  $\beta$ 3-floxed/Pdgfb-iCreER<sup>T2</sup> positive mice. Bone marrow derived cell suspensions isolated from  $\beta$ 3-floxed/Tie1Cre and  $\beta$ 3-floxed/Pdgfb-iCreER<sup>T2</sup> mice were double-immunostained with  $\beta$ 3-integrin in addition to markers for hematopoietic lineages (CD3, CD45, F4/80, Ly-6G, CXCR4) and analyzed by flow cytometry. Table shows the mean percentage ( $\pm$  SEM) of  $\beta$ 3-integrin expressing bone marrow derived subpopulations in  $\beta$ 3-floxed/Tie1-Cre and  $\beta$ 3-floxed/Pdgfb-iCreER<sup>T2</sup> mice (n=3 mice per genotype).

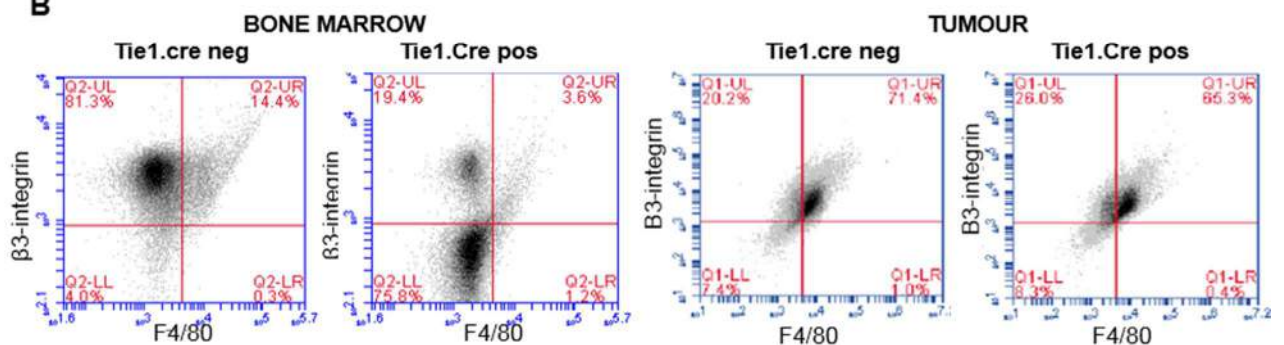
(B)  $\beta$ 3-integrin expression in F4/80 positive macrophages in bone marrow and 12-day-old tumours from in  $\beta$ 3floxed/Tie1Cre mice. Cell suspensions double-immunostained with  $\beta$ 3 integrin and F4/80, and analyzed by flow cytometry. Representative quadrant plots show the percentage of  $\beta$ 3+/F4/80+ macrophages (n=3 mice per genotype).

(C)  $\beta$ 3-integrin expression in platelets is not affected either in Tie1Cre or Pdgfb-iCreER<sup>T2</sup> mice. Western blot analysis confirms that  $\beta$ 3-integrin levels did not change in platelets isolated from  $\beta$ 3-floxed/Tie1Cre or  $\beta$ 3-floxed/Pdgfb-iCreER<sup>T2</sup> mice. ERK1/2 provided a loading control (n=3 mice per genotype).

**A**

Marker	% BMDCs expressing $\beta$ 3-integrin			
	Tie1.Cre negative	Tie1.Cre positive	Pdgfb.Cre negative	Pdgfb.Cre positive
CD3	5.2 $\pm$ 1.1	1.5 $\pm$ 0.7	5.6 $\pm$ 0.3	5.7 $\pm$ 0.5
CD45	98 $\pm$ 3.2	16.9 $\pm$ 1.5	95 $\pm$ 2.3	93 $\pm$ 2.4
F4/80	12.7 $\pm$ 2.4 (4.6 $\pm$ 0.1 of total BMDCs)	3.2 $\pm$ 0.8 (2.5 $\pm$ 0.9 of total BMDCs)	12.0 $\pm$ 1.2	10.9 $\pm$ 0.7
Ly6G	96 $\pm$ 7.5	17.1 $\pm$ 3.4	93 $\pm$ 4.8	95 $\pm$ 2.4
CXCR4	1.6 $\pm$ 0.1	1.4 $\pm$ 0.3	1.8 $\pm$ 0.2	2.0 $\pm$ 0.2

**B**



**C**

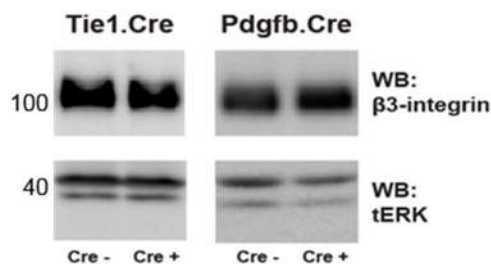


**Figure 3.8 Analysis of Cre specificity and efficiency *in vivo***

**(A)** Representative immunofluorescent analysis of tdTomato Cre reporter activity (in red) in whole tumour sections co-stained with endomucin (endothelial cell marker, in green) in tumours grown in Tie1Cre positive/tdTomato heterozygous and Pdgfb-iCreER<sup>T2</sup> positive/tdTomato heterozygous mice. Arrows point to colocalization signals, showing endothelial specific Cre activity (high magnification, scale bar=50µm). The pattern of Cre expression (in red) is similarly widespread in tumours grown in Tie1Cre positive/tdTomato heterozygous and Pdgfb-iCreER<sup>T2</sup> positive/tdTomato heterozygous mice. DAPI (blue) was used as a nuclear counterstain (low magnification, scale bar=400µm).

**(B)** Representative immunofluorescence analysis of endothelial cells (arrows) co-stained for IB4 (endothelial cell marker, in green) and β3-integrin (in red), which was labelled by systemic injection of PE-β3-integrin in β3-floxed/Tie1Cre and β3-floxed/Pdgfb-iCreER<sup>T2</sup> mice 10 minutes before sacrifice. DAPI (blue) was used as a nuclear counterstain (scale bar=50 µm).

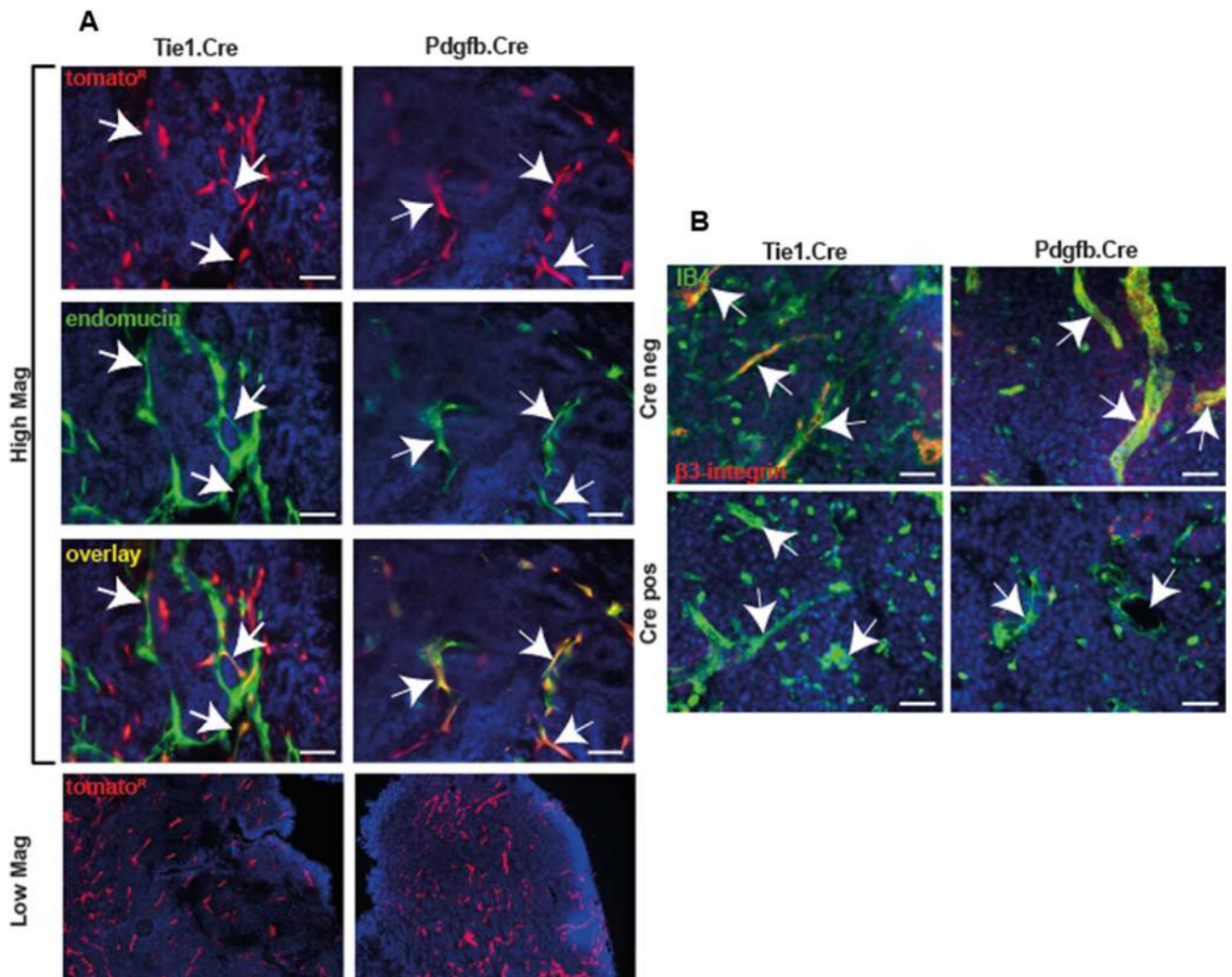


**Figure 3.9 The length of endothelial  $\beta$ 3-integrin deletion dictates the angiogenic response *in vivo***

(A) The difference in tumour growth is abolished when  $\beta$ 3-integrin deletion is induced long-term by 21-day-OHT treatment prior to CMT19T allograft implantation. A new tamoxifen pellet was implanted at the time of tumour cell injection.  $\beta$ 3-floxed/Pdgfb-iCreER<sup>T2</sup> mice were given subcutaneous injections of CMT19T tumour cells. Bar graph shows mean tumour volume (+/- SEM). Data are representative of 3 independent experiments (n=5 mice per genotype, NS=not significant).

(B) Representative Western blot analysis of endothelial  $\beta$ 3-integrin expression in tumour associated endothelial cells, isolated from 12-day-tumours grown in long OHT  $\beta$ 3-floxed/Pdgfb-iCreER<sup>T2</sup> positive and negative mice. HSC 70 provided a loading control.

(C) No difference in tumour blood vessel density was observed between long OHT  $\beta$ 3-floxed/Pdgfb-iCreER<sup>T2</sup> positive and negative tumours. Blood vessel density was assessed by counting the total number of endomucin positive vessels across entire tumour sections. Bar graph shows mean vessel number per mm<sup>2</sup> (+/- SEM, n=5 mice per genotype, NS=not significant).

(D) Representative immunofluorescence images of endothelial cells (arrows) co-stained with endomucin (endothelial cell marker, in green) and  $\alpha$ SMA (pericyte marker, in red) or nidogen (basement membrane marker, in red) in sections of 12-day-old tumours grown in long OHT  $\beta$ 3-floxed/Pdgfb-iCreER<sup>T2</sup> mice. Arrows point to examples of colocalization. DAPI (blue) was used as a nuclear counterstain (scale bar=50  $\mu$ m). Relative quantification of the level of pericyte and basement membrane coverage shows no difference in tumours grown in long OHT  $\beta$ 3-floxed/Pdgfb-iCreER<sup>T2</sup> positive and negative mice. Bar graphs represent the percentage of double-positive cells across each field (+/- SEM, n=10 fields per section, NS=not significant).

(E) Vessel distribution was evaluated in vibratome sections stained with endomucin (endothelial cell marker, in green) in tumours grown in long OHT  $\beta$ 3-floxed/Pdgfb-iCreER<sup>T2</sup> mice. DAPI (blue) was used as a nuclear counterstain. No difference in tumour vasculature distribution was observed (scale bar=400  $\mu$ m). Vessel perfusion was evaluated by systemic injection of PE-CD31 in long OHT  $\beta$ 3-floxed/Pdgfb-iCreER<sup>T2</sup> mice 10 minutes before sacrifice. Bar graph shows the mean depth of penetration in  $\mu$ m (+/- SEM) in tumours grown in long OHT  $\beta$ 3-floxed/Pdgfb-iCreER<sup>T2</sup> mice (n=3 mice per genotype, 5 fields per section, NS=not significant).

**Figure 3.9** The length of endothelial  $\beta 3$ -integrin deletion dictates the angiogenic response *in vivo*

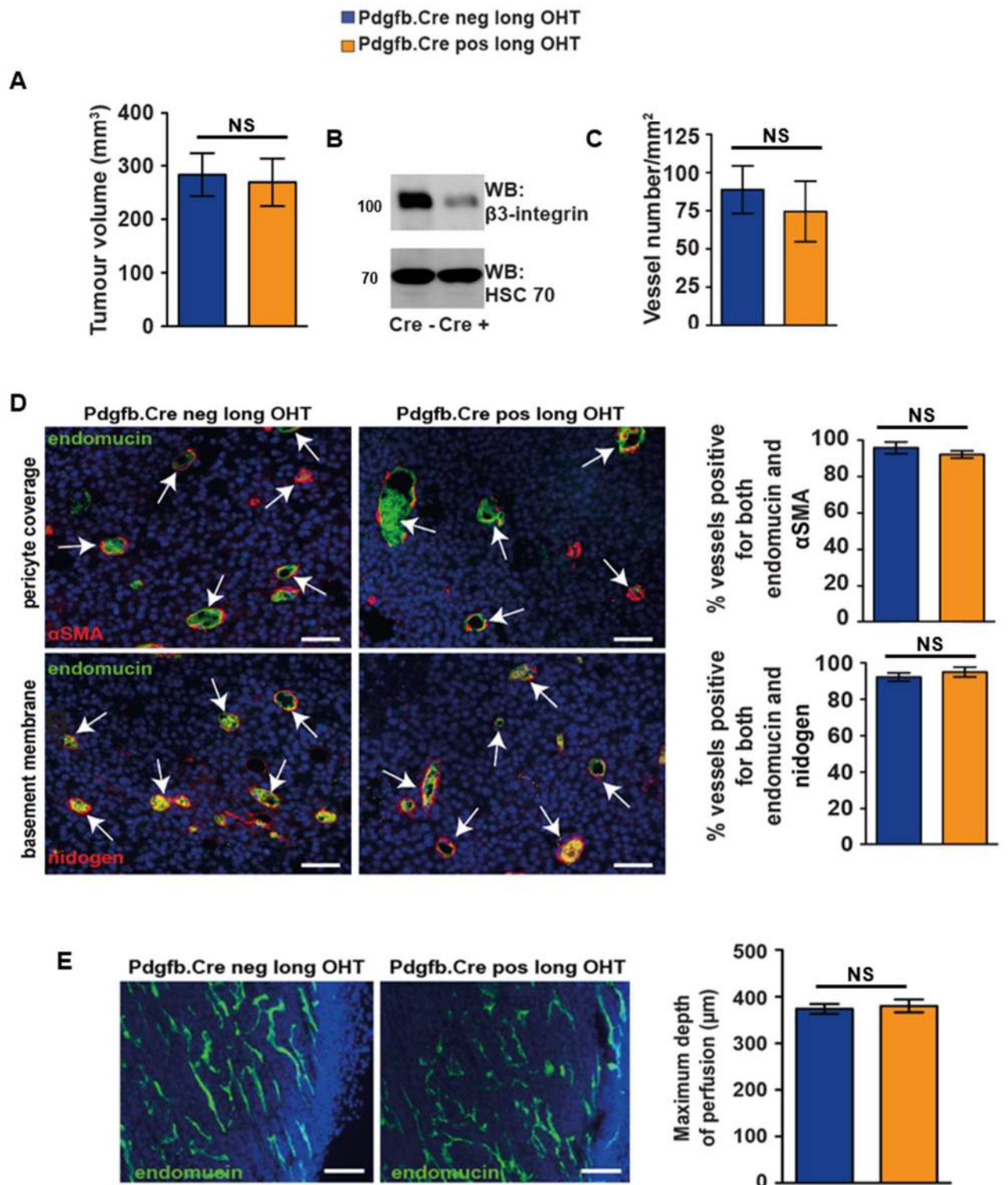


### Figure 3.10 The effects of endothelial $\beta$ 3-integrin deletion are time-dependent

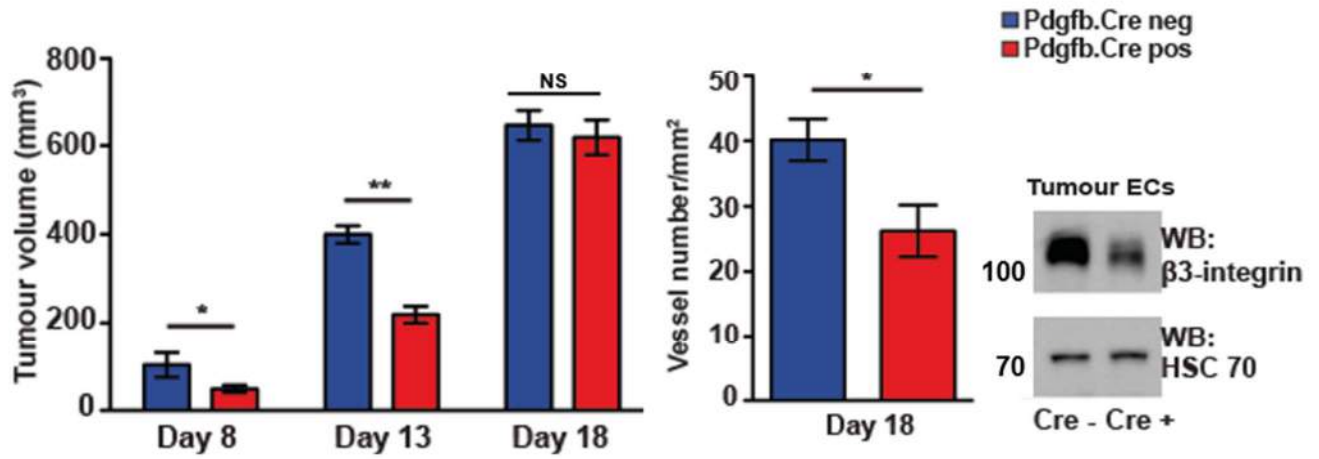
(A) The inhibition of tumour growth by inducible  $\beta$ 3-integrin deletion in endothelial cells dissipates with time.  $\beta$ 3-floxed/Pdgfb-iCreER<sup>T2</sup> positive and negative mice were given subcutaneous injections of CMT19T tumour cells. 8 and 13-day-old tumour volumes were significantly decreased in Cre positive mice when compared to negative; whereas by day 18 the difference in size was abrogated. Bar graph shows mean tumour volume (+/- SEM). Data are representative of 3 independent experiments (n=5 mice per genotype, \*p<0.05, \*\*p<0.01, NS=not significant). Similarly, blood vessel density in 18-day-tumours was reduced, but to a lesser degree than what was observed at day 12 in  $\beta$ 3-floxed/Pdgfb-iCreER<sup>T2</sup> positive tumours compared to negative tumours. Blood vessel density was assessed by counting the total number of endomucin positive vessels across entire tumour sections. Bar graph shows mean vessel number per mm<sup>2</sup> (+/- SEM, \*p<0.05). Representative Western blot analysis of endothelial  $\beta$ 3-integrin expression in tumour associated endothelial cells isolated from 18-day-tumours grown in  $\beta$ 3-floxed/Pdgfb-iCreER<sup>T2</sup> positive and negative mice. HSC 70 provided a loading control.

(B) Inducible deletion of endothelial  $\beta$ 3-integrin does not affect tumour progression, if deletion induced by OHT treatment occurs subsequent to tumour implantation.  $\beta$ 3-floxed/Pdgfb-iCreER<sup>T2</sup> mice were given subcutaneous injections of CMT19T tumour cells and  $\beta$ 3-integrin deletion was induced 8 days after tumour cell administration by tamoxifen pellet implantation (INTERVENTION scheme). 13 and 18-day-old CMT19T tumour volumes did not show any significant difference between  $\beta$ 3-floxed/Pdgfb-iCreER<sup>T2</sup> positive and negative mice. Bar graphs show mean tumour volume (+/- SEM). Data are representative of 3 independent experiments (n=5 mice per genotype, NS=not significant). Representative Western blot analysis of endothelial  $\beta$ 3-integrin expression in tumour associated endothelial cells isolated from 18-day-tumours grown in  $\beta$ 3-floxed/Pdgfb-iCreER<sup>T2</sup> positive and negative mice. HSC 70 provided a loading control.

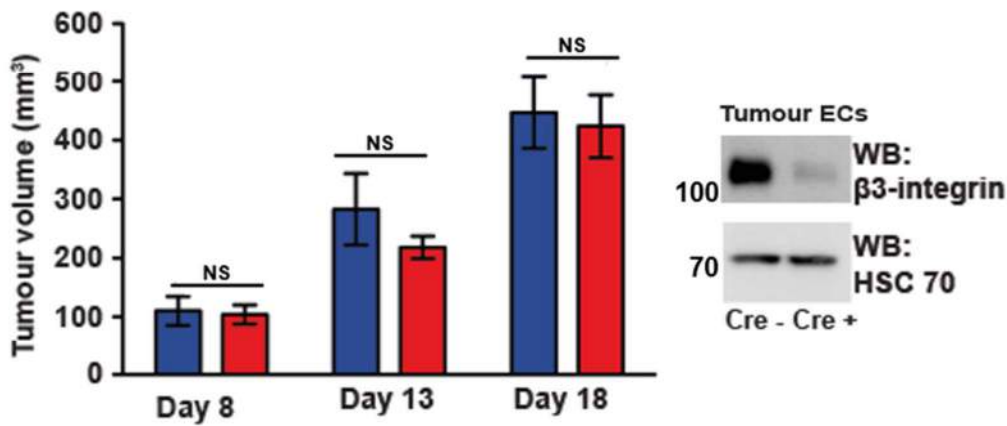
(C) No difference in tumour blood vessel density either in 13 or 18-day-old CMT19T tumours when comparing  $\beta$ 3-floxed/Pdgfb-iCreER<sup>T2</sup> positive to negative tumours. Bar graphs show mean vessel number per mm<sup>2</sup> (+/- SEM, NS=not significant).

Figure 3.10 The effects of endothelial  $\beta$ 3-integrin deletion are time-dependent

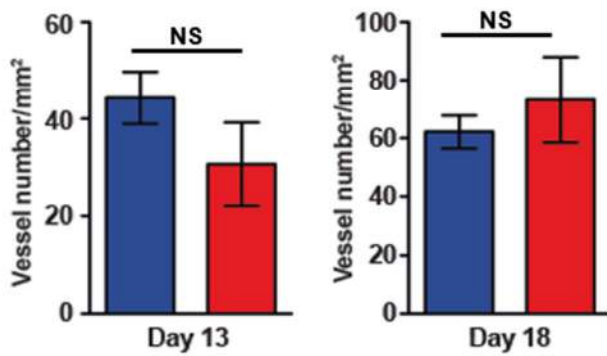
A



B



C



## DISCUSSION

### 3.5 The $\alpha\text{v}\beta\text{3}$ -integrin *conundrum*

Integrins play a crucial role in angiogenesis, both in physiological and pathological conditions and their functions and the molecular mechanisms involved in their regulation have been extensively studied (Robinson and Hodivala-Dilke, 2011). The interest beyond this is not purely from a fundamental interest in cell biology, but has gathered attention because of the clinically relevant potential of this knowledge to be translated into therapeutical options for a host of vascular and oncological diseases. With respect to tumour angiogenesis, after ten years of largely failed attempts at anti-angiogenic therapy, we have to take the lesson and go back to the bench because there are clearly aspects of pathological angiogenesis we do not understand fully and there are still issues which remain controversial (Atkinson *et al.*, 2014).

$\alpha\text{v}\beta\text{3}$ -integrin undoubtedly falls in this latter category. Its expression is upregulated during angiogenesis and is linked to endothelial cell proliferation, migration and survival (Hodivala-Dilke, 2008). Given that, it is surprising that genetic ablation of the  $\alpha\text{v}$ - or  $\beta\text{3}$ -subunits, does not lead to any major vascular defects:  $\alpha\text{v}$ -deficient mice die perinatally but without any obvious changes in blood vessel development or structure (Bader *et al.*, 1998), and  $\beta\text{3}$ -deficient mice are viable, fertile and adult mice develop normal vasculature (Hodivala-Dilke *et al.* 1999). The yet unsolved conundrum of  $\alpha\text{v}\beta\text{3}$ -integrin stems from the unexpected discrepancies between genetic data showing that  $\beta\text{3}$ -deficient mice support enhanced pathological angiogenesis (Reynolds *et al.*, 2002), whereas pharmacological inhibition of  $\alpha\text{v}\beta\text{3}$ -integrin can block angiogenesis in some models (Brooks *et al.*, 1995); in fact  $\alpha\text{v}\beta\text{3}$ -integrin antagonists have been investigated in clinical trials. This thesis was an attempt to shed light on these seeming discrepancies with the hope of adding a contribution to the clinical translation of  $\alpha\text{v}\beta\text{3}$ -integrin as a therapeutic target.

I took a genetic approach to elucidate the role of endothelial  $\alpha\text{v}\beta\text{3}$ -integrin in tumour angiogenesis, even though  $\alpha\text{v}\beta\text{3}$ -integrin antagonists were available (Stupp *et al.*, 2007). Genetics offered at least two advantages: cell-specificity achieved with the use of endothelial specific promoters and temporal regulation achieved with the use of an inducible promoter.

Cell specificity is fundamental as  $\alpha\beta$ 3-integrin is expressed by different cells all of which can contribute to angiogenesis: fibroblasts, macrophages, bone-marrow derived cells, pericytes, platelets and tumour cells themselves (Robinson and Hodivala-Dilke, 2011). For this reason previous genetic studies based on the global  $\beta$ 3-integrin knockout were muddled by the fact that  $\beta$ 3-integrin deletion was not restricted only to endothelial cells. In fact it has been shown that other cell types, such as bone marrow derived cells, contribute to the phenotype of increased pathological angiogenesis observed in  $\beta$ 3-integrin knockout mice (Taverna *et al.*, 2004; Watson *et al.*, 2010).

With respect to cell specific analysis, it has already been shown that  $\beta$ 3-integrin conditional deletion in platelets leads to a bleeding phenotype but has no effect on tumour growth and angiogenesis; whereas  $\beta$ 3-integrin deletion in myeloid cells caused osteopetrosis similar to that observed in  $\beta$ 3-null mice (Morgan *et al.*, 2010). My studies are the first to look at the effects of the endothelial-specific deletion of this molecule. I was able to show that the acute deletion of  $\beta$ 3-integrin in endothelial cells reduced tumour growth and angiogenesis in two different tumour models B16F0 melanoma and CMT19T lung carcinoma, drastically reducing the possibility that this effect is tumour specific. Therefore, my findings support the argument that endothelial  $\alpha\beta$ 3-integrin remains a valid target for anti-angiogenic tumour therapy.

Temporal regulation is a fundamental concept. Classically, there has been a distinct conceptual separation of angiogenesis studies into either developmental/physiological or adult/pathological. This approach, perhaps, is too reductionist in the context of cancer, which by definition is susceptible to selection and adaptation and as such a continuum of both “types” of angiogenesis are likely occurring in the same tissue at any one time.

Time matters and this is also reflected by the variability observed in clinical settings when applying anti-angiogenic therapies. When to start a therapeutical regime and how long to continue it are crucial parametres to consider to pinpoint exactly when  $\beta$ 3 integrin dependent functions take place in order to target it effectively. In line with this, the use of an inducible promoter enabled me to dissect specifically the time-dependency of  $\alpha\beta$ 3-integrin functions in tumour angiogenesis. Interestingly, I observed that the inhibitory effect on tumour growth and angiogenesis was transient, dissipated over time, and was not effective if tumour angiogenesis had already been established.

These findings indicate that the anti-tumourigenic/anti-angiogenic effects observed with the inducible deletion of endothelial  $\beta 3$ -integrin is time dependent, as demonstrated by the ability to escape the inhibitory effects of  $\beta 3$ -integrin blockade simply by extending the duration of the deletion in the inducible model. It is tempting to speculate that these findings help explain why long term pharmacological inhibition of  $\alpha v\beta 3$ -integrin functions do not work in the clinic: the molecule really only plays an essential role in the early stages of tumour growth.

This also correlates nicely with the finding that the constitutive deletion of endothelial  $\beta 3$ -integrin has no effect on tumour growth and angiogenesis. This might be explained by hypothesising that constitutive  $\beta 3$ -integrin deletion leads to the build up of compensatory mechanisms which circumvent  $\beta 3$ -integrin directed inhibition over time. Therefore, the constitutive model of  $\beta 3$ -integrin deletion might be a powerful tool to investigate the molecular and cellular changes which take over as a consequence of long term deletion of  $\beta 3$ -integrin and which might be responsible for acquired resistance to treatment in clinical settings. Taken as a whole, my findings highlight that both when to target  $\beta 3$ -integrin and for how long to target  $\beta 3$ -integrin to prevent tumour growth and angiogenesis are key aspects to consider for translational approaches.

The question of whether a genetic deletion elicits the same effect as a pharmacological inhibition is still open for debate. However, for the purpose of my studies a genetic approach was the most appropriate to accomplish an endothelial cell specific analysis of the role of  $\beta 3$ -integrin in tumour angiogenesis which cannot be achieved with pharmacological agents that will, of course, hit multiple cellular targets. Nonetheless, the light my studies shed on fundamental biology will certainly help improve pharmacological strategies.

### **3.6 Cre issues**

The Cre/loxP system is widely used in mice to achieve cell-type-specific gene deletion (Gu *et al.*, 1993), in particular for genes whose conventional null mutation is lethal. In my studies, I employed two endothelial specific Cre transgenic lines, where Cre expression was driven by *Tie1* and *Pdgfb* promoters which have been already used to study the functions of other endothelial integrins and of Focal Adhesion Kinase (Germain *et al.*, 2010; da Silva *et al.*, 2010; Tavora *et al.*, 2010).

*Tie1* promoter is active from E8.5 and allows Cre recombinase activity during embryogenesis and into adulthood (Gustafsson *et al.*, 2001), whereas *Pdgfb-iCreER<sup>T2</sup>* is a inducible promoter as Cre recombinase is activated only upon 4-hydroxytamoxifen administration (Claxton *et al.*, 2008).

Despite being extensively used, there are two main issues that need to be addressed when working with Cre transgenics: specificity and activity. The non-endothelial specificity of both *Tie1* and *Pdgfb* promoters was known since it had been extensively characterized in the publications in which these transgenic mice were originally described. This phenomenon also referred to as “leakiness of the promoter” involved certain neuronal populations and a small proportion of hematopoietic cells in *Tie1Cre* mice (Gustafsson *et al.*, 2001) and megakaryocytes in *Pdgfb-iCreER<sup>T2</sup>* mice (Claxton *et al.*, 2008). This issue was addressed by evaluating Cre recombinase activity and,  $\beta$ 3-integrin deletion, in these non-endothelial cell populations. This analysis was extremely relevant because both hematopoietic cells and megakaryocytes (which produce platelets), can contribute to angiogenesis to some extent. While no leakiness was detected in platelets, deletion of  $\beta$ 3-integrin was detected in bone marrow derived cells isolated from *Tie1Cre* positive bone marrow derived cells, but notably not in CXCR4+ (CD184) expressing cells. Therefore, I argued that the absence of  $\beta$ 3-integrin deletion in CXCR4+ bone marrow derived cells (mostly macrophages) explained why  $\beta$ 3-floxed/*Tie1Cre* positive mice did not exhibit enhanced tumour growth and angiogenesis *in vivo*, in marked contrast to  $\beta$ 3-integrin knockout mice (Reynolds *et al.*, 2002). This speculation was further supported by the finding that there was no change in  $\beta$ 3-integrin expression levels in tumour associated macrophages from  $\beta$ 3-floxed/*Tie1Cre* positive mice.

Nevertheless, it would be interesting to confirm this speculation by performing bone marrow transplant experiments in order to directly rule out the contribution of  $\beta$ 3-integrin expressed by bone marrow cells to the tumour growth and angiogenesis phenotype observed with the constitutive  $\beta$ 3-integrin deletion. This would require transplantation of wildtype ( $\beta$ 3-floxed/*Tie1Cre* negative) bone marrow into irradiated  $\beta$ 3-floxed/*Tie1Cre* positive mice. If my hypothesis is correct, I would expect to see no difference when comparing transplanted to non-transplanted mice.

With respect to Cre activity, this type of analysis was essential to enable a more direct comparisons between the two transgenic models. It was achieved by combining Western blot analyses to quantify the efficiency of  $\beta$ 3-integrin deletion in both lung and tumour associated endothelial cells and by performing Cre reporter analyses, which involved crossing the endothelial Tie1Cre and Pdgfb-iCreER<sup>T2</sup> lines with a Tomato Cre reporter line (Madisen *et al.*, 2010) to investigate the pattern of Cre activity *in vivo* and *ex vivo*. These combined strategies showed that Cre recombinase in both transgenic models behaved similarly, helping to rule out the possibility that differences observed when comparing the two models were due to intrinsic Cre related differences rather than to real biological ones.

The use of the inducible promoter requires Cre recombinase activation via tamoxifen administration. Difference in duration of induction required for activation of Cre might be influenced by the sensitivity of Cre recombinase itself (Weis *et al.*, 2008) and by the routes through which OHT is administered (for example intraperitoneal injection, oral gavage, tamoxifen enriched diet, slow release tamoxifen pellet). Since I have been comparing one Cre inducible system to a constitutive one (which does not require Cre activation), these considerations were not as relevant as they might have been if I were comparing two different inducible models; but they were still important with respect to investigating time-dependent effects of inducibly deleted genes.

Therefore, the choice of using 21-day-slow release tamoxifen pellets seemed to be the most preferable. It has been shown that efficient floxed gene deletion requires only 2 days in Pdgfb-iCreER<sup>T2</sup> mice (Indra *et al.*, 1999). I also confirmed it in aortic rings isolated from Pdgfb-iCreER<sup>T2</sup> positive/tdTomato heterozygous mice whereby I could detect Cre activity after 2 day of *ex vivo* OHT treatment. Moreover, tamoxifen pellets ensured controlled drug release in animals for 3 weeks, thereby reducing the variability of repeated OHT administration (intraperitoneal injection, oral gavage) or of relying on mice eating regularly (tamoxifen enriched diet) as confirmed by significantly reduced  $\beta$ 3-integrin protein levels in endothelial cells isolated from tumours grown  $\beta$ 3-floxed/Pdgfb-iCreER<sup>T2</sup> mice upon both short (3 days) and long (21 days) OHT treatments.

### **3.7 Endothelial $\alpha$ $\beta$ 3-integrin deficiency in the tumour vasculature**

Vessel density is a measure of how vascularised a tumour is. It is generally accepted that larger tumours have more vessels than smaller ones, but this is not necessarily

always true. Vessels can be present but function poorly or be leaky. Some tumours have been reported to have vessel pores 100 times bigger in size than those present in healthy vessels (Hobbs, 1998). Moreover, there is no definitive correlation between blood flow or oxygen consumption and tumour growth rate *in vivo* (Gullino, 1982).

However, my findings established a direct correlation between the reduction in tumour growth observed in the presence of an acute endothelial  $\beta$ 3-integrin deletion and reduction in vessel density. This angiogenic phenotype of increased tumour vascularization was shown not to be specific to a single tumour model; similar findings were observed in two strikingly different tumour models. These results are consistent with previous data from Mahabeleshwar *et al.* (2006) who showed that mice expressing a mutant of the  $\beta$ 3-integrin subunit in which both cytoplasmic tyrosine residues were mutated to phenylalanine and, unable to undergo phosphorylation (DiYF  $\beta$ 3 mutant mice); were deficient in angiogenesis thereby indicating a pro-angiogenic function for  $\beta$ -integrin in tumour angiogenesis. My studies narrowed down this pro-angiogenic function of  $\beta$ 3-integrin to endothelial cells and temporally defined it as important in the very early stages of angiogenesis. My findings suggest endothelial  $\beta$ 3-integrin plays a pivotal role in the early angiogenic processes; its acute deletion impairs tumour angiogenesis, thereby reducing tumour growth rate. However, when angiogenesis is already in full-swing endothelial  $\beta$ 3-integrin function becomes dispensable.

Abnormalities in pericyte and basement membrane support are associated with vessel structural deformities and reflect impaired vessel function (Jain, 2005). My structural analysis looking at pericyte coverage and endothelial basement membrane deposition, ruled out the involvement of endothelial  $\beta$ 3-integrin in these processes. In fact, despite the loss of endothelial  $\beta$ 3-integrin, tumour vessels exhibited normal pericyte and basement membrane support in line with findings of Taverna *et al.* (2004) showing enhanced tumour angiogenesis in mice lacking  $\beta$ 3 and  $\beta$ 3/ $\beta$ 5 integrins; whereas no difference in the structure of the vessels was reported. This was also described by McCarthy and colleagues (McCarthy *et al.*, 2002) who showed that cerebral microvessels were ultrastructurally normal in mice lacking  $\alpha$ v integrin.

Overall, I conclude that endothelial  $\beta$ 3-integrin is dispensable for vessel maturation and stabilization. Since the data indicate endothelial  $\beta$ 3-integrin as early pro-angiogenic regulator, some other functional parameters such as vessel leakiness and intratumoural hypoxia (Sadawa *et al.*, 2012) were not included in the functional vessel

analyses, as the absence of defects in vessel structure and function would at least in theory exclude them. However, I believe this evaluation would be extremely valuable to future studies investigating  $\alpha v\beta 3$ -integrin as a tumour endothelium targeted agent (Danhier *et al.*, 2012), but this is beyond the scope of this thesis.

## CONCLUSIONS

In this chapter, I have shown that:

- ***in vivo* tumour growth and angiogenesis are inhibited by inducible BUT NOT constitutive deletion of endothelial  $\beta 3$ -integrin;**
- **the *in vivo* efficiency of Cre induced deletion of endothelial  $\beta 3$ -integrin and the *in vivo* pattern of Cre activity are similar in both Tie1Cre and Pdgfb-iCreER<sup>T2</sup> models;**
- **extending the length of  $\beta 3$ -integrin deletion abrogates the *in vivo* inhibitory effect arising from its inducible deletion;**
- **the inhibitory effect of an inducible  $\beta 3$ -integrin deletion is transient and dissipates with time;**
- **an inducible  $\beta 3$ -integrin deletion has no effect when tumours have already been established.**

## 4. USING THE AORTIC RING ASSAY TO STUDY ENDOTHELIAL $\beta$ 3-INTEGRIN IN VESSEL SPROUTING

In order to fully understand the process of pathological angiogenesis, *in vivo* tumour experiments are required. However, the involvement of other cell types in angiogenic processes *in vivo* makes it difficult to discriminate endothelial specific responses from the contribution of other cells. On the other hand, *in vitro* angiogenesis assays often occur without actual sprouting of lumenised vessels or without involving the recruitment of supporting cells. The aortic ring assay, however, provides a more relevant model for studying angiogenesis *ex vivo*, as it allows to reproduce many of the key steps of microvessel sprouting over a timescale similar to that observed *in vivo* (Baker *et al.*, 2011). As such, I employed the aortic ring model to refine our understanding of the involvement of endothelial  $\beta$ 3-integrin in the angiogenic process, while at the same time excluding (at least to a degree) off-target contributors to *in vivo* phenotypes, such as bone marrow derived cells and inflammatory cells.

In this chapter, I will present my studies on the effect of the deletion of endothelial  $\beta$ 3-integrin in aortic ring angiogenesis and show that it largely recapitulates what I observed in the context of tumour angiogenesis.

### RESULTS AND FIGURES

#### 4.1 Inducible deletion of $\beta$ 3-integrin inhibits VEGF-induced microvessel sprouting *ex vivo*, while its constitutive deletion has the opposite effect

I evaluated the contribution of endothelial  $\beta$ 3-integrin to VEGF-induced angiogenesis to address whether it was affecting *ex vivo* angiogenesis and, if so, whether it reflected the pattern of pathological angiogenesis observed *in vivo*. In order to do that, I assessed microvessel sprouting in aortic ring explants from  $\beta$ 3-floxed/Tie1Cre and  $\beta$ 3-floxed/Pdgfb-iCreER<sup>T2</sup> positive and negative mice. Aortic rings were isolated, embedded in collagen and stimulated with VEGF. Sprouting microvessels were counted after 6 days of VEGF stimulation under phase-contrast microscopy and afterward, they were visualized by fluorescent labelling of endothelial cells with FITC-conjugated Isolectin B4 (IB4) (Baker *et al.*, 2011). Unstimulated (no VEGF treatment) rings acted as negative controls (Figure 4.1A). When compared to their Cre negative

counterparts, VEGF-induced sprouting was significantly enhanced in  $\beta 3$ -floxed/Tie1Cre positive rings; whereas it was inhibited in  $\beta 3$ -floxed/Pdgfb-iCreER<sup>T2</sup> positive rings, suggesting that inducible and constitutive deletion of  $\beta 3$ -integrin in endothelial cells elicited different angiogenic responses *ex vivo*.

The data are reminiscent of those observed *in vivo* where inducible deletion of endothelial  $\beta 3$ -integrin significantly inhibits tumour growth and angiogenesis; whereas its constitutive deletion does not. The data help strengthen the argument that endothelial  $\beta 3$ -integrin plays a role in the early stages of sprouting angiogenesis. The early inhibitory effects of blocking its expression are abolished upon long term deletion of the molecule, suggesting compensatory mechanisms are established over time.

#### **4.2 bFGF-induced microvessel sprouting *ex vivo* is not affected by loss of endothelial $\beta 3$ -integrin expression**

Tumour cells secrete VEGF, whose expression is driven by hypoxic conditions, but they can also produce many other angiogenic growth factors, e.g. basic Fibroblast Growth Factor, bFGF) (Carmeliet and Jain, 2011). Aside from being a more physiologically relevant model over other *in vitro* methods, the aortic ring assay also allows one to test several conditions, for instance different angiogenic growth factors. Therefore, I took advantage of this model to expand the analyses of the effect of endothelial  $\beta 3$  integrin deletion in *ex vivo* angiogenic responses dependent on bFGF stimulation.

Experimental studies have previously shown that bFGF stimulation requires embedding of aortic rings in a fibrin gel. (Nicosia, 2009; Zhu, 2003). Therefore, aortic rings were isolated from  $\beta 3$ -floxed/Tie1Cre and  $\beta 3$ -floxed/Pdgfb-iCreER<sup>T2</sup> mice, embedded in fibrin and stimulated with bFGF. Sprouting microvessels were counted after 6 days of bFGF stimulation via phase-contrast microscopy. Vessel sprouts were also visualised by fluorescent labelling of endothelial cells with FITC-conjugated IB4 (Figure 4.1B). Unstimulated (no bFGF treatment) rings acted as negative controls. Microvessel sprouting was similar when comparing all groups to one another suggesting, at least in the context of this assay, that endothelial  $\beta 3$ -integrin was not essential for bFGF induced microvessel sprouting.

### 4.3 *Ex vivo* Cre activity in aortic rings

A pre-requisite for these studies (as for the *in vivo* analyses) was determining the *ex vivo* pattern of Cre activity in the aortic ring model in both transgenic lines. Immunofluorescence analyses of collagen embedded Tie1Cre positive/tdTomato heterozygous and Pdgfb-iCreER<sup>T2</sup> positive/tdTomato heterozygous aortic rings showed that Tomato Cre reporter activity was expressed in all microvascular sprouts after 6 days of VEGF stimulation.

Cre activity appeared to be exclusively in endothelial cells, as demonstrated by overlapping fluorescent signals of Tomato and FITC-conjugated IB4+ angiogenic sprouts, but not overlapping signals when comparing Tomato fluorescence with NG2+ pericytes (Armulik *et al.*, 2011). This pattern was observed in both Tie1Cre positive/tdTomato heterozygous and Pdgfb-iCreER<sup>T2</sup> positive/tdTomato heterozygous aortic rings (Figure 4.2A). Since the Pdgfb promoter has been reported to be highly active in endothelial tip cells at the leading edge of angiogenic sprouts (Gerhardt *et al.*, 2003), differences in Cre activity within this population of cells between the 2 transgenic models could account for differences in angiogenic responses. Nevertheless, no differences were evident in the distribution of Cre activity when comparing microvessel sprouting from Tie1Cre positive/tdTomato heterozygous and Pdgfb-iCreER<sup>T2</sup> positive/tdTomato heterozygous aortic rings, suggesting that Cre activities *ex vivo* were similar in both tip and stalk cells in aortic ring sprouts (Figure 4.2A).

In parallel, the efficiency of  $\beta$ 3-integrin deletion was assessed by Western blot analysis whereby aortae were mechanically disrupted, aortic tissues lysed and then proteins extracted. Total  $\beta$ 3-integrin levels were reduced in Cre positive aortas compared to their Cre negative counterparts (Figure 4.2B). However, the reduction in  $\beta$ 3-integrin expression levels achieved in both transgenic model was only approximately 50% in  $\beta$ 3-floxed/Tie1Cre positive aortas and 60% in  $\beta$ 3-floxed/Pdgfb-iCreER<sup>T2</sup> positive aortas; this was likely due to the fact that  $\beta$ 3-integrin levels were quantified from the whole aortas, rather than only from neo-angiogenic sprouts where deletion has occurred (Figure 4.2B).

Overall these analyses show that *ex vivo* the two transgenic models behave similarly with respect to Cre specificity and efficiency. As such, a direct comparison of *ex vivo* angiogenic responses can be drawn between them.

#### **4.4 Microvessel sprouting is not suppressed by long OHT treatment of $\beta$ 3-floxed/Pdgfb-iCreER<sup>T2</sup> aortic rings**

In order to test whether it was the timing of  $\beta$ 3-integrin deletion in endothelial cells that determined angiogenic responses to VEGF-stimulation *ex vivo*, I adopted a similar strategy to the one I used *in vivo*: I mimicked the constitutive deletion of endothelial  $\beta$ 3-integrin that occurs in the Tie1Cre model by treating  $\beta$ 3-floxed/Pdgfb-iCreER<sup>T2</sup> mice for extended periods of time with OHT prior to conducting aortic ring assays.

This was achieved by taking aortic rings derived from  $\beta$ 3-floxed/Pdgfb-iCreER<sup>T2</sup> mice that had been treated with OHT *in vivo* for 33 days prior to embedding and by stimulating them with VEGF. Unstimulated rings were used as a negative control. Microvessel sprouts were visualized by fluorescent labelling of endothelial cells with FITC-conjugated IB4. I found that there was no difference in microvessel sprouting when comparing long OHT  $\beta$ 3-floxed/Pdgfb-iCreER<sup>T2</sup> positive and negative aortic rings, indicating that a prolonged deletion of endothelial  $\beta$ 3-integrin was sufficient to abolish the previously described inhibitory effect on aortic ring sprouting that occurred with an acute deletion (Figure 4.3A).

From these data, I conclude that the length of endothelial  $\beta$ 3-integrin deletion determines VEGF-dependent angiogenic responses both *ex vivo* and *in vivo*: long-term loss does not affect vessel sprouting, while acute loss significantly impairs it.

#### **4.5 $\beta$ 3-integrin deletion is ineffective when microvessel sprouting has already begun**

Based on the results presented here, it is reasonable to suggest that the timing of the deletion is critical in dictating whether VEGF-dependent angiogenic responses will be affected by the loss of endothelial  $\beta$ 3-integrin *ex vivo*. In order to test this hypothesis, I applied an *ex vivo* intervention strategy where  $\beta$ 3-integrin deletion in aortic rings derived from  $\beta$ 3-floxed/Pdgfb-iCreER<sup>T2</sup> animals was induced by OHT administration after microvessel sprouting had already begun, namely 3 days after the initiation of VEGF stimulation.

Microvessel sprouting was quantified after fluorescent labelling of endothelial cells with FITC-conjugated IB4 at day 8, which corresponded to 5 days of OHT treatment.

No significant differences were observed in the degree of sprouting when comparing  $\beta 3$  flox/flox/Pdgfb-iCreER<sup>T2</sup> positive and negative aortic rings (Figure 4.3B). Moreover, I showed that Cre recombinase became active within the first 24 hours of OHT treatment as displayed by Tomato fluorescence (Figure 4.3C).

These findings help sustain the hypothesis that endothelial  $\beta 3$ -integrin is required in the early stages of the angiogenic process both *in vivo* and *ex vivo*, but its contribution to angiogenesis becomes dispensable later on, once angiogenic sprouting has been established.

**Figure 4.1 Inducible deletion of  $\beta$ 3-integrin inhibits VEGF (but not bFGF) microvessel sprouting *ex vivo*, while the constitutive one has the opposite effect**

(A) Microvessel sprouting of aortic ring explants isolated from  $\beta$ 3-floxed/Tie1Cre and  $\beta$ 3-floxed/Pdgfb-iCreERT2 mice were embedded in collagen gel and stimulated with VEGF. Aortic rings from  $\beta$ 3-floxed/Pdgfb-iCreERT2 positive and negative mice were also supplemented with OHT (1  $\mu$ M). Unstimulated (no VEGF treatment) rings were used as a negative control. Sprouting microvessels were counted after 6 days of VEGF stimulation under phase-contrast and visualized by fluorescent labeling of endothelial cells with FITC-IB4. Bar graph shows total number of microvessel sprouts per aortic ring (means  $\pm$  SEM) after 6 days of stimulation. Data are representative of 3 independent experiments ( $n > 30$  rings per genotype,  $**p < 0.01$ , NS=not significant). Representative immunofluorescent images of FITC-IB4 (endothelial cell marker, in green) stained aortic ring explants isolated from  $\beta$ 3-floxed/Tie1Cre and  $\beta$ 3-floxed/Pdgfb-iCreERT2 positive and negative mice (scale bar=1 mm).

(B) Microvessel sprouting of aortic ring explants isolated from  $\beta$ 3-floxed/Tie1-Cre and  $\beta$ 3-floxed /Pdgfb-iCreERT2 mice were embedded in fibrin gel and stimulated with bFGF. Aortic rings from  $\beta$ 3-floxed/Pdgfb-iCreERT2 positive and negative mice were also supplemented with OHT (1  $\mu$ M). Unstimulated (no bFGF treatment) rings were used as a negative control. Sprouting microvessels were counted after 6 days of bFGF-stimulation under phase-contrast and visualized by fluorescent labeling of endothelial cells with FITC-IB4. Bar graph shows total number of microvessel sprouts per aortic ring (means  $\pm$  SEM) after 6 days of stimulation ( $n > 30$  rings per genotype, NS=not significant). Representative immunofluorescent images of FITC-IB4 stained aortic ring explants isolated from  $\beta$ 3-floxed/Tie1Cre and  $\beta$ 3-floxed/Pdgfb-iCreERT2 positive and negative mice (scale bar=0.5 mm).

Figure 4.1 Inducible deletion of  $\beta 3$ -integrin inhibits VEGF (but not bFGF) microvessel sprouting *ex vivo*, while the constitutive one has the opposite effect

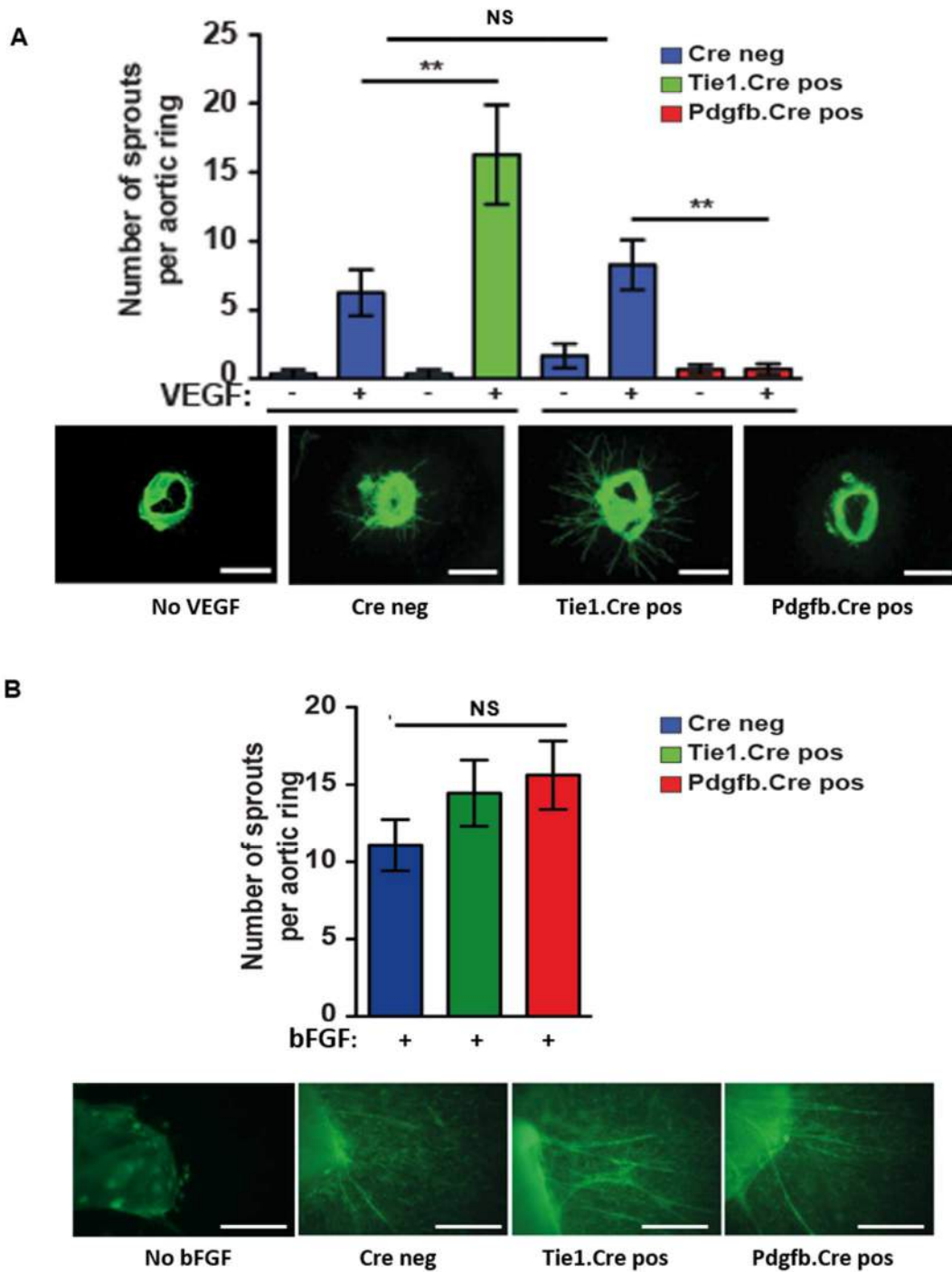


**Figure 4.2 Ex vivo Cre activity in aortic rings**

(A) Representative immunofluorescent analysis of aortic ring explants isolated from Tie1Cre positive/tdTomato heterozygous and Pdgfb-iCreER<sup>T2</sup> positive/tdTomato heterozygous mice which exhibit Tomato Cre reporter activity (in red) in all microvascular sprouts after 6 days of VEGF stimulation (low magnification, scale bar=0.5 mm). Aortic ring explants isolated from Tie1Cre positive/tdTomato heterozygous and Pdgfb-iCreER<sup>T2</sup> positive/tdTomato heterozygous mice were co-stained with FITC-IB4 (endothelial cell marker, in green) or NG-2 (pericyte marker, in green). Arrows point to examples of Tomato Cre reporter activity overlapping with endothelial cells but not with pericytes (scale bar=50  $\mu$ m).

(B)  $\beta$ 3-integrin is decreased ex vivo in microvascular aortic ring sprouts from  $\beta$ 3-floxed/Tie1-Cre and  $\beta$ 3-floxed/Pdgfb-iCreER<sup>T2</sup> mice. Representative Western blot analysis of protein lysates obtained from aortas of  $\beta$ 3-floxed/Tie1Cre and  $\beta$ 3-floxed/Pdgfb-iCreER<sup>T2</sup> positive and negative mice showed decreased  $\beta$ 3-integrin levels in Cre positive aortae in both models, whereas VEGFR2 levels were unchanged. HSC 70 provided a loading control. Bar graph shows  $\beta$ 3-integrin quantification relative to HSC 70 expression (mean  $\pm$  SEM, n=3 experiments; \*\*p<0.01).

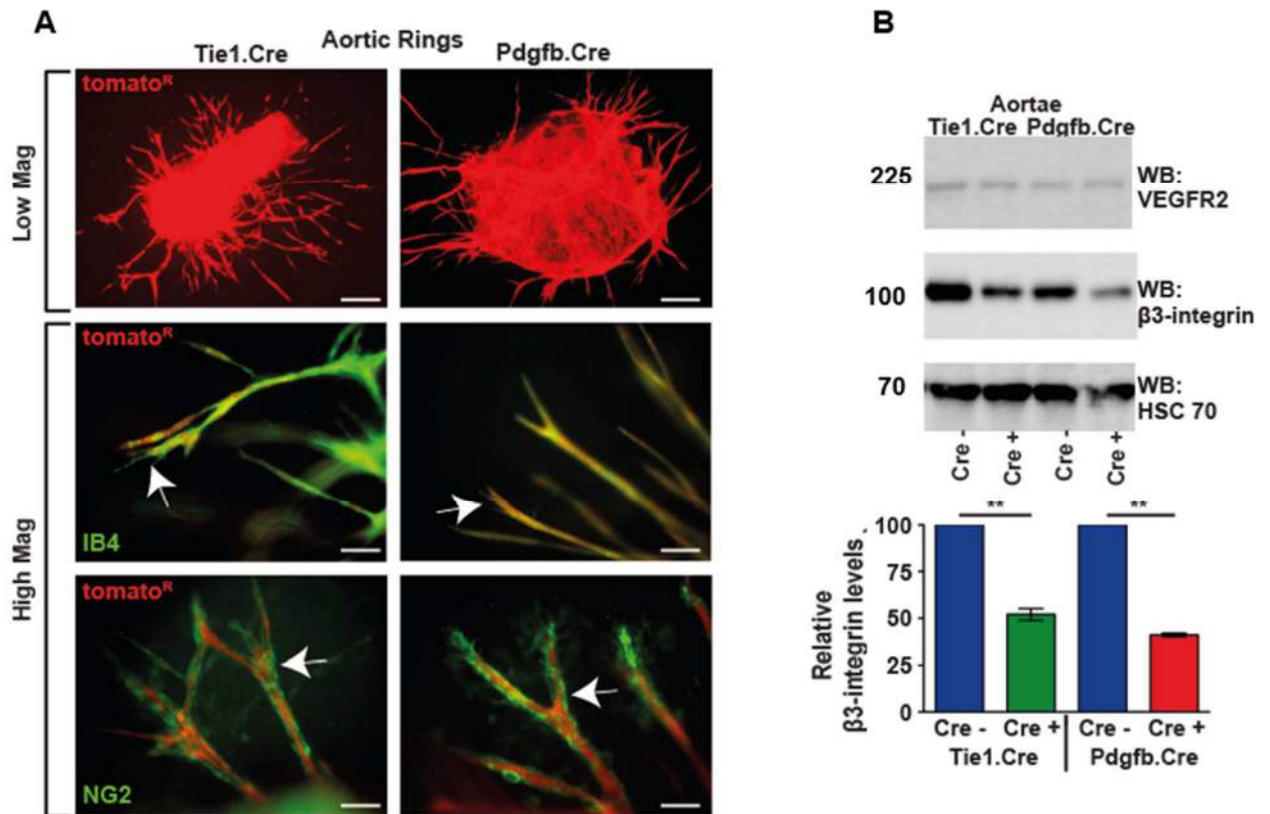


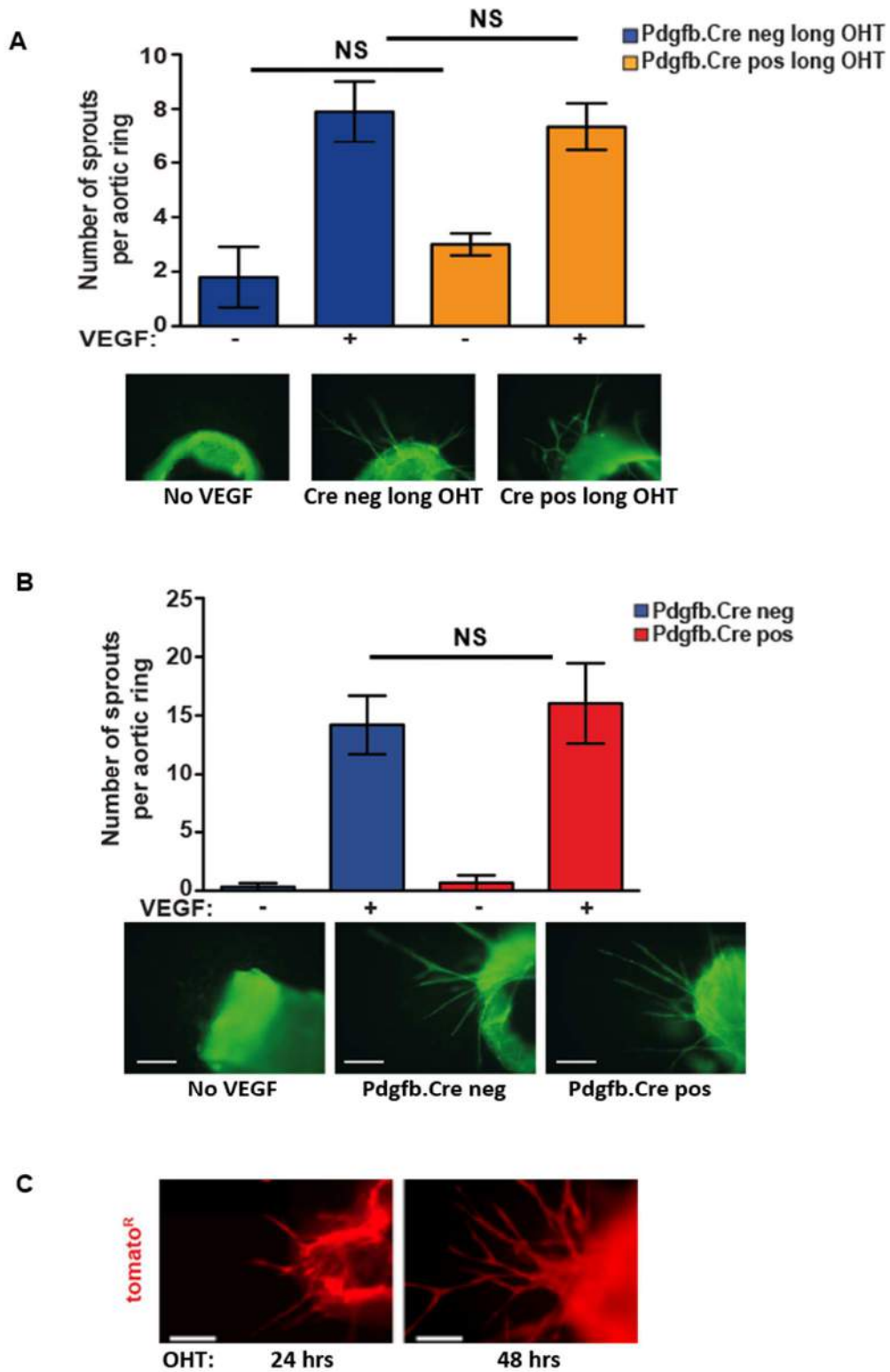
**Figure 4.3 The length of endothelial  $\beta$ 3-integrin deletion dictates the angiogenic response *ex vivo***

**(A)** Extending the inducible deletion of endothelial  $\beta$ 3-integrin by 21-day-OHT treatment reverses the inhibitory effect on VEGF-induced microvessel sprouting. Aortic ring explants isolated from long OHT  $\beta$ 3-floxed/Pdgfb-iCreER<sup>T2</sup> mice were embedded in collagen gel and stimulated with VEGF and supplemented with OHT (1  $\mu$ M). Unstimulated (no VEGF treatment) rings were used as a negative control. Sprouting microvessels were counted after 6 days of VEGF stimulation under phase-contrast and visualized by fluorescent labeling of endothelial cells with FITC-IB4 (endothelial cell marker, in green). Bar graph shows total number of microvessel sprouts per aortic ring (means  $\pm$  SEM) after 6 days of stimulation. Data are representative of 3 independent experiment (n>30 rings per genotype, NS=not significant). Representative immunofluorescent images of FITC-IB4 stained aortic ring explants isolated from long OHT  $\beta$ 3-floxed/Pdgfb-iCreER<sup>T2</sup> mice (scale bar=0.5 mm).

**(B)** Deletion of endothelial  $\beta$ 3-integrin when aortic angiogenesis is already established does not affect VEGF-induced microvessel sprouting. Aortic ring explants isolated from non-OHT-treated  $\beta$ 3-floxed/Pdgfb-iCreER<sup>T2</sup> mice were stimulated with VEGF and treated with OHT (1 $\mu$ m) after 3 days of culture. Unstimulated rings (no VEGF treatment) were used as a negative control. Bar graph shows total number of microvessel sprouts per aortic ring (means  $\pm$  SEM) after 8 days of stimulation. Data are representative of 3 independent experiments (n>20 ring per genotype, NS=not significant). Representative immunofluorescent images of FITC-IB4 stained aortic ring explants isolated from  $\beta$ 3-floxed/Pdgfb-iCreER<sup>T2</sup> mice treated with OHT 3 days after embedding (scale bar=0.5 mm).

**(C)** Representative immunofluorescent images of aortic ring explants isolated from Pdgfb-iCreER<sup>T2</sup> positive/tdTomato heterozygous mice displaying Tomato Cre reporter activity (in red) 24 and 48 hours after OHT administration (scale bar=0.5 mm).

Figure 4.3 The length of endothelial  $\beta 3$ -integrin deletion dictates the angiogenic response ex vivo



## DISCUSSION

### 4.5 The aortic ring model

The aortic ring model is based on the capacity of rat or mouse aortic explants to form new vessels in 3D gels. This was originally observed in the early 1980s by Joseph Leighton (Nicosia *et al.*, 1982), with a very good timing in the angiogenesis field, in fact less than 10 years before, Folkman hypothesised that tumour growth was angiogenesis dependent (Folkman, 1971) and soon after Folkman's group successfully isolated microvascular endothelial cells from bovine adrenal gland, showing they were capable of forming tubes *in vitro* (Folkman *et al.*, 1980). The aortic ring model rapidly became one of the most commonly used models of angiogenesis because it bridged the gap between *in vitro* and *in vivo* angiogenesis assays (Baker *et al.*, 2011).

The *ex vivo* microvessel sprouting produced by aortic rings is the result of the paracrine interaction between a mixed population of resident cells (endothelial cells, pericytes, fibroblasts, macrophages) under culture conditions. It mimicks the steps of the angiogenic process (Nicosia, 2009). Briefly, the first cells to migrate out of the aortic rings after one or two days are fibroblasts and macrophages, originating from the aortic adventitia. Endothelial sprouts first appear at the edges of the explants after two or three days of culture and are made of migratory cells which extend filopodia-like processes. As the outgrowth elongates, vessels develop a visible lumen and become surrounded by pericytes, which migrate and proliferate along the endothelium. After sprouting and branching for approximately one week, vessels stop growing and begin to regress. Therefore, this was a suitable model to investigate whether endothelium was positively regulating the early stages of physiological angiogenesis *ex vivo* (Nicosia, 2009).

### 4.6 $\alpha v\beta 3$ -integrin in aortic angiogenesis

The dualistic role  $\alpha v\beta 3$ -integrin has been described also in aortic ring angiogenesis. A number of studies have shown that angiogenesis was significantly enhanced in  $\beta 3$  deficient aortic explants (Reynolds *et al.*, 2004), or by treating aortic cultures with nanomolar concentrations of  $\alpha v\beta 3/\alpha v\beta 5$  inhibitors (Reynolds *et al.*, 2009); whereas it was impaired in aortic rings from DiYF  $\beta 3$ -mutant mice (Mahabeleshwar *et al.*,

2006), mirroring the conflicting responses observed in tumour models of pathological angiogenesis.

Consistent with the previously described *in vivo* phenotypes, my findings showed a time dependent inhibitory effect of endothelial  $\beta$ 3-integrin in *ex vivo* aortic ring angiogenesis. I also showed that this effect was VEGF-specific, (bFGF dependent angiogenesis did not elicit the same response). Moreover, I was able to confirm that this effect dissipated over time and did not affect aortic ring angiogenesis if the deletion of endothelial  $\beta$ 3-integrin was induced by *ex vivo* OHT treatment, when microvessel sprouting had already begun. These data help strengthen the argument that endothelial  $\beta$ 3-integrin plays a role in the early stages of sprouting angiogenesis (endothelial cell proliferation, migration and sprouting) which is really what *ex vivo* aortic ring model allows one to track precisely.

Despite the consistency with the *in vivo* data, it may be argued that the reduced microvessel sprouting observed with the acute  $\beta$ 3-integrin deletion might be due to a difference in functional Cre recombinase activity as it has been reported that the *Pdgfb* promoter is highly active in endothelial tip cells at the leading edge of angiogenic sprouts compared stalk cells (Gerhardt *et al.*, 2003). Tomato reporter analysis of Cre activity of both  $\beta$ 3-floxed/Tie1Cre and  $\beta$ 3-floxed/*Pdgfb*-iCreER<sup>T2</sup> positive aortic explants excluded this hypothesis by showing equal distribution of Tomato Cre fluorescence along the entire length of aortic sprouts.

Interestingly, VEGF aortic ring angiogenesis was enhanced in presence of constitutive endothelial  $\beta$ 3-integrin deletion (phenocopying  $\beta$ 3 knockout aortic rings - Reynolds *et al.*, 2004). This might be partially explained by the complexity of the *in vivo* angiogenic responses in the tumour *milieu*, whereas the *ex vivo* aortic ring model is a more defined microenvironment (Baker *et al.*, 2011) that largely excludes inflammatory and immune cells, although the involvement of macrophages has been reported (Gelati *et al.*, 2008). This helps discriminate the contribution of off-target cells in determining the *in vivo* phenotype.

Importantly,  $\beta$ 3-integrin is expressed by different cell types, all of which can contribute to tumour angiogenesis, particularly bone marrow derived cells (Robinson and Hovidala-Dilke, 2011). Considering the leakiness of the *Tie1* promoter on hematopoietic cells (Gustafsson *et al.*, 2001) and their role in tumour angiogenesis as demonstrated by the rescue of the KO and DiYF angiogenic phenotypes by wild-

type bone marrow transplants; I would speculate the effect of inducible  $\beta$ 3-integrin deletion is endothelial cell specific (as observed both *in vivo* and *ex vivo* in the Pdgfb model), whereas what happens with its long term deletion clearly implicates other non-endothelial cells in mediating the antiangiogenic effects; thereby explaining the difference in the *ex vivo* and *in vivo* phenotype in the constitutive model.

## CONCLUSIONS

In this chapter, I have shown that:

- ***ex vivo* VEGF-dependent angiogenesis is reduced by inducible BUT NOT constitutive loss of endothelial  $\beta$ 3-integrin;**
- **the *ex vivo* efficiency of Cre-induced  $\beta$ 3-integrin deletion and the *ex vivo* pattern of Cre activity are similar in the Tie1 Cre and Pdgfb-iCreER<sup>T2</sup> models;**
- **extending the length of  $\beta$ 3-integrin deletion abrogates the inhibitory effect arising from its inhibition in the aortic ring model;**
- **an inducible  $\beta$ 3-integrin endothelial deletion has no effect when microvessel sprouting has already begun.**

## **5. MECHANISTIC ANALYSIS OF THE ROLE OF ENDOTHELIAL $\beta$ 3-INTEGRIN: *IN VITRO* STUDIES**

The two transgenic models I have described so far differ from each other in the timing of endothelial  $\beta$ 3-integrin deletion. On whole, the results suggest that: (1) the expression of the molecule is required early on in primary tumour growth and angiogenesis; (2) long-term suppression of the molecule leads to  $\beta$ 3-integrin independent escape mechanisms, taking over in the early stages of primary tumour growth; and (3) already established tumours have a decreased need for endothelial  $\beta$ 3 integrin expression.

To explore the potential mechanisms underlying some of these conclusions, I investigated VEGF-induced endothelial cell signalling, proliferation and migration, which are crucial components of the initial phases of angiogenic sprouting (Carmeliet, 2000; Risau, 1997). I carried out these experiments *in vitro* using immortalized endothelial cells isolated from the lungs of Tie1Cre and Pdgfb-iCreER<sup>T2</sup> animals for the reasons which will be discussed in paragraph 5.1.1.

In this Chapter, I will describe some of the cellular and molecular changes I found in the two Cre models which correlated with the phenotypic differences described in previous chapters.

### **RESULTS AND FIGURES**

#### **5.1 *In vitro* cellular differences between the two Cre transgenic models**

I decided to investigate endothelial cell behaviour *in vitro* in order to characterize the cellular and molecular differences which may account for the *in vivo* phenotypic differences observed between inducible versus constitutive deletion of endothelial  $\beta$ 3-integrin; differences which may help explain why long-term genetic inhibition of the molecule leads to “treatment escape”.

##### **5.1.1 Why use immortalized rather than primary endothelial cells?**

Due to their slow growth and limited capacity to divide in culture, it is difficult to obtain sufficient quantities of primary endothelial cells to perform the *in vitro* analyses I

needed to address mechanistically the time dependent differences observed in the two transgenic models. I therefore opted to immortalize lung endothelial cells via polyoma-middle-T-(PyMT) antigen retroviral infection (May *et al.*, 2005). Being aware of the potential issues associated with interpreting the findings from these cells (e.g. phenotype stability and potentially altered behaviour in culture), I routinely monitored cell morphology, compared cells at similar passages (and not older than passage 15), and checked for expression of a number of endothelial cell markers (VEC, CD31, ICAM-2) (Figure 5.B, 5.1C). All cells appeared to maintain their endothelial cell identity and phenotypic characteristics over multiple passages in culture (Figure 5.1A).

### 5.1.2 Surface expression of endothelial integrin and adhesion properties

Sprouting angiogenesis is dependent on the regulation of integrin expression (Avramides *et al.*, 2008). Given the differences in angiogenic responses between  $\beta$ 3-floxed/Tie1-Cre and  $\beta$ 3-floxed/Pdgfb-iCreER<sup>T2</sup> models, it was conceivable to ask whether  $\beta$ 3-integrin deletion changed the surface expression pattern of other integrin subunits, which might lead to changes in endothelial cell behaviour or function. Therefore, the expression and function of several other endothelial integrins was analysed.

I used flow cytometric analyses to quantify the surface expression of endothelial  $\alpha$  ( $\alpha$ 1,  $\alpha$ 2,  $\alpha$ 5,  $\alpha$ v) and  $\beta$  ( $\beta$ 1,  $\beta$ 3) integrin subunits (Figure 5.2A) in  $\beta$ 3-floxed/Tie1Cre and  $\beta$ 3-floxed/Pdgfb-iCreER<sup>T2</sup> positive and negative endothelial cells. Whilst  $\alpha$ 2 integrin levels appeared to decrease in Cre positive cells from both models, no significant changes in expression were detected in any of the other integrin subunits I examined (except for  $\beta$ 3-integrin which decreased, as expected, in Cre positive endothelial cells). These findings suggest that integrin subunit expression at the cell surface was not altered by either an inducible or constitutive  $\beta$ 3-integrin deletion.

Since I was unable to detect surface expression of  $\beta$ 5-integrin, I analysed its total level by Western blot. Interestingly, a significant decrease of this integrin subunit was observed in  $\beta$ 3-floxed/Tie1Cre positive endothelial cells compared to  $\beta$ 3-floxed/Tie1-Cre negative endothelial cells; this difference was not observed in  $\beta$ 3-floxed/Pdgfb-iCreER<sup>T2</sup> positive endothelial cells (Figure 5.2B). It would be tempting to speculate that constitutive endothelial deletion of  $\beta$ 3-integrin is associated with a reduction in the

total level of  $\beta 5$ -integrin expression, though it remains to be determined whether this translates to changes at the surface.

Integrins are allosteric molecules that can exist in activated and non-activated states (Avramides *et al.*, 2008), and even when expressed at the cell surface, their expression levels do not necessarily predict their activity. To test whether endothelial integrin function was affected by the absence of  $\beta 3$ -integrin, adhesion capacity was tested on several extracellular matrices. Having observed minimal changes in the profile on surface integrin in the absence of  $\beta 3$ -integrin, I did not expect to find significant differences in adhesion to extracellular matrix components, except for vitronectin, the canonical ligand of  $\alpha v\beta 3$ -integrin.

Adhesion to collagen I, fibronectin, laminin I and vitronectin was quantified in  $\beta 3$ -floxed/Tie1Cre and  $\beta 3$ -floxed/Pdgfb-iCreER<sup>T2</sup> positive and negative endothelial cells. BSA was used as a negative control and the degree of adhesion was expressed as a percentage of relative adhesion to fibronectin (Figure 5.2C). The data confirmed that endothelial specific  $\beta 3$ -integrin deletion had no effect on adhesive properties to collagen I, fibronectin and laminin I. In contrast adhesion to vitronectin was significantly impaired. Similar results were obtained in both transgenic models supporting the conclusion that adhesion was not affected by the genetic deletion of  $\beta 3$ -integrin.

These data suggest the differences observed between the two transgenic models *in vivo* are not related to either changes in integrin expression at the cell surface (with the possible exception of  $\beta 5$ -integrin) or to changes in overall matrix adhesion.

### **5.1.3 VEGF-induced migration and proliferation**

Sprouting angiogenesis involves the migration and proliferation of endothelial cells in response to growth factor signals (Carmeliet, 2000; Risau, 1997). Given that  $\beta 3$ -integrin has been generally implicated in regulating both of these processes (Avramides *et al.*, 2008), I decided to examine whether constitutive or inducible  $\beta 3$ -integrin deletion in endothelial cells affected their *in vitro* migratory responses and/or proliferative behaviour to VEGF.

2D migration was examined by performing scratch wound healing assay on  $\beta 3$ -floxed/Tie1-Cre and  $\beta 3$ -floxed/Pdgfb-iCreER<sup>T2</sup> endothelial cell monolayers in the

presence or absence of VEGF stimulation. The scratch wound healing assay allows analysis of 2D *in vitro* non directional migration in response to a specific stimulus over time (until the scratch closes). VEGF treatment enhanced wound closure in both  $\beta$ 3-floxed/Tie1Cre positive and negative endothelial cells, but no differences were noted when comparing them to each other (Figure 5.3A). In contrast, VEGF-induced wound closure in  $\beta$ 3-floxed/Pdgfb-iCreER<sup>T2</sup> positive endothelial cells was significantly reduced in comparison to  $\beta$ 3-floxed/Pdgfb-iCreER<sup>T2</sup> negative endothelial cells (Figure 5.3A).

Proliferation of  $\beta$ 3-floxed//Tie1Cre and  $\beta$ 3-floxed//Pdgfb-iCreER<sup>T2</sup> endothelial cells was assessed over 48 hours in presence and absence of VEGF stimulation. Cell growth was measured indirectly as a function of the metabolic conversion of MTT (4,5-dimethylthiazol-2-yl)-2,5-diphenyltetrazolium bromide) to a chromogenic substrate which was then solubilized and quantified by optical density. No significant changes in proliferative rate were noted in either Cre model, when comparing Cre negative to Cre positive cells. Nor did I noted any differences when comparing the two Cre models to each other. This suggested that endothelial  $\beta$ 3-integrin expression is dispensable for initiating the proliferative process (Figure 5.3B).

Collectively, these results report a role for endothelial  $\beta$ 3-integrin in promoting VEGF-mediated cell migration, but not cell proliferation, *in vitro*. The effects on migration are seemingly dependent on the timing of the deletion. The inducible deletion of  $\beta$ 3 integrin in endothelial cells impaired 2D migration, but the impairment was overcome if the expression of the molecule was suppressed long term.

## **5.2 *In vitro* molecular differences between the two Cre transgenic models**

### **5.2.1 VEGFR2 analysis: total, surface, and phosphorylated levels**

Aside from the well-established role of VEGF/VEGFR2 in endothelial cell proliferation and migration (Cebe-Suarez *et al.*, 2006; Shibuya and Claesson-Welsh, 2006), another important function of  $\alpha$ v $\beta$ 3-integrin is the regulation of VEGFR2 recycling back to the cell surface (Caswell *et al.*, 2009).

Thus, I hypothesised that the differences in VEGF-mediated angiogenic responses between inducible versus constitutive deletion of endothelial  $\beta$ 3-integrin might be reflected in a change in VEGFR2 expression at the cell surface and/or in its function.

VEGFR2 expression and activity were analysed in  $\beta$ 3-floxed/Tie1Cre and  $\beta$ 3-floxed/Pdgfb-iCreER<sup>T2</sup> endothelial cells following VEGF stimulation. Western blot analyses showed that total levels of VEGFR2 expression did not change upon endothelial-specific deletion of  $\beta$ 3-integrin, regardless of the Cre driving the deletion (Figure 5.4B).

I further characterised VEGFR2 function by analysing its phosphorylation at tyrosine 1175 (Y1175) within the intracellular kinase domain, which has been extensively characterised as an important site in regulating intracellular downstream signalling pathways via phospholipase PLC $\gamma$  (as described in paragraph 1.4.2).  $\beta$ 3-floxed//Tie1Cre and  $\beta$ 3-floxed/Pdgfb-iCreER<sup>T2</sup> endothelial cells were stimulated with VEGF and phosphorylated (Y1175) levels of VEGFR2 were assessed by Western blot (Figure 5.3B).  $\beta$ 3-floxed//Pdgfb-iCreER<sup>T2</sup> positive endothelial cells displayed a reduction in VEGF-induced VEGFR2 phosphorylation at Y1175; whereas no changes were observed in  $\beta$ 3-floxed//Tie1-Cre positive endothelial cells, suggesting that VEGFR2 activity diminished only when endothelial  $\beta$ 3 integrin was deleted acutely.

Total expression levels may not reflect difference in expression at the cellular surface where receptors are meant to signal upon ligand binding. To address this point, surface levels of VEGFR2 were analysed by flow cytometry. A small but significant (and similar to that observed in  $\beta$ 3 knockout endothelial cells included as control) increase in surface expression of VEGFR2 was observed in  $\beta$ 3-floxed//Tie1Cre positive endothelial cells compared with  $\beta$ 3-floxed//Tie1Cre negative endothelial cells (Figure 5.4A). However, surface VEGFR2 levels were similar when comparing  $\beta$ 3-floxed/Pdgfb-iCreER<sup>T2</sup> positive and negative endothelial cells, suggesting that VEGFR2 expression was increased only when  $\beta$ 3-integrin was deleted constitutively in endothelial cells. It is conceivable that this small increase contributes to the enhanced *in vitro* responses observed in  $\beta$ 3-floxed/Tie1Cre positive endothelial cells (see below), though it is unclear why this did not correspond to an increase in VEGFR2 phosphorylation.

Overall, these results highlight the plasticity of the cross-talk between  $\beta$ 3-integrin and VEGFR2 in presence of VEGF in endothelial cells whereby its inducible deletion impaired receptor signalling; whereas its constitutive one is partially compensated for by increased receptor surface expression of VEGFR2.

## 5.2.2 VEGF/VEGFR2 signalling analysis

Given that my results showed a difference in VEGFR2 phosphorylation in the presence of acute deletion of  $\beta$ 3-integrin in endothelial cells, I examined in greater detail VEGFR2 signalling (as described in paragraph 1.4.2) in an attempt to determine which pathways were affected. One of the main VEGFR2 downstream signalling pathways is the MAPK/ERK pathway.

Therefore, I examined ERK1/2 levels (both total and phosphorylated) by Western blot analyses in a VEGF-stimulation time course in  $\beta$ 3-floxed/Tie1Cre and  $\beta$ 3-floxed/Pdgfb-iCreER<sup>T2</sup> endothelial cells. ERK1/2 phosphorylation was enhanced in  $\beta$ 3-floxed/Tie1Cre positive compared to  $\beta$ 3-floxed/Tie1Cre negative endothelial cells, but suppressed in  $\beta$ 3-floxed/Pdgfb-iCreER<sup>T2</sup> positive endothelial cells (Figure 5.4B). As for other intracellular signalling molecules, I further evaluated phosphorylated and total levels of c-Src and PLC $\gamma$  (as described in paragraph 1.4.2) by Western blot analyses in a VEGF-time course. No significant changes were noted between  $\beta$ 3-floxed/Tie1Cre and  $\beta$ 3-floxed/Pdgfb-iCreER<sup>T2</sup> positive and negative endothelial cells in either total or phosphorylated levels of c-Src or PLC $\gamma$  (Figure 5.4A).

I therefore focused my analyses on the VEGFR2 downstream effectors Focal Adhesion Kinase (FAK) and stress-activated protein kinase-2/p38 (SAPK2/p38). FAK is a non-receptor protein-tyrosine kinase which acts as point of convergence of VEGF/VEGFR2 and integrin-mediated signals for migration (Zachary and Glick, 2001). Interestingly, I detected a reduction in the levels of total FAK in  $\beta$ 3-floxed/Tie1Cre positive endothelial cells compared to  $\beta$ 3-floxed/Tie1Cre negative endothelial cells (Figure 5.4A). Since it has been recently shown that reduced FAK levels in FAK heterozygous mice display an imbalance in FAK phosphorylation at tyrosine 397 (Y397) and tyrosine 861 (Y861), which correlates with enhanced tumour growth and angiogenesis (Kostourou *et al.*, 2013), I expanded my analyses to examine these phosphorylation sites of FAK.

Western blot analyses indicated that no changes in FAK expression or phosphorylation were noted in  $\beta$ 3 flox/flox/Pdgfb-iCreER<sup>T2</sup> Cre positive endothelial cells when comparing them to their Cre negative counterpart (Figure 5.6A). However, total FAK levels were reduced by 50% in  $\beta$ 3-floxed/Tie1Cre positive endothelial cells when compared to  $\beta$ 3-floxed/Tie1Cre negative endothelial cells, as were levels of phosphorylated Y397 (Figure 5.6A). On opposite, the levels of phosphorylated Y861

were similar between the two cell lines, suggesting that the imbalance in tyrosine phosphorylation that occurs in FAK heterozygous mice was partially recapitulated by a long term loss of endothelial  $\beta$ 3-integrin. Importantly, immunohistochemical analysis of FAK expression in tumour vessels displayed the same result of reduced total FAK levels in  $\beta$ 3-floxed/Tie1Cre positive, but not from  $\beta$ 3-floxed/Pdgfb-iCreER<sup>T2</sup> positive tumours (Figure 5.6B). With respect to SAPK/p38, no significant changes were noted between  $\beta$ 3-floxed/Tie1Cre and  $\beta$ 3-floxed/Pdgfb-iCreER<sup>T2</sup> positive and negative endothelial cells in either total or phosphorylated levels (Figure 5.4A).

These findings suggest that long-term deletion of endothelial  $\beta$ 3-integrin leads to an increase in ERK phosphorylation, a reduction in FAK expression and a imbalance in FAK phosphorylation. Whilst still correlative (I have not tested the functional significance of these changes) these molecular changes may account for possible mechanisms of escape from long term genetic inhibition of  $\beta$ 3-integrin.

### **5.3 The differences observed in $\beta$ 3-integrin acutely deleted endothelial cells are abolished by long OHT treatment *in vitro***

Given that the two transgenic models appear to mostly differ in the amount of time that  $\beta$ 3 integrin has been deleted, extending the time of its deletion by long OHT treatment in the inducible model should abrogate the *in vitro* differences associated with its inducible deletion. To investigate further the time dependency of the differences noted above, I examined many of the same parameters in endothelial cells isolated from long OHT  $\beta$ 3-floxed Pdgfb-iCreER<sup>T2</sup> mice.

#### **5.3.1 Molecular differences upon long OHT treatment**

Flow cytometric analyses of endothelial integrin ( $\alpha$ 1,  $\alpha$ 2,  $\alpha$ 5,  $\alpha$ v,  $\beta$ 1, and  $\beta$ 3) subunit expression levels were performed on  $\beta$ 3-floxed/Pdgfb-iCreER<sup>T2</sup> lung endothelial cells which had been isolated from 33-day OHT treated mice. No significant changes were noted when comparing long OHT  $\beta$ 3-floxed/Pdgfb-iCreER<sup>T2</sup> positive to long OHT  $\beta$ 3-floxed/Pdgfb-iCreER<sup>T2</sup> negative endothelial cells (Figure 5.5A). On the other hand, Western blot analyses revealed a significant reduction in total levels of  $\beta$ 5 integrin in  $\beta$ 3-floxed/Pdgfb-iCreER<sup>T2</sup> positive endothelial cells, mimicking what I observed in  $\beta$ 3-floxed/Tie1Cre positive endothelial cells (Figure 5.5A).

I further assessed VEGFR2 expression and activity by Western blot in long OHT  $\beta 3$ -floxed/Pdgfb-iCreER<sup>T2</sup> endothelial cells. Cells were stimulated with VEGF and protein lysates were Western blotted for phosphorylated (Y1175) VEGFR2 and then reblotted for total VEGFR2. Total VEGFR2 levels were unchanged between the two genotypes, as were phosphorylated VEGFR2 levels (Figure 5.6C).

In parallel, flow cytometry was performed to quantify surface expression levels of VEGFR2 in long OHT  $\beta 3$ -floxed/Pdgfb-iCreER<sup>T2</sup> endothelial cells. Similarly to what was noted in  $\beta 3$ -floxed/Tie1Cre positive endothelial cells, long OHT  $\beta 3$ -floxed/Pdgfb-iCreER<sup>T2</sup> positive endothelial cells displayed increased VEGFR2 surface expression when compared to their Cre negative counterparts (Figure 5.6C).

Likewise, I examined total and phosphorylated levels of ERK1/2 and FAK proteins by Western blot analyses in long OHT  $\beta 3$ -floxed/Pdgfb-iCreER<sup>T2</sup> endothelial cells over a time course of VEGF stimulation. Protein lysates were Western blotted for phosphorylated ERK1/2 and phosphorylated (Y397 and Y861) FAK, then reblotted for total ERK1/2 and total FAK. Densitometric quantification of phosphorylated ERK 1/2 levels did not show any significant difference between long OHT  $\beta 3$ -floxed/Pdgfb-iCreER<sup>T2</sup> positive and negative endothelial cells (Figure 5.6D). In contrast, total FAK levels showed a significant decrease in long OHT  $\beta 3$ -floxed/Pdgfb-iCreER<sup>T2</sup> positive endothelial cells compared to long OHT  $\beta 3$ -floxed/Pdgfb-iCreER<sup>T2</sup> negative endothelial cells. Moreover, the ratio between phosphorylated Y397 and Y861 was affected in long OHT  $\beta 3$ -floxed/Pdgfb-iCreER<sup>T2</sup> positive endothelial cells: phosphorylated Y397 decreased, but phosphorylated Y861 did not (Figure 5.7A). Consistently immunohistological analysis of tumour vessels revealed the same result of reduced total FAK levels in tumour vessels from long OHT  $\beta 3$ -floxed/Pdgfb-iCreER<sup>T2</sup> positive tumours compared to long OHT  $\beta 3$ -floxed/Pdgfb-iCreER<sup>T2</sup> negative tumours (Figure 5.7B).

To summarize, while the endothelial  $\beta 3$ -integrin inducible deletion, driven by the Pdgfb-iCreER<sup>T2</sup> promoter, resulted in reduced VEGFR2 phosphorylation at Y1175, following long OHT treatment this difference was no longer observed. Moreover, long OHT  $\beta 3$ -floxed/Pdgfb-iCreER<sup>T2</sup> positive endothelial cells showed decreased total expression levels of  $\beta 5$  integrin, enhanced VEGFR2 surface levels, reduced FAK expression and misbalanced FAK phosphorylation; all of which seemingly phenocopied what was observed with constitutive endothelial  $\beta 3$ -integrin deletion driven by the Tie1Cre promoter (as summarized below).

	Tie1 Cre	Pdgfb-iCreER <sup>T2</sup>	long OHT Pdgfb-iCreER <sup>T2</sup>
Total VEGFR2	—	—	—
Surface VEGFR2	↑	↓	↑
Y1175 VEGFR	↑	↓	↑
p-ERK 1/2	↑	↓	↑
β5 integrin	↓	↑	↓
Total FAK	↓	↑	↓
Y397 FAK	↓	↑	↓
Y861 FAK	—	—	—

Taken together, these results represent compelling evidence supporting the conclusion that the timing of endothelial  $\beta$ 3-integrin deletion is important in determining endothelial cell intracellular signalling in response to VEGF stimulation. Extending the time during which  $\beta$ 3-integrin has been deleted by lengthening the OHT treatment of  $\beta$ 3-floxed/Pdgfb-iCreER<sup>T2</sup> mice prior to the isolation of endothelial cells, abolished the inhibitory phenotype otherwise associated with  $\beta$ 3-integrin inducible deletion. Indeed, in many respects, angiogenic responses in long OHT  $\beta$ 3-floxed /Pdgfb-iCreER<sup>T2</sup> positive endothelial cells mimicked those observed in  $\beta$ 3-floxed /Tie1Cre positive endothelial cells.

## Figure 5.1 Immortalized lung endothelial cell phenotype

(A) Representative phase contrast images of PyMT immortalized lung endothelial cells isolated from Tie1Cre and Pdgfb-iCreER<sup>T2</sup> transgenics mice (scale bar=100  $\mu$ m). After mechanical disruption and enzymatic digestion of lung tissue, primary lung cells were expanded and magnetically sorted for the expression of the endothelial cell marker ICAM2. Due to their slow in culture, they were subsequently immortalized by infection with PyMT viral supernatant containing. Immortalized lung endothelial cells were routinely passaged and used for *in vitro* experiments. Immortalized lung endothelial cells were assessed for their endothelial phenotype.

(B) Representative immunocytochemistry analysis of immortalized lung endothelial cells displaying VE-cadherin expression (in red). DAPI (blue) was used as nuclear counterstain (scale bar=20  $\mu$ m).

(C) Representative histograms of flow cytometric analysis of CD31 and ICAM2 endothelial cell marker expression of immortalized lung endothelial cells isolated from Tie1-Cre and Pdgfb-iCreER<sup>T2</sup> transgenics mice.

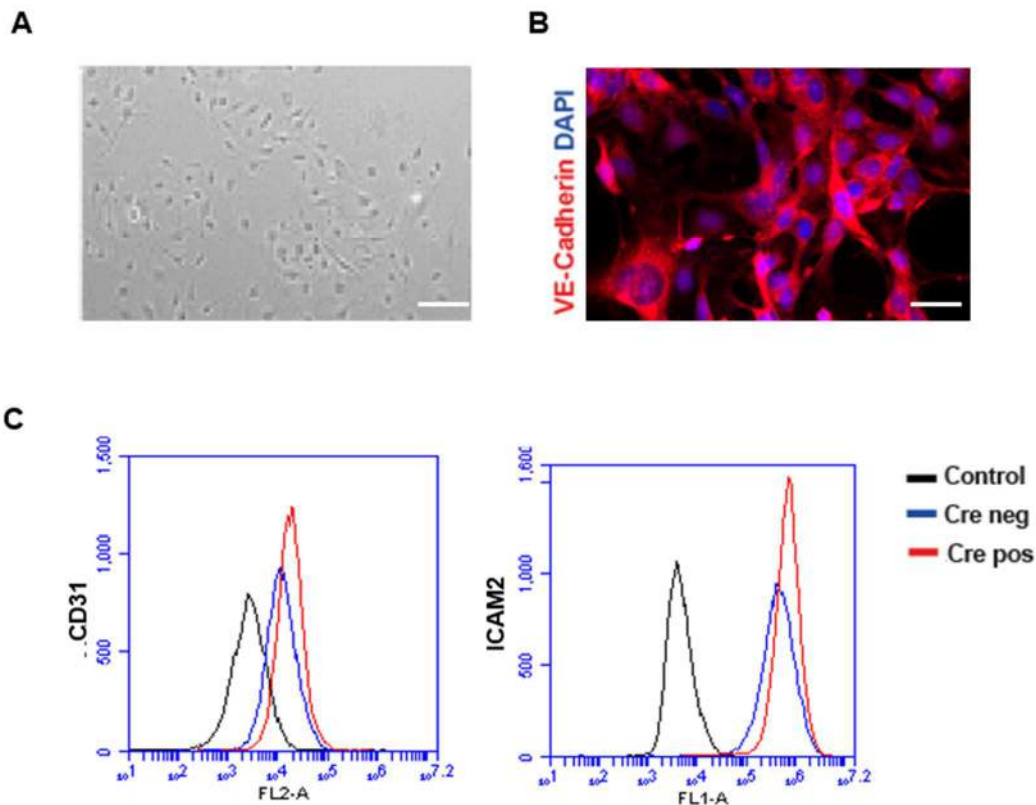


**Figure 5.2 Analysis of surface integrins and adhesive properties of  $\beta 3$ -integrin deleted endothelial cells**

(A) Representative histograms of flow cytometric analysis of endothelial  $\alpha$ - and  $\beta$ - integrin surface expression in endothelial cells isolated from  $\beta 3$ -floxed/Tie1Cre and  $\beta 3$ -floxed/Pdgfb-iCreER<sup>T2</sup> mice. Isotype matched-controls are shown in black.  $\beta 3$ -integrin was reduced as expected in both  $\beta 3$ -floxed/Tie1Cre and  $\beta 3$ -floxed/Pdgfb-iCreER<sup>T2</sup> positive cells. Except for  $\alpha 2$ -integrin, which was significantly reduced in both  $\beta 3$ -floxed/Tie1Cre and  $\beta 3$ -floxed/Pdgfb-iCreER<sup>T2</sup> positive cells, no other changes in integrin subunits were detected (n=3 mice per genotype, NS=not significant).

(B)  $\beta 5$ -integrin expression was analyzed by Western blot and showed significant decrease in  $\beta 3$ -floxed/Tie1Cre positive cells compared to negative cells. HSC 70 provided a loading control. Bar graphs shows  $\beta 5$ -integrin quantitation relative to HSC 70 expression (mean +/- SEM; \*\*p<0.01, n=3 mice per genotype, NS=not significant).

(C) Relative adhesion to the single extracellular matrix component fibronectin (Fn), collagen I (Col), laminin I (Ln) and vitronectin (Vn) was evaluated in endothelial cells isolated from  $\beta 3$ -floxed/Tie1Cre and  $\beta 3$ -floxed/Pdgfb-iCreER<sup>T2</sup> mice and expressed as mean percentage (+/- SEM) relative to Cre negative cells adhering to fibronectin. Data are representative of 3 independent experiments (\*\*p<0.01, NS=not significant). No differences in cell adhesion, except to vitronectin, were observed when comparing between Cre positive to Cre negative endothelial cells.

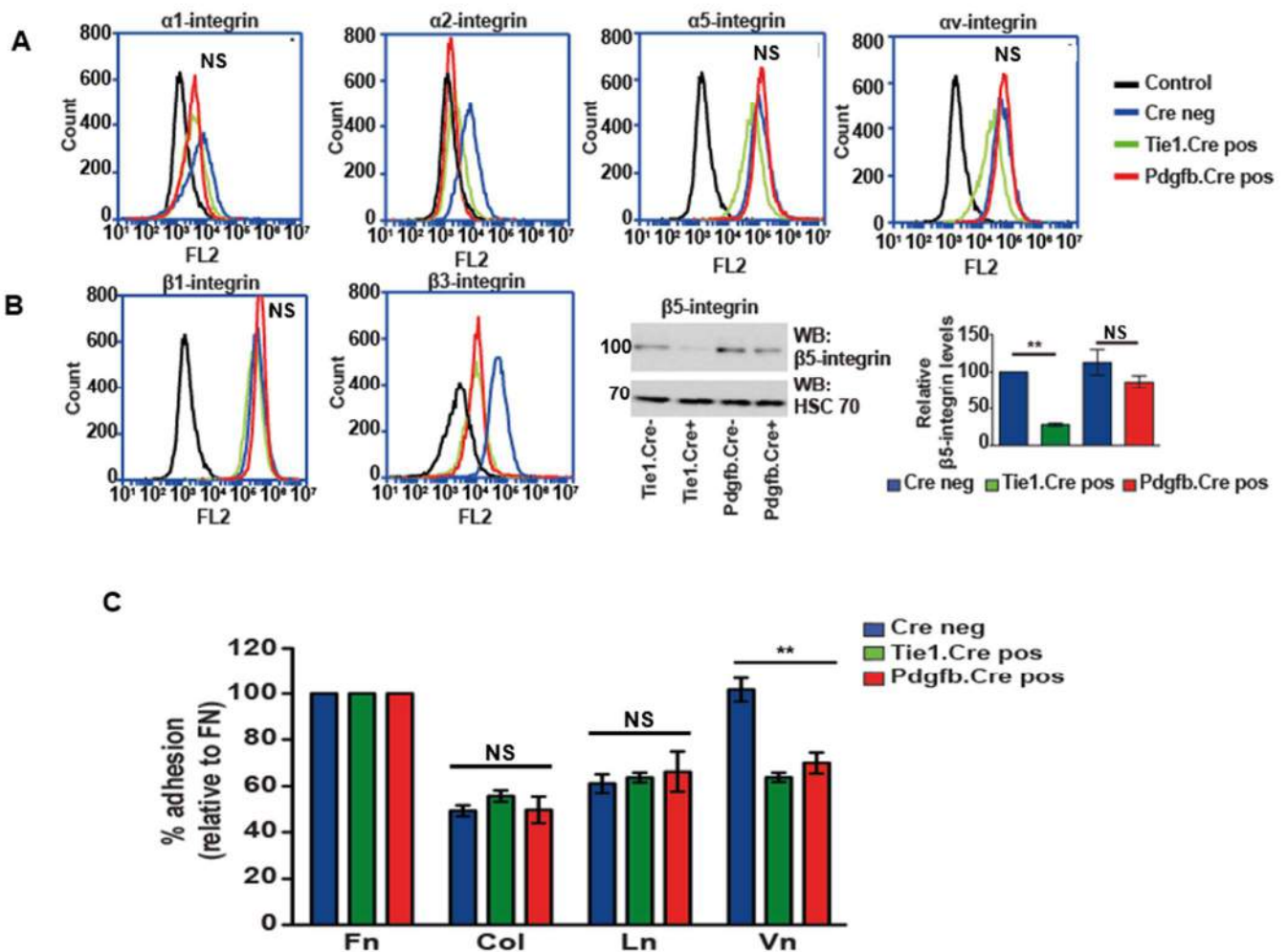


**Figure 5.3 Analysis of VEGF-induced migration and proliferation in  $\beta$ 3-integrin deleted endothelial cells**

(A) Representative phase contrast images of endothelial cells isolated from  $\beta$ 3-floxed/Tie1Cre and  $\beta$ 3-floxed/Pdgfb-iCreER<sup>T2</sup> mice show cell migration across a scratch wound. Cells were stimulated with VEGF to induce wound closure. After 24 hours, 2D migration was significantly reduced in  $\beta$ 3-floxed/Pdgfb-iCreER<sup>T2</sup> positive cells, but not in  $\beta$ 3-floxed/Tie1Cre positive cells (scale bar=100 $\mu$ m).

(B) Bar charts show the mean percentage (+/-SEM) of wound closure after 24 hours of VEGF stimulation relative to the 0 timepoint. Data are representative of 3 independent experiments (\*\*p<0.01, NS=not significant).

(C) VEGF-induced proliferation was evaluated in endothelial cells isolated from  $\beta$ 3-floxed/Tie1-Cre and  $\beta$ 3-floxed/Pdgfb-iCreER<sup>T2</sup> mice by an MTT assay in presence of VEGF stimulation. No differences in cell proliferation were detected between endothelial cells isolated from  $\beta$ 3-floxed/Tie1Cre and  $\beta$ 3-floxed/Pdgfb-iCreER<sup>T2</sup> mice. Line chart shows mean absorbance value after 24 and 48 hours of VEGF stimulation and relative to the 0 timepoint. Data are representative of 3 independent experiments (NS=not significant).

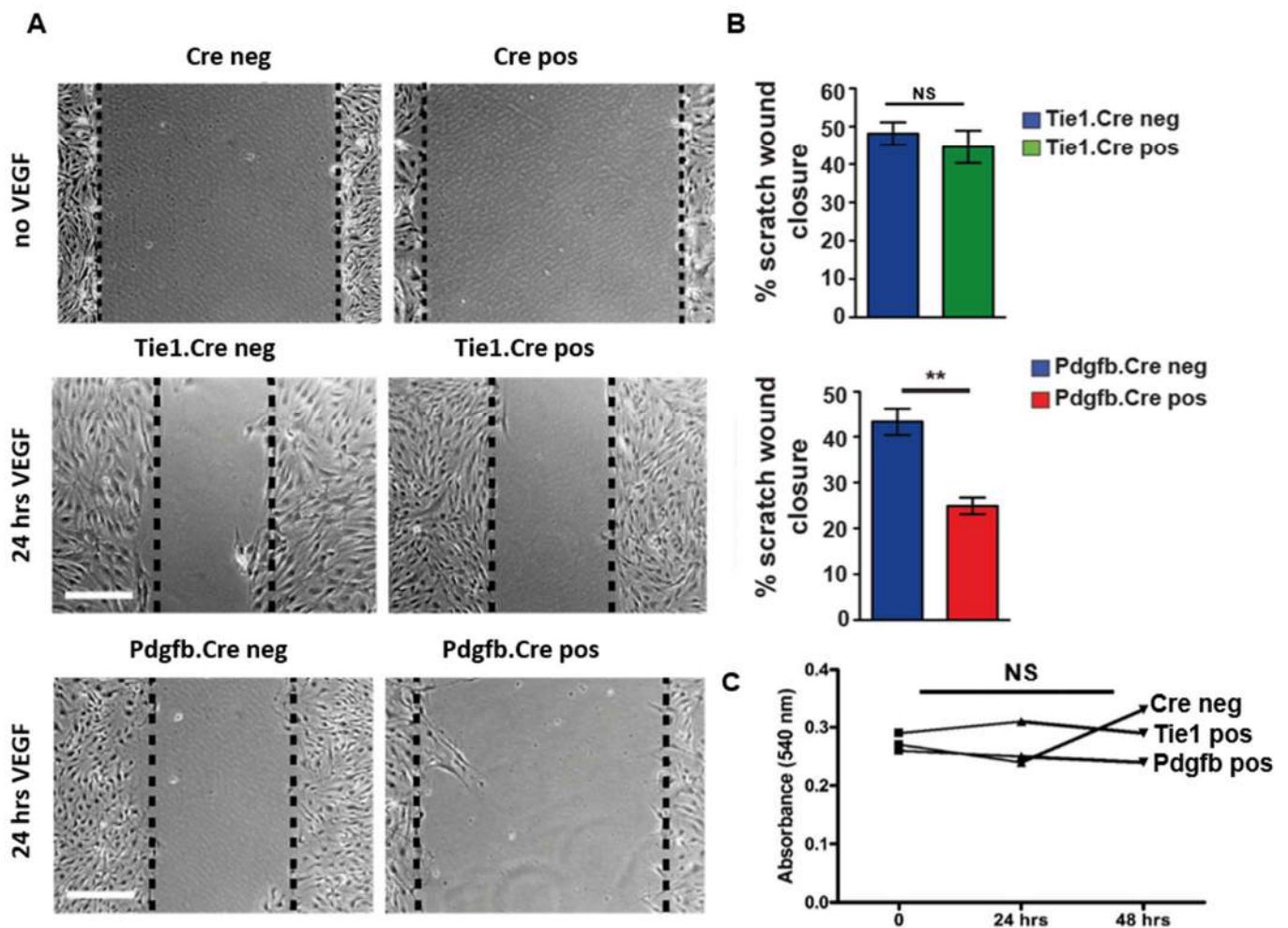


**Figure 5.4 Changes in VEGFR2 expression and activation**

(A) Representative histograms of flow cytometric analysis of VEGFR2 surface expression in endothelial cells isolated from  $\beta 3$ -floxed/Tie1Cre and  $\beta 3$ -floxed/Pdgfb-iCreER<sup>T2</sup> mice.  $\beta 3$ -floxed/Tie1Cre positive endothelial cells displayed a small but significant increase in VEGFR2 surface expression, whereas  $\beta 3$ -floxed/Pdgfb-iCreER<sup>T2</sup> positive did not. Isotype matched-controls are shown in black. B3 KO endothelial cells were included in the analysis as positive control for VEGFR2 overexpression (\*p<0.05, NS=not significant).

(B) Representative Western blot analysis of protein lysates obtained from endothelial cells shows decreased VEGFR2 phosphorylation (Y1175) in  $\beta 3$ -floxed/Pdgfb-iCreER<sup>T2</sup> positive cells compared to Cre negative cells, whereas no difference was observed between  $\beta 3$ -floxed/Tie1Cre positive and negative cells. Cells were stimulated with VEGF (30 ng/ml for 5 minutes). Protein lysates were blotted for phosphorylated VEGFR2 and subsequently reblotted for total VEGFR2. Bar graphs shows mean (+/- SEM) densitometric quantification of phosphorylated VEGFR2 relative to total VEGFR2 normalized to unstimulated cells. Data are representative of 3 independent experiments (\*p<0.05, NS=not significant).

(C) Schematic representation displaying  $\alpha v\beta 3$ -integrin and VEGFR2 cross-activation required for sustained activation of VEGFR2.

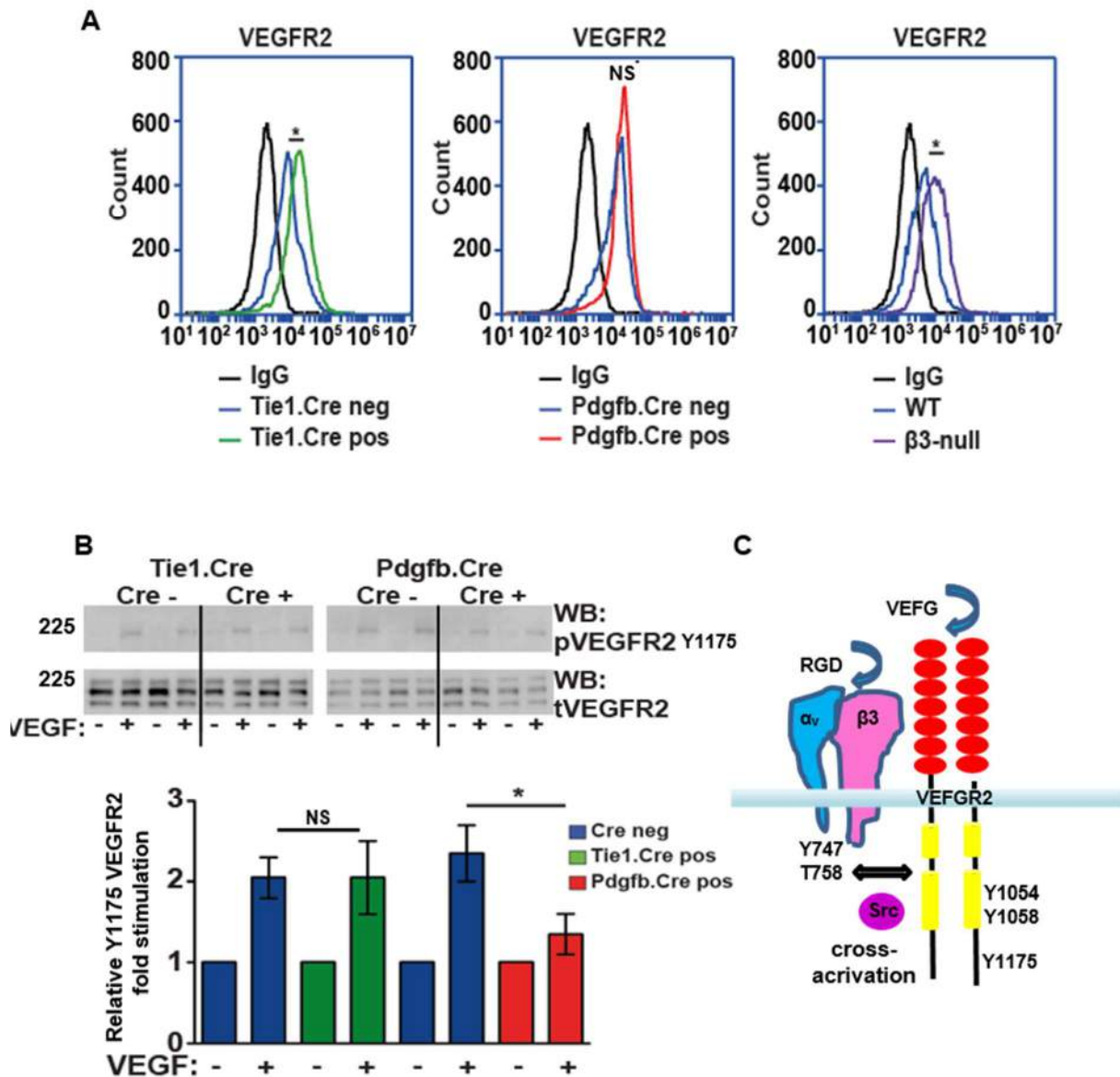


### Figure 5.5 VEGFR2 downstream signalling analyses

(A) Representative Western blot analysis of VEGF-induced phosphorylation of VEGFR2 downstream effectors (PLC $\gamma$ , FAK, c-Src, p38) in endothelial cells isolated from  $\beta$ 3-floxed/Tie1Cre and  $\beta$ 3-floxed/Pdgfb-iCreER<sup>T2</sup> mice. Endothelial cells were stimulated with VEGF (30 ng/ml) at the indicated timepoints. Protein lysates were blotted for phosphorylated forms and subsequently reblotted for total levels.

(B) Representative Western blot analysis of protein lysates obtained from endothelial cells shows decreased ERK 1/2 phosphorylation in  $\beta$ 3-floxed/Pdgfb-iCreER<sup>T2</sup> positive cells compared to Cre negative cells at 30-60 minute timepoints; whereas ERK 1/2 phosphorylation was enhanced in  $\beta$ 3-floxed/Tie1Cre positive cells compared to Cre negative controls at the 5-minute timepoint. Cells were stimulated with VEGF (30 ng/ml) at the indicated timepoints. Protein lysates were blotted for phosphorylated ERK 1/2 and subsequently reblotted for total ERK 1/2. Bar graphs shows mean ( $\pm$  SEM) densitometric quantification of phosphorylated ERK 1/2 relative to total ERK 1/2 normalized to unstimulated cells. Data are representative of 3 independent experiments (\* $p$ <0.05, hashed lines indicate baseline and 2-fold-stimulation).

(C) Schematic representation displaying main downstream effectors of  $\alpha$ v $\beta$ 3/VEGFR2 induced angiogenic signalling.

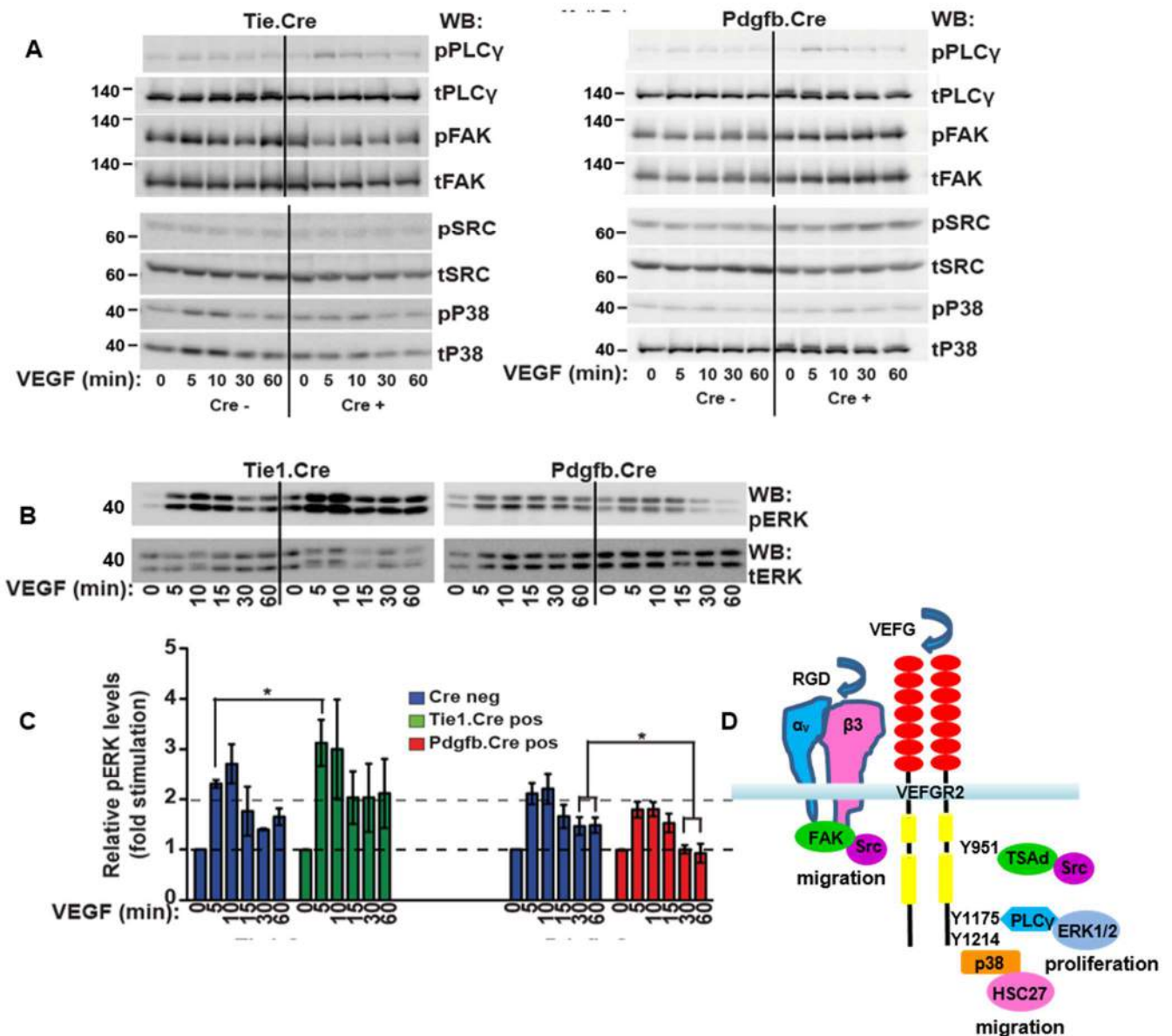


### Figure 5.6 Molecular differences are abolished by long OHT treatment

(A) Representative histograms of flow cytometric analysis of endothelial  $\alpha$ - and  $\beta$ - integrin surface expression in endothelial cells isolated from long OHT  $\beta$ 3-floxed/Pdgfb-iCreER<sup>T2</sup> mice. Isotype matched-controls are shown in black. Except for  $\beta$ 3-integrin, no other changes in surface  $\alpha$ - and  $\beta$ - integrins were detected (n=3 mice per genotype, NS=not significant).

$\beta$ 5-integrin expression was analysed by Western blot and showed a significant decrease. HSC 70 provided a loading control. Bar graph shows  $\beta$ 5-integrin densitometric quantification relative to HSC 70 expression (mean +/- SEM; \*\*p<0.01, NS=not significant).

(B) Analysis of VEGFR2 phosphorylation and surface expression in endothelial cells isolated from long OHT  $\beta$ 3-floxed/Pdgfb-iCreER<sup>T2</sup> mice. Representative Western blot analysis of protein lysates obtained from endothelial cells shows no changes in VEGFR2 phosphorylation (Y1175) in long OHT  $\beta$ 3-floxed/Pdgfb-iCreER<sup>T2</sup> cells. Cells were stimulated with VEGF (30 ng/ml for 5 and 60 minutes). Protein lysates were blotted for phosphorylated VEGFR2 and subsequently reblotted for total VEGFR2.

Representative histogram of flow cytometric analysis of surface expression of VEGFR2 displays a small but significant increase in VEGFR2 surface expression in long OHT  $\beta$ 3-floxed/Pdgfb-iCreER<sup>T2</sup> positive cells compared to negative cells. Isotype matched-controls are shown in black (n=3 mice per genotype, \*<0.05).

(C) Representative Western Blot analysis of protein lysates obtained from endothelial cells shows no difference in ERK 1/2 phosphorylation in long OHT  $\beta$ 3-floxed/Pdgfb-iCreER<sup>T2</sup> positive cells compared to Cre negative cells. Cells were stimulated with VEGF (30 ng/ml) at the indicated timepoints. Protein lysates were blotted for phosphorylated ERK 1/2 and subsequently reblotted for total ERK 1/2. Bar graph shows mean (+/- SEM) densitometric quantification of phosphorylated ERK 1/2 relative to total ERK 1/2 normalized to unstimulated cells. Data are representative of 3 independent experiments (NS=not significant).

Figure 5.6 Molecular differences are abolished by long OHT treatment

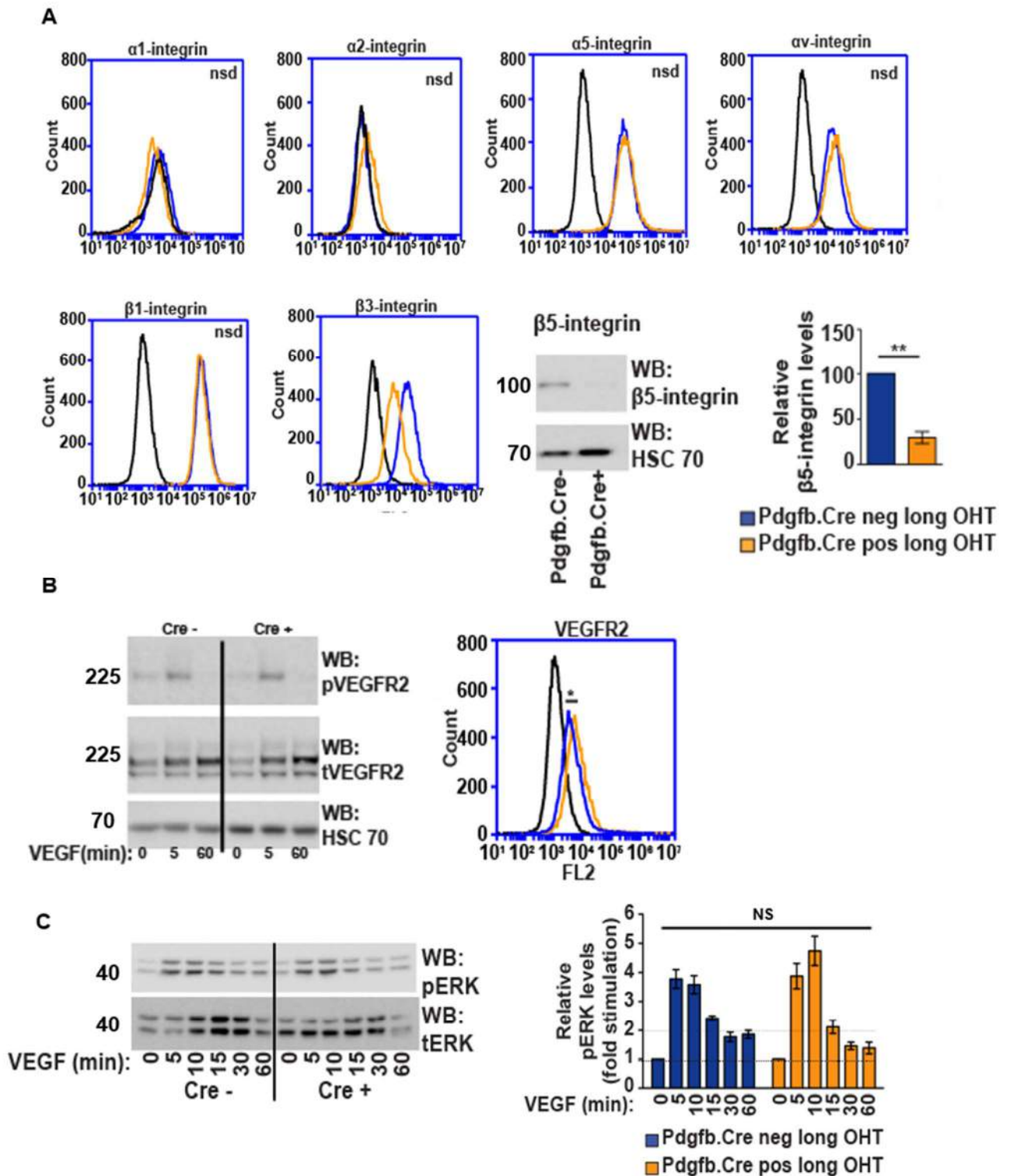
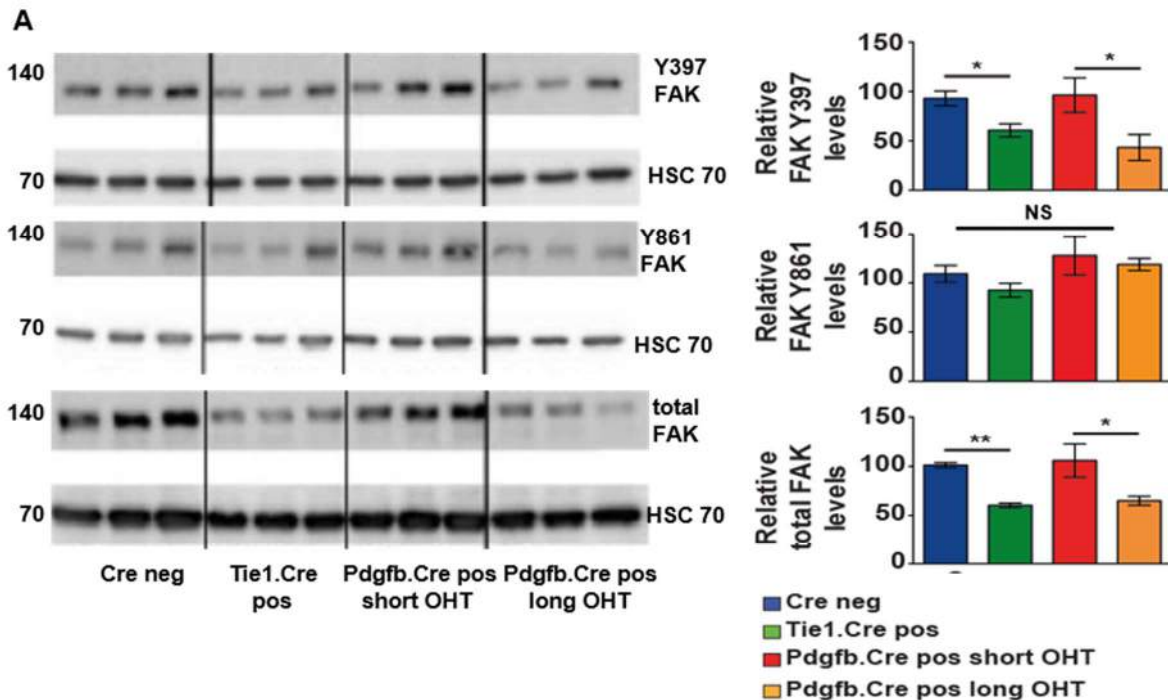


**Figure 5.7 Changes in FAK expression and phosphorylation after deletion of endothelial  $\beta$ 3-integrin**

**(A)** Representative Western blot analysis FAK expression and phosphorylation in endothelial cells isolated from  $\beta$ 3-floxed/Tie1Cre and  $\beta$ 3-floxed/Pdgfb-iCreER<sup>T2</sup> mice. Both total and phosphorylated FAK Y397 levels were significantly decreased in  $\beta$ 3-floxed/Tie1Cre positive and long OHT  $\beta$ 3-floxed/Pdgfb-iCreER<sup>T2</sup> positive cells compared to  $\beta$ 3-floxed/Pdgfb-iCreER<sup>T2</sup> positive cells, whereas phosphorylated FAK Y861 levels were unchanged across the 3 genotypes. Bar charts show the mean ( $\pm$  SEM) densitometric quantification of phosphorylated and total FAK in  $\beta$ 3-floxed/Tie1Cre,  $\beta$ 3-floxed/Pdgfb-iCreER<sup>T2</sup> and long OHT  $\beta$ 3-floxed/Pdgfb-iCreER<sup>T2</sup> endothelial cells. Phosphorylated FAK levels were normalized to total levels. Data are representative of 3 independent experiments (\* $p$ <0.05, \*\* $p$ <0.01, NS=not significant).

**(B)** Representative immunofluorescent images of FAK (in red) and endomucin (in green) in tumour sections from  $\beta$ 3-floxed/Tie1Cre,  $\beta$ 3-floxed/Pdgfb-iCreER<sup>T2</sup> and long OHT  $\beta$ 3-floxed/Pdgfb-iCreER<sup>T2</sup> tumours. Arrows point to examples of FAK staining in tumour vessels. Scatter plot shows mean fluorescent intensity ( $\pm$  SEM) of FAK in tumour blood vessels of the indicated genotypes ( $n$ =5 mice per genotype, 5 fields per section, \*\* $p$ <0.01, NS=not significant).



## DISCUSSION

### 5.4 $\alpha\beta3$ integrin and VEGFR2 in angiogenesis: a complex marriage

The cross-talk between  $\alpha\beta3$ -integrin and VEGFR2 on endothelial cells is crucial for angiogenesis. In fact it has been shown that  $\alpha\beta3$ -integrin and VEGFR2 interact synergistically: VEGFR2 activation induces  $\alpha\beta3$ -integrin tyrosine phosphorylation which, in turn, is essential for VEGF-induced receptor activation and downstream signalling (Somanath *et al.*, 2009). The importance of this crosstalk has been shown both *in vivo*, in  $\beta3$  knockout mice whereby the phenotype of enhanced tumour growth and angiogenesis could be normalized by administering VEGFR2 inhibitors (Reynolds *et al.*, 2002); and *in vitro*, in  $\beta3$  knockout endothelial cells where VEGFR2 expression and signalling were found to be enhanced (Reynolds *et al.*, 2004). Together this suggests that VEGFR2 dependent mechanisms can establish to compensate for the absence of  $\alpha\beta3$ -integrin.

Other studies have also described a functional mechanistic link between integrin genetic ablation and VEGFR2 expression and function. For example, Germain *et al.* (2010) showed that  $\alpha6$ -integrin knockout endothelial cells display increased levels of VEGFR2 and VEGF-mediated downstream ERK1/2 activation. In addition, da Silva *et al.* (2010) demonstrated that  $\alpha3$ -integrin knockout endothelial cells regulate endothelial-VEGF production, which ultimately controls of VEGFR2 expression. Therefore, VEGFR2 was a likely candidate involved in the mechanisms leading to the escape from long term deletion of endothelial  $\beta3$ -integrin. Despite no differences in total VEGFR2 expression levels (in tumour and lung endothelial cells as well as in aortae explants), my findings showed small but significant increases in surface expression levels of VEGFR2 in endothelial cells isolated from  $\beta3$ -floxed/Tie1Cre animals and from long OHT  $\beta3$ -floxed/Pdgfb-iCreER<sup>T2</sup>.

Receptor trafficking has been acknowledged as being essential for modulating temporal and spatial patterns of RTK signalling (Berger and Ballmer-Hofer, 2011). One may speculate that endothelial cells compensate for the long term loss of  $\beta3$ -integrin by increasing the amount of VEGFR2 receptor present at the surface of the cell and, as such, its responsiveness to VEGF stimulation. Although I have not tested it directly, there is precedent for suggesting that VEGFR2 trafficking is responsible for the changes I have noted in constitutively  $\beta3$  integrin deleted cells: in fact, it has

been shown that the mechanism by which low doses of CILENGITIDE (an  $\alpha v\beta 3/\alpha v\beta 5$  inhibitor) elicit pro-angiogenic responses is by increasing the recycling at the cell surface of VEGFR2 via internalization in Rab11 vesicles (Reynolds *et al.*, 2009) Note, I did attempt to examine VEGFR2 endocytosis and recycling directly but was never successful in my attempts to get the assays to work.

In contrast, VEGFR2 phosphorylation appeared to be reduced (likely as a result of decreased interactions between  $\alpha v\beta 3$ -integrin and VEGFR2), upon inducible but not constitutive endothelial  $\beta 3$ -integrin deletion; suggesting the absence of  $\alpha v\beta 3$ -integrin is compensated over time to restore VEGFR2 signalling. This was further sustained in lung endothelial cells isolated from long OHT  $\beta 3$ -floxed/Pdgfb-iCreER<sup>T2</sup> mice where extending the duration of endothelial  $\beta 3$ -integrin deletion was sufficient to rescue the phenotype of reduced VEGFR2 phosphorylation. Consistent with data from Germain *et al.* (2010), increased surface expression of VEGFR2 correlated with enhanced phosphorylation of ERK 1/2 (a known downstream effector VEGFR2 signalling) in endothelial cells isolated from  $\beta 3$ -floxed/Tie1Cre and from long OHT  $\beta 3$ -floxed/Pdgfb-iCreER<sup>T2</sup> mice. In short, the early preventive benefit observed with inducible deletion of endothelial  $\beta 3$ -integrin is transient and may be circumvented, at least in part, by enhancing VEGFR2 surface expression and function.

Notably though, I did not detect any increase in proliferation in VEGF stimulated  $\beta 3$   $\beta 3$ -floxed/Tie1Cre and long OHT  $\beta 3$ -floxed/Pdgfb-iCreER<sup>T2</sup> endothelial cells, which might have been expected as a result of enhanced VEGFR2/ERK1/2 signalling. It could be argued that this could be an artifact of immortalization. However, in a similar vein,  $\beta 3$ -integrin DiYF mutant endothelial cells do not show any defects in cell proliferation. Although it has been used to study proliferation in endothelial cells in culture (Kostourou *et al.*, 2013; Huang *et al.*, 2005) it could be argued that the MTT assay I employed to assess proliferation is indirect, as it is an index of cell metabolic activity. Perhaps this method is not sensitive enough, or I have not extended my analyses over a long enough time frame to detect subtle changes in proliferation. If I had time to extend these studies it would be interesting to compare these results with other experimental approaches such as BrdU incorporation or Propidium Iodide DNA staining, and to extend the time frame beyond the 48 hours.

Changes in VEGFR2 activity may help explain the molecular basis of the angiogenic changes observed with inducible and constitutive  $\beta 3$ -integrin deletion in endothelial cells, but do not exclude the possibility that there are other mechanisms involved.

Further molecular signalling analyses based on Western blot revealed decreased expression and misbalanced phosphorylation of FAK in  $\beta$ 3-floxed/Tie1Cre and long OHT  $\beta$ 3-floxed/Pdgfb-iCreER<sup>T2</sup> positive endothelial cells compared to Cre negative endothelial cells, suggesting it as a molecular adaptation occurring over time as a result of  $\beta$ 3-integrin deletion. This was strengthened by the same result of reduced total FAK levels in tumour vessels from  $\beta$ 3-floxed/Tie1Cre and long OHT  $\beta$ 3-floxed/Pdgfb-iCreER<sup>T2</sup> mice. With respect to FAK phosphorylation, the results observed are in line with Kostourou *et al.* (2013), who have recently shown that reduced FAK levels in FAK heterozygous mice results in an imbalance in the ratio of phosphorylated FAK at Y397 and Y861 sites (whereby the ratio Y397/total FAK decreases while Y861/total FAK does not). This appears to ultimately lead to enhanced tumour growth and angiogenesis.

Full phosphorylation of VEGFR2 induced by synergistic signalling interplay between VEGFR2 and  $\alpha$  $\beta$ 3-integrin has shown to be required for the activation of cell motility pathways involving FAK and SAPK2/p38 in endothelial cells (Masson-Gadais *et al.*, 2003). Moreover, Tavora *et al.* (2010) have shown that endothelial FAK deficiency reduced VEGF-induced migration. Despite no difference in p38 levels (total and phosphorylated) across the three genotypes, it was reasonable to predict that the decrease in total FAK levels associated with constitutive deletion of endothelial  $\beta$ 3-integrin may affect endothelial cell migration.

As expected, VEGF treatment enhanced 2D migration in scratch wound closure assays in  $\beta$ 3-floxed/Tie1Cre positive endothelial cells; whereas it significantly inhibited it in  $\beta$ 3-floxed/Pdgfb-iCreER<sup>T2</sup> positive endothelial cells. Although this does not reflect what might be predicted based on the role of FAK in endothelial cell migration, it still could be explained by picturing a more complex scenario of molecular adaptation whereby different level of expression might regulate biological outcomes. Thus, wild-type levels of endothelial  $\beta$ 3-integrin can positively regulate migration independently of FAK, in fact its acute deletion impairs 2D migration without any effects on FAK (neither expression nor phosphorylation). However, over time,  $\beta$ 3-integrin loss can be circumvented by reducing FAK levels, whose partial loss has been shown to enhance angiogenic responses (Kostourou *et al.*, 2013).

## 5.5 Molecular compensation of other endothelial integrins

A conceivable consequence of the genetic deletion of the  $\beta 3$ -integrin subunit would be the increased expression of other members of the integrin family, as a result of functional redundancy. It has been shown, for example, that  $\alpha v\beta 5$  integrin can compensate for the loss of  $\alpha 5\beta 1$  integrin (Yang *et al.*, 1996). Most endothelial integrins I examined were unchanged in response to  $\beta 3$ -integrin deletion (in both Cre models). I did notice changes in  $\alpha 2$  integrin levels which decreased in Cre-positive endothelial cells from both models. As of yet, I have no explanation for this finding. However it might be interesting to explore because also  $\alpha 2\beta 1$  seems to play opposite functions: it is known to promote VEGF-driven signaling, tumor angiogenesis (Senger *et al.*, 2002; Hong *et al.*, 2004) and developmental angiogenesis (San Antonio *et al.*, 2009) it has also been reported that its ablation resulted in enhanced angiogenesis in skin wound healing and sponge implants.

Interestingly, however,  $\beta 5$ -integrin (albeit total levels, as assessed by Western blot analysis because I was unable to detect its surface expression) was reduced in  $\beta 3$ -floxed/Tie1-Cre positive endothelial cells and long OHT  $\beta 3$ -floxed/Pdgfb-iCreER<sup>T2</sup> positive endothelial cells, but not in  $\beta 3$ -floxed/Pdgfb-iCreER<sup>T2</sup> positive endothelial cells. The reduction of  $\beta 5$ -integrin has not been observed before in  $\beta 3$ -integrin genetic deletion models. One hypothesis may be that over time,  $\beta 3$ -integrin is needed to stabilize  $\beta 5$ -integrin and as a consequence of  $\beta 3$ -integrin constitutive deletion,  $\beta 5$ -integrin levels decrease. The functional consequences of this loss have not been directly tested and the observation is, to date, strictly correlative.

However, considering that  $\beta 3$  and  $\beta 5$ -integrins seem to have discrete roles in angiogenesis (Friedlander *et al.*, 1995), the concomitant loss (reduction) of both integrin heterodimers is surprising and may be significant. It is known that unligated integrins initiate apoptosis selectively via caspase-8 (Stupack *et al.*, 2001). This process, termed Integrin Mediated Death (IMD), occurs in response to the accumulation and apparent clustering of unligated integrins on the cell surface and it is a function of both the local microenvironment around the cell and the integrin “repertoire” expressed by that cell (Lathi *et al.*, 2006). The depletion of both integrins may, therefore, benefit cell survival, and the prediction arising would be that reduced levels of  $\alpha v\beta 5$ -integrin would be advantageous because a natural pathway that keeps angiogenesis in check has been removed.

Any one of the changes described above (and likely a combination of these and others yet discovered) could contribute to an escape from angiogenic inhibition directed against  $\beta$ 3-integrin. Similarly to  $\beta$ 3 knockout endothelial cells (Reynolds *et al.*, 2004), constitutive deletion of endothelial  $\beta$ 3-integrin resulted in increased surface expression of VEGFR2. However, unlike the  $\beta$ 3 knockout studies, constitutive deletion of endothelial  $\beta$ 3-integrin does not result in enhanced pathological angiogenesis *in vivo*, thereby highlighting that this aspect of the knockout phenotype is primarily a result of  $\beta$ 3-integrin deletion in non-endothelial cells. In fact, it is partially rescued by restoring wild-type expression of  $\beta$ 3-integrin in BMDCs through bone marrow transplants (Feng *et al.*, 2008).

Together, these findings emphasise the complexity of  $\beta$ 3-integrin regulation and when developing translation approaches, one should take into consideration its cell specific targeting and possible compensatory changes resulting from its suppression.

## CONCLUSIONS

In this chapter, I have shown that:

- **the inducible loss of endothelial  $\beta$ 3-integrin impairs VEGF dependent 2D-migration albeit not proliferation *in vitro*;**
- **the constitutive deletion of endothelial  $\beta$ 3-integrin leads to molecular changes *in vitro* in the form of increased surface expression and phosphorylation of VEGFR2, enhanced ERK 1/2 phosphorylation, reduced total expression of  $\beta$ 5-integrin, and reduced and misbalanced FAK phosphorylation;**
- **the constitutive deletion of endothelial  $\beta$ 3-integrin does not result in overcompensation by other endothelial integrin subunits.**

## **6. DEVELOPING MOUSE MODEL OF SPONTANEOUS METASTASIS TO ADDRESS THE ROLE OF ENDOTHELIAL $\beta$ 3-INTEGRIN**

In the previous chapters, I examined the role of endothelial  $\beta$ 3-integrin during the initial stages of tumour growth; however there is certainly precedence for exploring its role in later stages of tumour progression. Clinical evidence suggests  $\beta$ 3-integrin may play a role in metastatic spread as its expression positively correlates with tumour grade, and it has been found to be highly expressed by bone and lymphatic metastases from several types of primary tumours including melanoma, prostate, breast, cervical and pancreatic carcinomas (Desgrosseillers and Cheresch, 2010).

In the current chapter, I will describe the development of a model of spontaneous metastasis to the lung in order to investigate the role of endothelial  $\beta$ 3-integrin in tumour progression and metastasis. In parallel to this model, I also exploited a breast carcinoma cell line which spontaneously metastasises to lung and bone, which was developed in the laboratory of Katherine Weilbacher at the Washington University of St Louis where I spent a summer internship period. Using these models, I was able to collect preliminary data suggesting that long-term endothelial specific deletion of  $\beta$ 3-integrin has the potential to reduce metastases to the lung, despite no changes in primary tumour growth or angiogenesis. Furthermore, I attempted to elucidate the cellular and molecular pathways associated with this phenotype. Although the findings from these studies are still very preliminary, they are clearly encouraging. They show there is merit in further investigating the potential targeting of endothelial  $\beta$ 3-integrin therapeutically to reduce tumour metastasis.

## **RESULTS AND FIGURES**

### **6.1 Mouse models of metastasis**

*In vivo* standard models of spontaneous metastasis include ectopic (subcutaneous) or orthotopic transplantation of metastatic variants of established tumour cells lines in mice. These metastatic tumour cells can be either syngeneic or xenografts, in which case they need to be transplanted in immunocompromised mice. Such spontaneous metastases assays involve establishing a primary tumour, which is then allowed to grow and spread, especially if the primary tumour is surgically resected

(for reasons that will be explained in the paragraph 6.1.1) to metastasise to distant sites.

Additionally, genetically engineered mouse models (GEMMs) whereby oncogenes such as Polyoma Middle T (PyMT) or SV40 T antigen (Tag) have been expressed under the control of mouse viruses, such as the Mouse Mammary Tumour Virus (MMTV) or endogenous tissue specific promoters such as the Rat Insulin Promoter (RIP) to induce the tumourigenic process spontaneously, have been developed to investigate several aspects of tumour biology, including metastatic spread (Francia *et al.*, 2011). These models offer the advantage of generating syngeneic orthotopic tumours which mimic the progression of the disease from benign to invasive malignant tumours; but, importantly in immune competent hosts containing the vasculature and the stroma of the same species.

Alternatively, metastatic tumour cells can be injected systemically in mice (experimental metastasis assay). Despite the advantage of requiring a shorter time for the evidence of metastases compared to spontaneous metastases models, experimental metastases assays circumvent the initial growth and dissemination phases, as a result of injecting tumour cells directly in the circulation through, for example, the tail vein. As a consequence, the analysis of the metastatic cascade is limited to post-extravasation steps.

### **6.1.1 CMT19T F1**

Instead of exploiting the B16 melanoma cell line which I had already used for my initial studies and which is widely used in experimental metastases experiments, my initial approach was to develop an *in vivo* model that would allow spontaneous metastases formation in endothelial specific  $\beta$ 3-integrin transgenic mice, yet avoid the shortcomings associated with experimental metastases assays.

I moved to the CMT19T tumour cell line (which was used in previous chapters in parallel with B16F0 cells) and tried to derive a highly metastatic variant. I achieved this through a single round of *in vivo* selection, which involved subcutaneous CMT19T tumour cell implantation followed by tumour resection and, finally, isolation of metastatic cells from the lung. The metastatic variant generated from the parental CMT19T cell line will be, hereafter, referred to as CMT19T F1.

The next step I took was to characterize the biological behaviour of CMT19T F1 cells in order to establish the experimental conditions which would give the highest number of metastases in the least amount of time. Because I wanted, at least initially, to focus solely on the role of endothelial  $\beta$ 3-integrin in regulating metastasis, for the sake of simplicity and reduced experimental costs, a comparative characterisation was performed between  $\beta$ 3-floxed/Tie1Cre negative and positive mice.

Since I opted for subcutaneous tumour cell implantation, which is known to have a less efficient rate of metastatic spread compared to orthotopic transplants (Cruz-Munoz *et al.*, 2008), I maximized the chance of getting distant metastasis by performing surgical resection of the primary tumours. Surgical resection of the primary tumour prolongs mouse survival and allows extra time for metastatic cells originating from the primary tumour to develop into established metastases at distant sites. The kinetics of CMT19T F1 growth in  $\beta$ 3-floxed/Tie1Cre negative and positive mice was monitored every other day starting from day 10 by taking external caliper measurements. As I observed with CMT19T cells, there was no difference in primary tumour growth of the F1 variant when comparing  $\beta$ 3-floxed/Tie1Cre negative and positive mice (Figure 6.1A).

Tumours were grown until they reached 1 cm<sup>3</sup> (the limit set out in our Home Office Project Licence). In both genotypes, this corresponded to approximately 20 days after initial tumour cell injection and neither genotype showed any adverse effects of carrying this level of tumour burden; thus this defined the timepoint for tumour resection. Finally, in order to determine the optimal timing for detecting metastatic outgrowth without compromising animal welfare, health was monitored daily. Lungs were harvested at the first signs of cachexia. In  $\beta$ 3-floxed/Tie1Cre negative animals this was first noted 12 days after tumour resection. Therefore, this timing was used in all subsequent experiments. I was able to observe macroscopically evident lung metastases upon visual examination (Figure 6.1D). Lungs were then processed for Hematoxylin and Eosin (H&E) staining. Macroscopic examinations did not reveal metastatic spread to any other organs.

Overall, these data describe the development of a metastatic carcinoma model obtained through the derivation of a metastatic variant of the CMT19T tumour cell line, the CMT19T F1. The use of this line was optimised to allow for the development of overt lung metastases ~5 weeks after ectopic transplantation followed by surgical resection of the primary tumour.

### 6.1.2 B6 LV-1

B6 LV-1 is a breast carcinoma cell line which has been established in the laboratory of Katherine Weilbaecher. MMTV-PyMT is a reliable model of metastatic breast cancer, which recapitulate the stages of breast cancer from benign and well-differentiated adenoma to metastatic and poorly differentiated adenocarcinoma. Existing models of breast cancer primarily metastasise to lung, but bone is a more common site of metastasis in humans, and is associated with high morbidity and pain. This is the reason why the Weilbaecher lab has generated, through multiple rounds of *in vivo* selection, a C57BL/6 compatible MMTV-PyMT-derived transplant cell line (B6 LV-1), which spontaneously metastasises to bone. In this model, B6 LV-1 cells are orthotopically transplanted in the inguinal mammary fat-pad, tumour resection (mastectomy) is performed after 2 weeks and bone metastases appear in another 3-5 weeks. Furthermore, B6 LV-1 cells are GFP and luciferase tagged, thus allowing tumour cell tracking both *in vitro* in histological sections and *in vivo* by bioluminescent imaging, whereby tumour burden and metastatic dissemination can be quantified and followed over time without the need to kill the animal.

B6 LV-1 cells (kindly provided to us by Katherine Weilbaecher) are the first-ever model of breast cancer that spontaneously metastasise to bone. The initial aim was to investigate the role of endothelial  $\beta$ 3-integrin in the two different metastases tumour models just described. However, without *in vivo* imaging capabilities, which have only very recently become available at UEA, characterising the B6 LV-1 model proved difficult (however, see paragraph 6.3.1). I therefore mainly focused my studies on the CMT19T F1 model.

### 6.2 Endothelial $\beta$ 3-integrin deletion reduces CMT19T F1 spontaneous, but not experimental, metastasis

To study the effect of endothelial  $\beta$ 3-integrin deletion on lung metastasis,  $\beta$ 3-floxed/Tie1Cre negative and positive mice were injected subcutaneously with CMT19T F1 carcinoma cells. Tumours were grown until day 20 and then surgically resected under anaesthesia. Primary tumours were histologically processed to analyse the degree of tumour angiogenesis. After 12 days, both genotypes were sacrificed and lungs were inflated via a tracheal injection of 4% PFA prior to overnight fixation. Lungs were subsequently processed for histological analysis and metastases evaluation.

In parallel, experimental metastases experiments were performed by injecting CMT19T F1 tumour cells into the tail vein of  $\beta$ 3-floxed/Tie1Cre negative and positive mice. Lungs were harvested and processed, as described above, 14 days post injection.

### **6.2.1 The number of spontaneous CMT19T F1 lung metastases is reduced, but not their size or vascularisation, in the absence of endothelial $\beta$ 3-integrin**

The histological quantification of lung metastases based on H&E staining revealed a significant decrease in the number of spontaneous lung metastases in  $\beta$ 3-floxed/Tie1Cre positive mice compared to  $\beta$ 3-floxed/Tie1Cre negative mice (Figure 6.1B). I decided to further investigate this unexpected phenotype by evaluating the average size of metastatic outgrowths on H&E stained sections (Figure 6.1E). In parallel, I also examined the degree of angiogenesis within the metastatic area by immunofluorescent staining. No difference was observed with respect to average metastasis size when comparing the two genotypes to one another (Figure 6.2A), suggesting that once CMT19T F1 cells had established colonies in the lungs, their growth proceeded at the same rate. Similarly, the number of vessels associated with the lung metastatic area was similar in both genotypes (Figure 6.2B), thus suggesting that metastatic cells can equally make up their own vessels at distant sites, regardless of the presence of  $\beta$ 3-integrin in the endothelium. Resected tumours were also analysed for angiogenic markers. There was no difference in the degree of angiogenesis in CMT19T F1 primary tumours grown in  $\beta$ 3-floxed/Tie1Cre positive mice compared to  $\beta$ 3-floxed/Tie1Cre negative mice, a result which is consistent with the tumour volume data.

Taken together, these results suggest that endothelial  $\beta$ 3-integrin facilitates the process of spontaneous lung metastasis through a mechanism which is independent of angiogenic potential at the metastatic site.

### **6.2.2 Tumour-Associated macrophages are reduced in the CMT19T F1 metastatic lung when endothelial $\beta$ 3-integrin is absent**

Over the last decade, a growing body of literature has highlighted the importance of the tumour microenvironment in cancer progression. The tumour microenvironment contains many resident cell types, such as adipocytes and fibroblasts, but it is also

populated by migratory bone marrow derived cells, which can play pivotal roles in the progression and metastasis of tumours (Kaplan *et al.*, 2005).

Macrophages are myeloid cells which represent an important cellular component of the tumour microenvironment. It is well established that tumour associated macrophages (TAMs) induce tumour growth (Sica and Mantovani, 2011), so I asked whether their recruitment to the lung was involved in supporting the establishment of metastatic outgrowth, thus potentially contributing to the difference in metastases observed in  $\beta 3$ -floxed/Tie1Cre mice. To test this hypothesis the macrophage infiltration in the metastatic lung tissue was quantified by F4/80 (a macrophage marker, Schmieder *et al.*, 2012) immunofluorescent staining of lung histological sections (Figure 6.2D). The number of F4/80 positive macrophages present in the metastatic lung tissue was significantly reduced in  $\beta 3$ -floxed/Tie1Cre positive mice compared to lungs from  $\beta 3$ -floxed/Tie1Cre negative mice (Figure 6.2C), thus correlating with the reduced number of lung metastases.

These preliminary observations imply that the loss of endothelial  $\beta 3$ -integrin affects the tumour microenvironment at the site of metastases by reducing the number of tumour associated macrophages in the lung.

### **6.2.3 Loss of endothelial $\beta 3$ -integrin is sufficient to affect lung metastasis**

In order to understand the cellular basis of metastatic phenotype described above, I addressed the contribution of endothelial  $\beta 3$ -integrin in the process of metastatic dissemination by performing an experimental metastasis experiment. CMT19T F1 tumour cells were injected via the tail vein into  $\beta 3$ -floxed/Tie1Cre mice. 14 days after tumour cell injection, lungs were processed for metastases evaluation. Sections of lung tissues were stained with H&E and metastases counted. The number of metastatic foci was not statistically different between the two genotypes (Figure 6.1C), implying that, once in the circulation, tumour cells can equally invade and colonise the lung, regardless of the expression of  $\beta 3$ -integrin on the endothelium. Moreover, the number of experimental metastases was lower than the number of spontaneous metastases that developed in the spontaneous model.

From these data, I concluded that endothelial  $\beta 3$ -integrin is dispensable for the process of lung colonization, but it is required for establishing a pre-metastatic niche in the lung during the growth of the primary tumour. It would be tempting to speculate

that endothelial  $\beta$ 3-integrin exerts a pro-metastatic function through the regulation of macrophage infiltration at the metastatic site and, as such, seeds the lung microenvironment to make it more permissive for metastasis. Since the establishment of the pre-metastatic niche precedes tumour colonization, this would also explain why in an experimental metastasis setting the difference in the number of lung metastases was abolished, regardless of endothelial  $\beta$ 3-integrin absence.

### **6.3 *In vivo* and *in vitro* mechanistic analysis of the role of endothelial $\beta$ 3-integrin in metastasis**

In order to identify the mechanistic link underlying the role of endothelial  $\beta$ 3-integrin in metastasis, I formulated two different, but not mutually exclusive, hypotheses based on my preliminary data and evidence from the literature: first, according to Paget's theory of "Seed and Soil" (Paget 1989), the primary tumour while growing is already sending out signals to prepare the soil to make it more permissive for metastatic tumour cells to grow at distant sites (a process referred to as "pre-metastatic niche formation") and/or second, the reduced number of lung metastases observed in  $\beta$ 3-floxed/Tie1Cre positive mice might be due to a reduced number of metastatic cells leaving the primary tumour.

#### **6.3.1 F4/80+ macrophages are reduced in the CMT19T F1 pre-metastatic lung when endothelial $\beta$ 3-integrin is absent**

Since I observed a difference in the macrophage infiltration in the metastatic lung, I wanted to know if this difference was already established before metastases appeared in the lung, therefore suggesting macrophages were involved in favouring a pro-metastatic microenvironment. It has previously been shown that the recruitment of myeloid cells can predetermine lung metastases (Hiratsuka *et al.*, 2006); therefore, with respect to my first hypothesis, I determined whether endothelial  $\beta$ 3 integrin played a role in seeding the lung via mobilization of myeloid cells.

In order to achieve this, I quantified the myeloid cell population in the lungs of CMT19T F1 tumour bearing mice during the pre-metastatic phase (i.e. at the time of tumour resection). Flow cytometric analyses of the pre-metastatic lung (Figure 6.3A) showed no difference in the total amount of infiltrating CD45+/CD11b+ myelomonocytes when comparing  $\beta$ 3-floxed/Tie1Cre negative and positive mice (Figure 6.3B). However, when analysing specifically the macrophage subset (F4/80+ cells)

a significant difference became evident. The number of total F4/80+ macrophages was significantly reduced in the pre-metastatic lungs of  $\beta$ 3-floxed/Tie1Cre positive mice (Figure 6.3C). This result agrees with the previously observed difference in macrophage infiltration in the metastatic lung and suggests endothelial  $\beta$ 3-integrin modulates macrophage homing to metastatic sites, thus generating a pro-metastatic microenvironment.

To recapitulate, reduced macrophage infiltration in the absence of endothelial  $\beta$ 3-integrin was observed before and once metastases had established in the lung and it correlated with a reduced number of metastatic foci. These observations are likely to indicate that endothelial  $\beta$ 3-integrin is involved in the process of formation of a pre-metastatic niche in the lung by promoting macrophage infiltration.

### **6.3.2 Loss of endothelial $\beta$ 3-integrin within the tumour does not affect either vascular permeability, or circulating tumour cells *in vivo***

My previous findings suggest that endothelial  $\beta$ 3-integrin regulates metastases. I then asked whether endothelial  $\beta$ 3 integrin was affecting tumour vascular permeability, which might lead to differences in the number of tumour cells entering the blood circulation. I investigated the effect on vessel permeability *in vivo* by performing FITC-dextran perfusion assay and by quantifying blood tumour circulating cells at the time of tumour resection.

Recent work from Jean *et al.* (2014) showed that inhibition of endothelial FAK did not alter primary tumour growth, but did result in reduced metastases *in vivo* by affecting primary tumour vascular permeability via VE-cadherin (VEC) barrier function. Since it is well established that FAK acts downstream of  $\beta$ 3 integrin signalling, I wondered whether  $\beta$ 3 integrin could affect tumour vascular permeability through a FAK/VEC dependent mechanism, thereby leading to decreased tumour cell extravasation in  $\beta$ 3-floxed/Tie1Cre positive mice.

Increased vascular permeability causes endothelial cells to partially lose their close contacts and the endothelium becomes permeable to small proteins such as low-molecular weight dextran. As such, FITC-dextran extravasation is considered a measure of vascular permeability (Eliceiri *et al.*, 1999). Day 20 B6 LV-1 tumour bearing  $\beta$ 3-floxed/Tie1Cre negative and positive mice were injected systemically with low molecular weight FITC-dextran. 30 minutes later, specimens were harvested and

FITC-dextran was extracted by immersion in formamide buffer. The amount of FITC-dextran in each tumour tissue sample was quantified by fluorescence emission at 520 nm and normalized to tumour weight. No difference in tumour vascular permeability was detected when comparing B6 LV-1 tumours grown in the two genotypes (Figure 6.4A), suggesting the endothelial  $\beta$ 3-integrin deletion was not altering tumour vascular permeability.

In parallel, to test whether the loss of endothelial  $\beta$ 3-integrin affected the number of circulating tumour cells the degree of circulating B6 LV-1 (luciferase tagged) cells was quantified by luciferase semiquantitative-PCR from nucleated cells isolated from peripheral blood. In agreement with tumour permeability data, the relative number of tumour circulating cells indirectly measured by the quantification of luciferase gene expression showed no statistical difference between blood samples from  $\beta$ 3-floxed/Tie1Cre negative and positive mice (Figure 6.4B), suggesting that endothelial  $\beta$ 3 integrin is not required for tumour cell extravasation during the metastatic process.

Taken together these data help exclude the premise that endothelial  $\beta$ 3-integrin exerts a pro-metastatic role by increasing the permeability of the vasculature in the primary tumour or by enhancing the process of tumour cell extravasation from the primary tumour, which would then result in an increased number of tumour cells in the circulation. Though negative, these results are very important because they help rule out two possible mechanisms contributing to the reduced metastatic potential observed in  $\beta$ 3-floxed/Tie1Cre positive mice.

I have presented preliminary data which are likely to imply a role for endothelial  $\beta$ 3 integrin in the establishment of a pre-metastatic niche. However, I am fully aware that further investigation is needed. For example, it would be elegant to show that after systemic macrophage depletion the difference in lung metastasis is abolished. Moreover, it would be interesting to more fully characterize the immune cell infiltration in the pre-metastatic lung, as well as, investigate environmental changes in the pre-metastatic lung by, for example, chemokine/cytokine and protease profiling (see DISCUSSION).

### **6.3.3 VEC Y731 phosphorylation is affected by endothelial $\beta$ 3-integrin *in vitro***

To address mechanistically how endothelial  $\beta$ 3-integrin might affect macrophage recruitment to the pre-metastatic site, I moved to *in vitro* analyses. As the secondary

site in this model is the lung, endothelial cells isolated from the lung provided a realistic representation of the metastatic site.

Recent work from Wessel *et al.* (2014) showed that different phosphorylation sites of VEC are involved distinctly and specifically in the induction of vascular permeability or leukocyte extravasation across the endothelium. In more detail, phosphorylation of VEC Y731 has been implicated in leukocyte transmigration and has a high baseline phosphorylation; while its de-phosphorylation, mediated by SHP-2, has been associated with an increase in leukocyte extravasation (Turowski *et al.*, 2007; Wessel *et al.*, 2014). In fact, Y731 phosphorylation has been shown to decrease by 50% following Tumour Necrosis Factor (TNF) stimulation of T cells and bone marrow derived cells, resulting in leukocyte extravasation (Wessel *et al.*, 2014). Furthermore, in culture, VEC Y731 has been shown to be responsive to VEGF stimulation (Monaghan-Benson and Burridge, 2009). This evidence led me to hypothesise that endothelial  $\beta$ 3 integrin can modulate macrophage extravasation to the lung via VEC Y731 phosphorylation.

To investigate this hypothesis, quantification of phosphorylation of VEC Y731 followed over a VEGF stimulation time course was performed by Western blot analyses on protein lysates from lung endothelial cells isolated from  $\beta$ 3-floxed/Tie1Cre mice. Interestingly, in  $\beta$ 3-floxed/Tie1Cre negative lung endothelial cells, a significant reduction in the phosphorylation of VEC Y731 was observed over time (Figure 6.4C). However, this change in VEC Y731 phosphorylation status did not occur in  $\beta$ 3-floxed/Tie1Cre positive lung endothelial cells.

This preliminary findings are likely to suggest that the absence of endothelial- $\beta$ 3 integrin at metastatic sites causes the inability of VEC Y731 to dephosphorylate in response to VEGF and, as a consequence, endothelial junctions do not open to allow leukocyte extravasation. Therefore, the reduction in macrophage infiltration in presence of VEC Y731 at high levels is not conducive to tumour cell extravasation and therefore metastases are reduced. However, this is only one interpretation and our data, though promising, are not yet conclusive: *in vitro* adhesion and transmigration assays of macrophages across endothelium are essential to support this hypothesis, as well as the identification of the molecular player linking  $\beta$ 3-integrin and VEC (see DISCUSSION).

**Figure 6.1 Constitutive endothelial  $\beta$ 3-integrin deletion reduces CMT19T F1 spontaneous, but not experimental, metastasis**

(A) CMT19T F1 tumour cells were grown subcutaneously in  $\beta$ 3-floxed/Tie1Cre mice. Line graph shows CMT19T F1 growth curve based on external measurement of tumour size taken with a digital caliper every other day, until day 20, when tumours were surgically removed. Following resection of CMT19T F1 tumours, mice were housed for a further 12 days, until they were sacrificed and lungs were isolated for histological analysis with H&E staining to quantify metastases.

(B) The number of spontaneous lung metastases was reduced in  $\beta$ 3-floxed/Tie1Cre positive lungs compared to  $\beta$ 3-floxed/Tie1Cre negative lungs. Bar chart shows the mean (+SEM) number of lung metastases in the whole lung. Data are representative of 3 independent experiments (n=3 per genotype, \*p<0.05).

(C) CMT19T F1 were systemically injected through the tail vein in  $\beta$ 3-floxed/Tie1Cre mice. After 14 days, lungs were isolated and histologically analysed with H&E staining to quantify metastases. No difference in the number of experimental lung metastases was observed between  $\beta$ 3-floxed/Tie1Cre positive and negative lungs. Data is representative of a single experiment (n=3 per genotype, NS=not significant).

(D) Macroscopic appearance of lungs isolated from  $\beta$ 3-floxed/Tie1Cre positive and negative mice 12 day after tumour resection. Arrows point to examples of CMT19T F1 metastasis (scale bar=1 cm)

(E). Representative images of H&E stained sections of lungs isolated  $\beta$ 3-floxed/Tie1Cre positive and negative mice (scale bar=1 mm).

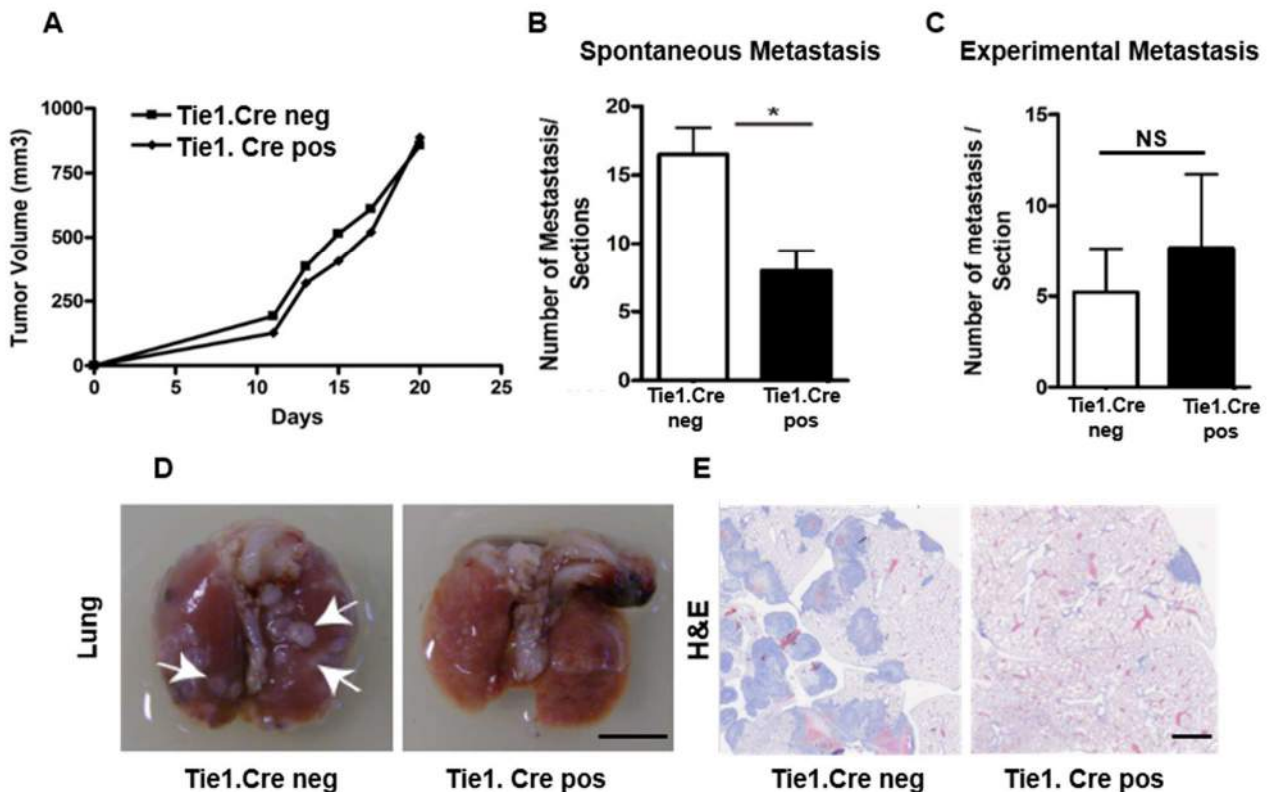


**Figure 6.2 Constitutive deletion of endothelial  $\beta 3$ -integrin does not affect average metastasis size or vascularisation, but fewer macrophages are present in the lung**

(A) CMT19T F1 lungs from  $\beta 3$ -floxed/Tie1Cre positive and negative mice were evaluated histologically with H&E to measure metastasis size. No differences in the average metastasis size were observed when comparing  $\beta 3$ -floxed/Tie1Cre positive and negative lungs. Average metastasis size was quantified using ImageJ on H&E stained sections. Bar chart shows the mean (+ SEM) area of single metastatic foci present in the lung. Data are representative of 3 independent experiments (n=3 per genotype, NS=not significant).

(B) CMT19T F1 lungs from  $\beta 3$ -floxed/Tie1Cre positive and negative mice were immunostained for endomucin to assess vessel density in metastatic foci. No differences in vessel density in lung metastatic areas were observed when comparing  $\beta 3$ -floxed/Tie1Cre positive and negative lungs. Bar chart shows the mean (+ SEM) vessel number in metastatic areas of the lungs. Data are representative of 3 independent experiments (n=3 per genotype, NS=not significant).

(C) Fewer F4/80+ macrophages were found in metastatic lungs from  $\beta 3$ -floxed/Tie1Cre positive mice compared to those from  $\beta 3$ -floxed/Tie1Cre negative mice. Bar chart shows the mean (+ SEM) number of F4/80 positive cells infiltrating lung metastatic areas (mm<sup>2</sup>). Data are representative of 3 independent experiments (n=3 per genotype, \*p<0.05). Representative immunofluorescent images from lung sections immunostained for F4/80 (in green) to detect infiltrating macrophages. DAPI (blue) was used as a nuclear counterstain (scale bar=50 $\mu$ m).

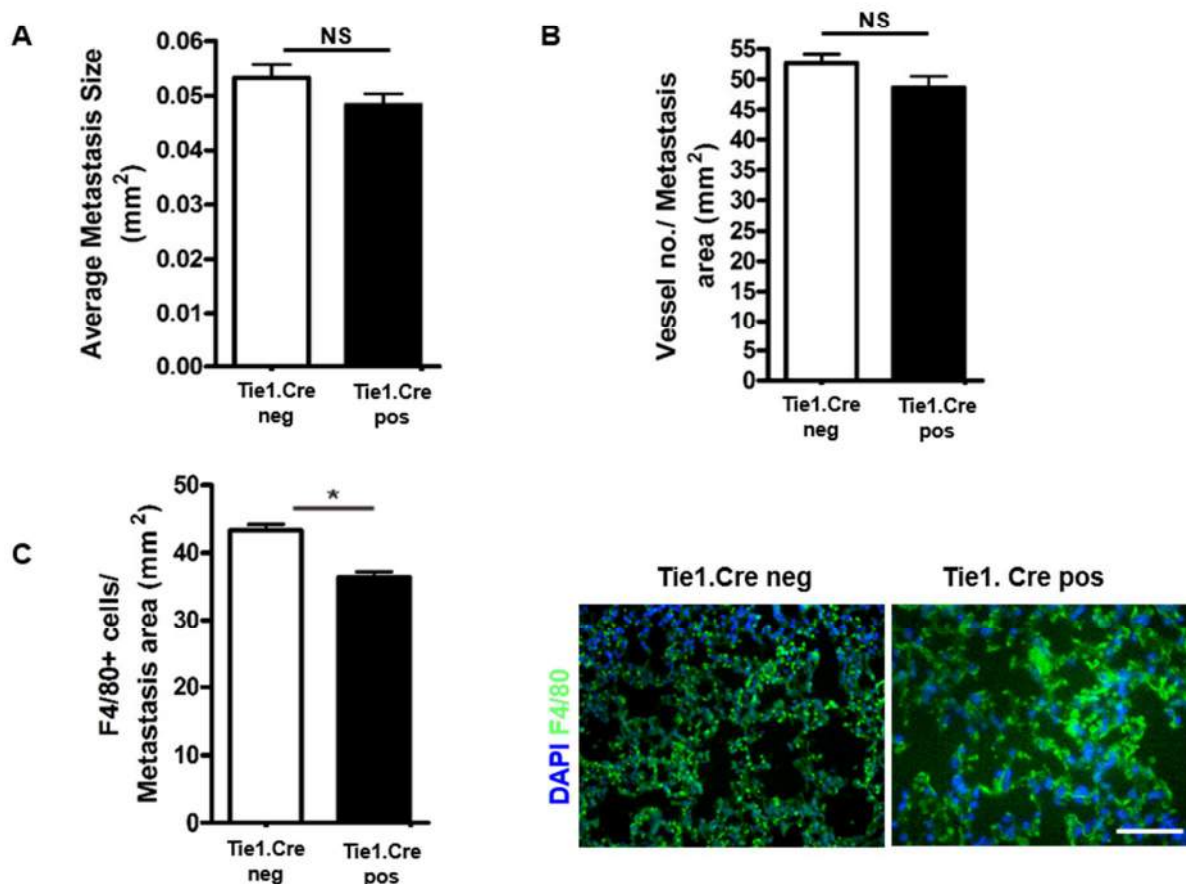


**Figure 6.3 F4/80+ macrophages are reduced in CMT19T F1 pre-metastatic lungs when endothelial  $\beta$ 3-integrin is absent**

(A) Macrophage infiltration in the lungs of  $\beta$ 3-floxed/Tie1Cre mice before tumour cell arrival was assessed at day 20, corresponding to the day of resection of the primary tumours. Lung cell suspensions were double-immunostained with the myeloid markers CD45 and CD11b, and with  $\beta$ 3 integrin and F4/80, respectively; then analyzed by flow cytometry (representative dot plots displaying gating strategy). Despite no difference in the total amount of infiltrating myeloid cells in the pre-metastatic lungs, the percentage of F4/80+ macrophages and  $\beta$ 3 integrin+/F4/80+ macrophages were significantly reduced in  $\beta$ 3-floxed/Tie1Cre positive lungs compared to  $\beta$ 3-floxed/Tie1Cre negative lungs.

Scatter plots show mean percentage of CD45+/CD11b+ myeloid cells (B) F4/80+ macrophages (C) and  $\beta$ 3 integrin+/F4/80+ macrophages (D) relative to the total lung population isolated from  $\beta$ 3-floxed/Tie1Cre positive and negative mice. Data are representative of a single experiment (n=5 mice per genotype, \*\*p<0.01, NS=not significant).

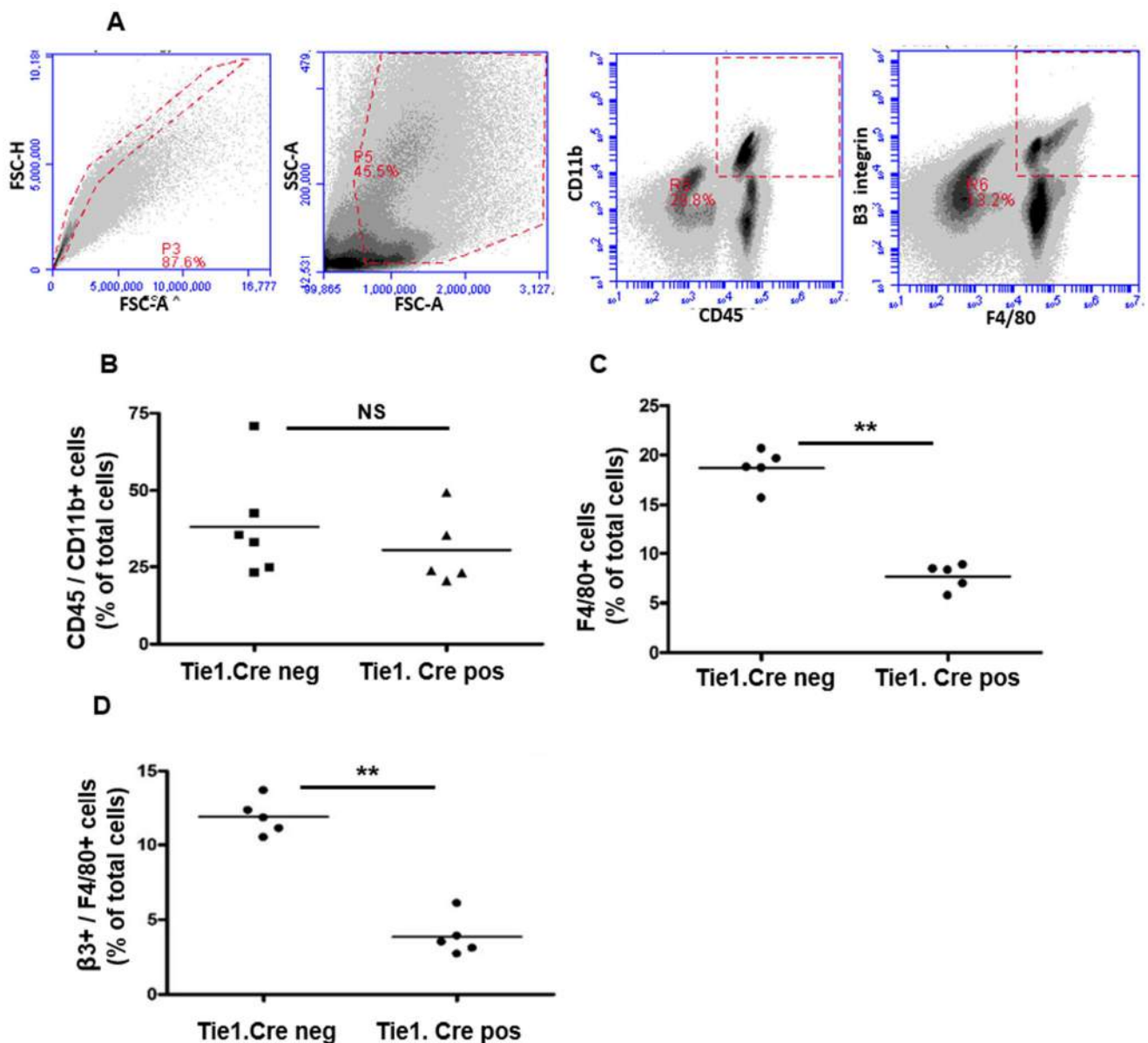


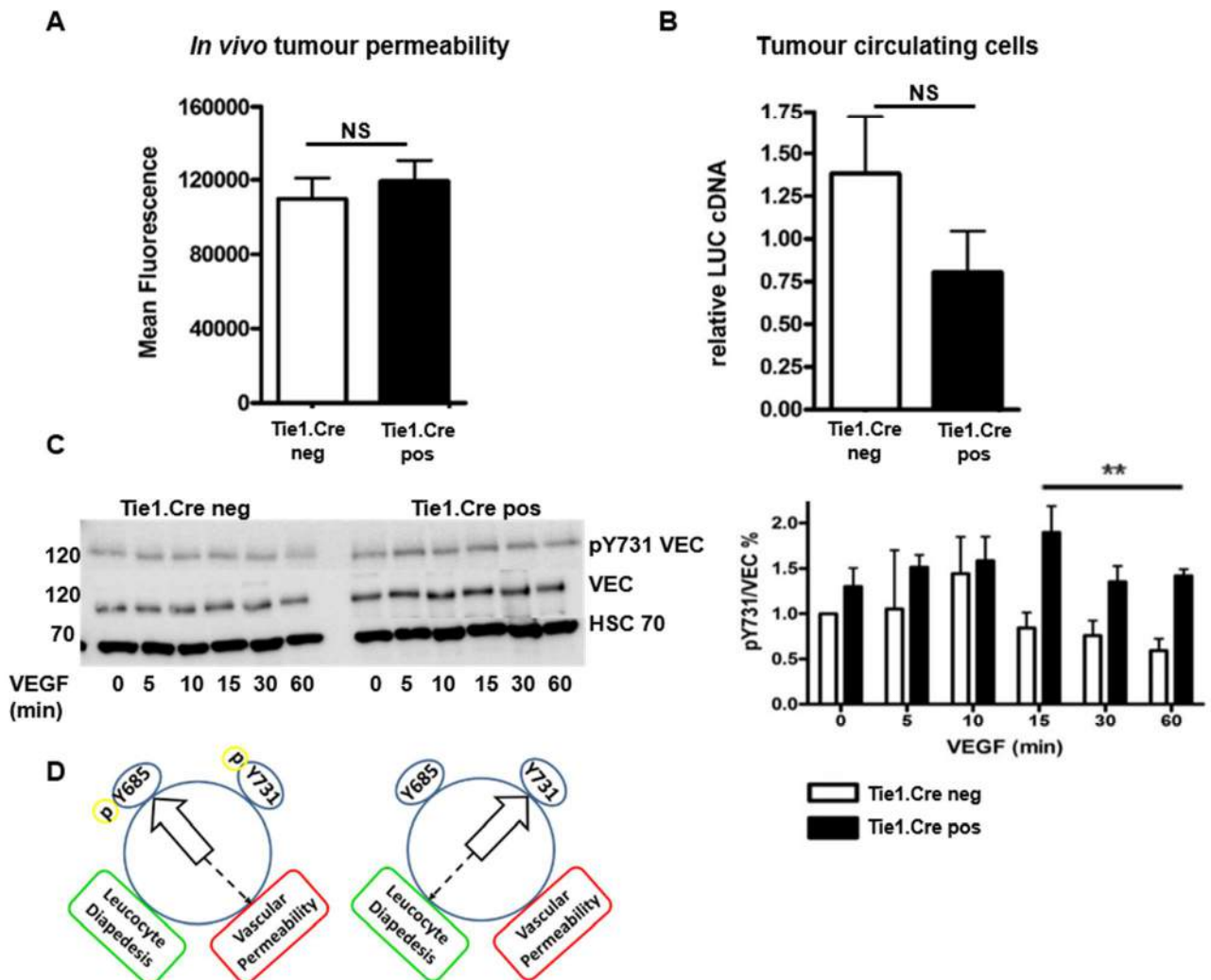
**Figure 6.4** Constitutive deletion of endothelial  $\beta 3$ -integrin: *in vivo* and *in vitro* effects

(A) Tumour vascular permeability was assessed by systemic FITC-dextran injection in tumour B6 LV-1 tumour-bearing  $\beta 3$ -floxed/Tie1Cre positive and negative mice, 30 minutes before sacrifice. Tumours were isolated and weighed. FITC fluorescence due to dextran extravasation was extracted by incubation with formamide and quantified by fluorescence analysis. Bar chart shows the mean (+ SEM) fluorescent value of single tumours normalized to weight. Data are representative of a single experiment (n=5 per genotype, NS=not significant).

(B) The amount of tumour circulating cells was measured in B6 LV-1 tumour-bearing  $\beta 3$ -floxed/Tie1Cre positive and negative mice by luciferase q-PCR analysis on blood mononucleated cells. GAPDH provided a loading control. Bar chart shows the mean (+ SEM) densitometric quantification of luciferase cDNA relative to GAPDH cDNA. Data are representative of a single independent experiment (n=5 per genotype, NS=not significant).

(C) Representative Western Blot analysis of time-course of VEGF stimulation in endothelial cells isolated from  $\beta 3$ -floxed/Tie1Cre mice. Cells were stimulated with VEGF (30 ng/ml) at the indicated timepoints. Protein lysates were blotted for phosphorylated VEC Y731 and subsequently reblotted for total VEC. Bar graph shows mean (+ SEM) densitometric quantification of phosphorylated VECY731 relative to total VEC normalized to unstimulated cells. Data are representative of 3 independent experiments (\*\*p<0.01).

(D) Schematic displaying the mechanism for the control of permeability and diapedesis by phosphorylated VE-Cadherin.



## DISCUSSION

### 6.4 Metastasis: the real killer

Metastasis is the leading cause of tumour related death, lung and bone being the most common site for metastasis in breast and prostate cancers. In the UK alone, 12,000 women will die from breast cancer each year, the large majority as a result of metastatic disease (Eccles *et al.*, 2013). In the US in 2014, one and a half million people were diagnosed with cancer and half a million died of cancer. This statistic reflects the 5 year overall survival index, which for cancer has been estimated to be 66.1% in the latest 10 years (2004-2014) in the US. In other words 2/3 of people diagnosed with cancer are still alive after 5 years but the remaining 1/3 of them die, not from primary cancer, but rather from secondary disease (from <http://seer.cancer.gov/>). Metastatic dissemination is a multi-step process in which invasive cells spread from the primary tumour by extravasating and entering the circulation (either blood or lymphatic), to then intravasate and colonize distant tissues and organs. In order to become invasive and metastasise, malignant tumours require a sufficient blood supply. This is achieved through the remodelling of the host vasculature via angiogenesis.

I have shown that acute deletion of endothelial  $\beta$ 3-integrin inhibits tumour growth and angiogenesis preventatively, but not in already established tumours, while its long term deletion is ineffective. This implies that timing and length of inhibition are critical factors to be considered when targeting endothelial  $\beta$ 3-integrin expression. In follow-on studies, I aimed to determine whether endothelial  $\beta$ 3-integrin plays a role in the process of metastatic spread; in order to assess whether its targeting could prevent or delay tumour dissemination or metastatic outgrowth. In fact, targeting the tumour vasculature offers many advantages compared to targeting neoplastic cancer cells. Such a strategy bypasses the problems of tumour heterogeneity, genomic instability and different degrees of metastases common to many cancers.

### 6.5 Metastasis models: not enough

There are various ways to mimic cancer growth and metastasis in tumour transplantation experiments as described in paragraph 6.1. Implantation of human cancer cell lines derived from human cancer (xenograft models) is simple, but has limitations: the immune responses are impaired in immunocompromised mice and

stromal components are not of tumour origin. Syngeneic transplantation bypasses the immunologic rejection and allows the investigation of the contribution of the immune system to malignant tumour progression and metastasis (Francia *et al.*, 2011). On the other hand, genetically modified mice which develop metastatic disease spontaneously mimic the entire process of tumourigenesis *in vivo* and, as such, they are more reliable as clinically predictive tools for evaluating the efficacy of therapeutic agents for the treatment of metastatic disease (Talmadge *et al.*, 2007).

Nevertheless, even encouraging preclinical therapeutic findings employing either transplanted or spontaneous tumour metastasis models often fail to reproduce the successful outcomes when translated to the clinic (Francia *et al.*, 2011). There are several reasons for this including a failure to establish appropriate and accurate models. One example of this discrepancy is the poor predictability of xenograft tumour models of whether a treatment is likely to be effective in a metastatic setting as a consequence of the differential response of metastasis and primary tumours to the therapy. Therefore, it would be beneficial to combine orthotopic or subcutaneous tumours model with spontaneous models of advanced metastasis when testing new anticancer strategies (Francia *et al.*, 2011). It is thus important to generate mouse models that more accurately recapitulate clinical scenarios and this is the reason behind the choice to develop spontaneous models through several rounds of syngeneic tumour cell transplantation and selection of metastatic cells, such as the subcutaneous tumour model of lung metastases CMT19T F1 and the orthotopic tumour model of lung and bone metastases B6 LV-1 (developed at Washington University).

However, spontaneous metastasis models are challenging to set up and optimize for a number of reasons. Tumours can grow asynchronously and metastases can appear unevenly, making it difficult to decide when to resect tumours and harvest organs for metastatic evaluation. In general, not all mice survive for the entire experiment as poor health may require premature sacrifice, meaning that large cohorts of mice are required. Finally, metastatic phenotypes can vary significantly from animal to animal, even within the same experimental group. This actually reflects what is seen in the clinic: every individual presents differently and our results may simply reflect individual variation. The only way to reduce this variable is with further repeats to achieve a greater end number, thus making these experiments more labour-intensive and expensive. For these reasons, I decided to perform my initial analyses in the

constitutive model of endothelial  $\beta$ 3-integrin deletion (Tie1Cre transgenic mice): it is a simpler model as it does not require tamoxifen treatment.

## 6.6 Is endothelial $\beta$ 3-integrin anti-metastatic?

My studies have for the first time addressed the potential for targeting endothelial  $\beta$ 3-integrin for the prevention of metastasis: preliminary findings in CMT19 T F1 model suggest that, while constitutive deletion of endothelial  $\beta$ 3-integrin did not affect primary tumour growth, it significantly reduced metastatic spread to lung.  $\alpha$ v $\beta$ 3-integrin expression in primary tumours has been found to associate with greater metastatic potential (Liu *et al.*, 2012, Desgrosellier *et al.*, 2009, Felding-Habermann 2003, Sloan *et al.*, 2006), therefore I further investigated the role of  $\beta$ 3-integrin in the process of metastasis.

Surprisingly, although constitutive deletion of endothelial  $\beta$ 3-integrin decreased the number of spontaneous metastasis, it did not appear to alter metastatic angiogenesis in the lung, as confirmed by no difference in the average size of metastatic foci, regardless of endothelial  $\beta$ 3-integrin expression. Interestingly, the difference in the number of metastasis between the two genotypes was not observed in an experimental metastasis setting.

One explanation may be that fewer tumour cells entered the blood circulation as a result of reduced tumour vascular permeability, as reported by Jean *et al.* (2014), whereby inhibition of endothelial FAK was shown to prevent tumour metastasis by enhancing barrier function at the primary site. I was able to rule out this hypothesis by showing that there was no difference *in vivo*, in either tumour vascular permeability or in the amount of tumour circulating cells.

A second explanation may be that the tumour releases signals, such as pro-inflammatory cytokines, to prepare the metastatic site prior to spread (Langley and Fidler, 2011). It is also becoming increasingly recognised that immune cells can be mediators of tumour development and metastasis (De Nardo *et al.*, 2008, Lin and Pollard 2007, Joyce and Pollard 2009). Enhanced leukocyte infiltration, causing conditions of inflammation, have been suggested to disrupt the normal microenvironment preparing the 'soil' for metastasising tumour cells (Hu and Polyak, 2008).

To this end, I was able to show that, in absence of endothelial  $\beta 3$ -integrin, the number of tumour associated macrophages in the lung was reduced before and after metastasis had established, thereby suggesting that they may be involved in the formation of a pre-metastatic niche. These very interesting, but preliminary, findings raise at least 3 questions, yet unaddressed:

- *first, how does endothelial  $\beta 3$ -integrin regulate the infiltration of macrophages in the lung?*

The recruitment of leukocytes into peripheral tissues involves interactions with endothelium. Leukocytes need to establish transient and dynamic adhesive contacts with endothelial cells to transmigrate (Lindbom and Werr, 2002).  $\alpha v\beta 3$ -integrin has been shown to function as a heterotypic ligand for CD3, in controlling the arrest and extravasation of hematopoietic cells (Lindbom and Werr, 2002). While its expression on leukocytes (monocytes and neutrophils) has been described to be involved in the transition between adhesion to the endothelium and diapedesis (Weerasinghe *et al.*, 1998). Therefore, it would be interesting to investigate whether  $\beta 3$ -integrin on endothelial cells is involved in the recruitment and/or retention of leucocytes to the pre-metastatic lung to promote metastasis outgrowth.

- *second, how do macrophages contribute to the formation of a pre-metastatic niche in the lung?*

Macrophages infiltrating the tumour contribute to the formation of an inflammatory microenvironment which sustains tumour growth and progression and have been reported to have a M2 phenotype (Biswas *et al.*, 2006). Macrophages are also associated with increased metastatic potential (De Nardo *et al.*, 2009; Joyce and Pollack, 2009). They have been shown to upregulate the expression of Cathepsin B which leads to increased lung metastasis (Vasiljieva *et al.*, 2006) and they have been found to express a truncated isoform of fibronectin which acts as a potent chemoattractant for tumour cells (Solinas *et al.*, 2010). Macrophages can also promote angiogenesis and exert immunosuppressive activity (Galdiero *et al.*, 2013). No difference in vessel density in the metastatic lung would imply at least in theory mechanisms other than increased angiogenesis are induced by tumour associated macrophage to promote metastatic growth. This mechanistic analysis needs to be followed up and investigated further.

- *Third, are there other cells involved in setting up the pre-metastatic niche? If so, who are they and how do they do it?*

A wide spectrum of immune cells take part in the tumour environment, such as neutrophils and myeloid derived suppressor cells. Interestingly, neutrophils can up-regulate  $\beta$ 2-integrin to interact with ICAM-1 on melanoma cells and promote lung metastasis (Huh *et al.*, 2010). Myeloid derived suppressor cells have been found to promote metastasis in the pre-metastatic lung via different mechanisms: up-regulation of MMP9 which leads to aberrant and leaky vasculature (Yan *et al.*, 2010); inhibition of Interferon- $\gamma$  (IFN $\gamma$ ) which promotes an immune-suppressive environment and inflammatory environment (Yan *et al.*, 2010); versican expression, which leads to Mesenchymal to Epithelial Transition (MET), thus favouring metastases formation (Gao *et al.*, 2012). These evidences would suggest that other immune cells might be involved in setting up the pre-metastatic niche and their contribution would require further investigation.

My preliminary data on the role of endothelial  $\beta$ 3-integrin in metastatic prevention are encouraging and suggest they should be further investigated. These studies will lead to a better understanding of the integrin-mediated interactions between endothelial cells and tumour microenvironment which mediate metastasis, and will help us understand how to manipulate these interactions when designing novel therapeutic strategies.

### **6.7 Mechanisms of pre-metastatic niche formation**

Vascular Endothelial cadherin (VEC) is a type I transmembrane protein which mediates endothelial cell adhesion and barrier function (Sidibe and Imhof, 2014). This protein has a range of phosphorylation sites, each having a unique role in various processes. For example, phosphorylation of VEC Y658 has been shown to induce vessel permeability via the dissociation of the VEC- $\beta$ -catenin-p120-catenin- $\alpha$ -catenin complex (Potter *et al.*, 2005). More recently, this same residue has been reported to be phosphorylated by endothelial FAK to control endothelial barrier function and facilitate tumour spread (Jean *et al.*, 2014). Instead, VEC Y731 phosphorylation site has been reported to control a different aspect of endothelial barrier function which is leukocytes extravasation (Wessel *et al.*, 2014). VEC Y731 has a high baseline phosphorylation and in order for extravasation to occur, leukocytes trigger dephosphorylation of Y731.

The unaltered level of VEC Y731 phosphorylation I observed in  $\beta$ 3-floxed/Tie1Cre positive lung endothelial cells would suggest that in absence of endothelial  $\beta$ 3-integrin, VEC Y731 is unable to be dephosphorylated and, as such, the potential for leukocyte extravasation is reduced. Therefore, this was consistent with the *in vivo* results of decreased tumour associated macrophages in the metastatic lung of  $\beta$ 3-floxed/Tie1Cre positive mice. Similarly to endothelial FAK regulating endothelial barrier function via VEC Y658 phosphorylation in the primary tumour, I hypothesised a model whereby endothelial  $\beta$ 3-integrin controls leukocytes extravasation via VEC Y731 phosphorylation in the lung. As such, the lung would become less conducive to tumour cell colonisation, therefore reducing metastasis. This would also imply that endothelial  $\beta$ 3 is not required for tumour cell colonisation at distant site, but it might be for macrophage infiltration into the lung during the growth of the primary tumour to establish the pre-metastatic niche.

However, this model, envisioned by combining preliminary data and evidence from the literature, though promising, is still only a model. A pre-condition for any further investigation is the confirmation that the anti-metastatic effect is endothelial  $\beta$ 3-integrin specific, despite the leakiness of the *Tie1* promoter in the bone marrow derived cells (20%, Gustafsson *et al.*, 2001). This is essential because bone marrow derived cells have also been shown to prepare the pre-metastatic niche (Kaplan *et al.*, 2005). More importantly,  $\beta$ 3-integrin on bone marrow derived cells is crucial for the adhesion and transmigration at sites of neovascularization, such as tumour sites (Feng *et al.*, 2008). To exclude that an anti-metastatic effect was due to  $\beta$ 3-integrin deletion in some bone marrow lineages, it would be necessary to transplant wild-type bone marrow into  $\beta$ 3-floxed/Tie1Cre positive and see if there is a reversal of the phenotype of reduced lung metastasis. Alternatively, spontaneous metastasis experiments could be performed in the inducible endothelial transgenic model (Pdgfb-iCreER<sup>T2</sup>), whereby Cre recombinase is not active in the bone marrow (Claxton *et al.*, 2008) to assess whether the phenotype of reduced lung metastasis could be replicated.

Moreover, to prove this model to be right, it would be crucial to identify the molecular players involved in the cross-talk between integrin  $\alpha$ v $\beta$ -integrin and VEC. Based on the recent works from Jean *et al.* (2014) and Wessel *et al.* (2014), potential candidates may be SHP-2 and FAK/c-Src. SHP-2 is a non-transmembrane protein tyrosine phosphatase which associates with SHPS-1 upon its phosphorylation

(Tsuda *et al.*, 1998) and it has been shown to mediate dephosphorylation of VEC Y731 to allow leucocytes passage across endothelial junctions (Wessel *et al.*, 2014). Interestingly, there is evidence suggesting that SHPS-1/SHP-2 complex promote a positive feedback loop leading to c-Src/FAK activation during integrin signalling (Oh *et al.*, 1998). The precise order in which c-Src and FAK are activated upon integrin signalling is still controversial. Regardless, it leads to SHPS-1/SHP-2 complex formation and SHP-2 activation. Therefore, it would be tempting to speculate that the absence of endothelial  $\beta 3$  integrin causes defective SHP-2 activity, which then results in reduced leukocyte extravasation, as a consequence of unaltered level of phosphorylated VEC Y731. Consistent with this idea, impaired expression and function of FAK would be accommodated in this model, as a result of constitutive endothelial  $\beta 3$ -integrin deletion.

Further investigation is required for a more thorough understanding of what is occurring at the secondary site. Whilst I have not clearly defined the mechanism(s) which could explain my metastases findings, I have provided preliminary evidence that targeting endothelial  $\beta 3$ -integrin could have a potential therapeutic benefit in preventing metastatic spread and suggested lines of investigation to move forward with these studies.

## **CONCLUSIONS**

This final result chapter contains preliminary data I collected in my last year which I have not had the time to follow up. In fact this project will be continued by a new PhD student. I thought it was worthwhile to include it as a final part of my work.

In this chapter I have presented initial findings suggesting that:

- **Constitutive endothelial  $\beta 3$ -integrin deletion reduces the number of lung metastasis;**
- **the reduction in lung metastases which occurs in constitutively  $\beta 3$ -integrin deleted mice correlates with reduced tumour associated macrophage infiltration in the lung prior to tumour cell arrival;**

- further *in vivo* and *in vitro* analyses are needed to confirm that it is endothelial specific phenotype and to explain it mechanistically.

## 7. SUMMARY AND CONCLUSION

### 7.1 Novelty and significance

*Do these studies help to reconcile the seemingly conflicting findings regarding  $\alpha\beta 3$ -integrin functions in tumour angiogenesis?*

I believe they do. Genetic data from  $\beta 3$ -integrin knockout mice have already helped explain some reasons for discrepancies in the literature. Their phenotype of enhanced tumor growth and angiogenesis is caused, at least in part, by the upregulation of VEGFR2-dependent angiogenic pathways (Reynolds *et al.*, 2002; Reynolds *et al.*, 2004). However, multiple cell types express  $\beta 3$ -integrin and contribute to tumour angiogenesis, making it difficult to discriminate between endothelial cell contributions to the process from that of other cells (Robinson and Hodivala-Dilke, 2011). This is an important question, though, as the original observation that spear-headed the development of  $\beta 3$ -integrin antagonists, and the generation of the knockout mice for that matter, was marked up-regulation of the protein in the vasculature.

My studies have specifically addressed this point. By dissecting its role specifically in endothelial cells, I have confirmed  $\beta 3$ -integrin plays a proangiogenic role in the early steps of angiogenesis. However, as ever, this comes with caveats. I have shown that timing is critical. In fact suppressing  $\beta 3$ -integrin expression for too long leads to “treatment” escape. Moreover, once tumour growth and angiogenesis are firmly established, suppressing  $\beta 3$ -integrin, at least alone, has little effect on the progression of the cancer. I would like to speculate that these results recapitulate what is often seen in the clinic: patients become resistant to initially successful  $\beta 3$  integrin blockade and tumours begin to regrow (Desgrosellier and Cheresh, 2010). My finding suggests that the antiangiogenic function of  $\alpha\beta 3$  inhibition occurs transiently and is confined to a specific window during tumour progression. Targeting the molecule at later stages will not prove effective (inherent resistance) and, even if successful to begin with, over time inhibitory effects are lost (acquired resistance).

Importantly, I was able to identify potentially useful cellular and molecular mechanisms accounting for long term adaptation to endothelial  $\beta 3$ -integrin “blockade” (the most interesting may involve with a FAK feedback loop). The pathways I have

identified may provide useful clues for improving on existing antiangiogenic therapies and may, ultimately, help guide future clinical strategies.

In conclusion, my studies help marry up the two sides of the  $\beta$ 3-integrin conundrum. They cement the concept that the function of  $\beta$ 3-integrin in angiogenesis depends on the cell expressing it (Robinson and Hodivala-Dilke, 2011) and contribute to further understanding the complexity of how endothelial cells can adapt their cellular and molecular programmes to circumvent attempts at blocking angiogenesis in pathological conditions.

*And if so, what is their clinical significance?*

My finding that the inducible deletion of endothelial  $\alpha$ v $\beta$ 3-integrin can reduce tumour angiogenesis, clearly re-establish the molecule as a valuable antiangiogenic target. This is important because, with the recent failure of CILENGITIDE in a phase III glioblastoma trial, the field is in danger of giving up on the molecule (<http://merckgroup.com/en/>). However, I believe this might be premature. The models I have described provide a powerful tool for the development of novel therapies that, in combination with  $\alpha$ v $\beta$ 3-integrin inhibition, could improve therapeutic outcomes in clinical settings. For example, my studies helped identify the potential involvement of FAK in promoting escape from  $\beta$ 3-integrin inhibition. One prediction may be that combining the antagonism of integrin  $\alpha$ v $\beta$ 3-integrin with FAK inhibition will result be effective in reducing tumour growth and angiogenesis of micrometastases by exploiting  $\alpha$ v $\beta$ 3-integrin preventative antiangiogenic effect at secondary site and with FAK providing a second barrier to tumour spread (Jean *et al.*, 2014). Since both  $\alpha$ v $\beta$ 3-antagonists and FAK inhibitors are already available and well-tolerated (Eskens *et al.*, 2003; Infante *et al.*, 2012), their efficacy when used together could be tested (as proof-of-concept) in our spontaneous metastases models.

I showed that different molecular and cellular changes correlate with a constitutive deletion of endothelial  $\beta$ 3-integrin. What does this mean clinically? It means that the therapeutic benefit of these agents (anti-angiogenic drugs along with others) is often short lived and resistance develops within a matter of months. Tumours adapt quickly under the selective pressure of drug treatment and that explains why the concept of drug holiday has recently emerged (Das Thakur *et al.*, 2013). I interpret this as following on from a paradigm shift in cancer chemotherapy. In the year 2000 Fidler and Ellis said "*cancer is a chronic disease and should be treated like other chronic*

*disease*" (Scharovsky *et al.*, 2009). This idea has led to a new therapeutic philosophy from "the maximum tolerated dose" of standard chemotherapy to the "less is better, regularly" of metronomic chemotherapy (Hanahan *et al.*, 2000).

Therefore, preclinical models of resistance, such as the Tie1Cre model of constitutive deletion of endothelial  $\beta$ 3-integrin, will likely provide critical insights in elucidating potential mechanisms leading to resistance (as a consequence of chronic treatment), and ultimately, to effective treatments. This might take the form of combinatorial targeting or of modulating the timing and dosing of treatments.

## 7.2 Final conclusions and future works

Overall, my findings have answered some questions and created many more. I envision two main lines of investigation spinning off from this project which will likely contribute to translational knowledge. These are:

- to directly address the differences between genetic versus pharmacological inhibition of  $\beta$ 3-integrin, including different classes of  $\beta$ 3-integrin inhibitors, dosing and treatment schemes;
- to address the mechanisms of resistance that build up to compensate for long-term loss of endothelial  $\beta$ 3-integrin, in order to identify and validate molecular targets that might be co-targeted alongside  $\beta$ 3 integrin to sustain, or at least extend, tumour inhibition.

In my last year, I started to investigate the role of endothelial  $\beta$ 3-integrin in the process of metastasis and revealed a potential anti-metastatic effect which I believe, deserves further investigation. Previous work from Taverna *et al.* (2005) showed that the total absence of  $\beta$ 3-integrin has very little effect on tumor progression and metastasis in a spontaneous model of breast carcinogenesis. However, as I have pointed out, this may reflect non-endothelial cell contributions to the process.

My preliminary findings point to a potential anti-metastatic role for endothelial  $\beta$ 3-integrin. I have uncovered a complex scenario in which pre-metastatic niche and inflammation act together to promote tumour progression. Whether this is true or not still needs further analyses and confirmation. These findings might provide a rationale for synergistically targeting the endothelium and immune cells. This represents a

completely new and exciting project which has been inspiring me for my next step and leading me to focus my research interest in the field of immunoangiogenesis.

## ACKNOWLEDGEMENTS

Since I believe that most of what a Phd is about, it is looking for differences and thinking differently, I would like to thank first, and above all, the person that has made the difference to me in this last three years.

The person beyond the "I" in this thesis,

there would have been no "I" without "WE".

A beautiful thank, Stephen.

For everything and forever.

And then, of course, I would like to thank all the people that have been supporting me in these years both academically and personally:

Prof Dylan Edwards, his lab (present and former members);

My supervisory teams, Dr Mohammad Hajhosseini and Dr Ernst Poschl;

Faculty members Dr Jelena Gavrilovic, Prof Ulriche Mayer, Prof Andrea Munsterberg and Dr Grant Wheeler;

My labmates, Tim Sam Ben Alex (after all it was fun guys);

UEA counselling and NEDS;

Medusa Volleyball team;

Sprinters ( from JCI Sprint Programme-2014)

Special "thank you" section for friends: to all real friends, nearby and faraway, italians and not italians, scientist and not scientists; all of you have been part of this and help me through this and so deserve all my gratitdude and affection.

Final last thank you to mamma e papa' e marco (my loves, my strenght).

## LIST OF PUBLICATIONS

Su X, Esser A, Amend SR, Xiang J, Yalin Xu Y, Ross MH, Steri V, Roomp K, Fontana F, Hurchla MA, Knolhoff B, Meyer MA, Morgan E, Zou W, Tomasson JC, Faccio R, Novack DV, Robinson SR, Steven Teitelbaum S, DeNardo DG, Schneider JG, Weilbaecher KN. *Integrin beta3 Regulates Macrophage Polarization in the Tumor Microenvironment*. Submitted to JCI

Ellison TS, Atkinson SJ, Steri V, Kirkup BM, Preedy MEJ, Johnson RT, Ruhrberg C, Dylan R. Edwards DR, Schneider JG, Katherine Weilbaecher K, Stephen D. Robinson SD. *Suppressing  $\beta$ 3-integrin triggers a neuropilin-1 dependent focal adhesion turnover pathway that can be targeted to block pathological angiogenesis*. In press

Atkinson SJ, Ellison TS, Steri V, SD Robinson. *Redefining the role(s) of endothelial  $\alpha$ v $\beta$ 3-integrin in angiogenesis*. Biochem Soc Trans. 2014 Dec; 42(6):1590-5

Steri V, Ellison TS, Weilbaecher KN, Schneider JG, Edwards DR, Gontarczyk A, Fruttiger M, Hodivala-dilke KM, Robinson SD. *Acute depletion of endothelial  $\beta$ 3-integrin transiently inhibits tumor growth and angiogenesis in mice*. Circ Res. 2014 Jan 3; 114(1):79-91.

## REFERENCES

- Abedi H**, Zachary I. Vascular endothelial growth factor stimulates tyrosine phosphorylation and recruitment to new focal adhesions of focal adhesion kinase and paxillin in endothelial cells. *J. Biol. Chem.* 1997. 272: 15442–15451.
- Alghisi GC**, Ponsonnet L, Rüegg C. The integrin antagonist cilengitide activates  $\alpha$ V $\beta$ 3, disrupts VE-cadherin localization at cell junctions and enhances permeability in endothelial cells. *PLoS One.* 2009.4(2):e4449.
- Algire GH**, Chalkley HW, Legallais FY, Park HD. Vascular reactions of normal and malignant tissues in vivo. I. Vascular reactions of mice to wounds and to normal and neoplastic transplants. *J Natl Cancer Inst.* 1945; 6:73–85.
- Armulik A**, Genové G, Betsholtz C. Pericytes: developmental, physiological, and pathological perspectives, problems, and promises. *Dev Cell.* 2011. Aug 16; 21(2):193-215.
- Aumailley M**, Gurrath M, Muller G, Calvete J, Timpl R, Kessler H. Arg-Gly-Asp constrained within cyclic pentapeptides. Strong and selective inhibitors of cell adhesion to vitronectin and laminin fragment P1. *FEBS Lett.* 1991. 291: 50–54.
- Asahara T**, Murohara T, Sullivan A, Silver M, van der Zee R, Li T, Witzenbichler B, Schatteman G, Isner JM. Isolation of putative progenitor endothelial cells for angiogenesis. *Science.* 1997. 275 (5302), 964–967.
- Atkinson SJ**, Ellison TS, Steri V, Gould E, Robinson SD. Redefining the role(s) of endothelial  $\alpha$  $\beta$ 3-integrin in angiogenesis. *Biochem Soc Trans.* 2014 Dec; 42(6):1590-5.
- Avraamides CJ**, Garmy-Susini B, Varnier JA. Integrins in angiogenesis and lymphangiogenesis. *Nat Rev Cancer.* 2008. Aug; 8(8):604-17.
- Bader BL**, Rayburn H, Crowley D, Hynes RO. Extensive vasculogenesis, angiogenesis, and organogenesis precede lethality in mice lacking all alpha v integrins. *Cell.* 1998 Nov 13; 95(4):507-19.
- Baker M**, Robinson SD, Lechertier T, Barber PR, Tavora B, D'Amico G, Jones DT, Vojnovic B, Hodivala-Dilke K. Use of the mouse aortic ring assay to study angiogenesis. *Nat Protoc.* 2011 Dec 22; 7(1):89-104.
- Balkwill F**, Mantovani A. Inflammation and cancer: back to Virchow? *Lancet.* 2001. Feb 17; 357(9255):539-45.
- Bates DO**, Harper SJ. Regulation of vascular permeability by vascular endothelial growth factors. *Vascul Pharmacol.* 2002. 39, 225-237.
- Bendas G**, Borsig L. Cancer cell adhesion and metastasis: selectins, integrins, and the inhibitory potential of heparins. *Int J Cell Biol.* 2012; 2012:676731.
- Bergers G**, Song S. The role of pericytes in blood-vessel formation and maintenance. *Neuro Oncol.* 2005. Oct; 7(4):452-64.

**Bergers G**, Hanahan D. Modes of resistance to anti-angiogenic therapy. *Nat Rev Cancer* 2008; 8:592–603.

**Biswas SK**, Sica A, Lewis CE. Plasticity of macrophage function during tumor progression: regulation by distinct molecular mechanisms. *J Immunol.* 2008 Feb 15; 180(4):2011-7.

**Black WC**, Welch HG. Advances in diagnostic imaging and overestimations of disease prevalence and the benefits of therapy. *N Engl J Med.* 1993. Apr 29; 328(17):1237-43.

**Branco-Price C**, Zhang N, Schnelle M, Evans C, Katschinski DM, Liao D, Ellies L, Johnson RS. Endothelial cell HIF-1 $\alpha$  and HIF-2 $\alpha$  differentially regulate metastatic success. *Cancer Cell.* 2012 Jan 17; 21(1):52-65.

**Brooks PC**, Clark RA., and Cheresh, D. A. Requirement of vascular integrin  $\alpha v$   $\beta 3$  for angiogenesis. *Science.* 1994. 264, 569-571.

**Brooks PC**, Montgomery AM, Rosenfeld M, Reisfeld RA, Hu T, Klier G, Cheresh DA. Integrin  $\alpha v \beta 3$  antagonists promote tumor regression by inducing apoptosis of angiogenic blood vessels. *Cell.* 1994. 79: 1157–1164.

**Brooks PC**, Stromblad S, Klemke R, Visscher D, Sarkar FH, Cheresh DA. Antiintegrin  $\alpha v \beta 3$  blocks human breast cancer growth and angiogenesis in human skin. *J Clin Invest.* 1995. 96, 1815-1822.

**Cai W**, Chen X. Anti-angiogenic cancer therapy based on integrin  $\alpha v \beta 3$  antagonism. *Anticancer Agents Med Chem.* 2006. Sep; 6(5):407-28.

**Carmeliet P**, Lampugnani MG, Moons L, Breviario F, Compernelle V, Bono F, Balconi G, Spagnuolo R, Oosthuysen B, Dewerchin M, Zanetti A, Angellilo A, Mattot V, Nuyens D, Lutgens E, Clotman F, de Ruiter MC, Gittenberger-de Groot A, Poelmann R, Lupu F, Herbert JM, Collen D, Dejana E. Targeted deficiency or cytosolic truncation of the VE-cadherin gene in mice impairs VEGF-mediated endothelial survival and angiogenesis. *Cell* 98, 1999. 147–157.

**Carmeliet P**. Mechanisms of angiogenesis and arteriogenesis. *Nat. Med.* 6:389-395. 2000.

**Carmeliet P**, Jain RK. Angiogenesis in cancer and other diseases. *Nature.* 2000. 407, 249-257.

**Carmeliet P**, Ferreira V, Breier G, Pollefeyt S, Kieckens L, Gertsenstein M, Fahrig M, Vandenhoeck A, Harpal K, Eberhardt C, Declercq C, Pawling J, Moons L, Collen, D, Risau W, Nagy A. Abnormal blood vessel development and lethality in embryos lacking a single VEGF allele. *Nature.* 2006. 380, 435-439.

**Carmeliet P**, Jain RK. Molecular mechanisms and clinical applications of angiogenesis. *Nature*, 2011. 473 (7347), 298-307.

**Caswell PT**, Vadrevu S, Norman JC. Integrins: masters and slaves of endocytic transport. *Nat Rev Mol Cell Biol.* 2009 Dec; 10(12):843-53.

**Cébe-Suarez S**, Zehnder-Fjällman A, Ballmer-Hofer K. The role of VEGF receptors in angiogenesis; complex partnerships. *Cellular and molecular life sciences*, 2006. 63(5), 601-15.

**Charo IF**, Nannizzi L, Smith JW, Cheresh DA. The vitronectin receptor alpha v beta 3 binds fibronectin and acts in concert with alpha 5 beta 1 in promoting cellular attachment and spreading on fibronectin. *J Cell Biol.* 1990. Dec;111(6 Pt 1):2795-800.

**Claxton S**, Kostourou V, Jadeja S, Chambon P, Hodivala-Dilke K, Fruttiger M. Efficient, inducible Cre-recombinase activation in vascular endothelium. *Genesis*. 2008. Feb;46(2):74-80.

**Cleaver O**, Melton DA. Endothelial signaling during development. *Nat Med.* 2003. Jun; 9(6):661-8.

**Cruz-Munoz W**, Man S, Xu P, Kerbel RS. Development of a preclinical model of spontaneous human melanoma central nervous system metastasis. *Cancer Res.* 2008 Jun 15; 68(12):4500-5.

**Danhier F**, Le Breton A, Préat V. RGD-based strategies to target alpha(v) beta(3) integrin in cancer therapy and diagnosis. *Mol Pharm.* 2012 Nov 5; 9(11):2961-73.

**da Silva RG**, Tavora B, Robinson SD, Reynolds LE, Szekeres C, Lamar J, Batista S, Kostourou V, Germain MA, Reynolds AR, Jones DT, Watson AR, Jones JL, Harris A, Hart IR, Iruela-Arispe ML, Dipersio CM, Kreidberg JA, Hodivala-Dilke KM. Endothelial alpha3beta1-integrin represses pathological angiogenesis and sustains endothelial-VEGF. *Am J Pathol.* 2010 Sep; 177(3):1534-48.

**Das Thakur M**, Stuart DD. The evolution of melanoma resistance reveals therapeutic opportunities. *Cancer Res.* 2013 Oct 15; 73(20):6106-10.

**Davis GE**, Senger DR. Endothelial extracellular matrix: biosynthesis, remodeling, and functions during vascular morphogenesis and neovessel stabilization. *Circ Res.* 2005. Nov 25; 97(11):1093-107.

**Dejana E**, Bazzoni G. and Lampugnani M. G. Vascular endothelial (VE)-cadherin: only an intercellular glue? *Exp.Cell Res.* 1999. 252: 13–19

**Dejana E**. Endothelial cell-cell junctions: happy together. *Nat. Rev. Mol. Cell Biol.* 2004. 5:261-270.

**Delbaldo C**, Raymond E, Vera K, Hammershaimb L, Kaucic K, Lozahic S, Marty M, Faivre S. Phase I and pharmacokinetic study of etaracizumab (Abegrin), a humanized monoclonal antibody against  $\alpha v \beta 3$  integrin receptor, in patients with advanced solid tumors. *Invest New Drugs.* 2008. 26: 35–43.

**DeNardo DG**, Johansson M, Coussens LM. Immune cells as mediators of solid tumor metastasis. *Cancer Metastasis Rev.* 2008. Mar; 27(1):11-8.

**DeNardo DG**, Barreto JB, Andreu P, Vasquez L, Tawfik D, Kolhatkar N, Coussens LM. CD4(+) T cells regulate pulmonary metastasis of mammary carcinomas by enhancing protumor properties of macrophages. *Cancer Cell.* 2009. Aug 4; 16 (2):91-102.

**De Palma M**, Venneri MA, Roca C, Naldini L., Targeting exogenous genes to tumor angiogenesis by transplantation of genetically modified hematopoietic stem cells. *Nat. Med.* 2003. 9(6), 789–795.

**Desgrosellier JS**, Barnes LA, Shields DJ, Huang M, Lau SK, Prévost N, Tarin D, Shattil SJ, Cheresh DA. An integrin alpha(v)beta(3)-c-*Src* oncogenic unit promotes anchorage-independence and tumor progression. *Nat Med.* 2009. Oct; 15(10):1163-9.

**Desgrosellier JS**, Cheresh DA. Integrins in cancer: biological implications and therapeutic opportunities. *Nat Rev Cancer.* 2010. Jan; 10(1):9-22.

**Ding Q**, Stewart J, Olman MA, Klobe MR, and Gladson CL. The Pattern of Enhancement of *Src* Kinase Activity on PDGF Stimulation of Glioblastoma Cells Is Affected by The Integrin Engaged. *Journal of Biological Chemistry.* 2003 Oct 10:278(41):39882-91.

**Dingemans AM**, van den Boogaart V, Vosse BA, van Suylen RJ, Griffioen AW, Thijssen VL. Integrin expression profiling identifies integrin alpha5 and beta1 as prognostic factors in early stage non-small cell lung cancer. *Mol Cancer.* 2010 Jun 17; 9:152.

**Dougher M**, Terman BI. Autophosphorylation of KDR in the kinase domain is required for maximal VEGFs stimulated kinase activity and receptor internalization. *Oncogene.* 1999. 18: 1619–1627.

**Downs KM.** Florence Sabin and the mechanism of blood vessel lumenization during vasculogenesis. *Microcirculation.* 2003.10:5-25.

**Drake CJ**, Cheresh, DA, Little CD. An antagonist of integrin alpha v beta 3 prevents maturation of blood vessels during embryonic neovascularization. *J Cell Sci.* 1995. 108 (Pt 7), 2655-2661.

**Duval M**, Bedard-Goulet S, Delisle C. Gratton JP. Vascular endothelial growth factor-dependent down regulation of Flk-1/KDR involves Cbl-mediated ubiquitination: consequences on nitric oxide production from endothelial cells. *J. Biol. Chem.* 2003. 278: 20091–20097.

**Dvorak HF**, Nagy JA, Feng D, Brown, Dvorak AM. Vascular permeability factor/vascular endothelial growth factor and the significance of microvascular hyperpermeability in angiogenesis. *Curr Top. Microbiol. Immunol.* 1999.237:97-132. Purves WK, Sadava D, Orians GH, Heller C. *Life: the Science of Biology.* 2004.

**Eccles SA**, Aboagye EO, Ali S, Anderson AS, Armes J, Berditchevski F, et al. Critical research gaps and translational priorities for the successful prevention and treatment of breast cancer. *Breast Cancer Res.* 2013 Oct 1; 15(5):R92.

**Eliceiri BP**, Paul R, Schwartzberg PL, Hood JD, Leng J, Cheresh DA. Selective requirement for *Src* kinases during VEGF-induced angiogenesis and vascular permeability. *Mol Cell.* 1999 Dec;4(6):915-24.

**Eliceiri BP**, Cheresh, DA. Adhesion events in angiogenesis. *Curr Opin Cell Biol.* 2001. 13, 563-568.

**Eliceiri, BP.** Integrin and growth factor receptor crosstalk. *Circ Res.* 2001. 89, 1104-

1110.

**Enestein J**, Kramer RH. Confocal microscopic analysis of integrin expression on the microvasculature and its sprouts in the neonatal foreskin. *J Invest Dermatol.* 1994 Sep; 103(3):381-6.

**Eskens FA**, Dumez H, Hoekstra R, Perschl A, Brindley C, Böttcher S, Wynendaele W, Dreys J, Verweij J, van Oosterom AT. Phase I and pharmacokinetic study of continuous twice weekly intravenous administration of Cilengitide (EMD 121974), a novel inhibitor of the integrins  $\alpha v \beta 3$  and  $\alpha v \beta 5$  in patients with advanced solid tumours. *Eur J Cancer.* 2003. May; 39(7):917-26.

**Esser S.**, Lampugnani M. G., Corada M., DeJana E. and Risau W. Vascular endothelial growth factor induces VE-cadherin tyrosine phosphorylation in endothelial cells. *J. Cell Sci.* 1998.111: 1853–1865.

**Felding-Habermann B.** Integrin adhesion receptors in tumor metastasis. *Clin Exp Metastasis.* 2003; 20(3):203-13.

**Feng W**, McCabe NP, Mahabeleshwar GH, Somanath PR, Phillips DR, Byzova TV. The angiogenic response is dictated by  $\beta 3$  integrin on bone marrow-derived cells. *J Cell Biol.* 2008. Dec 15; 183(6):1145-57.

**Ferrara N**, Gerber HP, Le Couter J. The biology of VEGF and its receptors. *Nat. Med.* 2003. 9, 669-676.

**Ferrara N**, Carver-Moore K, Chen H, Dowd M, Lu L, O'Shea KS, Powell- Braxton L, Hillan KJ, Moore, MW. Heterozygous embryonic lethality induced by targeted inactivation of the VEGF gene. *Nature.* 1996.380, 439-442.

**Francia G**, Cruz-Munoz W, Man S, Xu P, Kerbel RS. Mouse models of advanced spontaneous metastasis for experimental therapeutics. *Nat Rev Cancer.* 2011 Feb; 11(2):135-41.

**Fridlender ZG**, Sun J, Kim S, Kapoor V, Cheng G, Ling L, Worthen GS, Albelda SM. Polarization of tumor-associated neutrophil phenotype by TGF- $\beta$ : "N1" versus "N2" TAN. *Cancer Cell.* 2009 Sep 8; 16(3):183-94.

**Friedlander M**, Brooks PC, Shaffer RW, Kincaid CM, Varner JA, Cheresh DA. Definition of two angiogenic pathways by distinct  $\alpha v$  integrins. *Science.* 1995 Dec 1; 270(5241):1500-2.

**Fidler IJ.** Selection of successive tumour lines for metastasis. *Nat New Biol.* 1973. Apr 4; 242(118):148-9.

**Fiedler U**, Augustin HG. Angiopoietins: a link between angiogenesis and inflammation. *Trends Immunol.* 2006.27:552-558.

**Florey L.** The endothelial cell. *Br. Med. J.* 1966. 5512, 487-490.

**Folkman J.** Tumor angiogenesis: therapeutic implications. *N Engl J Med.* 1971 Nov 18; 285(21):1182-6.

**Folkman J**, Haudenschild C. Angiogenesis by capillary endothelial cells in culture. *Trans Ophthalmol Soc U K.* 1980 Sep; 100(3):346-53.

**Fulton D**, Gratton J. P., McCabe T. J., Fontana J., Fujio Y., Walsh K. et al. (1999) Regulation of endothelium-derived nitric oxide production by the protein kinase Akt. *Nature*. 1999. 399:597–601

**Gaengel K**, Genové G, Armulik A, Betsholtz C. Endothelial-mural cell signaling in vascular development and angiogenesis. *Arterioscler Thromb Vasc Biol*. 2009 May;29 (5):630-8.

**Galdiero MR**, Bonavita E, Barajon I, Garlanda C, Mantovani A, Jaillon S. Tumor associated macrophages and neutrophils in cancer. *Immunobiology*. 2013 Nov; 218(11):1402-10.

**Gao AG**, Lindberg FP, Dimitry JM, Brown EJ, Frazier WA. Thrombospondin modulates alpha v beta 3 function through integrin-associated protein. *J Cell Biol*. 1996 Oct; 135(2):533-44.

**Gao D**, Joshi N, Choi H, Ryu S, Hahn M, Catena R, Sadik H, Argani P, Wagner P, Vahdat LT, Port JL, Stiles B, Sukumar S, Altorki NK, Raffi S, Mittal V. Myeloid progenitor cells in the premetastatic lung promote metastases by inducing mesenchymal to epithelial transition. *Cancer Res*. 2012 Mar 15; 72(6):1384-94.

**Gelati, M**, Aplin AC, Fogel E, Smith KD, Nicosia RF. The angiogenic response of the aorta to injury and inflammatory cytokines requires macrophages. *J. Immunol*. 2008. 181, 5711–5719.

**Gerber HP**, McMurtrey A, Kowalski J, Yan M, Keyt BA, Dixit V. Vascular endothelial growth factor regulates endothelial cell survival through the phosphatidylinositol 3-kinase/Akt signal transduction pathway: requirement for Flk-1/KDR activation. *J. Biol. Chem*. 1998. 273: 30336–30343.

**Gerber HP**, Dixit V, Ferrara N. Vascular endothelial growth factor induces expression of the antiapoptotic proteins Bcl-2 and A1 in vascular endothelial cells. *J Biol Chem*. 1998. 273, 13313-13316.

**Gerhardt H**, Betsholtz C. Endothelial-pericyte interactions in angiogenesis. *Cell Tissue Res*. 2003 Oct; 314(1):15-23.

**Gerhardt H**, Golding M, Fruttiger M, Ruhrberg C, Lundkvist A, Abramsson A, Jeltsch M, Mitchell C, Alitalo K, Shima D, and Betsholtz C. VEGF guides angiogenic sprouting utilizing endothelial tip cell filopodia. *J. Cell Biol*. 2003.161:1163-1177.

**Germain M**, De Arcangelis A, Robinson SD, Baker M, Tavora B, D'Amico G, Silva R, Kostourou V, Reynolds LE, Watson A, Jones JL, Georges-Labouesse E, Hodivala-Dilke K. Genetic ablation of the alpha 6-integrin subunit in Tie1Cre mice enhances tumour angiogenesis. *J Pathol*. 2010 Feb; 220(3):370-81.

**Geudens I**, Gerhardt H. Coordinating cell behaviour during blood vessel formation. *Development*. 2011. Nov; 138(21):4569-83.

**Giancotti FG**, Ruoslahti E. Integrin signaling. *Science*.1999. 285, 1028-1032.

**Giavazzi R**, Decio A. Syngeneic murine metastasis models: B16 melanoma. *Methods Mol Biol*. 2014. 1070:131-40.

**Ginsberg MH**, Partridge A, Shattil, SJ. Integrin regulation. *Curr Opin Cell Biol.* 2005 17, 509-516.

**Giordano FJ**, Johnson RS. Angiogenesis: the role of the microenvironment in flipping the switch. *Curr Opin Genet Dev.* 2001 Feb; 11(1):35-40.

**Gladson CL**. Expression of integrin alpha v beta 3 in small blood vessels of glioblastoma tumors. *J Neuropathol Exp Neurol.* 1996 Nov; 55(11):1143-9.

**Gladson CL**, Cheresh DA 1991. Glioblastoma expression of vitronectin and the  $\alpha v \beta 3$  integrin. Adhesion mechanism for transformed glial cells. *J Clin Invest.* 1991. 88: 1924–1932

**Grunewald M**, Avraham I, Dor Y, Bachar-Lustig E, Itin A, Jung S, Chimenti S, Landsman L, Abramovitch R, Keshet E.. VEGF-induced adult neovascularization: recruitment, retention, and role of accessory cells. *Cell.* 2006 Jan 13; 124(1):175-89.

**Gu H**, Zou YR, Rajewsky K. Independent control of immunoglobulin switch recombination at individual switch regions evidenced through Cre-loxP-mediated gene targeting. *Cell.* 1993. Jun 18; 73(6):1155-64.

**Gullino PM**. Consideration on blood supply and fluid exchange in tumors. *Prog. Clin. Biol. Res.* 1982. 107, 1–20.

**Hammes HP**, Brownlee M, Jonczyk A, Sutter A, Preissner KT. Subcutaneous injection of a cyclic peptide antagonist of vitronectin receptor-type integrins inhibits retinal neovascularization. *Nat Med.* 1996. 2, 529-533.

**Hanahan D**, Bergers G, Bergsland E. Less is more, regularly: metronomic dosing of cytotoxic drugs can target tumor angiogenesis in mice. *J Clin Invest.* 2000 Apr; 105(8):1045-7.

**Hanahan D**, Weinberg RA. Hallmarks of cancer: the next generation. *Cell.* 2011. Mar 4; 144 (5):646-74.

**Hanahan D**, Coussens LM. Accessories to the crime: functions of cells recruited to the tumor microenvironment. *Cancer Cell.* 2012 Mar 20; 21 (3):309-22.

**Hendrix MJ**, Seftor EA, Meltzer PS, Gardner LM, Hess AR, Kirschmann, DA, Schatteman, GC, Seftor, RE. Expression and functional significance of VE-cadherin in aggressive human melanoma cells: role in vasculogenic mimicry. *Proc. Natl. Acad. Sci.* 2001. 98 (14), 8018–8023.

**Hersey P**, Sosman J, O'Day S, Richards J, Bedikian A, Gonzalez R, Sharfman W, Weber R, Logan T, Buzoianu M, et al. A randomized phase 2 study of etaracizumab, a monoclonal antibody against integrin  $\alpha v \beta 3$ , + or – dacarbazine in patients with stage IV metastatic melanoma. *Cancer.* 2010. 116: 1526–1534.

**Hicklin DJ**, Ellis LM. Role of the vascular endothelial growth factor pathway in tumour growth and angiogenesis. *J Clin Oncol*, 2005. Feb 10; 23(5):1011-27.

**Hiratsuka S**, Nakamura K, Iwai S, Murakami M, Itoh T, Kijima H, Shipley JM, Senior RM, Shibuya M. MMP9 induction by vascular endothelial growth factor receptor-1 is involved in lung-specific metastasis. *Cancer Cell.* 2002 Oct; 2(4):289-300.

**Hiratsuka S**, Watanabe A, Aburatani H, Maru, Y. Tumour-mediated upregulation of chemoattractants and recruitment of myeloid cells predetermines lung metastasis. *Nat. Cell Biol.* 2006. 8 (12), 1369–1375

**Hobbs, S. K.** Regulation of transport pathways in tumor vessels: role of tumor type and microenvironment. *Proc. Natl Acad. Sci.* 1998. 95, 4607–4612.

**Hodivala-Dilke KM**, McHugh KP, Tsakiris DA, Rayburn H, Crowley D, Ullman-Culleré M, Ross FP, Collier BS, Teitelbaum S, Hynes RO. Beta3-integrin-deficient mice are a model for Glanzmann thrombasthenia showing placental defects and reduced survival. *J Clin Invest.* 1999 Jan; 103(2):229-38.

**Hodivala-Dilke, KM**, Reynolds, AR, Reynolds LE. (2003). Integrins in angiogenesis: multitasking molecules in a balancing act. *Cell Tissue Res* 314,131-144.

**Holash J**, Maisonpierre PC, Compton D, Boland P, Alexander CR, Zagzag D, Yancopoulos, GD, Wiegand SJ. Vessel cooption, regression, and growth in tumors mediated by angiotensins and VEGF. *Science.* 1999. 284 (5422), 1994–1998.

**Hong YK**, Lange-Asschenfeldt B, Velasco P, Hirakawa S, Kunstfeld R, Brown LF et al. (2004) VEGF-A promotes tissue repair-associated lymphatic vessel formation via VEGFR-2 and the alpha1beta1 and alpha2beta1 integrins. *FASEB J* 18:1111–1113

**Hosotani R**, Kawaguchi M, Masui T, Koshihara T, Ida J, Fujimoto K, Wada M, Doi R, Imamura M. Expression of integrin alphaVbeta3 in pancreatic carcinoma: relation to MMP-2 activation and lymph node metastasis. *Pancreas.* 2002 Aug; 25(2):e30-5.

**Houghton AM**, Rzymkiewicz DM, Ji H, Gregory AD, Egea EE, Metz HE, Stolz DB, Land SR, Marconcini LA, Kliment CR, Jenkins KM, Beaulieu KA, Mouded M, Frank SJ, Wong KK, Shapiro SD. Neutrophil elastase-mediated degradation of IRS-1 accelerates lung tumor growth. *Nat Med.* 2010 Feb; 16(2):219-23.

**Hu M**, Polyak K. Microenvironmental regulation of cancer development. *Curr Opin Genet Dev.* 2008 Feb; 18(1):27-34.

**Huang J**, Roth R, Heuser JE, Sadler JE. Integrin alpha(v)beta(3) on human endothelial cells binds von Willebrand factor strings under fluid shear stress. *Blood.* 2009. Feb 12; 113(7):1589-97.

**Huang MT**, Mason JC, Birdsey GM, Amsellem V, Gerwin N, Haskard DO, Ridley AJ, Randi AM. Endothelial intercellular adhesion molecule (ICAM)-2 regulates angiogenesis. *Blood.* 2005 Sep 1; 106(5):1636-43.

**Huh SJ**, Liang S, Sharma A, Dong C, Robertson GP. Transiently entrapped circulating tumor cells interact with neutrophils to facilitate lung metastasis development. *Cancer Res.* 2010 Jul 15; 70(14):6071-82.

**Humphries MJ.** The molecular basis and specificity of integrin-ligand interactions. *J Cell Sci* 1990; 97:585-92

**Hurwitz H.** Integrating the anti-VEGF-A humanized monoclonal antibody bevacizumab with chemotherapy in advanced colorectal cancer. *Clin Colorectal Cancer.* 2004 Oct; 4 Suppl 2:S62-8.

**Hynes RO.** Integrins: bidirectional, allosteric signaling machines. *Cell*. 2002. Sep 20; 110(6):673-87.

**Ide AG,** Baker NH, Warren SL. Vascularisation of the Brown Pearce rabbit epithelioma transplant as seen in the transparent ear chamber. *Am. J. Roentgenol* 1939. 42, 891-899.

**Igreja, C.,** Courinha, M., Cachaco, A.S., Pereira, T., Cabecadas, J., da Silva, M.G., Dias, S., 2007. Characterization and clinical relevance of circulating and biopsy derived endothelial progenitor cells in lymphoma patients. *Haematologica* 92 (4), 469–477.

**Iljin K,** Dube A, Kontusaari S, Korhonen J, Lahtinen I, Oettgen P, Alitalo K. Role of ets factors in the activity and endothelial cell specificity of the mouse Tie gene promoter. *FASEB J*. 1999 Feb; 13(2):377-86.

**Indra AK,** Warot X, Brocard J, Bornert JM, Xiao JH, Chambon P, Metzger D. Temporally-controlled site-specific mutagenesis in the basal layer of the epidermis: comparison of the recombinase activity of the tamoxifen-inducible Cre-ER(T) and Cre-ER(T2) recombinases. *Nucleic Acids Res*. 1999 Nov 15; 27(22):4324-7.

**Infante JR,** Camidge DR, Mileskin LR, Chen EX, Hicks RJ, Rischin D, Fingert H, Pierce KJ, Xu H, Roberts WG, Shreeve SM, Burris HA, Siu LL. Safety, pharmacokinetic, and pharmacodynamic phase I dose-escalation trial of PF-00562271, an inhibitor of focal adhesion kinase, in advanced solid tumors. *J Clin Oncol*. 2012 May 1; 30(13):1527-33.

**Jain RK.** Normalizing tumour vasculature with anti-angiogenic therapy: a new paradigm for combination therapy. *Nature medicine*, 2001.7(9), 987-9.

**Jain RK.** Normalization of tumor vasculature: an emerging concept in antiangiogenic therapy. *Science*.2005. 307, 58–62.

**Jakobsson L,** Kreuger J, Holmborn K, Lundin L, Eriksson I, Kjellén L, Claesson-Welsh L. Heparan sulfate in trans potentiates VEGFR-mediated angiogenesis. *Dev Cell*. 2006. May; 10(5):625-34.

**Jean C,** Chen XL, Nam JO, Tancioni I, Uryu S, Lawson C, Ward KK, Walsh CT, Miller NL, Ghassemian M, Turowski P, Dejana E, Weis S, Cheresh DA, Schlaepfer DD. Inhibition of endothelial FAK activity prevents tumor metastasis by enhancing barrier function. *J Cell Biol*. 2014. Jan 20; 204(2):247-63.

**Joyce JA,** Pollard JW. Microenvironmental regulation of metastasis. *Nat Rev Cancer*. 2009 Apr; 9(4):239-52.

**Kaplan RN,** Riba RD, Zacharoulis S, Bramley AH, Vincent L, Costa, C, MacDonald DD, Jin DK, Shido K, Kerns SA, Zhu Z, Hicklin D, Wu Y, Port JL, Altorki N, Port ER, Ruggero D, Shmelkov, SV, Jensen KK, Rafii S, Lyden D. VEGFR1-positive haematopoietic bone marrow progenitors initiate the pre-metastatic niche. *Nature* 2005. 438 (7069), 820–827.

**Kashiwagi S,** Izumi Y, Gohongi T, Demou ZN, Xu L, Huang PL, Buerk DG, Munn LL, Jain RK, Fukumura D. NO mediates mural cell recruitment and vessel

morphogenesis in murine melanomas and tissue-engineered blood vessels. *J Clin Invest.* 2005. Jul; 115(7):1816-27.

**Kato H**, Liao Z, Mitsios JV, Wang HY, Deryugina EI, Varner JA, Quigley JP, Shattil SJ. The primacy of  $\beta 1$  integrin activation in the metastatic cascade. *PLoS One.* 2012; 7(10):e46576.

**Kerbel RS**, 2008. Tumor angiogenesis. *N. Engl. J. Med.* 358 (19), 2039–2049.

**Khalili P**, Arakelian A, Chen G, Plunkett ML, Beck I, Parry GC, et al. A non-RGD based integrin binding peptide (ATN-161) blocks breast cancer growth and metastasis in vivo. *Mol Cancer Ther.* 2006; 5: 2271–80.

**Kim R**, Emi M, Tanabe K. Cancer immunoediting from immune surveillance to immune escape. *Immunology.* 2007 May; 121(1):1-14.

**Kohfeldt E**, Sasaki T, Göhring W, Timpl R. Nidogen-2: a new basement membrane protein with diverse binding properties. *J Mol Biol.* 1998 Sep 11; 282(1):99-109.

**Koistinen P**, Heino J. Integrins in Cancer Cell Invasion. *Landes Bioscience* 2000.

**Kostourou V**, Lechertier T, Reynolds LE, Lees DM, Baker M, Jones DT, Tavora B, Ramjaun AR, Birdsey GM, Robinson SD, Parsons M, Randi AM, Hart IR, Hodivala-Dilke K. FAK-heterozygous mice display enhanced tumour angiogenesis. *Nat Commun.* 2013; 4:2020.

**Kren A**, Baeriswyl V, Lehembre F, Wunderlin C, Strittmatter K, Antoniadis H, Fässler R, Cavallaro U, Christofori G. Increased tumor cell dissemination and cellular senescence in the absence of beta1-integrin function. *EMBO J.* 2007 Jun 20; 26(12):2832-42.

**Krilleke D**, DeErkenez A, Schubert W, Giri I, Robinson GS, Ng YS, Shima DT. Molecular mapping and functional characterisation of the VEGF164 heparin-binding domain. *J Biol Chem.* 2007. Sep 21; 282(38):28045-56.

**Kroll J**, Waltenberger J. A novel function of VEGF receptor-2 (KDR): rapid release of nitric oxide in response to VEGF-A stimulation in endothelial cells. *Biochem Biophys Res Commun.* 1999. 265, 636-639.

**Kumar CC**, Malkowski M, Yin Z, Tanghetti E, Yaremko B, Nechuta T, Varner J, Liu M, Smith EM, Neustadt B, Presta M, Armstrong L. Inhibition of angiogenesis and tumor growth by SCH221153, a dual  $\alpha(v)\beta 3$  and  $\alpha(v)\beta 5$  integrin receptor antagonist. *Cancer Res* 61. 2001. 2232-2238.

**Lampugnani MG**, Corada M, Andriopoulou P, Esser S, Risau W, Dejana E. Cell confluence regulates tyrosine phosphorylation of adherens junction components in endothelial cells. *J. Cell Sci.* 1997. 110 (Pt 17):2065-2077.

**Lampugnani MG**, Zanetti A, Corada M, Takahashi T, Balconi G, Breviario F, Orsenigo F, Cattelino A, Kemler R, Daniel TO, Dejana E. Contact inhibition of VEGF-induced proliferation requires vascular endothelial cadherin, beta-catenin, and the phosphatase DEP-1/CD148. *J. Cell Biol.* 2003. 161:793- 804.

**Lampugnani MG**, Dejana E. Adherens junctions in endothelial cells regulate vessel maintenance and angiogenesis. *Thromb Res.* 2007. 120 Suppl 2, S1-6.

**Langley RR**, Fidler IJ. The seed and soil hypothesis revisited--the role of tumor-stroma interactions in metastasis to different organs. *Int J Cancer*. 201. Jun 1; 128(11):2527-35.

**Layton MG**, Franks LM. Selective suppression of metastasis but not tumorigenicity of a mouse lung carcinoma by cell hybridization. *Int J Cancer*. 1986. May 15; 37(5):723-30.

**Leite de Oliveira R**, Hamm A, Mazzone M. Growing tumor vessels: more than one way to skin a cat - implications for angiogenesis targeted cancer therapies. *Mol Aspects Med*. 2011. Apr; 32(2):71-87.

**Liaw L**, Skinner MP, Raines EW, Ross R, Cheresch DA, Schwartz SM, Giachelli CM.. The adhesive and migratory effects of osteopontin are mediated via distinct cell surface integrins. Role of alpha v beta 3 in smooth muscle cell migration to osteopontin in vitro. *J Clin Invest*. 1995. Feb; 95(2):713-24.

**Limaverde-Sousa G**, Sternberg C, Ferreira CG. Antiangiogenesis beyond VEGF inhibition: a journey from antiangiogenic single-target to broad-spectrum agents. *Cancer Treat Rev*. 2014 May; 40(4):548-57.

**Lin EY**, Pollard JW. Tumor-associated macrophages press the angiogenic switch in breast cancer. *Cancer Res*. 2007 Jun 1; 67(11):5064-6.

**Lindbom L**, Werr J. Integrin-dependent neutrophil migration in extravascular tissue. *Semin Immunol*. 2002. 14(2):115-21.

**Liu H**, Radisky DC, Yang D, Xu R, Radisky ES, Bissell MJ, Bishop JM. MYC suppresses cancer metastasis by direct transcriptional silencing of  $\alpha v$  and  $\beta 3$  integrin subunits. *Nat Cell Biol*. 2012 May 13; 14(6):567-74.

**Liu Z**, Jia B, Zhao H, Chen X, Wang F. Specific targeting of human integrin  $\alpha v \beta 3$  with (111) in-labeled abegrin in nude mouse models. 2010. *Mol Imaging Biol* 13: 112–120.

**Lyden D**, Hattori K, Dias S, Costa C, Blaikie P, Butros L, Chadburn A, Heissig B, Marks W, Witte L, Wu Y, Hicklin D, Zhu Z, Hackett NR, Crystal RG, Moore MA, Hajjar KA, Manova K, Benezra R, Rafii S. Impaired recruitment of bone-marrow-derived endothelial and hematopoietic precursor cells blocks tumor angiogenesis and growth. *Nat Med*. 2001 Nov; 7(11):1194-201.

**Mackey JR**, Kerbel RS, Gelmon KA, McLeod DM, Chia SK, Rayson D, Verma S, Collins LL, Paterson AH, Robidoux A, Pritchard KI. Controlling angiogenesis in breast cancer: a systematic review of anti-angiogenic trials. *Cancer Treat Rev*. 2012 Oct; 38(6):673-88.

**Madisen L**, Zwingman TA, Sunkin SM, Oh SW, Zariwala HA, Gu H, Ng LL, Palmiter RD, Hawrylycz MJ, Jones AR, Lein ES, Zeng H. A robust and high-throughput Cre reporting and characterization system for the whole mouse brain. *Nat Neurosci*. 2010 Jan; 13(1):133-40

**Mahabeleshwar GH**, Feng W, Phillips DR, Byzova TV. Integrin signalling is critical for pathological angiogenesis. *J Exp Med*. 2006. Oct 30; 203 (11):2495-507.

**Maniotis AJ**, Folberg R, Hess A, Seftor EA, Gardner LM, Pe'er J, Trent JM, Meltzer PS, Hendrix MJ. Vascular channel formation by human melanoma cells in vivo and in vitro: vasculogenic mimicry. *Am. J. Pathol.* 1999. 155 (3), 739–752.

**Mantovani A**, Allavena P, Sica A, Balkwill F. Cancer-related inflammation. *Nature.* 2008 Jul 24; 454(7203):436-44.

**Mantovani A**, Cassatella MA, Costantini C, Jaillon S. Neutrophils in the activation and regulation of innate and adaptive immunity. *Nat Rev Immunol.* 2011 Jul 25; 11(8):519-31.

**Masson-Gadais B**, Houle F, Laferrière J, Huot J. Integrin  $\alpha$ v $\beta$ 3, requirement for VEGFR2-mediated activation of SAPK2/p38 and for Hsp90-dependent phosphorylation of focal adhesion kinase in endothelial cells activated by VEGF. *Cell Stress Chaperones.* 2003. Spring; 8 (1):37-52.

**Matsumoto T**, Bohman S, Dixelius J, Berge T, Dimberg A, Magnusson P, Wang L, Wikner C, Qi JH, Wernstedt C, Wu J, Bruheim S, Mugishima H, Mukhopadhyay D, Spurkland A, Claesson-Welsh L. VEGF receptor-2 Y951 signaling and a role for the adapter molecule TSAd in tumor angiogenesis. *Embo J.* 2005. 24, 2342-2353.

**May T**, Mueller PP, Weich H, Froese N, Deutsch U, Wirth D, Kröger A, Hauser H. Establishment of murine cell lines by constitutive and conditional immortalisation. *J Biotechnol.* 2005. Oct 17; 120(1):99-110.

**Mazzone M**, Dettori D, Leite de Oliveira R, Loges S, Schmidt T, Jonckx B, Tian YM, Lanahan AA, Pollard P, Ruiz de Almodovar C, De Smet F, Vinckier S, Aragonés J, Debackere K, Lutun A, Wyns S, Jordan B, Pisacane A, Gallez B, Lampugnani MG, Dejana E, Simons M, Ratcliffe P, Maxwell P, Carmeliet P. Heterozygous deficiency of PHD2 restores tumor oxygenation and inhibits metastasis via endothelial normalization. *Cell.* 2009. 136(5):839-51.

**McCarty JH**, Monahan-Earley RA, Brown LF, Keller M, Gerhardt H, Rubin K, Shani M, Dvorak HF, Wolburg H, Bader BL, Dvorak AM, Hynes RO. Defective associations between blood vessels and brain parenchyma lead to cerebral hemorrhage in mice lacking  $\alpha$ v integrins. *Mol Cell Biol.* 2002. Nov; 22(21):7667-77.

**McLean GW**, Carragher NO, Avizienyte E, Evans J, Brunton VG, Frame MC. The role of focal-adhesion kinase in cancer - a new therapeutic opportunity. *Nat Rev Cancer.* 2005. Jul; 5(7):505-15.

**Meadows KN**, Bryant P, Pumiglia KM. VEGF induction of the angiogenic phenotype requires Ras activation. *J. Biol. Chem.* 2001. 276: 49289–49298.

**Miranti CK**, Brugge, JS. Sensing the environment: a historical perspective on integrin signal transduction. *Nat Cell Biol.* 2002. Apr; 4(4):E83-90.

**Miyauchi A**, Alvarez J, Greenfield EM, Teti A, Grano M, Colucci S, Zamboni-Zallone A, Ross FP, Teitelbaum SL, Cheresch D. Binding of osteopontin to the osteoclast integrin  $\alpha$ v $\beta$ 3. *Osteoporos Int.* 1993. 3 Suppl 1:132-5.

**Monaghan-Benson E**, Burridge K. The regulation of vascular endothelial growth factor-induced microvascular permeability requires Rac and reactive oxygen species. *J Biol Chem.* 2009. Sep 18; 284(38):25602-11.

**Morgan EA**, Schneider JG, Baroni TE, Uluçkan O, Heller E, Hurchla MA, Deng H, Floyd D, Berdy A, Prior JL, Piwnica-Worms D, Teitelbaum SL, Ross FP, Weilbaecher KN Dissection of platelet and myeloid cell defects by conditional targeting of the beta3-integrin subunit. *FASEB J.* 2010. Apr; 24(4):1117-27.

**Morgan SM**, Samulowitz U, Darley L, Simmons DL, Vestweber D. Biochemical characterization and molecular cloning of a novel endothelial-specific sialomucin. *Blood.* 1999. Jan 1; 93(1):165-75.

**Mould AP**, Humphries MJ. Regulation of integrin function through conformational complexity: not simply a knee-jerk reaction? *Curr Opin Cell Biol.* 2004 Oct; 16(5):544-51.

**Naik RP**, Jin D, Chuang E, Gold EG, Tousimis EA, Moore AL, Christos PJ, de Dalmas T, Donovan D, Rafii S, Vahdat LT. Circulating endothelial progenitor cells correlate to stage in patients with invasive breast cancer. *Breast Cancer Res. Treat.* 2008.107 (1), 133–138.

**Nicosia RF**, Tcho R, Leighton J. Histotypic angiogenesis in vitro: light microscopic, ultrastructural, and radioautographic studies. *In Vitro.* 1982 Jun; 18(6):538-49.

**Nicosia RF**. The aortic ring model of angiogenesis: a quarter century of search and discovery. *J Cell Mol Med.* 2009 Oct; 13(10):4113-36.

**Oh ES**, Gu H, Saxton TM, Timms JF, Hausdorff S, Frevert EU, Kahn BB, Pawson T, Neel BG, Thomas SM. Regulation of early events in integrin signaling by protein tyrosine phosphatase SHP-2. *Mol Cell Biol.* 1999 Apr; 19(4):3205-15.

**Ostrand-Rosenberg S**. Immune surveillance: a balance between protumor and antitumor immunity. *Curr Opin Genet Dev.* 2008 Feb; 18(1):11-8.

**Otrock ZK**, Makarem JA, Shamseddine AI. Vascular endothelial growth factor family of ligands and receptors: review. *Blood Cells Mol Dis.* 2007 May-Jun; 38(3):258-68.

**Paget S**. The distribution of secondary growths in cancer of the breast. *Cancer Metastasis Rev.* 1989 Aug; 8 (2):98-101.

**Patan S**, Tanda S, Roberge S, Jones RC, Jain RK, Munn LL. Vascular morphogenesis and remodeling in a human tumor xenograft: blood vessel formation and growth after ovariectomy and tumor implantation. *Circ. Res.* 2001.89 (8), 732–739.

**Petit V**, Thiery JP. Focal adhesions: structure and dynamics. *Biol Cell.* 2000. Oct; 92(7):477-94.

**Potente M**, Gerhardt H, Carmeliet P. Basic and therapeutic aspects of angiogenesis. *Cell.* 2011. Sep 16; 146(6):873-87.

**Potter MD**, Barbero S, Cheresh DA. Tyrosine phosphorylation of VE-cadherin prevents binding of p120- and beta-catenin and maintains the cellular mesenchymal state. *J Biol Chem.* 2005 Sep 9; 280 (36):31906-12.

**Purves WK**, Sadava D, Orians GH, Heller C. *Life: the Science of Biology.* 2004.

**Quail DF**, Joyce JA. Microenvironmental regulation of tumor progression and metastasis. *Nat Med.* 2013 Nov; 19 (11):1423-37.

**Reardon DA**, Fink KL, Mikkelsen T, Cloughesy TF, O'Neill A, Plotkin S, et al. Randomized phase II study of cilengitide, an integrin-targeting arginine-glycine-aspartic acid peptide, in recurrent glioblastoma multiforme. *J Clin Oncol: Off J Am Soc Clin Oncol* 2008; 26:5610–7.

**Reynolds AR**, Reynolds LE, Nagel TE, Lively JC, Robinson SD, Hicklin DJ, Bodary SC, and Hodivala-Dilke K. M. Elevated Flk1 (vascular endothelial growth factor receptor 2) signaling mediates enhanced angiogenesis in beta3-integrin-deficient mice. 2004. *Cancer Res* 64, 8643-8650.

**Reynolds AR**, Hart IR, Watson AR, Welte JC, Silva RG, Robinson SD, Da Violante G, Gourlaouen M, Salih M, Jones MC, Jones DT, Saunders G, Kostourou V, Perron-Sierra F, Norman JC, Tucker GC, Hodivala-Dilke KM. Stimulation of tumor growth and angiogenesis by low concentrations of RGD-mimetic integrin inhibitors. *Nat Med*. 2009 Apr; 15(4):392-400.

**Reynolds LE**, Wyder L, Lively JC, Taverna D, Robinson SD, Huang X., Sheppard D, Hynes, RO, Hodivala-Dilke, KM. Enhanced pathological angiogenesis in mice lacking beta3 integrin or beta3 and beta5 integrins. *Nat Med*. 2002. 8, 27-34.

**Risau W**, Flamme I. Vasculogenesis. *Annu Rev Cell Dev Biol*. 1995. 11:73-91.

**Risau W**. Mechanisms of angiogenesis. *Nature*. 1997 Apr 17; 386(6626):671-4.

**Rivera LB**, Bergers G. Angiogenesis. Targeting vascular sprouts. *Science*. 2014. Jun 27; 344(6191):1449-50.

**Robinson SD**, Reynolds LE, Kostourou V, Reynolds AR, Silva RG, Tavora B, Baker M, Marshall JF, Hodivala-Dilke KM. Alpha5 beta3 integrin limits the contribution of neuropilin-1 to vascular endothelial growth factor-induced angiogenesis. *The Journal of biological chemistry*. 2009. 284(49), 33966-81.

**Robinson SD**, Hodivala-Dilke KM. The role of  $\beta$ 3-integrins in tumor angiogenesis: context is everything. *Curr. Opin. Cell Biol*. 2011. 23, 630–637.

**Rouget, C**. Memoire sur le developpement, la structures et les proprietes des capillaires sanguins et lymphatiques. *Archs Physiol Norm Pathol*. 1873. 5, 603–633.

**Rousseau S**, Houle F, Kotanides H, Witte L, Waltenberger J, Landry J. Vascular endothelial growth factor (VEGF)-driven actin-based motility is mediated by VEGFR2 and requires concerted activation of stress-activated protein kinase 2 (SAPK2/p38) and geldanamycin-sensitive phosphorylation of focal adhesion kinase. *J. Biol. Chem*. 2000. 275: 10661–10672.

**Roy H**, Bhardwaj S, Yla-Herttuala S. Biology of vascular endothelial growth factors. *FEBS Lett*. 2006. 580, 2879-2887.

**Sakurai Y**, Ohgimoto K, Kataoka Y, Yoshida N, Shibuya M. Essential role of Flk-1 (VEGF receptor 2) tyrosine residue 1173 in vasculogenesis in mice. *Proc. Natl. Acad. Sci*. 2005. 102: 1076–1081.

**San Antonio JD**, Zoeller JJ, Habursky K, Turner K, Pimpong W, Burrows M, Choi S, Basra S, Bennett JS, DeGrado WF, Iozzo RV. A key role for the integrin  $\alpha$ 2 $\beta$ 1

in experimental and developmental angiogenesis. *Am J Pathol.* 2009 Sep;175(3):1338-47.

**Sandhu JK**, Privora HF, Wenckebach G, Birnboim HC. Neutrophils, nitric oxide synthase, and mutations in the mutatest murine tumor model. *Am J Pathol.* 2000 Feb; 156(2):509-18.

**Sawada J**, Urakami T, Li F, Urakami A, Zhu W, Fukuda M, Li DY, Ruoslahti E, Komatsu M. Small GTPase R-Ras regulates integrity and functionality of tumor blood vessels. *Cancer Cell.* 2012 Aug 14; 22(2):235-49.

**Schaller MD**, Hildebrand JD, Shannon JD, Fox JW, Vines RR, Parsons JT. Autophosphorylation of the focal adhesion kinase, pp125FAK, directs SH2-dependent binding of pp60src. *Mol Cell Biol.* 1994 Mar; 14(3):1680-8.

**Scharovsky OG**, Mainetti LE, Rozados VR. Metronomic chemotherapy: changing the paradigm that more is better. *Curr Oncol.* 2009 Mar; 16(2):7-15.

**Scharpfenecker M**, Fiedler U, Reiss Y, Augustin HG. The Tie-2 ligand angiopoietin-2 destabilizes quiescent endothelium through an internal autocrine loop mechanism. *J. Cell Sci.* 2005.118:771-780.

**Schmieder A**, Michel J, Schönhaar K, Goerdts S, Schledzewski K. Differentiation and gene expression profile of tumor-associated macrophages. *Semin Cancer Biol.* 2012 Aug; 22(4):289-97.

**Senger DR**, Galli SJ, Dvorak AM, Perruzzi CA, Harvey VS, Dvorak HF. Tumor cells secrete a vascular permeability factor that promotes accumulation of ascites fluid. *Science.* 1983 Feb 25; 219 (4587):983-5.

**Senger DR**, Perruzzi CA, Streit M, Kotliansky VE, De Fougères AR, Detmar M (2002) The  $\alpha(1)\beta(1)$  and  $\alpha(2)\beta(1)$  integrins provide critical support for vascular endothelial growth factor signaling, endothelial cell migration, and tumor angiogenesis. *Am J Pathol* 160:195–204

**Shalaby F**, Rossant J, Yamaguchi TP, Gertszenstein M, Wu XF, Breitman ML, Schuh AC. Failure of blood-island formation and vasculogenesis in Flk-1-deficient mice. *Nature.* 1995. Jul 6; 376(6535):62-6.

**Sheldrake HM**, Patterson LH. Function and antagonism of  $\beta(3)$  integrins in the development of cancer therapy. *Curr Cancer Drug Targets.* 2009 Jun; 9(4):519-40.

**Shibuya M**, Claesson-Welsh L. Signal transduction by VEGF receptors in regulation of angiogenesis and lymphangiogenesis. *Exp Cell Res.* 2006. Mar 10; 312 (5):549-60.

**Sica A**, Bronte V. Altered macrophage differentiation and immune dysfunction in tumor development. *J Clin Invest.* May 1, 2007; 117(5): 1155–1166.

**Sica A**, Mantovani Macrophage plasticity and polarization: in vivo veritas. *A.J Clin Invest.* 2012. Mar 1; 122(3):787-95.

**Sidibé A**, Imhof BA. VE-cadherin phosphorylation decides: vascular permeability or diapedesis. *Nat Immunol.* 2014 Mar; 15(3):215-7.

**Sloan EK**, Pouliot N, Stanley KL, Chia J, Moseley JM, Hards DK, Anderson RL. Tumor-specific expression of  $\alpha v \beta 3$  integrin promotes spontaneous metastasis of breast cancer to bone. *Breast Cancer Res.* 2006; 8(2):R20.

**Smith JW**, Ruggeri ZM, Kunicki TJ, Cheresh DA 1990. Interaction of integrins  $\alpha v \beta 3$  and glycoprotein IIb-IIIa with fibrinogen. Differential peptide recognition accounts for distinct binding sites. *J Biol Chem.* 1990. 265: 12267–12271.

**Soffietti R**, Trevisan E, Rudà R. What have we learned from trials on antiangiogenic agents in glioblastoma? *Expert Rev Neurother.* 2014 Jan; 14(1):1-3.

**Soker S**, Takashima S, Miao HQ, Neufeld G, Klagsbrun M. Neuropilin-1 is expressed by endothelial and tumor cells as an isoform-specific receptor for vascular endothelial growth factor. *Cell.* 1998. 92:735-745.

Soldi R, Mitola S, Strasly M, Defilippi P, Tarone G, Bussolino F. Role of  $\alpha v \beta 3$  integrin in the activation of vascular endothelial growth factor receptor-2. *EMBO J.* 1999 February 15; 18(4): 882–892.

**Solinas G**, Schiarea S, Liguori M, Fabbri M, Pesce S, Zammataro L, Pasqualini F, Nebuloni M, Chiabrando C, Mantovani A, Allavena P. Tumor-conditioned macrophages secrete migration-stimulating factor: a new marker for M2-polarization, influencing tumor cell motility. *J Immunol.* 2010 Jul 1; 185(1):642-52.

**Somanath PR**, Malinin NL, Byzova TV. Cooperation between integrin  $\alpha v \beta 3$  and VEGFR2 in angiogenesis. *Angiogenesis.* 2009; 12(2):177-85.

**Soriano P**. Generalized lacZ expression with the ROSA26 Cre reporter strain. *Nat Genet.* 1999. Jan; 21(1):70-1

**Staton CA**, Kumar I, Reed MW, Brown NJ. Neuropilins in physiological and pathological angiogenesis. *J Pathol.* 2007. Jul; 212(3):237-48.

**Stupack DG**, Puente XS, Boutsaboualoy S, Storgard CM, Cheresh DA. Apoptosis of adherent cells by recruitment of caspase-8 to unligated integrins. *J Cell Biol.* 2001. Oct 29; 155(3):459-70.

**Stupp R**, Rugg C. Integrin inhibitors reaching the clinic. *J Clin Oncol.* 2007. May 1; 25(13):1637-8.

**Swift MR**, Weinstein BM. Arterial-venous specification during development. *Circ Res.* 2009. Mar 13; 104(5):576-88.

**Takagi J**, Petre BM, Walz T, Springer TA. Global conformational rearrangements in integrin extracellular domains in outside-in and inside-out signaling. *Cell.* 2002 Sep 6; 110 (5):599-11.

**Takahashi H**, Shibuya M. The vascular endothelial growth factor (VEGF)/VEGF receptor system and its role under physiological and pathological conditions. *Clin Sci* 2005. Sep; 109 (3):227-41.

**Takahashi T**, Yamaguchi S, Chida K, Shibuya M. (2001)A single autophosphorylation site on KDR/Fik-1 is essential for VEGF-A-dependent activation of PLC-gamma and DNA synthesis in vascular endothelial cells. *EMBO J.* 2001. 20: 2768–2778.

**Talmadge, JE**, Singh RK, Fidler, IJ, Raz, A. Murine models to evaluate novel and conventional therapeutic strategies for cancer. *Am. J. Pathol.* 2007. 170, 793–804

**Talmadge JE**. Immune cell infiltration of primary and metastatic lesions: mechanisms and clinical impact. *Semin Cancer Biol.* 2011 Apr; 21(2):131-8.

**Taverna D**, Crowley D, Connolly M, Bronson RT, Hynes RO. A direct test of potential roles for beta3 and beta5 integrins in growth and metastasis of murine mammary carcinomas. *Cancer Res.* 2005 Nov 15; 65(22):10324-9.

**Taverna D**, Moher H, Crowley D, Borsig L, Varki A, Hynes RO. Increased primary tumor growth in mice null for beta3- or beta3/beta5-integrins or selectins. *Proc Natl Acad Sci.* 2004.101, 763-768.

**Tavora B**, Reynolds LE, Batista S, Demircioglu F, Fernandez I, Lechertier T, Lees DM, Wong PP, Alexopoulou A, Elia G, Clear A, Ledoux A, Hunter J, Perkins N, Gribben JG, Hodivala-Dilke KM. Endothelial-cell FAK targeting sensitizes tumours to DNA-damaging therapy. *Nature.* 2014 Oct 2; 514(7520):112-6.

**Tsuda M**, Matozaki T, Fukunaga K, Fujioka Y, Imamoto A, Noguchi T, Takada T, Yamao T, Takeda H, Ochi F, Yamamoto T, Kasuga M. Integrin-mediated tyrosine phosphorylation of SHPS-1 and its association with SHP-2. Roles of Fak and Src family kinases. *Mol Cell Biol.* 1999 Apr; 19(4):3205-15.

**Turowski P**, Martinelli R, Crawford R, Wateridge D, Papageorgiou AP, Lampugnani MG, Gamp AC, Vestweber D, Adamson P, Dejana E, Greenwood J. Phosphorylation of vascular endothelial cadherin controls lymphocyte emigration. *J Cell Sci.* 2008 Jan 1; 121(Pt 1):29-37.

**van der Flier**, A, Sonnenberg, A. Function and interactions of integrins. 2001. *Cell Tissue Res* 305, 285-298.

**Vasiljeva O**, Papazoglou A, Krüger A, Brodoefel H, Korovin M, Deussing J, Augustin N, Nielsen BS, Almholt K, Bogyo M, Peters C, Reinheckel T. Tumor cell-derived and macrophage-derived cathepsin B promotes progression and lung metastasis of mammary cancer. *Cancer Res.* 2006 May 15; 66(10):5242-50.

**von Tell D**, Armulik A, Betsholtz C. Pericytes and vascular stability. *Exp. Cell Res.* 2006.312:623-629.

**Wallez Y**, Cand F, Cruzalegui F, Wernstedt C, Souchelnytskyi S, Vilgrain I, Huber P. Src kinase phosphorylates vascular endothelial-cadherin in response to vascular endothelial growth factor: identification of tyrosine 685 as the unique target site. *Oncogene.* 2007. Feb 15; 26(7):1067-77.

**Weerasinghe D**, McHugh KP, Ross FP, Brown EJ, Gisler RH, Imhof BA. A role for the alphavbeta3 integrin in the transmigration of monocytes. *J Cell Biol.* 1998 Jul 27; 142(2):595-607.

**Weis SM**, Lim ST, Lutu-Fuga KM, Barnes LA, Chen XL, Gothert JR, Shen TL, Guan JL, Schlaepfer DD, Cheresh DA (Compensatory role for Pyk2 during angiogenesis in adult mice lacking endothelial cell FAK. *J Cell Biol.* 2008.181: 43-50

**Weis SM**, Cheresh DA.  $\alpha$ V integrins in angiogenesis and cancer. *Cold Spring Harb Perspect Med*. 2011 Sep; 1(1):a006478.

**Welti J**, Loges S, Dimmeler S, Carmeliet P. Recent molecular discoveries in angiogenesis and antiangiogenic therapies in cancer. *J Clin Invest*. 2013 Aug 1; 123(8):3190-200.

**Wessel F**, Winderlich M, Holm M, Frye M, Rivera-Galdos R, Vockel M, Linnepe R, Ipe U, Stadtmann A, Zarbock A, Nottebaum AF, Vestweber D. Leukocyte extravasation and vascular permeability are each controlled in vivo by different tyrosine residues of VE-cadherin. *Nat Immunol*. 2014 Mar; 15(3):223-30.

**Williams CK**, Li JL, Murga M, Harris AL, Tosato G. Up-regulation of the Notch ligand Deltalike 4 inhibits VEGF-induced endothelial cell function. *Blood*. 2006. 107:931-939.

**Wilson A**, Trumpp A. Bone-marrow haematopoietic-stem-cell niches. *Nat Rev Immunol*. 2006 Feb; 6(2):93-106.

**Yachida S**, Jones S, Bozic I, Antal T, Leary R, Fu B, Kamiyama M, Hruban RH, Eshleman JR, Nowak MA, Velculescu VE, Kinzler KW, Vogelstein B, Iacobuzio-Donahue CA. Distant metastasis occurs late during the genetic evolution of pancreatic cancer. *Nature*. 2010 Oct 28; 467(7319):1114-7.

**Yan HH**, Pickup M, Pang Y, Gorska AE, Li Z, Chytil A, Geng Y, Gray JW, Moses HL, Yang L. Gr-1+CD11b+ myeloid cells tip the balance of immune protection to tumor promotion in the premetastatic lung. *Cancer Res*. 2010 Aug 1; 70(15):6139-49.

**Yang JT**, Hynes RO. Fibronectin receptor functions in embryonic cells deficient in alpha 5 beta 1 integrin can be replaced by alpha V integrins. *Mol Biol Cell*. 1996 Nov; 7(11):1737-48.

**Yurchenco PD**. Basement Membranes: Cell Scaffoldings and Signaling Platforms. *J Biol Chem*. 2009 Mar 27; 284(13):8984-94.

**Zachary I**, Glikli, G. Signaling transduction mechanisms mediating biological actions of the vascular endothelial growth factor family. *Cardiovasc Res*. 2001. 49, 568-581.

**Zachary, I**. VEGF signalling: integration and multi-tasking in endothelial cell biology. *Biochem Soc Trans*. 2003. 31, 1171-1177.

**Zeng H**, Zhao D, Mukhopadhyay D. KDR stimulates endothelial cell migration through heterotrimeric G protein Gq/11-mediated activation of a small GTPase RhoA. *J Biol Chem*. 2002. 277, 46791-46798.

**Zimmermann, KW**. Der feinere bau der blutcapillares. *Z. Anat. Entwicklungsgesch*. 1923. 68, 3-109.

**Zhu WH**, Iurlaro M, MacIntyre A, Fogel E, Nicosia RF. The mouse aorta model: influence of genetic background and aging on bFGF- and VEGF-induced angiogenic sprouting. *Angiogenesis* 6, 193-199. 2003

## APPENDIX